Copyright Notices

Notice 1

Notice 2

AN INVESTIGATION INTO THE EFFECT OF *IN UTERO* HYPOXIA ON CEREBRAL BLOOD VESSELS AND BRAIN ACTIVITY IN LATE GESTATION FETAL SHEEP.

Ana Aradhna Baburamani

BBNSc (Hons)

Department of Physiology and
The Ritchie Centre,
Monash Institute of Medical Research
Monash University

This thesis is submitted in fulfilment of the requirement for the Degree of Doctor of Philosophy at Monash University.

December 2011

To my Family ...

Mum & Dad
Kaushik & Carol
Thatha

"A pessimist sees the difficulty in every opportunity;

An optimist sees the opportunity in every difficulty."

Winston Churchill

TABLE OF CONTENTS

LIST OF FIGURES AND TABLES

Appendices

*Denotes figures in which permission to adapt (Figures 1.3, 1.5, 1.8, 1.9, 1.12, 1.14) and reproduce (Figures 1.4, 2.9, 3.1) have been attained from the publisher.
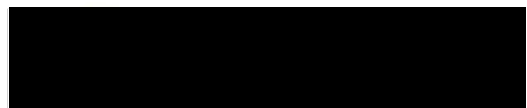
GENERAL DECLARATION

In accordance with Monash University Doctrate Regulation 17/Doctor of Philosophy regulations the following regulations are made:

I hereby declare that, to the best of my knowledge and belief, that this thesis contains no material that has been accepted for the award of any other degree or diploma in any other university and that, it contains no material previously published or written by another person except when due reference is made.

Under the Copyright Act 1968, this thesis must be used only under the normal conditions of scholarly fair dealing. In particular no results or conclusions should be extracted from it, nor should it be copied or closely paraphrased in whole or in part without the written consent of the author. Proper written acknowledgement should be made for any assistance obtained from this thesis.

I certify that I have made all reasonable efforts to secure copyright permissions for third-party content included in this thesis and have not knowingly added copyright content to my work without the owner's permission.

Ana Aradhna Baburamani

CONTRIBUTION TO THESIS

In general terms, experiments on large animals are quite involved and require a number of people to conduct such studies. Due to this, a number of people assisted Ms Baburamani in her experiments. For the studies conducted in Chapter 3 and 4, animal experiments were conducted by Ana A. Baburamani with assistance from Dr. Edwin Yan, Dr. Margie Castillo-Melendez and Prof David W. Walker. All animal studies reported in Chapter 5 and 6 were run by Ana A. Baburamani with assistance from both supervisors.

All experimental procedures and analyses were conducted by Ana A. Baburamani, with the exception of the counting of VEGF cell numbers in Chapter 4 which was done by Dr. Castillo-Melendez to allow for a 'blinded' assessment of the results.

Advice was also received from Dr. Camden Lo (MIMR) for the method of analysis of blood vessel morphology presented in Chapter 3.

SUMMARY

Fetal hypoxia contributes significantly to the pathogenesis of permanent perinatal brain injury. Cerebrovascular pathology following hypoxia can lead to devastating and debilitating brain injury, such as that seen following stroke and haemorrhage, but the effect of *in utero* fetal hypoxia on the developing cerebrovasculature is not well understood. In the adult brain, robust up-regulation of vascular endothelial growth factor (VEGF) occurs following hypoxia and cerebral ischemia which results in the formation of new blood vessels, as an adaptive response to protect and repair the brain from hypoxic injury. However, newly-formed blood vessels are fragile and prone to rupture.

The aims of the studies described in this thesis were to determine how a single brief, but severe episode of **fetal** hypoxia in late gestation in sheep affects VEGF expression and the cerebral vasculature. We also determined the effects of this global hypoxia on *fetal* and *neonatal* behaviour to determine if the fetal brain can repair itself following a single brief hypoxic insult. The results show that 48 h after an *in utero* hypoxic insult, produced by 10 min of complete umbilical cord occlusion, the distribution of mean blood vessel size is greater in white matter but not gray matter, and there was greater blood vessel-associated VEGF expression white matter compared to gray matter. This was associated with disruption in blood brain barrier (BBB) permeability seen by increased extravasation of plasma albumin in white matter. When the fetuses were left *in utero* (5 – 10 days following UCO) until the onset of labour, increased VEGFR-2 expression was again seen in white, not gray matter.

These studies highlight the importance of assessing VEGF/VEGFR system following *in utero* hypoxia in the developing fetal brain. Studies assessing both **fetal** and **newborn** behaviour following *in utero* global hypoxia showed that **fetal** electrocortical (ECoG) activity and breathing movements were disturbed throughout late gestation, and after birth there were delays in the **newborn lamb** achieving important behavioural milestones such as the ability to stand,

use all four legs, and find the udder and suckle. Therefore, it is concluded that an antepartum hypoxic event late in gestation does not result in the fetal brain being able to recover fully, resulting in persistent and profound changes in brain structure and pre- and post-natal behaviour.

ACKNOWLEDGMENTS

My deepest and sincere thanks must first go to my supervisors David and Margie for their continued guidance, advice, friendship and enthusiasm. DW, who would have thought that a coming into the lab as a summer research student at the start of third year (in 2005), would land us here, 7 years on? Your continual support, patience, understanding and the endless opportunities that you have given me through the years has truly been exceptional. Many chats over coffee about life, cricket and science, along with your "inspirational" and at times quirky anecdotes, has given me a real passion and excitement for research.

Margie, massive thank you for all the knowledge, support and opportunities you have given me over the last few years. Right from the beginning your enthusiasm for the exciting, new and unknown was contagious. The last few years have been an extremely enjoyable, at times crazy, experience. You have taught me many invaluable lessons about science and life, too many of which to list, all of which I am grateful for.

Edwin, always a source of important yet quirky facts. The lessons (both good and bad) you taught me all the way back in Honours, are still priceless. Thank you. Alex Satragano – Thank you for the many lessons you taught me during surgery. The many conversations we also had will always remind me to live for the moment. Physiology Animal House Staff (Lily, Jade and Erin), many thanks for your time and effort in helping to look after and take care of our sheep, including the numerous 'in labour' phone calls. Jan Loose, for your assistance in the lab and with Cortisol RIA. Camden Lo (MMI), massive thank you for your advice, assistance and expertise.

Ree, my little guardian angel, can't thank you enough for the endless chats, hugs and coffees, not to mention valuable advice you gave me along the way. My immediate support crew – Tam, Burcu and Amy; you guys have always been there and I'm sending out a massive thanks your way!! Whether it was helping with sheep emergencies, being free for a coffee break, always ready for a chat about science, life or other and forever prepared with some motivating words with a shoulder to lean on - couldn't have done it without your support. Kel, can't thank you enough – always ready for a chat, coffee and a pep up, the advice and feedback have been invaluable.

To the Walker Lab all past and present: Edwin, Ree, Hayley, Lisa, Bobbi, Zoe, Tam, Dave C, Tracey, Udani, Bree, Carlos, Icha, Wani, Daphne, Karin; to have a lab environment that was

My amazing Mum and Dad (& Chachi); you are both incredibly inspirational and have always taught me that hard work, dedication and a positive attitude are the key to success. Your endless love, support and advice (and constant reminder that these things take time) are simply invaluable. Dad, you are such a valuable source of knowledge and advice, thank you for always being able to calm me down. Mum, a.k.a."Super-Woman" in our eyes, even though you scared us for a while there you have always been a pillar of strength, and been prime example of what hard work and determination can achieve. Although you are to blame for my strong ability to always keep talking, I thank you for always teaching me to dream big, reach for the stars and that everything is possible.

PUBLICATIONS & PRESENTATIONS

PUBLICATIONS

1. Polglase GR, Nitsos I, **Baburamani AA**, Crossley KJ, Slater MK, Gill AW, Allison BJ, Moss TJ, Pillow JJ, Hooper SB, Kluckow M. Inflammation *in utero* exacerbates ventilation induced brain injury in preterm lambs.(2011) *J Appl Physiol*. Nov 3. [Epub ahead of print]

2. Yan EB, **Baburamani AA**, Walker AM, Walker DW. Changes in cerebral blood flow, cerebral metabolites and breathing movements in the sheep fetus sheep following asphyxia produced by occlusion of the umbilical cord. (2009) *American Journal of Physiology- Regulatory Integrative and Comparative Physiology,* 297 (1) R60 – R69

PUBLISHED ABSTRACTS

1. **Baburamani AA,** Crossley KJ, Allison BJ, Chalmers D, Hooper SB, Walker DW, Castillo-Melendez M. (2010) What effect does ventilation have on the preterm ovine brain? *Journal of Paediatrics and Child Health, 46 (S1), p14 – A026.*

2. **Baburamani AA**, Walker DW, Castillo-Melendez M. (2009) Cerebro-vascular responses to brief global asphyxia in late gestation fetal sheep: evidence for vascular re-modelling? *Journal of Cerebral Blood Flow and Metabolism, 29 (S1),* pS538-9*.*

3. **Baburamani AA**, Yan EB, Walker DW. (2009) Prolonged decrease in cerebral blood flow following a transient severe hypoxia in late gestation fetal sheep. *Journal of Cerebral Blood Flow and Metabolism, 29 (S1),* pS102*.*

4. Castillo-Melendez M, **Baburamani AA**, Alwis D, Walker DW. (2009) Temporal-Spatial expression of VEGF and Ki67 in the germinal matrix of mid to late gestation fetal sheep. *Reproductive Sciences, 16(3)*, p323A.

5. **Baburamani AA,** Cabalag C, Castillo-Melendez M, Hutton LC, Walker DW. (2009) Effect of prenatal asphyxia on pregnancy outcome, brain and behaviour in newborn sheep. *Developmental Medicine and Child Neurology, 51(2)*, p20.

6. Castillo-Melendez M, **Baburamani AA**, Walker DW. (2009) Endothelial cell proliferation and neovascularisation in the late gestation fetal sheep brain is associated with increased VEGF expression. *Developmental Medicine and Child Neurology, 51(2),* p59.

ABSTRACTS

1. **Baburamani AA**, Walker DW, Castillo-Melendez M. *Cerebrovascular response to brief hypoxia in fetal sheep: Contribution to selective vulnerability of white matter in the developing brain?* - XXVth International Symposium on Cerebral Blood Flow, Metabolism and Function - Barcelona – Spain, 2011 (May)

2. Polglase GR, Hooper SB, Gill AW, Wong F, Allison BJ, Moss TJW, **Baburamani AA**, Kluckow M. *Resuscitation of preterm lambs with high tidal volumes causes cerebral haemodynamic disturbance and related brain injury.* Pediatric Academic Society – Asian Society for Pediatric Research (PAS/ASPR) – Denver, USA, 2011 (April)

3. Polglase GR, Hooper SB, Gill AW, Wong F, Allison BJ, Moss TJW, **Baburamani AA**, Kluckow M. *Resuscitation of preterm lambs with high tidal volumes causes cerebral haemodynamic disturbance and related brain injury.* PSANZ 15th Annual Congress – Hobart, Australia, 2011 (April)

4. Walker DW, **Baburamani AA**, Lo C, Castillo-Melendez M *Consequence of umbilical cord occlusion in late gestational fetal sheep on the developing cerebrovasculature.* PSANZ 15th Annual Congress – Hobart, Australia, 2011 (April)

5. **Baburamani AA**, Walker DW, Castillo-Melendez M. *Cerebrovascular responses following in utero umbilical cord occlusion in late gestation fetal sheep.* – International Anatomical Sciences and Cell Biology Conference (IASCBC) – Singapore, 2010

6. **Baburamani AA,** Crossley KJ, Allison BJ, Chalmers D, Hooper SB, Walker DW, Castillo-Melendez M. *What effect does ventilation have on the preterm ovine brain?-* PSANZ 14th Annual Congress – Wellington, New Zealand, 2010

7. **Baburamani AA,** Cabalag C, Witjaksono A, Walker DW, Castillo-Melendez M. *Could early upregulation of VEGF following hypoxia predetermine post-natal bleeding in the brain?* – NGED Forum, Palm Cove, Australia, 2009

8. **Baburamani AA**, Walker DW, Castillo-Melendez M. *Cerebro-vascular responses to brief global asphyxia in late gestation fetal sheep: evidence for vascular re-modelling?-* XXIVth International Symposium on Cerebral Blood Flow, Metabolism and Function - Chicago - USA, 2009

9. **Baburamani AA**, Yan EB, Walker DW. *Prolonged decrease in cerebral blood flow following a transient severe hypoxia in late gestation fetal sheep.* - XXIVth International Symposium on Cerebral Blood Flow, Metabolism and Function - Chicago - USA, 2009

10. Castillo-Melendez M, **Baburamani AA**, Alwis D, Walker DW. *Temporal–Spatial Expression of VEGF and Ki67 in the Germinal Matrix of Mid to Late Gestation Fetal Sheep.* – Society for Gynaecological Investigation – Glasgow, United Kingdom, 2009

11. **Baburamani AA,** Cabalag C, Castillo-Melendez M, Hutton LC and Walker DW. *Effect of prenatal asphyxia on pregnancy outcome, brain and behaviour in newborn sheep.* – International Cerebral Palsy Conference – Sydney, Australia, 2009

12. Castillo-Melendez M, **Baburamani AA** and Walker DW. *Endothelial cell proliferation and neovascularization in the late gestation fetal sheep brain is associated with increased VEGF expression.* - International Cerebral Palsy Conference – Sydney, Australia, 2009

13. Castillo-Melendez M, **Baburamani AA** and Walker DW. *Early Cerebro-vascular Responses to a Brief Global Asphyxia in Late Gestation Fetal Sheep.* – Society for Neuroscience – Neuroscience 2008, Washington DC, USA, 2008

14. **Baburamani AA,** Cabalag C, Castillo-Melendez M, Hutton LC and Walker DW. *Consequences of a brief, prenatal asphyxia on pregnancy outcome, brain development, and newborn behaviour in sheep.* - 35th Annual Fetal and Neonatal Physiological Society, Maastrict, The Netherlands, 2008

15. **Baburamani AA,** Walker DW and Castillo-Melendez M. *Vasculogenic responses after umbilical cord occlusion in late gestation fetal sheep.* – 35th Annual Fetal and Neonatal Physiological Society, Maastrict, The Netherlands, 2008

16. **Baburamani AA,** Walker DW and Castillo-Melendez M. *Induction of vascular endothelial growth factor in the late gestation fetal brain following intrauterine hypoxia*

produced by umbilical cord occlusion, - Sixth Hershey Conference on Developmental Brain Injury, Paris, France, 2008.

17. Cabalag C, **Baburamani AA,** Castillo-Melendez M, Hutton LC and Walker DW. *Consequences of a prenatal asphyxial insult on pregnancy outcome, neonatal behaviour and brain development in sheep*,- PSANZ 12th Annual Congress, Gold Coast, Australia.

18. **Baburamani AA**, Yan EB, Walker DW. *Changes in regional cerebral blood flow following transient severe hypoxia in late gestation fetal sheep*, - Healthy Start to Life: *A Wintour's Tale*, Melbourne Australia 2007.

AWARDS FROM CONFERANCE MEETINGS

1. Young Investigator Travel Bursary, XXVth International Symposium on Cerebral Blood Flow and Metabolism and Function, 2011

2. 2nd Prize (4th year Category)– Oral Presentation, MIMR Postgraduate Symposium, 2010

3. Conference Participation Award, ARC/NHMRC funded Network in Genes and Environment in Development (NGED), 2009

4. Young Investigator Travel Bursary, XXIVth International Symposium on Cerebral Blood Flow and Metabolism and Function, 2009

5. Best Oral Presentation, 35th Annual Fetal and Neonatal Physiological Society Meeting (Maastricht, The Netherlands), 2008

6. Conference Participation Award, NGED - 2008

7. Postgraduate Travel Grant Award, Monash Research Graduate School (MRGS) - 2008

SYMBOLS AND ABBREVIATIONS

%	Percent
±	Plus or minus
*	Significance ($p < 0.05$)
/	Per
~	Approximately
<	Less than
=	Equal
>	Greater than
°C	Degrees Celsius
ACTH	Adrenocorticotropic hormone
Angpt-1	Angiopoietin-1
Angpt-2	Angiopoietin-2
Angptl-1	Angiopoietin like-1
ANOVA	Analysis of variance
BBB	Blood brain barrier
BPM	Beats per minute
BrdU	Bromodeoxyuridine
BSA	Bovine serum albumin
CBF	Cerebral blood flow
cm	Centimetre
CREB/Akt/ERK	cAMP response element-binding/ protein kinase /extracellular signal related kinase
d	Day
DAB	Diaminobenzidine
dH$_2$O	Distilled water
DPX	Distyrene, plasticizer and xylene
ECoG	Electrocorticogram
EMG	Electromyogram
EO	Ethylene Oxide
EOG	Electro-oculogram

Epo	Erythropoietin
Epo-R	Erythropoietin Receptor
ERR-α	oestrogen related receptor-α
FBM	Fetal breathing movements
G	Gram
GA	Gestational age
GM-IVH	Germinal matrix-intraventricular haemorrhage
h	Hour
H$_2$O$_2$	Hydrogen peroxide
HIF-1α	Hypoxia inducible factor-1α
HR	Heart rate
HRP	Horseradish peroxidise
HV	High voltage
Hz	Hertz
i.v.	Intravenous
ID	Inner diameter
IgG	Immunoglobulin G
IHC	Immunohistochemistry
IL	Interleukin
IU	International Units
L	Litre
LV	Low voltage
M	Molar
m	metre
MAP	Mean arterial blood pressure (fetal)
MCAO	Middle Cerebral Artery Occlusion
Mg	milligram
min	Minute
mL	millilitre
mm	millimetre
mmHg	Millimetres of mercury
MMP	Matrix metalloproteinase
n	Sample size

N_2	Nitrogen
NaCl	Sodium chloride
NGS	Normal goat serum
NO	Nitric oxide
NOS	Nitric oxide synthase
NREM	Non rapid eye movement
NRS	Normal Rabbit Serum
OD	Outer diameter
PBS	Phosphate buffered saline
pCO_2	Partial pressure of carbon dioxide
PEG	Polyethylene glycol
PET	Positron emission tomography
PFA	paraformaldehyde
PG	prostaglandin
PGC-1α	peroxisome-proliferator-activated receptor-γ coactivator-1α
pH	Potential of Hydrogen
PM	Post mortem
pO_2	Partial pressure of oxygen
Pty Ltd	Propriety limited
PVL	Periventricular leukomalacia
REM	Rapid eye movement
RIA	Radioimmunoassay
ROS	Reactive oxygen species
rpm	Rotations per minute
SD	Standard deviation
SEM	Standard error of the mean
sO_2	Oxygen saturation
SOD2	Superoxide dismutase
SSbfv	Sagittal Sinus blood flow velocity
TBS	Tris Buffered Saline
UCO	Umbilical cord occlusion
USA	United States of America
VEGF	Vascular endothelial growth factor

(VPF)	Vascular permeability factor
VEGFR-2 (KDR/Flk-1)	Vascular endothelial growth factor receptor -2 (kinase insert domain receptor/fetal liver kinase 1)
ZO	Zona Occludin

Chapter 1

INTRODUCTION

TABLE OF CONTENTS

As clinicians attempt to understand the underlying reasons for inherent vulnerability of brain regions which result in brain injury, little is known as to how hypoxia-ischemia affects the cerebrovasculature in the developing infant. Most of the research investigating the pathogenesis of perinatal brain injury following hypoxia-ischemia has focussed on excitotoxicity, oxidative stress and inflammatory response, with the response of the developing cerebrovasculature being vastly overlooked. This is surprising as the presentation of devastating and permanent injury such as germinal matrix-intraventricular haemorrhage (GM-IVH) and perinatal stroke are of vascular origin. Even the incidence of periventricular leukomalacia (PVL) is thought to occur due to poor perfusion of the white matter. Inadequate functioning cerebrovascular and vascular injury following hypoxia could be primarily responsible for the injury seen in all these conditions.

Interestingly the response of blood vessels could also explain both the regional protection and vulnerability due to the highly dynamic nature of the cerebral blood vessels in the fetus, and also the fluctuations of cerebral blood flow and metabolic demand that occur following hypoxia. However research into how blood vessels respond following hypoxia-ischemia have mostly been conducted in adult models of ischemia or stroke, further highlighting the need to investigate how the developing cerebrovasculature responds and contribution to perinatal brain injury following hypoxia.

This literature review will detail the current concepts on the pathogenesis of perinatal brain injury, the development of the fetal cerebrovasculature and the blood brain barrier (BBB), key mediators involved with the response of cerebral blood vessels to hypoxia. The key modulators of cerebral blood flow will also be reviewed to understand how these may contribute to pathogenesis of perinatal brain injury.

1.1   PERINATAL HYPOXIA

The occurrence of intrapartum asphyxia is present in up to 25 per 1000 live births in term deliveries (Low, 2004). However the incidence of antepartum and/or intrauterine (occurring before birth) asphyxia is much more difficult to determine. Post mortem studies indicate that hypoxic-ischemic and asphyxic episodes that occur during pregnancy significantly contribute to brain injury, morbidity and mortality (Sims *et al.*, 1985; Low *et al.*, 1989; Low, 2004). Intrauterine asphyxia also contributes to cognitive impairment, developmental delay, epilepsy, motor deficits and cerebral palsy (Low *et al.*, 1989; Cowan *et al.*, 2003; Low, 2004; Glass *et al.*, 2009). The Australian Cerebral Palsy Foundation states that the incidence of cerebral palsy (approximately 1 in 400 live births) has remained relatively unchanged over the last 40 years, despite the rate of perinatal morbidity reducing (Stanley & Watson, 1992). This highlights the importance of understanding the contribution of intrauterine events, such as asphyxia, to the pathogenesis of brain injury.

Common causes of asphyxia and hypoxia that result in reduced blood flow and oxygen to the fetus include maternal infection, hypertension, diabetes and placental insufficiency. Fetal factors can range from multiple births, growth retardation, and umbilical tangling (Figure 1.1 A). The extent of injury that can occur as a consequence of hypoxia are dependent on the duration, degree and frequency of the insult. The gestational age (GA) at which hypoxia may occur also affects the brain regions involved (Figure 1.1 B).

1.1.1   Defining fetal asphyxia

Asphyxia describes an insufficiency to exchange respiratory gases (Blair, 1993; Parer, 1998). The severity of asphyxia and hypoxia-ischemia are thereby defined as a series of responses; including hypoxia (decreased pO_2), hypercapnia (increased pCO_2), hypoxemia, metabolic acidosis (increased lactate), impaired blood gas exchange and ischemia (decreased oxygen to tissue). Some argument exists over whether "asphyxia" is an accurate definition when occurring

during gestation, as in the adult, asphyxia describes deficient oxygen supply arising from the inability to breathe (such as seen during strangulation). *In utero* the fetus does not breathe, but fetal asphyxia does arise from insufficient umbilical or uterine blood flow resulting in impaired blood gas exchange (Parer, 1998; Low, 2004). However without measurement of blood gases and cardiovascular parameters defining asphyxia accurately is difficult. *In this literature review to describe the pathophysiology of both neonatal asphyxia and hypoxia, the terms hypoxia or hypoxia-ischemia will be used.*
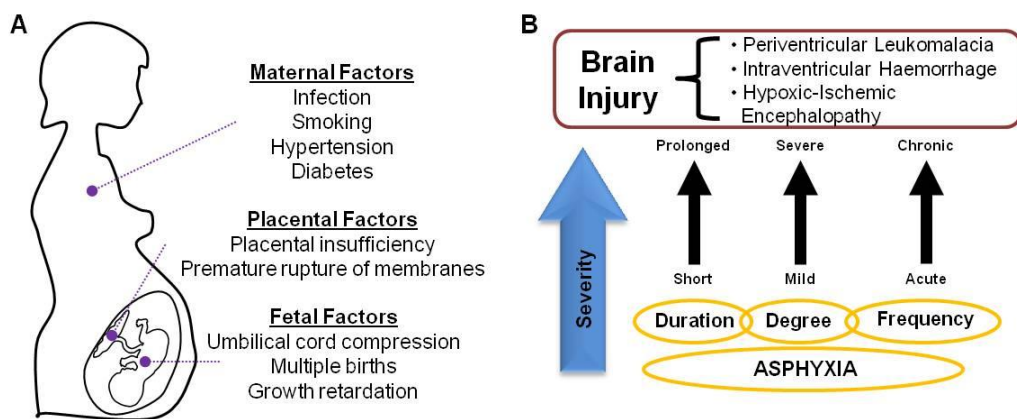
Figure 1.1: Factors contributing to brain injury. Maternal, placental and fetal factors can all contribute to brain injury in the developing fetus (A). The duration, degree and frequency of asphyxia all contribute to the pathogenesis of hypoxic-ischemic injury (B).

1.1.2 Patterns of brain injury

Hypoxia is one of the most common causes of neonatal brain injury, and it still remains to be well understood as to why some brain regions are more vulnerable to injury than others. From human infant autopsy tissue it was found the most prominent injury that occurred was haemorrhage and areas of necrotic tissue, with exacerbated injury seen in neonates that had suffered hypoxia-ischemia or a complicated pregnancy. To understand the impact hypoxia had on the developing brain, the most prominent types of brain injury are explained below.

1.1.2.1 Germinal Matrix – Intraventricular Haemorrhage

The source of GM-IVH was classified by Takashima and Tanaka (1978b), Wigglesworth and Pape (1978) and Volpe (1989) who described bleeding occurring around the subependymal germinal matrix (around the lateral ventricle) extending into the white matter. PVL is characterised by hemorrhagic necrosis of the white matter surrounding the lateral ventricles. It can be diffuse or focal and commonly occurs in the preterm infant. (Reviewed by Volpe (1998).

1.1.2.2 Perinatal Stroke

Perinatal stroke is defined as a cerebrovascular event that can occur between 28 weeks gestation to 28 days postnatal age. The incidence of perinatal stroke (thromboembolism) is approximately 1 in 4000 live births, with < 5 % also being associated with asphyxia (Estan & Hope, 1997; Lynch *et al.*, 2002). An increase in the incidence of neonatal seizures is also associated with perinatal asphyxia resulting in worse neuro-developmental outcome (Miller *et al.*, 2002; Glass *et al.*, 2009). Clinical studies from full term neonates that have experienced perinatal arterial stroke, also show a greater incidence of cerebral palsy, epilepsy, language delay, behavioural abnormalities, and brain injury to the basal ganglia, internal capsule Broca's and Wernicke's area. Increased stroke size also further increases the incidence of cerebral palsy (Lee *et al.*, 2005).

Clinical manifestation of infants who have experienced stroke include seizure activity and apnoea from the second postnatal day (Koelfen *et al.*, 1995; Perlman, 2004), this can also persist to neonatal encephalopathy (Ramaswamy *et al.*, 2004). Focal stroke in the term infant is most common with the presentation of seizure activity without associated encephalopathy. However if neonatal encephalopathy also occurred, neurodevelopmental outcome was significantly worse (de Vries *et al.*, 1997; Perlman, 2004; Ramaswamy *et al.*, 2004).

1.1.3 The influence of gestational age on brain injury

Premature neonates who are also of a low birth weight are at the highest risk of PVL and GM-IVH. Term neonates who undergo hypoxia-ischemia late in gestation tend to have injury in the hippocampus, cortical and thalamic regions. PVL and haemorrhage tend to occur at a lower but still significant incidence (Wigglesworth & Pape, 1978; Inder & Volpe, 2000; Perlman, 2004). Cellular immaturity (such as oligodendrocytes) is also thought to significantly contribute to regional vulnerability of white matter (Alvarez-Diaz *et al.*, 2007; Back *et al.*, 2007). This "selective vulnerability" governs the responses and subsequent manifestation of injury. Cowan *et al.,* (2003) studied MRI and post mortem tissue of full term infants and found that the perinatal period immediately preceding birth was most important in contributing to neonatal encephalopathy and brain injury.

From studies in fetal sheep it was found that younger fetuses can tolerate longer periods of complete cessation of umbilical blood flow, up to 25 minutes, however near-term fetuses can only withstand up to 10 minutes (Mallard *et al.*, 1994; Keunen *et al.*, 1997). The differing tolerance across gestation to duration is suggested to be due to differing metabolic maturity hence response (Bennet *et al.*, 1999).

1.1.4 Animal models investigating the effect of hypoxia during pregnancy

The use of animal models has been widely employed to understand the pathophysiology of brain injury that occurs following hypoxia and/or ischemia. Numerous considerations are made before choosing an adequate animal model including pattern of brain development, length of gestation, body size (both maternal and fetal) and organ development. Following this, the type of insult and duration is an important consideration. Each model has its strengths and weaknesses.

Smaller animal models, such as rats and mice are commonly used. Rodents are "postnatal brain developers" (Dobbing & Sands, 1979) due to their short gestation, so the timing of insults are usually given *ex-utero* or after birth. This allows for post natal behavioural measurements to also be conducted. The effects of **global** hypoxia can be investigated by hypobaric chambers that allow for differing concentrations of oxygen and both acute and chronic studies to be conducted (Kaur *et al.*, 2006a). Another global insult has also been done in the Spiny Mouse using a model of birth asphyxia (Hutton *et al.*, 2009; Ireland *et al.*, 2009). The most common models for studying hypoxia-ischemia in rats and mice is one developed by Rice-Vannucci, in which unilateral ligation of the carotid artery with subsequent hypoxia at postnatal day 7 results in severe brain injury (Rice *et al.*, 1981). Many variations of this model are commonly used; however this is a **focal** insult, comparable to neonatal stroke (Derugin *et al.*, 1998; Vexler *et al.*, 2006). Rabbit kits have been used in a model of uterine ischemia which results in a cerebral palsy like condition (Derrick *et al.*, 2004).

Larger animal models (such as pigs, sheep, llamas) are used due to their long gestation, tolerance to surgical intervention and being perinatal brain developers (similar to humans) allowing for a greater opportunity to closely monitor responses to an insult (Foster *et al.*, 2001). Brain development in the ovine fetus has been characterised as mature at birth (146 days GA); 0.65 GA and 0.9 GA are deemed equivalent to 24 – 26 weeks and 37 – 42 weeks in the human, respectively (McCrabb & Harding, 1995; Hagberg *et al.*, 2002; Back *et al.*, 2006). In fetal sheep a model of cerebral ischemia is achieved by unilateral carotid artery occlusion (McClure *et al.*, 2008).

Occlusion of the umbilical cord, single or repeated, in mid and late gestation has been widely used to investigate the consequence of acute global asphyxia (Bocking, 1992; Mallard *et al.*, 1994; Richardson *et al.*, 1996; Ikeda *et al.*, 1998b; Bennet *et al.*, 1999; Castillo-Melendez *et al.*, 2004; Duncan *et al.*, 2004). Chronic hypoxia, leading to growth restriction has also been conducted in guinea pigs by uterine artery ablation (McKendry *et al.*, 2010) and pregnant sheep

by single umbilical artery ligation (Miller *et al.*, 2007). Studies in the non-human primate were some of the foundation studies used to investigate perinatal brain injury following hypoxia (Myers, 1975), however the cost and ethical difficulties make these a rarely used model. For the studies conducted in this thesis, late gestation fetal sheep were used to investigate the effects of a single *in utero* hypoxic insult, produced by umbilical cord occlusion (UCO) for the study of fetal and newborn behaviour and the analysis of the fetal (near term) brain.

1.1.5 Pathophysiology of hypoxia-ischemia in the neonatal brain

The developing brains' response to global hypoxia-ischemia is a multi-step process. Within the first few hours a regional increase followed by a decrease in cerebral blood flow and subsequent excitotoxicity, energy depletion and generation of free radicals collectively result in increased apoptotic and necrotic cell death (Wigglesworth & Pape, 1978; Shalak & Perlman, 2004). A secondary phase of injury occurs in subsequent hours to days resulting in a neuroinflammatory response, reperfusion and a loss of cerebral autoregulation which can also lead to increased free radical production (Inder & Volpe, 2000; Hamrick & Ferriero, 2003; McLean & Ferriero, 2004; Leonardo & Pennypacker, 2009). These are briefly explained below.

1.1.5.1 Cardiovascular response

The systemic and haemodynamic responses following a severe hypoxic-ischemic insult have been studied using chronically catheterised fetal sheep. Both immature and mature ovine fetuses when subjected to complete UCO subsequently resulted in severe hypoxia (decreased pO_2), hypercapnia (increased pCO_2), academia (decreased pH) and metabolic acidosis (increased lactate), measured from systemic arterial blood samples. These fetuses then fully recover to pre-occlusion values (Bennet *et al.*, 1999; Yan *et al.*, 2009). Mean arterial blood pressure initially increases resulting in hypertension and subsequently hypotension at the end of occlusion. Initially, bradycardia occurs when the cord is occluded, followed with tachycardia. All

parameters return to pre-occlusion values within 2-3 hours (Bennet *et al.*, 1999; Yan *et al.*, 2009).

In response to partial or complete UCO redistribution of cardiac output occurs; increased blood flow to the brain, heart and adrenal glands and decreased blood flow to the lungs, kidneys, intestines and carcass (muscle and skin) (Figure 1.2). Increased blood flow through the ductus venosus also results in decreased blood flow to the liver (Itskovitz *et al.*, 1987; Ball *et al.*, 1994; Jensen *et al.*, 1999). Similar responses in cardiac output also occur following maternal hypoxemia and reductions in uterine blood flow (reviewed by (Jensen *et al.*, 1999; Low, 2004).
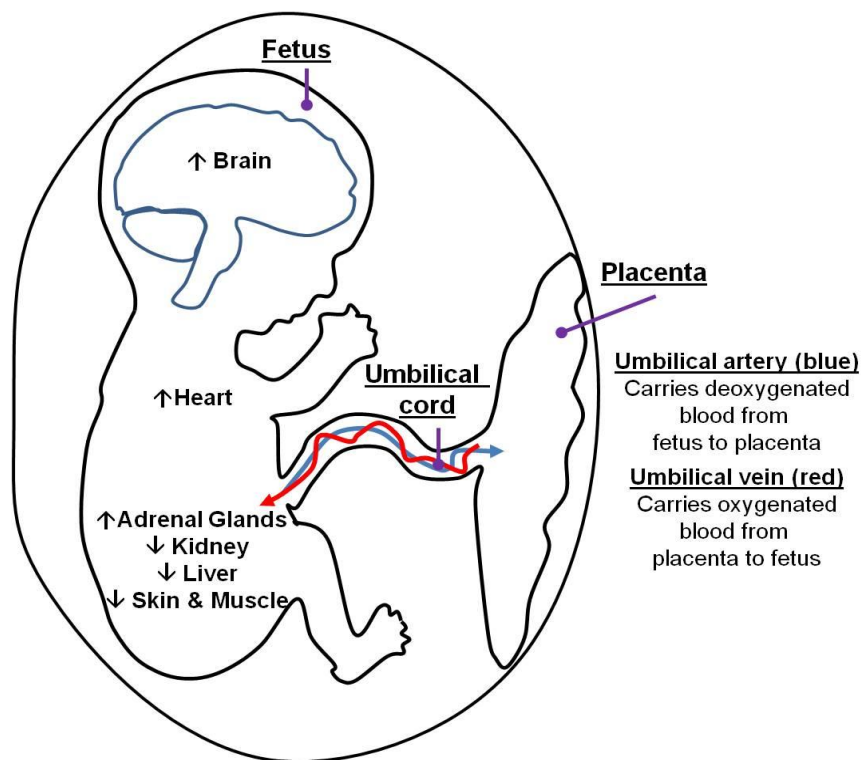
Figure 1.2: Fetal physiological responses to umbilical cord occlusion. Redistribution of blood flow occurs following UCO. Increased blood flow to the brain, heart and adrenals while decreased blood flow to the kidney, liver, skin and muscles occur (Jensen *et al.*, 1999).

1.1.5.2 Excitotoxicity and energy failure

Excitotoxicity refers to neuronal cell death that occurs due to excitability of amino acid receptors (Beal, 1992). Neurons are more vulnerable than glial cells to hypoxic induced injury

due to their high dependence on oxygen. Neuronal glutamate release, re-uptake and resynthesis is a tightly regulated metabolic pathway that is closely coupled with cerebral glucose oxidation demand. There is high density and activity of glutamate receptors during perinatal development, so any severe fluctuations, such as those resulting from hypoxia can have devastating consequences (Low, 2004; McLean & Ferriero, 2004). Oxygen and glucose deprivation can then lead to energy failure.

Prolonged neuronal depolarisation increases neurotransmitter release resulting in excitotoxicity. Astrocytic re-uptake of glutamate is restricted due to low availability of ATP, so overstimulation of glutamate receptors occurs by the presence of excess extracellular glutamate (McLean & Ferriero, 2004). Overstimulation of receptors can result in damage to neurons, particularly seen in the hippocampus, this increased excitability can also lead to neonatal seizure activity (Jensen *et al.*, 1998). NMDA, important in excitatory neurotransmission and adenosine, whose receptors are expressed on excitatory neurons are both implicated in excitatory mediated injury following hypoxia (McLean & Ferriero, 2004). Energy depletion, mitochondrial dysfunction and accumulation of cytosolic calcium all caused by excitotoxicity lead to the development of free radicals (McLean & Ferriero, 2004).

1.1.5.3 Oxidative stress

The developing brain has high lipid content, with the amount of polyunsaturated fatty acids increasing during gestation; this leaves the term brain extremely vulnerable to free radical damage (O'Brien & Sampson, 1965; Mishra & Delivoria-Papadopoulos, 1999; McLean & Ferriero, 2004). During normal metabolism, reactive oxygen species (ROS) are produced in low concentrations acting as signalling molecules to modulate vasodilatation and cerebral blood flow (Paravicini *et al.*, 2004). The generations of ROS induces the production of highly reactive molecules such as nitric oxide (NO), superoxide dismutase (SOD) and hydrogen peroxide (H_2O_2). Increased production of hydroxyl radicals, lipid peroxidation and DNA fragmentation

occur following *in utero* UCO in the near term fetal sheep (Ikeda *et al.*, 1998b; Castillo-Melendez *et al.*, 2004; Miller *et al.*, 2005).

In response to hypoxia-ischemia, and involved in both excitotoxicity and oxidative stress, the biosynthesis of NO from nitric oxide synthase (NOS) occurs. NO and NOS are involved in hypoxic-ischemic induced programmed cell death (Parikh *et al.*, 2003; McLean & Ferriero, 2004; Kaur *et al.*, 2006a) and important for modulation of cerebral blood flow (Section 1.4.2.2). Three well know isoforms exist; neuronal NOS (nNOS), endothelial NOS (eNOS) and inducible NOS (iNOS). Each serve a different function; iNOS is produced in macrophages, microglia, endothelial cells and astrocytes, eNOS in endothelial cells and nNOS in neurons (McLean & Ferriero, 2004; Kaur & Ling, 2009). Increase in intracellular calcium results in active nNOS and eNOS, whereas iNOS is calcium independent (Kaur & Ling, 2009).

1.1.5.4 Response of inflammatory cells

Cell death that is mediated by a neuroinflammatory response is complex. Resident microglia are some of the first cells to become "activated". Amoeboid microglial cells, important for phagocytosis in the developing brain, are found in clusters in the periventricular white matter and are in close association with blood vessels in many brain regions (Fujimoto *et al.*, 1989; Kaur *et al.*, 2007). Microglia are the resident immune cells in the nervous system, whose presence is also related to vascularisation, particularly in the early developmental stages of the human brain (Fujimoto *et al.*, 1989). Microglia are also associated with active myelination during development (Hutchins *et al.*, 1992; Ling & Wong, 1993; Kaur *et al.*, 2007; Kaur & Ling, 2009). Activated microglia are known to produce inflammatory cytokines interleukin-1β (IL-1β), IL-6 and tumour necrosis factor-α (TNF-α), as well as ROS and reactive nitrogen species (Kaur & Ling, 2009).

Activated microglia and astrocytes migrate to necrotic regions and attempt to clean up cellular debris (Leonardo & Pennypacker, 2009). Following hypoxia-ischemia, compromise of the BBB

(Section 1.3.3) allows the entry of macrophages and cytokines into the circulation (Alvarez-Diaz *et al.*, 2007; Leonardo & Pennypacker, 2009). Circulating cytokines can then exacerbate excitotoxicity by again stimulating glutamate, free radicals and NO (McLean & Ferriero, 2004).

1.1.6 Contribution of the cerebrovasculature to perinatal brain injury

The most devastating permanent injury that occurs in the developing fetus is GM-IVH. Although the incidence is greater in premature and low birth weight babies, term infants are more susceptible to breakdown of the BBB and impaired metabolism (Wigglesworth & Pape, 1978). Volpe (1989) suggests that consequences and subsequent neuropathology that originate from GM-IVH include destruction of the germinal matrix, periventricular haemorrhagic infarction (possibly of venous origin), PVL, hydrocephalus and pontine neuronal necrosis. Analysis of neonates with PVL suggest that this area of infarct contained poorly perfused vessels of an irregular capillary shape, suggesting a relationship between vascular supply to this region and the pathology of PVL (Takashima & Tanaka, 1978a). Figure 1.3 shows the main vascular supply to the germinal matrix and white matter.

Clinicians have long sought to understand the inherent vulnerability of the sub-ependymal germinal matrix to haemorrhage and periventricular white matter to necrosis. Observations of infarctions in these periventricular areas were seen to occur in watershed vascular or border "end zones" (areas where long and penetrating arteries end). These areas were deemed more vulnerable to poor perfusion and less capable of tolerating fluctuations of cerebral blood flow and cerebral venous pressure especially following hypoxia-ischemia and/or reperfusion (De Reuck, 1971; Takashima & Tanaka, 1978a, b; Wigglesworth & Pape, 1978; Volpe, 1989).

Ballabh (2010) also suggests that the germinal matrix may have an inherent fragility during development deeming it vulnerable to haemorrhage, which may be further exacerbated following hypoxia. Interestingly, Volpe (1989) also highlights that many thin walled cerebral blood vessels are the source of bleeding. This finding was also seen in the beagle puppy model

of germinal matrix haemorrhage (Trommer *et al.*, 1987; Ment *et al.*, 1991) but not in the rhesus monkey (Lenn & Whitmore, 1985). The observation of thin walled blood vessels could be indicative of structural immaturity or ongoing angiogenesis. However, Back and colleagues believe injury occurring in periventricular white matter is more likely due to cellular immaturity especially of oligodendrocyte progenitors than of vascular end zones (Back *et al.*, 2007; McClure *et al.*, 2008).
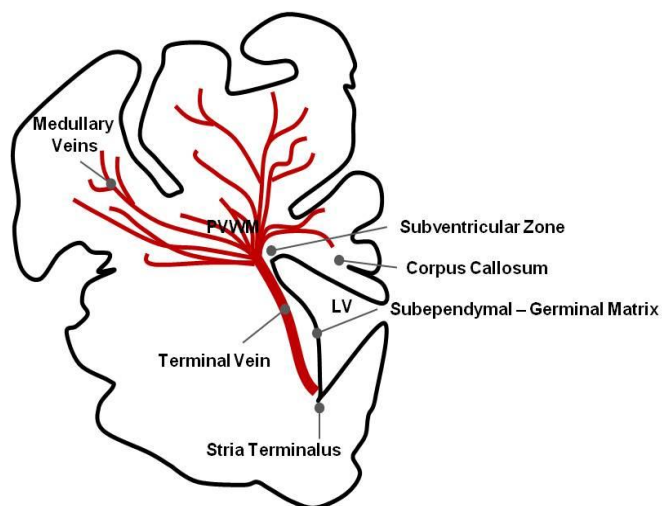
Figure 1.3: Coronal schematic of venous drainage of cerebral white matter. Medullary veins drain into the terminal vein that runs along the subependymal-germinal matrix. Adapted from (Volpe, 1998). A Licence Agreement from the publisher (Elsevier) for permission to adapt this figure has been attained.

The response of the cerebrovasculature following hypoxia-ischemia and how this may contribute to perinatal brain injury is not well investigated. The response of blood vessels including blood flow and the expression of proteins by the vasculature could influence the processes of excitotoxicity and oxidative stress which are already known to be closely inter-related. It is not known whether developmental vulnerability or the functionality of blood vessels are the underlying reasons for the pathogenesis of brain injury. However the prominent occurrence of injury such as haemorrhage and leukomalacia highlight that the response of the vasculature is pivotal. Understanding the development of the cerebrovasculature, important processes such as angiogenesis and BBB development and key mediators, could reveal reasons for regional vulnerability.

1.2 Fetal Cerebrovascular Development

1.2.1 Cerebrovascular development

Vascularisation occurs for the entire duration of gestation and well into the newborn period. For optimal development and function, the formation of blood vessels by vasculogenesis and angiogenesis is a tightly regulated process. In the human embryo, intra-cerebral blood vessels begin to appear from 7 weeks GA, this is when the basement membrane of the capillary network also forms (Korzhevskii & Otellin, 2000). The developing cerebrum contains cerebral arteries that originate from the peripheral system and branch within the cortex, and both a superficial and deep (Galenic) vein system (Wigglesworth & Pape, 1978). Early in development the formation of large blood vessels occurs by vasculogenesis, followed by angiogenesis where endothelial cells differentiate and proliferate into avascular tissue (See Section 1.1.2) (Yancopoulos *et al.*, 2000). Up to 35 weeks gestation, the process of neovascularisation is equivalent to white matter growth but more rapid than cortical expansion (Mito *et al.*, 1991).

The subependymal germinal matrix (also referred to as the area surrounding the lateral ventricle) is the source of neuroblasts from 10 – 20 weeks gestation, and of glioblasts in the third trimester (to become oligodendrocytes and astrocytes) (Wigglesworth & Pape, 1978; Volpe, 1989). Heubner's artery is a main blood vessel that provides nutrients to the germinal matrix (shown in Figure 1.4), while the matrix is also a terminal area for the medullary artery which extends into deep white matter (Takashima & Tanaka, 1978b; Wigglesworth & Pape, 1978; Volpe, 1989).

During gestation the matrix undergoes a decrease in size from 2.5 mm at 23 – 24 weeks when basal ganglia regions have a well developed circulation. By 36 weeks the germinal matrix is nearly involuted, at this time cortical regions are undergoing vascular development (Wigglesworth & Pape, 1978; Volpe, 1989). The progression of arterial development is shown in Figure 1.4. The time when the germinal matrix is undergoing change could reveal a window

of vulnerability. During development, the caudate and thalamus have a fine, circular capillary network in comparison to white matter and subependymal regions where vessels run perpendicular to the ventricle and have an elliptical shape (Takashima & Tanaka, 1978b).
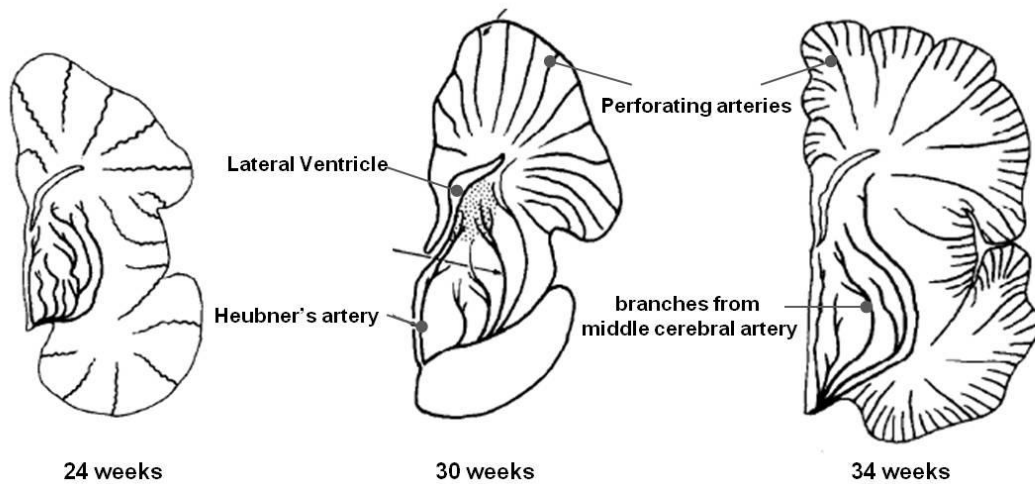
Figure 1.4: Arterial development in the human fetal brain. Figure shows the arterial development from the human fetal brain at 24 weeks (A), 30 weeks (B) and 34 weeks (C) gestational age. With increasing gestation, increasing branching of the arterial network also occurs. The Heubner artery is the main arterial supply to the lateral ventricle. From Wigglesworth and Pape (1978). A Licence Agreement from the publisher (Elsevier) for permission to reproduce this figure has been attained.

During development, blood vessels have a large diameter, irregular shape and are permeable to hydrophillic substances (Stonestreet *et al.*, 1996). As development continues vessels becomes thinner with a regular shape and endothelial tight junctions become more interconnected (Engelhardt, 2003). The vascular density of tissue is closely correlated with cerebral blood flow and metabolic demand (Miyawaki *et al.*, 1998). During normal development in the human fetal brain, as GA increases so does vascular density in the putamen, germinal matrix and cortex. There is some conflicting findings about the vascularisation of the white matter, Mito *et al.,* (1991) found no change of vascular density during gestation, but others suggest a smaller increase across gestation, and a lower blood vessel density compared to the above brain regions (Gould & Howard, 1988; Mito *et al.*, 1991; Miyawaki *et al.*, 1998; Ballabh *et al.*, 2004a).

1.2.2 Angiogenesis

Angiogenesis describes the sprouting of new vessels from pre-existing ones into avascular tissue (Yancopoulos *et al.*, 2000; Carmeliet, 2003). Vascular remodelling can occur when the existing vascular network is modified by pruning and vessel enlargement to form interconnecting branching (Yancopoulos *et al.*, 2000). Angiogenesis begins by basement membrane dissolution (which is facilitated by the presence of proteases such as matrix metalloproteinase (MMP). Mitogens (such as vascular endothelial growth factor (VEGF) are then activated to enhance endothelial cell migration and proliferation. Finally, tube and basement membrane formation occur triggering vessel maturation processes which involve the recruitment of pericytes by endothelial cells (Tomanek & Schatteman, 2000). See Figure 1.5.
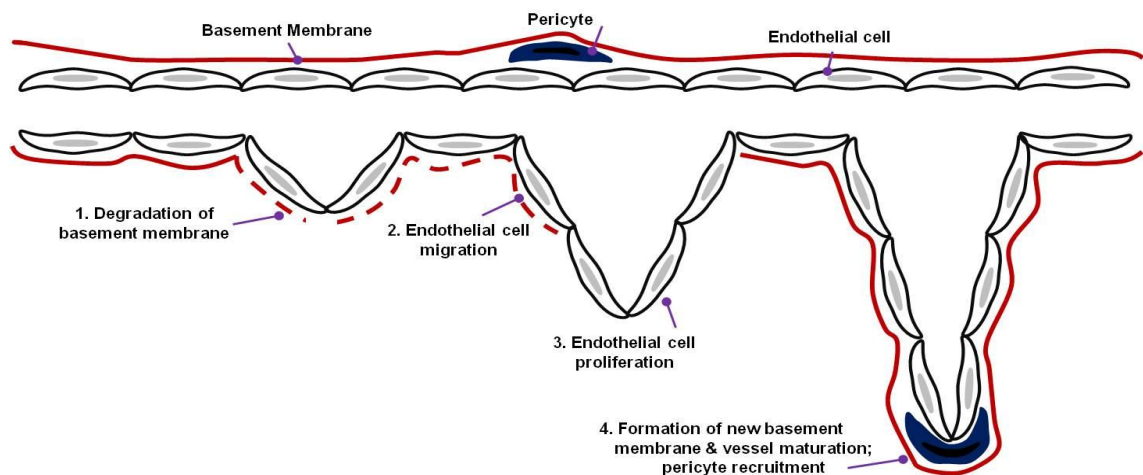
Figure 1.5: Angiogenesis. The process of angiogenesis occurs firstly by degradation of the basement membrane, followed by endothelial cells migration and proliferation. The formation of a new basement membrane and recruitment of pericytes occurs allowing vessel maturation Adapted from Tomanek & Schatteman (2000). A Licence Agreement from the publisher (John Wiley and Sons) for permission to adapt this figure has been attained.

Initiation of angiogenesis occurs by the extensive interplay between a variety of cells and numerous growth factors. These include fibroblast growth factor (FGF; both acidic and basic), VEGF, platelet derived growth factor (PDGF), transforming growth factor (TGF) and the angiopoietins (angpt) (Tomanek & Schatteman, 2000). *In vitro* models have provided further

understanding of the importance of neurovascular structures during cerebrovascular and BBB development. Astrocytes induce endothelial cell and pericyte differentiation, but pericytes appear to migrate and cover capillary like structures faster than astrocytes (Ramsauer *et al.*, 2002). Interestingly, hypoxia is also a key regulator of angiogenesis and effects the expression of key angiogenic proteins (See Section 1.3).

1.2.2.1 Vascular endothelial growth factor and receptors

VEGF is a key regulator of vasculogenesis and angiogenesis (Breier *et al.*, 1992; Breier & Risau, 1996). Being a potent, secreted angiogenic mitogen, VEGF was first described as vascular permeability factor (VPF), and is closely related to PDGF (Keck *et al.*, 1989; Leung *et al.*, 1989). During angiogenesis, endothelial cells that express VEGF produce plasminogen activators and MMPs to initiate extracellular matrix degradation (the first step in angiogenesis, Figure 1.5 (1)). Subsequently, VEGF is also important in stimulating the proliferation of endothelial cells (Breier *et al.*, 1992).

VEGF has six homologous family members - VEGF-A, placental growth factor (PIGF), VEGF-B, VEGF-C, VEGF-D and VEGF-E. Three high-affinity tyrosine kinase receptors also exist - VEGFR-1 (Flt-1), VEGFR-2 (fetal liver kinase (Flk-1) in the mouse/ kinase insert domain receptor (KDR) in the human) and VEGFR-3 (Flt-4) (Breier, 2000). VEGF-A is the most active, involved in blood vessel growth, endothelial cell mitogenesis, vasodilatation (via NO dependant pathways) and vascular permeability (Leung *et al.*, 1989; Breier *et al.*, 1992; Breier, 2000). VEGF and VEGFR-2 activation is important for promoting neuronal growth, migration, maturation, survival as well as axonal and dendritic outgrowth (Hermann & Zechariah, 2009; Sentilhes *et al.*, 2010). Figure 1.6 summaries the actions of both VEGF family members and associated receptors. There are also four VEGF isoforms; 121, 165, 189 and 206 (Dvorak *et al.*, 1995).
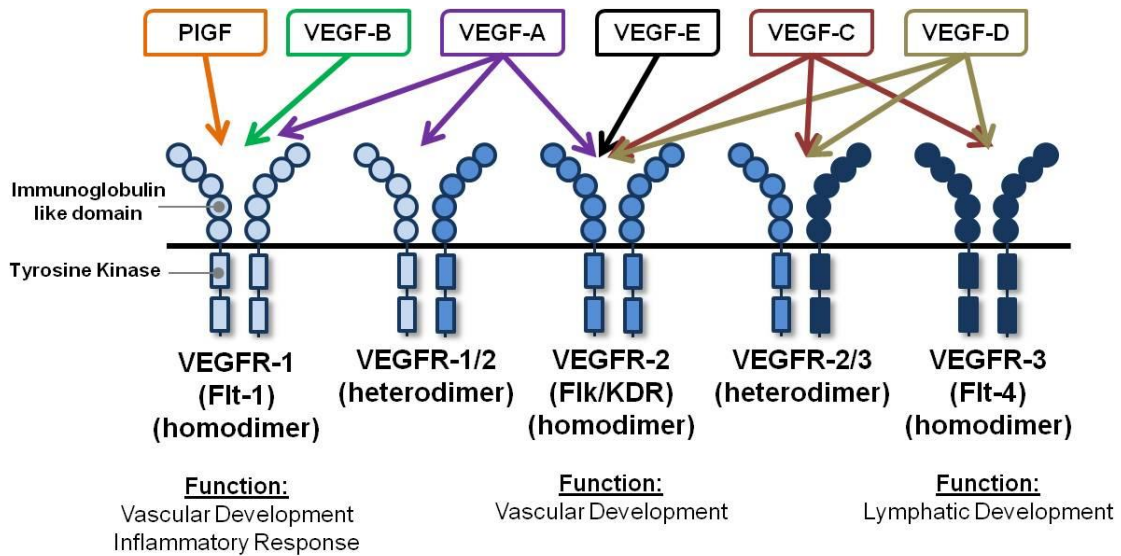
Figure 1.6: Schematic representation of VEGF/VEGF receptor system. The specific binding of the VEGF isoforms (A, B, C, D, E and placental growth factor (PIGF) and their associated tyrosine kinase receptors (VEGFR-1, -2, -3) (Breier, 2000; Dimberg *et al.*, 2009).

VEGF has been implicated in embryogenesis and normal development of organs as well as tumour growth. During embryogenesis, the formation of new blood vessels is guided by the actions of VEGF. VEGF is expressed by the embryonic neuroectoderm, the epithelium of the stem cell and progenitor region of the brain (i.e., ventricular zone). All of these are important for vascularisation and brain development, while VEGF receptors are expressed mainly on endothelial cells (Breier *et al.*, 1992; Carmeliet & Storkebaum, 2002).

During development it is predominantly VEGF-A, through binding with VEGFR-2, that is responsible for both vascular and neuronal development (Carmeliet, 2003). It is suggested that during development VEGFR-1 may act as a decoy receptor, but this isoform becomes functionally important following hypoxia, in the adult rodent at least (Marti & Risau, 1998). VEGF-B and VEGF-C isoforms are present in the brain early in embryonic life (Lagercrantz *et al.*, 1998), but in the adult brain VEGF-B appears to have greater expression in neurons (Boer *et al.*, 2008). Importantly, VEGF-C through the binding with VEGFR-3 has recently been shown to be important in mice from E15.5 to E18.5, by stimulating growth of progenitor cells, such as oligodendrocyte progenitors in the optic nerve (Le Bras *et al.*, 2006). While several VEGF

isoforms are clearly important during development, this thesis focused on the expression of VEGF-A in the late gestation fetal sheep brain as it is the most characterized isoform, important for vascular development and responses to hypoxia.

In the developing brain, the temporal and spatial expression of VEGF is correlated closely with vascularisation and endothelial cell growth (Breier *et al.*, 1992). In studies from the human fetus and postnatal rat, it was found that VEGF protein is expressed by many cell types including neuroblasts, neuroepithelial, radial glia, pericytes, neuronal and endothelial cells (Virgintino *et al.*, 2003; Rosenstein & Krum, 2004; Sentilhes *et al.*, 2010). Early in development neurons express VEGF, possibly a signal that initiates angiogenesis and also coincides with increasing neuronal metabolism. Increased glial VEGF expression occurs as stabilisation of the cerebrovasculature is reached, when glial end-feet ensheath blood vessels (Ogunshola *et al.*, 2000).

From 9 weeks gestation, VEGF is strongly expressed in the developing human telencephalon (Virgintino *et al.*, 2003). From 14 to 34 weeks there is strong expression of VEGF and VEGFR-2 by neurons, glia and blood vessels throughout the brain and cerebellum. During 21 − 34 weeks VEGF is also strongly expressed in the cortex and white matter (Arai *et al.*, 1998). By 34 weeks, neurons, astrocytes and endothelial cells weakly express VEGF which is thought to correspond with a functioning blood brain barrier (BBB) (Sentilhes *et al.*, 2010). Figure 1.7 summaries the numerous suggested physiological actions of VEGF.
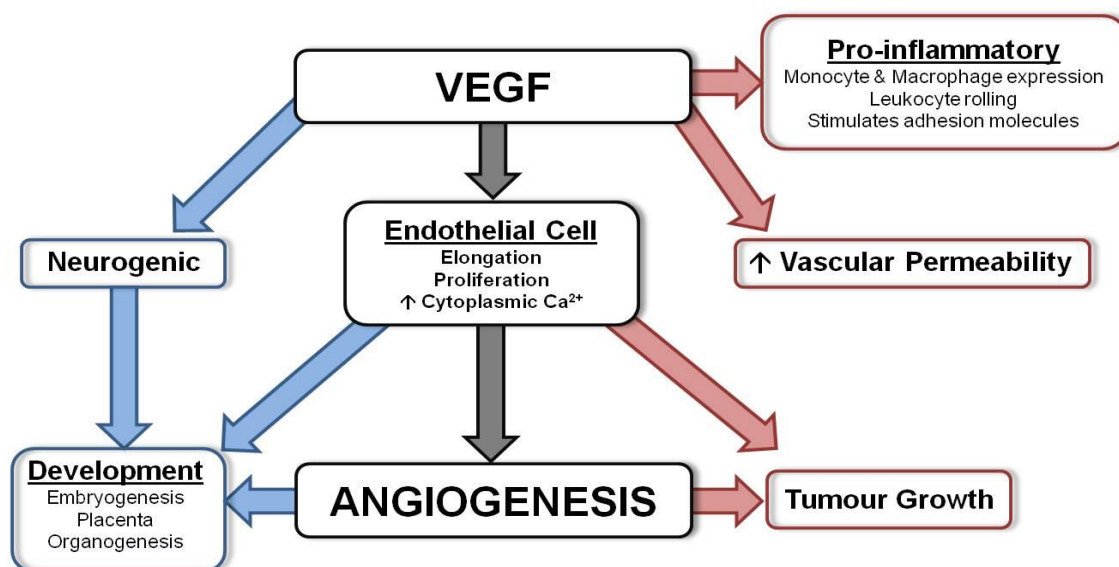
Figure 1.7: Diagram summarising the actions of VEGF. VEGF is involved in numerous important physiological processes. Angiogenesis is the main function of VEGF, however it also has protective actions (shown in blue) which include neurogenesis and involvement during development, and detrimental actions (shown in red) including being a pro-inflammatory mediator, vascular permeability factor and involved in tumour growth.

1.2.2.2 Angiopoietins

Working in close conjunction with VEGF are angpt and their ligand receptor Tie (-1 and -2), part of the tyrosine receptor kinases. There are four members of the angpt family, although angpt-1 and angpt-2 are the most understood (Yancopoulos *et al.*, 2000; Carmeliet, 2003; Otrock *et al.*, 2007; Hansen *et al.*, 2008). Their actions are mediated by binding to Tie-2 receptors on endothelial cells in a concentration dependant manner (Mustonen & Alitalo, 1995; Bogdanovic *et al.*, 2006). From studies in tumour growth the significance of angpt-1 and angpt-2 have been elucidated.

Angpt-1 is important for stimulating vessel growth, branching, maintenance and stabilisation, and is expressed by endothelial cells, astrocytes and pericytes (Yancopoulos *et al.*, 2000; Carmeliet, 2003; Kim *et al.*, 2008). Angpt-1 knockout mice develop a normal vasculature however they are incapable of adequate vascular remodelling. Whereas, over-expression leads to a functional vasculature that is resistant to being permeable (Suri *et al.*, 1996; Thurston *et al.*,

1999; Yancopoulos *et al.*, 2000), highlighting that angpt-1 is important for inhibiting vascular permeability.

Angpt-1 also exhibits anti-inflammatory effects, particularly inflammatory mediated vascular leakage and more recently has been shown to inhibit neuronal apoptosis (Thurston *et al.*, 1999; Thurston *et al.*, 2000; Valable *et al.*, 2003; Hansen *et al.*, 2008). Increased expression of angpt-1 promotes the "tightening" of vessels by increasing expression of tight junctional proteins and thereby resulting in decreased permeability with vessels that are resistant to plasma leakage (Thurston *et al.*, 1999; Thurston *et al.*, 2000; Valable *et al.*, 2005). Increased expression is also implicated in promoting endothelial cell survival, migration and enhancing the interaction between endothelial cells and neighbouring cells such as the recruitment of pericytes (Suri *et al.*, 1996).

Angpt-2, important in initiating vascular remodelling, has both agonistic and antagonistic actions to angpt-1 when binding to Tie-2. The presence or absence of VEGF may dictate the function of angpt-2, whether vessel remodelling or destabilisation and subsequent vessel regression occur (Maisonpierre *et al.*, 1997; Beck *et al.*, 2000; Yancopoulos *et al.*, 2000; Gale *et al.*, 2002). Over-expression of angpt-2 can also lead to vascular discontinuity, embryonic death and pathology similar to angpt-1 knockout mice and an inability for vascular remodelling (Maisonpierre *et al.*, 1997). In the adult mouse brain the presence of angpt-2 and VEGF resulted in increased microvascular density, increased MMP-9 and a decrease in zona-occludin expression, leading to increased permeability (Zhu *et al.*, 2005). However high angpt-2 expression in the absence of VEGF can result in vessel regression, seen to occur following hypoxia and in tumour growth (Holash *et al.*, 1999; Beck *et al.*, 2000). Expressed mostly by endothelial cells, angpt-2 has been seen to degrade the extracellular matrix and disrupt junctions between endothelial cells in tumour vessels (Gale *et al.*, 2002; Carmeliet, 2003).

1.2.3 The blood-brain barrier

The cerebral microvascular system has two functional and anatomical barriers to protect surrounding tissue; the BBB and the basement membrane (Scholler *et al.*, 2007; Burk *et al.*, 2008). The three major functions of the mature BBB include protection of the brain from the chemical environment of blood, selective transport of substances into and out of the brain, and metabolism of blood and brain substances (Risau & Wolburg, 1990). The structure of the BBB is composed of capillary endothelial cells, tight junctions, astrocytes, pericytes, and the basement membrane (detailed below; Figure 1.8).

The maturity of the BBB and corresponding permeability characteristics are a consequence of changes in endothelial cell morphology and function (Risau & Wolburg, 1990). However, there is some argument over the correlating maturation and permeability of the BBB. Permeability to large molecules is consistently restricted in both the fetus and adult, although smaller molecules can enter the younger, fetal brain more readily (Keep *et al.*, 1995; Engelhardt, 2003). BBB development has been investigated in rats and results indicate that invasion of blood vessels is associated with neurogenesis and development of tight junctions which occur prior to astrocyte end-feet development (Stewart & Hayakawa, 1994; Ballabh *et al.*, 2004b; Kaur & Ling, 2008). In fetal sheep, BBB permeability to small molecules was greatest earlier in gestation (0.6), and decreased as GA increased, with regional heterogeneity observed that was consistent with that seen in the adult brain (Stonestreet *et al.*, 1996).

1.2.3.1 Endothelial cells

Endothelial cells are thin and elongated interacting readily with the extracellular matrix and have the capability of sensing change in blood flow and pressure (Carmeliet, 2003) (Figure 1.8). The high density of mitochondria and a high capacity for sodium/potassium pumps are key characteristics of endothelial cells (Bradbury, 1984). During development, the differentiation of endothelial cells is important for the maturation of the BBB. Endothelial cell proliferation and

growth is strongly influenced by VEGF, which is highly expressed in these cells in the developing brain (Breier *et al.*, 1992).
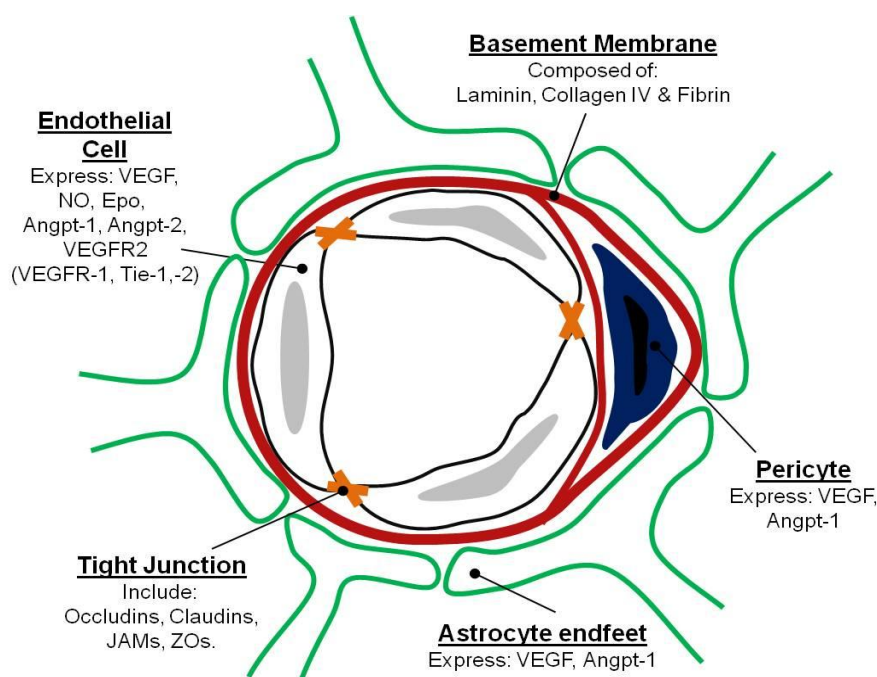
Figure 1.8: Schematic diagram of a coronal cross section of the neurovascular unit. Tight junctions form between endothelial cells. Separating endothelial cells and astrocyte end-feet is the basement membrane. Pericytes are also enclosed by the basement membrane. Adapted from Balabanov and Dore-Duffy (1998) and Kaur & Ling (2008). A Licence Agreement from the publisher (John Wiley and Sons and Bentham Science) for permission to adapt this figure has been attained.

1.2.3.2 Tight junctions and adheren junctions

A tight junctional complex exists within the BBB between endothelial cells (Figure 1.8 and 1.9). They provide an important structural component that impedes the diffusion of molecules from the blood vessel lumen across the brain parenchyma and are composed of cytoplasmic and transmembrane proteins (Ballabh *et al.*, 2004b; Ballabh *et al.*, 2005; Kaur & Ling, 2008). Adheren junctions are located near endothelial cells and form a continuous barrier holding neighbouring cells together. They are composed with cadherin-catenins complex and their associated proteins (Schulze & Firth, 1993).

Ballabh *et al.,* (2005) have closely studied the expression of tight junctional molecules claudin-1, -5, occludin and JAM-1, -2 and -3 in the germinal matrix, cerebral cortex and white matter of 16 – 40 week old babies. Their findings suggest that key tight junctional proteins may develop and mature early, their observations are detailed below. Important in controlling paracellular permeability, disruptions of tight junctions can occur following pathological conditions such as hypoxia-ischemia.
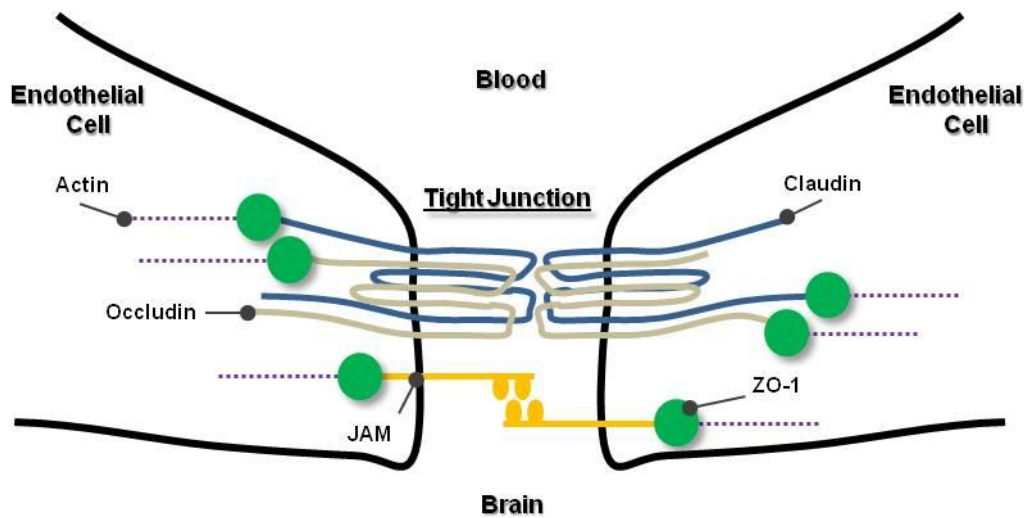
Figure 1.9: Schematic diagram of tight junctional complex between endothelial cells. Key components of the tight junction include claudin (blue), occludin (grey), zona-occludin-1 (ZO-1; green) junctional adhesion molecules (JAM; yellow) and actin (purple).

Claudins

The claudin family consists of 24 members that bind to each other on adjacent endothelial cells to form a primary seal of tight junctions (Figure 1.9) (Furuse *et al.*, 1999). Claudin-1 and claudin-5 are highly expressed in cerebral capillaries (Furuse *et al.*, 1999). Claudin-5 is expressed as early at 12 weeks gestation in the telencephalon of the human fetus (Virgintino *et al.*, 2004), and only claudin-5 (not claudin-1) is consistently expressed from 16 – 40 weeks gestation in the developing human brain (Ballabh *et al.*, 2005).

Occludins

Occludins are highly expressed by brain capillary endothelial cells, and their presence is related to increased electrical resistance across the barrier. Occludins appear to be able to alter paracellular permeability with increased expression being indicative of greater barrier properties (Furuse *et al.*, 1993; Hirase *et al.*, 1997). Occludin is expressed as early as 12 weeks gestation in the developing human brain with no change in expression for the duration of pregnancy (Virgintino *et al.*, 2004; Ballabh *et al.*, 2005).

Junctional adhesion molecules and Cytoplasmic accessory proteins

Junctional adhesion molecules (JAM) are important for tight junctional integrity and permeability (Martin-Padura *et al.*, 1998). Three JAM proteins exists; JAM-1, JAM-2 and JAM-3, although JAM-2 has not been seen to be expressed in cerebral blood vessels to date (Aurrand-Lions *et al.*, 2001). Ballabh *et al.,* (2005) found JAM-1, but not JAM-2 or JAM-3, was expressed from 16 weeks, with no change of expression across gestation. The most abundant cytoplasmic accessory group of proteins are the zona occludins (ZO), important for the structural support of tight junctions (Stevenson *et al.*, 1986).

1.2.3.3 Astrocytes

Astrocyte end-feet that ensheath blood vessels in the brain (Figure 1.8) are in close proximity to endothelial cell plasma membrane and are separated by the basement membrane (Risau & Wolburg, 1990; Risau, 1991; Bernstein & Karp, 1995; El-Khoury *et al.*, 2006). This "glial sheath" that surrounds cerebral blood vessels is thought to be important for vascular structure and function and can express tight junctional proteins (Bradbury, 1984; Willis *et al.*, 2004). Perivascular astrocytes have the important function of enhancing the development of endothelial tight junctions (Janzer & Raff, 1987; Brightman, 1991; Nagy & Martinez, 1991). Regions that have a discontinuous ensheathment of astrocytes also show a disintegrated basement membrane *in vitro* (Wolff *et al.*, 1974). An absence of the endothelial cell-astrocyte interaction, seen in the

hypothalamus and brainstem, produces areas that are highly permeable with an opening of tight junctions (Coomber & Stewart, 1984; Goldstein, 1988; Hamm *et al.*, 2004).

El-Khoury and colleagues (2006) investigated astrocyte end-feet coverage in the germinal matrix, white matter and cortex of human fetuses from 16 – 40 weeks gestation using glial fibrillary acidic protein (GFAP; cytoskeleton protein forming the intermediate filament), S-100β (cytosolic calcium binding protein) and aquaporin-4 (AQP4; water channel protein). Most remarkably they found that in the germinal matrix, a region vulnerable to haemorrhage; only few end-feet and processes were labelled (with GFAP or S-100β) but this increased across gestation. The cortex and white matter showed strong perivascular coverage from 16 weeks gestation.

1.2.3.4 Pericytes

Pericytes are cells that wrap around endothelial cells (Figure 1.8) and provide structural support, stability and integrity to the vessel wall (Ballabh *et al.*, 2004b; Nakagawa *et al.*, 2007; Kaur & Ling, 2008). Important in vasculogenesis, pericytes are recruited by endothelial cells and involved in the processes of blood vessel and BBB development (Balabanov & Dore-Duffy, 1998). Pericytes and endothelial cells communicate via gap junctions and their interaction is important for maintenance and maturation of the vasculature and contractile function to aid in modulating cerebral blood flow (Cuevas *et al.*, 1984). Pericytes that are in close association with endothelial cells are also more resistant to apoptosis (Ramsauer *et al.*, 2002). For detailed reviews on pericytes see (Hirschi & D'Amore, 1996; Balabanov & Dore-Duffy, 1998; Bergers & Song, 2005; Dore-Duffy, 2008).

The pluripotency of perciytes make them quite a mystery, as they exhibit multipotential stem cell activity, phagocytic activity and even express macrophage markers (Balabanov *et al.*, 1996; Dore-Duffy *et al.*, 2006). Pericytes may also be involved in autoregulatory processes as they express receptors and are modulated by catecholamines, endothelin-1 and vasopressin (van

Zwieten *et al.*, 1988; Elfont *et al.*, 1989; Dehouck *et al.*, 1997; Balabanov & Dore-Duffy, 1998; Ballabh *et al.*, 2004b). Pericytes and their modulation of capillary diameter is reviewed by Hamilton *et al.,* (2010) and is further detailed in Section 1.4.2.1.

Pericytes are present in the cerebrovasculature from as early at 10 weeks gestation, however in comparison to the cortex and white matter the germinal matrix has fewer pericytes present during gestation (Povlishock *et al.*, 1977; Braun *et al.*, 2007). Importantly, decreased pericyte expression could help explain the regional vulnerability of the germinal matrix to haemorrhage, particularly in pre-term neonates. Al Ahmad and colleagues (2010) set up an *in vitro* model to reproduce the interaction of cell types during BBB development. They found, consistent with *in vivo* studies, pericytes play an important role in the development and maintenance of the BBB. Hori *et al.,* (2004) also suggest that *in vitro* pericyte expression of angpt-1 in important for maintaining BBB integrity via increased expression of occludin.

1.2.3.5 Basement membrane

The basement membrane (also commonly referred to as the basal lamina) exists between endothelial cells and astrocytes (del Zoppo & Mabuchi, 2003). Functionally, it is important in protecting the brain from extravasation of protein rich fluids and blood components into the parenchyma (Hamann *et al.*, 1996; Scholler *et al.*, 2007). The basement membrane is composed of collagens, non-collagen glycoproteins (including laminin, fibrinogen), glycosamineglycans and proteoglycans (heparin sulphate). A direct consequence of the binding of collagen IV and laminin is the tissue support it provides the basement membrane (Charonis *et al.*, 1985; Yurchenco & Schittny, 1990; Hamann *et al.*, 1995; Lukes *et al.*, 1999; Jakobsson *et al.*, 2008). Ment *et al.,* (1991) suggested that basement membrane proteins (laminin and collagen IV) are important in providing structural integrity to blood vessels, particularly in the germinal matrix (subventricular zone) to prevent rupture. Changes in expression are also seen to occur following ischemia (Section 1.3.2).

Laminin

Laminin is a non-colleganous constituent of the basement membrane and during development is an indicator of vascular maturation (Timpl *et al.*, 1979; Risau & Lemmon, 1988). It separates endothelial cells from other brain cells and is made up of a family of heterotrimeric glycoprotein, containing one of 5α, 3β or 3γ chains, with α-chains being highly bioactive and important in vascular development (Veltkamp *et al.*, 2006; Jakobsson *et al.*, 2008). Normally laminin expression is confined to the basement membrane; however during development laminin expression is induced by endothelial cells and precursors of neurons and glia and in response to injury by reactive astrocytes (Liesi *et al.*, 1984; Liesi, 1985; Wagner *et al.*, 1997). Maturation of blood vessels is also associated with an up-regulation of laminin signalling and expression during angiogenesis (Risau & Lemmon, 1988; Milner & Campbell, 2002). Xu *et al.,* (2008) measured laminin α1, α4 and α5 isoforms in germinal matrix, gray and white matter of both human tissue and rabbit pups and found regional, developmental regulation of expression for each isoforms (germinal matrix greater expression for α1).

Collagen IV

Collagen IV is derived from a triple helical molecule, [α1(IV), $_2$α2(IV)] and is present at similar levels to laminin (Sanes *et al.*, 1990; Yurchenco & Schittny, 1990; Ment *et al.*, 1991). Collagen IV plays a fundamental role in the maintenance of integrity and function particularly when there is increased metabolic demand (Poschl *et al.*, 2004). Studies from knockout mice suggest collagen IV does not appear to be important until embryonic day 10, while other studies indicate it is important earlier in development, possibly influencing neurite outgrowth (Laurie *et al.*, 1980; Poschl *et al.*, 2004).

Fibronectin

Fibronectins are a family of glycoproteins that are another important constituent of the basement membrane and promote endothelial cell adhesion, migration and organisation of the

cytoskeleton (Wang & Milner, 2006). Integrins are extracellular matrix receptors, α5β1 (important postnatally) and αvβ3 are important during angiogenesis and in fibronectin signalling (Wang & Milner, 2006). Fibronectin is expressed highly during developmental angiogenesis and is essential during embryogenesis (George *et al.*, 1993).

1.2.3.6 Blood-brain barrier transport

Glucose transporter-1 (GLUT-1)

Glucose transporter (Glut)-1 is one of the earliest markers of a functionally competent BBB, expressed once blood vessels begin sprouting, and is strongly expressed in endothelial cells with low expression seen in pericytes (Virgintino *et al.*, 1998; Virgintino *et al.*, 2000; Engelhardt, 2003). Glucose transport is mediated by a family of glucose transporter proteins (Glut) 1 – 7. In the brain, Glut-1 and Glut-3 mediate glucose transport (Pardridge *et al.*, 1990; Pessin & Bell, 1992; Maher *et al.*, 1993). Early in human fetal development, between 12 to 18 weeks of gestation, Glut-1 expression increases (Virgintino *et al.*, 1998). Dermietzel *et al.,*(1992) also suggests as the BBB matures, endothelial Glut-1 expression decreases and non-vascular Glut-1 and Glut-3 (neuronal) increase expression to allow for adequate glucose utilisation, as seen in the postnatal rat (Vannucci *et al.*, 1994).

1.3 CONSEQUENCE OF HYPOXIA ON THE CEREBROVASCULATURE

During development any perturbations, such as hypoxia, can significantly alter the expression of key angiogenic genes and could result in an inadequately functioning vasculature. This can contribute to the pathogenesis of brain injury, however the response could also be neuroprotective. The consequence of hypoxia on the cerebrovasculature in the developing fetus has not been widely investigated. Much of what we know is from adult rodent studies and is detailed below.

1.3.1 Hypoxia induced angiogenesis

In the adult, hypoxia induced angiogenesis occurs in an attempt to increase vascularisation to increase oxygen supply to deprived tissue (Shweiki *et al.*, 1993). This process occurs in tumour growth (Kim *et al.*, 1993; Breier & Risau, 1996; Banerjee *et al.*, 1997; Breier, 2000) as well as during wound healing (Bates & Jones, 2003; Otrock *et al.*, 2007), diabetic retinopathy (Boulton *et al.*, 1998; Aiello, 2005) and following stroke (Krupinski *et al.*, 1994; Zhang *et al.*, 2000; del Zoppo & Mabuchi, 2003). Neovascularisation and vascular remodelling is a tightly regulated process and in the brain, there is a complex interplay of multiple genes (hypoxia inducible factor-1 (HIF-1α), VEGF and erythropoietin (Epo) expressed by different cell types (Marti *et al.*, 2000b). Following stroke, regions of high angiogenesis have also been correlated with increased neuronal survival (Krupinski *et al.*, 1994). Although hypoxic induced angiogenesis is thought to be a protective response, in many cases, there are associated detrimental effects that can occur (such as alterations in BBB permeability, discussed in 1.3.3). Widely investigated in the adult, the consequence of this occurring in the neonatal brain and whether it could explain possible regional protection or vulnerability are yet to be determined.

1.3.1.1 Hypoxia inducible factors

In response to hypoxia, HIF-1, a key regulator of oxygen homeostasis is transcriptionally activated to improve oxygen availability (Semenza, 2009b). Increased HIF-1α also contributes to increased expression of angiogenic genes including; VEGF, angpt-2, PDGF-B and placental growth factor (Fan *et al.*, 2009; Semenza, 2009b). Composed of α and β subunits, once in the nucleus, HIF-1α dimerises HIF-1β and binds to target genes (including Epo and VEGF) at the hypoxia response element (Semenza, 2009b). Three alpha isoforms exist; HIF-1α, HIF-2α, HIF-3α although less is known about the actions of the latter 2. HIF-1α is expressed in many cell types throughout the body whereas expression of HIF-2α is restricted to vascular endothelial cells (Wiener *et al.*, 1996; Semenza, 2009b; Skuli *et al.*, 2009).

During embryonic and brain development physiological hypoxia stimulates vasculogenesis and angiogenesis, this is mediated by HIF (Trollmann & Gassmann, 2009). HIF-1α knockout mice exhibit an open neural tube, impaired erythropoiesus and are embryonic lethal by embryonic day 8.5 (Iyer *et al.*, 1998; Semenza, 2009a)   HIF-2α endothelial deletion shows normal development but increased vascular permeability, and decreased angpt-2 expression and angiogenesis (Skuli *et al.*, 2009). It is therefore suggested that in endothelial cells, HIF-1α may be important for proliferation, metabolism and survival, HIF-2α could trigger cell migration, adhesion and vascular integrity (Skuli & Simon, 2009), summarised is Figure 1.10.

Following hypoxia in the neonatal brain, HIF-1α predominantly accumulates in neurons first as they are oxygen sensing cells and most sensitive to fluctuations in oxygen. This can result in apoptotic and/or necrotic neuronal death, but sustained high expression of HIF-1α in neurons has been shown to be protective and anti-apoptotic (Fan *et al.*, 2009; Trollmann & Gassmann, 2009). Inhibiting HIF-1α soon after hypoxia-ischemia has been shown to decrease infarct size, attenuate BBB permeability changes and neuronal death in neonatal rats (Chen *et al.*, 2008).
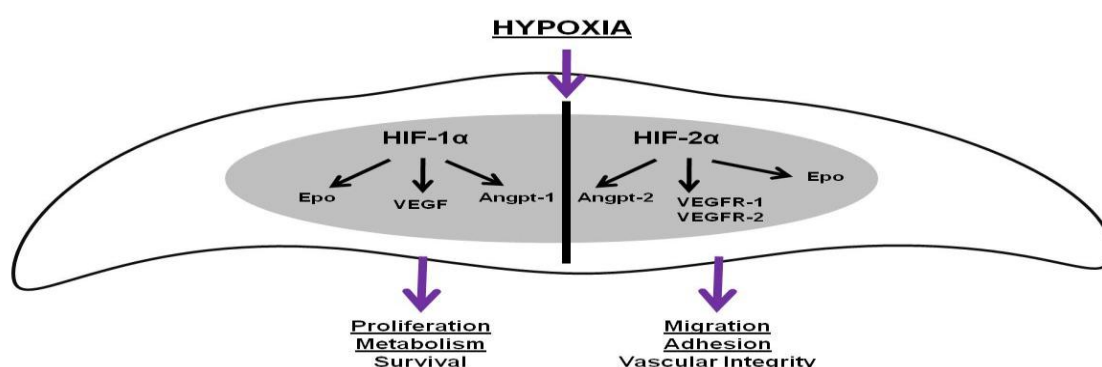
Figure 1.10: Schematic diagram of endothelial cell responses to hypoxia. Suggested responses of HIF-1α and HIF-2α in endothelial cells from studies in the lung, heart and brain. Adapted from Skuli *et al.,* (2009), Skuli and Simon (2009).

1.3.1.2 Implications of VEGF

The response of VEGF following hypoxia and/or hypoxia-ischemia has been widely studied in the adult (Cobbs *et al.*, 1998; Lennmyr *et al.*, 1998; Plate *et al.*, 1999; Marti *et al.*, 2000b;

Zhang *et al.*, 2000; Zhang *et al.*, 2002b; Sun *et al.*, 2003) and to a lesser extent in the developing fetus (Arai *et al.*, 1998; Mu *et al.*, 2003; Kaur *et al.*, 2006a; Aly *et al.*, 2009). As previously described, a potent stimulator and key transcriptional regulator of VEGF expression is HIF-1α (Forsythe *et al.*, 1996; Marti & Risau, 1998). However, it was recently observed that following hypoxia astrocytic expression of VEGF is not entirely HIF-1α dependant (Schmid-Brunclik *et al.*, 2008). Up-regulation of VEGF following hypoxia has also been seen to be mediated by peroxisome-proliferator-activated receptor-gamma coactivator-1alpha (PGC-1α), and this is independent of HIF-1α (Arany *et al.*, 2008). Hypoxia induced VEGF expression in the brain can have both neuroprotective and neurotoxic actions (Figure 1.11; this has been reviewed by several authors (Carmeliet & Storkebaum, 2002; Skold & Kanje, 2008; Hermann & Zechariah, 2009) and is briefly summarised below.

Neurotoxic actions of VEGF

Increased circulating serum VEGF from umbilical cord blood of infants who had experienced birth asphyxia was strongly correlated with hypoxic-ischemic encephalopathy and lower Apgar scores (Aly *et al.*, 2009). Arai *et al.,* (1998) also found increased astrocytic and endothelial expression of VEGF in the foci of necrosis in infants who suffered PVL. From postnatal rat studies of either hypobaric (chronic or acute) hypoxia or middle cerebral artery occlusion (MCAO), increased VEGF expression was seen as quickly at 3 hours following the insult to being sustained for up to 7 days (Ment *et al.*, 1997; Ogunshola *et al.*, 2000; Mu *et al.*, 2003; Kaur *et al.*, 2006a). Following hypobaric hypoxia, high VEGF expression is seen with high eNOS, iNOS and, nNOS expression suggesting vasodilation and possibly excitotoxicity (Kaur & Ling, 2009). Astrocytic and neuronal expression of VEGF is high following hypoxia when compared to normoxic controls, high neuronal VEGF expression following hypoxia is also seen in the adult (Marti & Risau, 1998; Ogunshola *et al.*, 2000).

The most profound consequence of increased VEGF expression is the increased permeability that leads to the leakage of harmful substances into the brain parenchyma and possible

vasogenic oedema (Schoch *et al.*, 2002; Kaur *et al.*, 2006b). In adult models of global hypoxia, focal cerebral ischemia and brain trauma, increased BBB leakage was associated with acute up-regulation of VEGF (Nag *et al.*, 1997; Zhang *et al.*, 2000; Schoch *et al.*, 2002; Zhang *et al.*, 2002b; Kaur *et al.*, 2006b). Astrocytic expression of VEGF is suggested to contribute to BBB leakage (Schmid-Brunclik *et al.*, 2008). This is discussed in further detail in Sections 1.3.3 and Figure 1.12.

Intravenous administration of VEGF in the newborn mouse has also shown to open the BBB within 2 h (Young *et al.*, 2004). VEGF has a direct action on endothelial cells and pericytes, where by pericytes have been implicated in exacerbating disruption of the BBB (Hippenstiel *et al.*, 1998; Yamagishi *et al.*, 1999; Al Ahmad *et al.*, 2009; Thanabalasundaram *et al.*, 2010). Following hypoxia pericytes are the first cells to respond by migrating and producing factors such as VEGF which are thought to contribute to vascular instability (Gonul *et al.*, 2002; Al Ahmad *et al.*, 2009; Thanabalasundaram *et al.*, 2010) The involvement of VEGF and tight junctions, ZO-1 and occludin has been investigated *in vitro*. In brain microvascular endothelial cells, disruption and disassembly of tight junction proteins occluding and ZO-1, and regulation of occludin is VEGF mediated (Wang *et al.*, 2001). Fischer *et al.,* (2002) also found that VEGF mediates changes in ZO-1 expression following hypoxia.

Neuroprotective actions of VEGF

Hypoxia induced angiogenesis occurs in an attempt to increase vascularisation, to increase cerebral blood flow and oxygenation in ischemic tissue. VEGF can increase the survival of endothelial cells as well as stimulate and sustain neurogenesis and inhibit apoptosis (Gora-Kupilas & Josko, 2005). Schmid-Brunclik and colleagues (2008) also found that following hypoxia VEGF contributes to astrocyte proliferation and survival.

Experimental studies from the adult brain suggest that the 'early' up-regulation (between 1 - 3 h post-MCAO) of VEGF could be associated with alterations in BBB permeability and contribute

to exacerbating injury. The neuroprotective actions of VEGF including neovascularisation and neuronal protection are more likely to occur in the days (after 48 h) following hypoxia (MCAO), when both VEGF and VEGFR-2 have been shown to be up-regulated (Marti *et al.*, 2000b). Most interestingly it is studies that use VEGF treatment that show the best neuroprotective outcome. In both neonatal and adult models following hypoxia, intracerebroventricularly injection of VEGF resulted in reduced gross brain injury, subsequently alleviating the decrease in brain weight (i.e. decreased infarct volume), decreased apoptotic cells without increasing BBB permeability. Both studies suggest this is related to the activation of the Akt/ERK pathway (Kaya *et al.*, 2005; Feng *et al.*, 2008).
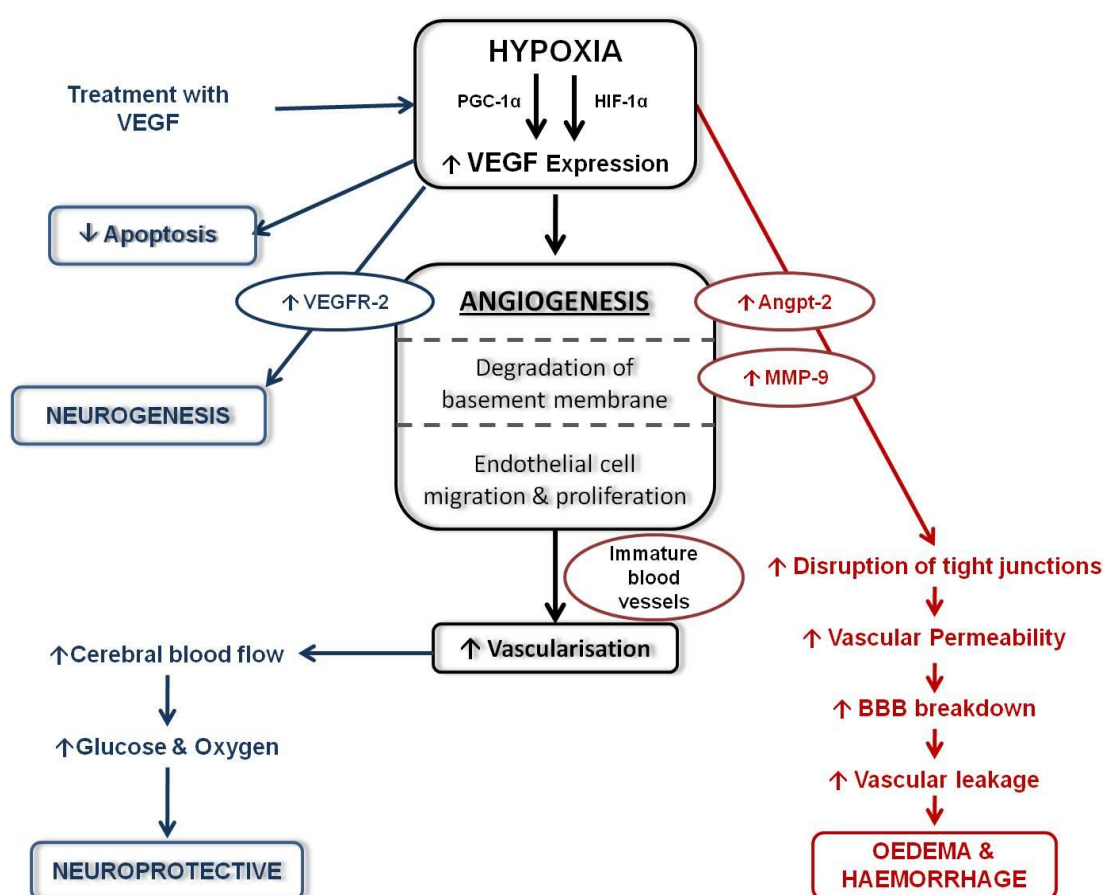
Figure 1.11: Schematic diagram of the effects of VEGF following hypoxia. Following hypoxia, increased VEGF expression stimulated angiogenesis leading to increase vascularisation. Increased VEGF expression can have detrimental effects (shown in red) which can lead to oedema and haemorrhage formation. Beneficial effects of increased VEGF (shown in blue) help stimulate neurogenesis, decrease apoptosis and are neuroprotective.

Studies from the neonatal rat following hypobaric hypoxia (Kaur *et al.*, 2006a) and MCAO (Mu *et al.*, 2003) have found that VEGF is unregulated leading to increased vascular permeability as well as being a possible neuroprotectant. The response of VEGF following an *in utero* hypoxic insult such as UCO in late gestation fetal sheep has not been investigated. One of the primary aims of this thesis is to investigate VEGF following UCO and the implications (protective or detrimental) this can have on the developing fetal brain. More specifically, the response of the vascular morphology (Chapter 3), and VEGF hours (24 and 48 h – Chapter 4) to days (up to 14 days – Chapter 5) after UCO in the late gestation fetal sheep brain.

1.3.1.3 Erythropoietin

Another key hypoxia inducible gene is Epo which, following hypoxia, is increasingly important for regulating red blood cell production to increase the capacity of red blood cells to transport and ultimately increase oxygen supply (Marti, 2004; Fan *et al.*, 2009). Hypoxic up-regulation of Epo is regulated by HIF-1α, however, growing evidence suggests HIF-2α may also play a significant role is transcriptionally regulating Epo expression in the brain *in vivo* and in cultured astrocytes *in vitro* (Chavez *et al.*, 2006; Yeo *et al.*, 2008; Fan *et al.*, 2009). Epo is widely expressed in the brain by astrocytes, neurons, microglia and endothelial cells (Bernaudin *et al.*, 1999; Marti, 2004; Castillo-Melendez *et al.*, 2005). Following cerebral ischemia, endothelial cells are the first to increase Epo expression (Bernaudin *et al.*, 1999), which could implicate Epo as being important for the vasculature following hypoxia. More recently it has been reported that Epo mediated angiogenesis can occur by stimulating the expression of VEGF and its' receptor on endothelial cells (Iwai *et al.*, 2007; Hermann & Zechariah, 2009). *In vitro*, Epo can modulate angiogenesis by stimulating endothelial cell migration and proliferation (Anagnostou *et al.*, 1990; Yamaji *et al.*, 1996).

Suggested to be neuroprotective following hypoxia, increased Epo expression has also been shown to increase anti-apoptotic genes and promote survival in oligodendrocytes, neurons, astrocytes and microglia (Marti, 2004; Fan *et al.*, 2009). Treatment with recombinant human

Epo following focal hypoxia-ischemia in neonatal rats results in enhanced revascularisation, neurogenesis, endothelial cell and neuronal survival and increased Glut-1, Tie-1 and angpt-2 expression which resulted in enhanced neurovascular unit repair (Iwai *et al.*, 2007; Keogh *et al.*, 2007).

1.3.1.4 Angiopoietins

There is a close interaction between VEGF and angpt (-1 and -2) expression following hypoxia. Down regulation of angpt-1, important for blood vessel stabilisation occurs in response to hypoxia, and this correlates with increased BBB permeability and vascular leakage (Zhang *et al.*, 2002b; Valable *et al.*, 2005). Whether vascular remodelling or regression occurs following cerebral ischemia in the adult (rat) is dependent upon the presence of VEGF. Increased angpt-2 and VEGF expression by blood vessels promotes vascular growth; however regression occurs in the absence of VEGF (Beck *et al.*, 2000). Persistent up-regulation of Tie-1 and Tie-2, the angpt receptors, occurs for up to 2 weeks following MCAO and this correlates closely with increased angpt-1 and angpt-2 expression resulting in neovascularisation (Lin *et al.*, 2000; Lin *et al.*, 2001). However, increased angpt-2 expression can also persist with no change in angpt-1 or Tie-2 expression seen to occur following MCAO or chronic hypobaric hypoxia in the adult rat (Beck *et al.*, 2000; Pichiule & LaManna, 2002).

Interestingly, treatment with dexamethasone *in vitro* was seen to increase angpt-1 expression and decrease VEGF in astrocytes and pericytes. However, endothelial cells showed no change in expression following dexamethasone treatment in angpt-1, -2 or VEGF expression (Kim *et al.*, 2008). The implications of this study suggest that dexamethasone, a glucocorticoid routinely used to mature preterm lungs (Halliday *et al.*, 2009) could possibly have beneficial effects for the premature and vulnerable brain.

1.3.2 Degradation of basal lamina

Degradation of laminin is consistent with disruptions of the BBB (Figure 1.12) and can contribute to oedema formation and haemorrhage (del Zoppo & Mabuchi, 2003; Veltkamp *et al.*, 2006). Degradation of the basal lamina following hypoxia (Figure 1.12) is due to plaminogen-plasmin system and matrix metalloproteinase (MMP) 2 and 9. MMPs belong to a family of proteins that control tissue degradation (Hamann *et al.*, 1995; Burk *et al.*, 2008). Following hypoxia-ischemia, MMP-9 is upregulated, and being a substrate of laminin, is thought to correlate with laminin degradation (Zalewska *et al.*, 2002). Following ischemia, decreased collagen IV is associated with increased infarct volume and changes in BBB permeability (Hamann *et al.*, 1995; Hamann *et al.*, 2002; Scholler *et al.*, 2007). However another basement membrane constituent fibronectin and its' α5β1 integrin receptor are seen to be upregulated by endothelial cells following hypobaric hypoxia in the adult, possibly highlighting its angiogenic role (Milner *et al.*, 2008).

1.3.3 Compromise of the blood brain barrier

The severity of oxygen deprivation contributes to the rate of BBB function loss during acute hypoxic exposure (Al Ahmad *et al.*, 2009). In newborns that developed hypoxic-ischemic encephalopathy due to perinatal asphyxia, increased BBB permeability was seen to be correlated with increased malondialdehyde (a marker of lipid peroxidation) and nitrate/nitrite levels (Kumar *et al.*, 2008). Increased BBB permeability was also observed within 24 h and persisting for up to 7 days following hypoxia-ischemia in neonatal rats (Yang *et al.*, 2009; Ferrari *et al.*, 2010). However in a model of hypoxia in the newborn piglet BBB integrity, measured as permeability to small ions, was maintained (Stonestreet *et al.*, 1992). Interestingly, maternal treatment with glucocorticoids such as dexamethasone has shown to up-regulate key tight junctional proteins and decreases BBB permeability in the ovine fetus (Stonestreet *et al.*, 1999; Sadowska *et al.*, 2010), consistent with *in vitro* studies that also show endothelial up-regulation of angpt-1 for treatment with dexamethasone (Kim *et al.*, 2008).

As previously mentioned (Section 1.3.1.2), increased VEGF expression following hypoxia-ischemia results in a compromise of BBB permeability. Figure 1.12 summarises the consequence of hypoxia on the neurovascular unit. Synthesis and release of soluble guanylate cyclase, NO, tissue type plasminogen activator, prostaglandins (PG) and increased calcium influx all contribute to changes in vascular permeability (Bates & Curry, 1997; Murohara *et al.*, 1998; Mayhan, 1999; Yang *et al.*, 2009). Following hypoxia and brain injury (trauma), BBB leakage triggers the activation of astrocytes, corresponding with an increase in AQP4, an astrogilal water channel which facilitates water in and out of the brain, this response could contribute to formation of oedema (Papavassiliou *et al.*, 1997; Kaur *et al.*, 2006b; Ferrari *et al.*, 2010).
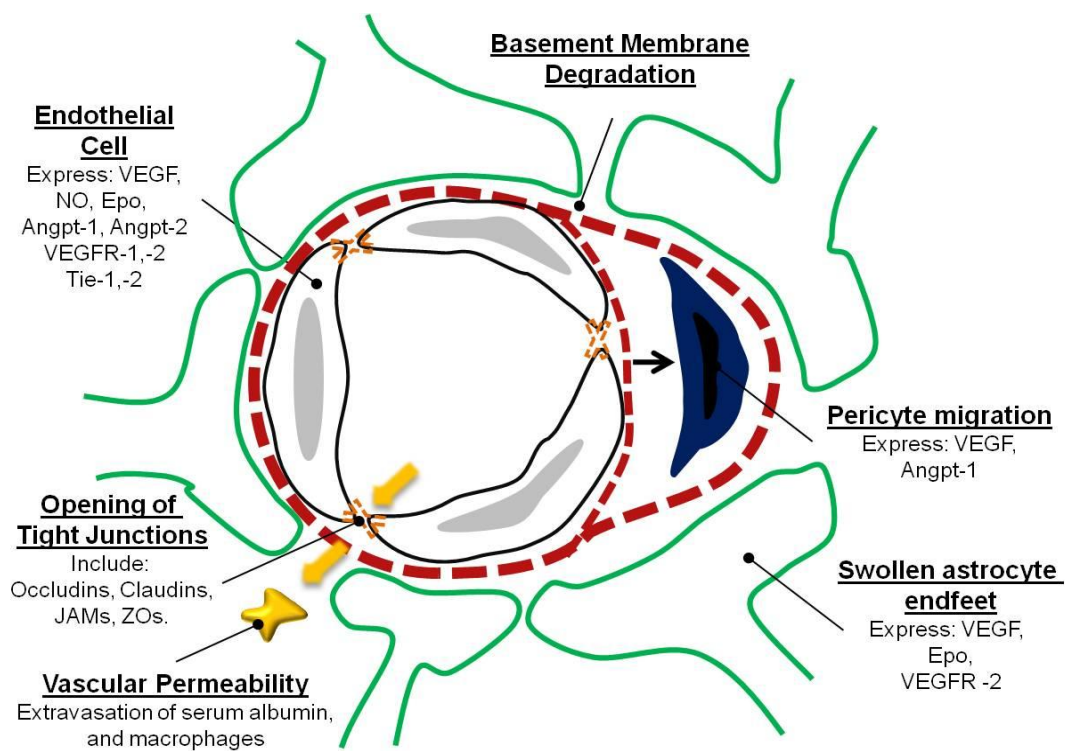
Figure 1.12: Schematic cross section of the consequence of hypoxia on the neurovascular unit. Following hypoxia, astrocyte end-feet become swollen, basement membrane degradation occurs, pericytes may migrate away and the opening of tight junctions occur resulting in the changes in BBB permeability leading to extravasation of serum albumin into the brain parenchyma (Kaur & Ling, 2008). A Licence Agreement from the publisher (Bentham Science) for permission to adapt this figure has been attained.

Disruptions in BBB permeability, elevation in mean arterial blood pressure and subsequent accumulation of water content into the brain parenchyma all contribute to the formation of vasogenic oedema (Kuroiwa *et al.*, 1985; Klatzo, 1987). Two forms of oedema exist; cytotoxic oedema and vasogenic oedema. Cytotoxic oedema is swelling of cellular elements and is suggested to occur in severe cardiovascular and hypoxic collapse seen following pneumothorax (Temesvari *et al.*, 1984; Klatzo, 1987). Vasogenic oedema is associated with increased vascular permeability, retention of water and entry of serum proteins into the brain parenchyma (Klatzo, 1987).

1.4 CEREBRAL BLOOD FLOW

In response to hypoxia, angiogenesis ultimately attempts to improve oxygen supply by providing a greater vascular network to allow for increased cerebral blood flow. Interestingly, during reperfusion regions of increased cerebral blood flow have also been seen to correlate closely with areas undergoing angiogenesis (Lin *et al.*, 2001). It is therefore important that whilst understanding the pathogenesis of brain injury we also understand the alterations of cerebral blood flow that may occur that can either contribute to or protect against injury. Cerebral blood flow is closely coupled with metabolic demand, and the delivery of oxygen is dependent on the rate of cerebral blood flow, oxygen content and consumption (Ashwal *et al.*, 1984; Pearce, 2006). Glucose is a major metabolite of the brain and provides 50 – 70% of oxidative metabolic needs in the fetus (Richardson & Bocking, 1998).

1.4.1 Cerebral autoregulation

Cerebral autoregulation refers to the ability to regulate and maintain a constant cerebral blood flow despite fluctuations in mean arterial blood pressure (Papile *et al.*, 1985). Immature fetal sheep (92 days gestation) show a decreased capacity to regionally autoregulate in response to increased intracranial pressure and cerebral perfusion pressure. However, by the last third of

gestation fetal sheep appear to have a better cerebral autoregulatory capacity, between 30-78 mmHg (Ashwal *et al.*, 1984; Helou *et al.*, 1994).

1.4.2 Modulators of cerebral blood flow

Cerebral blood vessels are innervated by both extrinsic and intrinsic neurons. Extrinsic innervation originates from the peripheral nervous system and makes synaptic contact with large blood vessels. Sympathetic nerves release noradrenaline and neuropeptide Y to elicit contractile effects and shift the upper limit of cerebral autoregulation. Parasympathetic nerves release vasoactive intestinal peptide, acetylcholine and NOS to dilate blood vessels. Trigeminal nerves are also important in restoring vascular tone following ischemia (Hamel, 2006).

Numerous factors contribute to the modulation of cerebrovascular tone. In response to neural activity astrocytes and interneurons can regulate cerebral blood flow (Hamel, 2006). Neurotransmitters, peptides and free radicals that can control cerebral blood flow include; PG, NO, adenosine, catecholamines and potassium induced vasodilation (endothelium derived hyperpolarising factor), some of these are discussed below. Figure 1.13 details the interplay between ROS generation and modulation of cerebral vascular tone.

1.4.2.1 Pericytes

Pericytes are sensitive to alterations O_2 and CO_2 levels suggesting they have the capacity to modulate capillary diameter, however this is a relatively new concept that has been very recently reviewed by Hamilton *et al.,* (2010). Briefly, pericytes act as contractile cells and based on their morphology and location (close contact with the basement membrane and endothelial cells) has the capability to modulate vascular tone. *In vitro*, decreased pH can result in pericyte dilation and in the presence on noradrenalin, pericyte constriction can occur (Chen & Anderson, 1997; Peppiatt *et al.*, 2006; Hamilton *et al.*, 2010).

Pericyte contraction is suggested be controlled by intracellular calcium (depolarisation), and dilation can occur by hyperpolarisation of potassium channels (Sakagami *et al.*, 1999; Sakagami *et al.*, 2001; Hamilton *et al.*, 2010). Finally, following ischemia (and traumatic brain injury) pericytes have been seen to migrate away from the vessel wall, coinciding with hypoperfusion (Takahashi *et al.*, 1997; Dore-Duffy *et al.*, 2000; Gonul *et al.*, 2002; Melgar *et al.*, 2005; Hamilton *et al.*, 2010). What is known about the role that pericytes play in modulating cerebrovascular tone is limited, most studies have been done *in vitro* and in the retina, so the implications this could have in the brain following hypoxia need to be further investigated.

1.4.2.2 Nitric Oxide

The activity of NOS is developmentally regulated during gestation (from studies in sheep), with close correlation to neuronal and metabolic activity and in close correlation with increases in cerebral blood flow (Northington *et al.*, 1997). The production of NO by eNOS has a fundamental role in regulating blood flow by causing vasodilatation (Figure 1.13), to increase cerebral blood flow, seen to occur following hypoxia-ischemia (Bolanos & Almeida, 1999; Rodrigo *et al.*, 2005; Kaur & Ling, 2009). It has also been suggested that increased vascular permeability induced by VEGF, may be mediated by eNOS (Fukumura *et al.*, 2001).

1.4.2.3 Prostaglandins

Prostaglandins are suggested to mediate NO induced vasodilatation. From *in vitro* studies, astrocytes have been seen to express PG and NO, particularly following hypoxia (Mollace *et al.*, 1997). Blocking PG resulted in no change in cerebral blood flow despite increased NO production, suggesting PGs are more important in mediating NO vasodilatory effects than NO production (VanBel *et al.*, 1997).
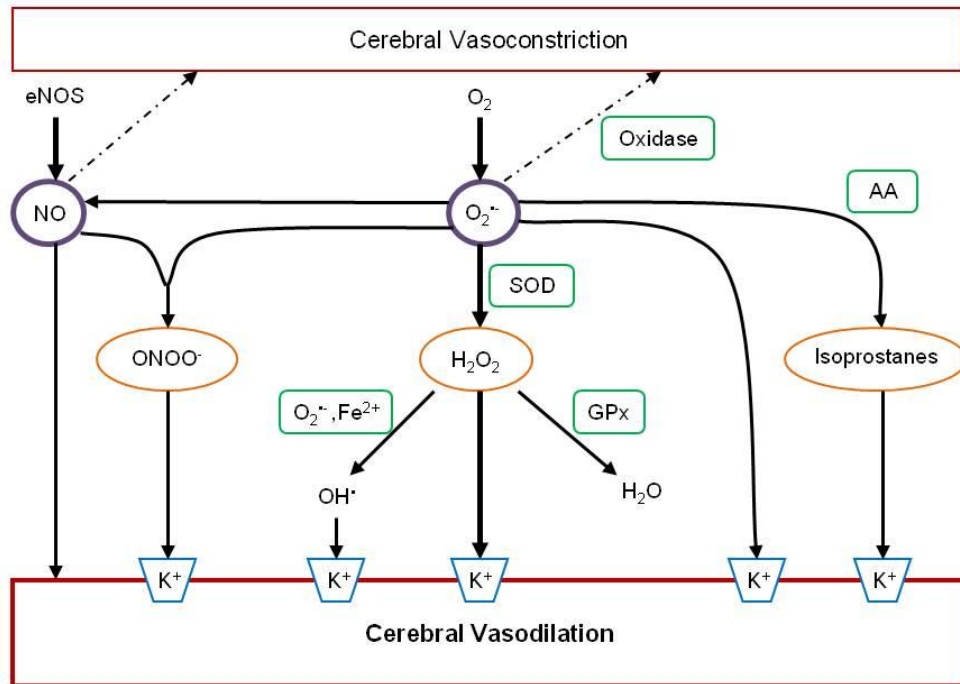
Figure 1.13: Reactive oxygen species (ROS) involved in the stimulation of cerebral vasodilation and vasoconstriction. Superoxide (O2•-) is produced by nicotinamide-adenine dinucleotide phosphate (NADPH) and xanthine in the mitochondria. O2•- itself has vasodilatory effects, and can form many reactive molecules following further reactions, These molecules have predominate vasodilation effects, including isoprostanes, hydrogen peroxide (H_2O_2), hydroxyl radical (OH•-) and perioxinitrite (ONOO-). To a lesser extent (shown by dotted lines), O2•- can cause vasoconstriction. arachidonic acid (AA); superoxide dismutase (SOD); glutathione peroxidise (GPx); endothelial NOS (eNOS). (Faraci & Heistad, 1998; Paravicini *et al.*, 2004).

1.4.2.4 Adenosine

Adenosine is a neuroprotective vasodilator, important in maintaining oxygen supply to oxygen demand. In response to hypoxia and during periods of decreased nutrient supply adenosine (both plasma and cerebral) concentrations increase (Kubonoya & Power, 1997; O'Regan, 2005). Adenosine is also involved in the suppression of cortisol production (Chau *et al.*, 1999; Jensen *et al.*, 2010) From studies in near-term fetal sheep, adenosine has been shown to increase cerebral blood flow following hypoxia and inhibit fetal breathing movements (FBM; Section 1.4.4.1) (Koos *et al.*, 2001; Blood *et al.*, 2002; Koos *et al.*, 2002; Watson *et al.*, 2002; Blood *et al.*, 2003). Meininger *et al.,* (1988) also suggest that following hypoxia *in vitro*, adenosine

stimulates endothelial cell proliferation and migration thereby also acting as a stimulator of angiogenesis.

1.4.3 Consequence of hypoxia

Although brain regions develop a greater oxygen sensing ability with advancing gestation, studies in the near term fetal sheep brain suggest regional responses exist, and white matter vulnerability may still have an incomplete autoregulatory capacity (Szymonowicz *et al.*, 1988). Following hypoxia or hypoxemia, initially cerebral blood flow increases in an attempt to sustain oxygen supply and demand, and this is seen in both immature and near term fetal sheep (Ashwal *et al.*, 1980; Ashwal *et al.*, 1984; Bocking *et al.*, 1988; McCrabb & Harding, 1995; Bennet *et al.*, 1998). Hypercapnia also results in increased cerebral blood flow, however it has been suggested that the effects of hypoxia and hypercapnia are independent rather than synergistic (Shapiro *et al.*, 1966; Ashwal *et al.*, 1984; Massik *et al.*, 1989). Studies using near infrared spectroscopy in near term fetal sheep suggest that during asphyxia blood flow drops, and then increases once asphyxia (10 min UCO) has completed (Bennet *et al.*, 1998), however when using microspheres, an increase in regional cerebral blood flow occurs during UCO (Yan *et al.*, 2009).

Ischemia occurs when there is decrease of available oxygen to the tissue. It is complex and involves a multi-factorial physiological response, where the ischemic core can respond differently to the surrounding ischemic tissue (Kulik *et al.*, 2008). During ischemia in preterm fetal sheep, regional cerebral blood flow decreases and during reperfusion cerebral blood flow increases (McClure *et al.*, 2008). Figure 1.14 summarises how fluctuations in cerebral blood flow can contribute to brain injury in the developing fetus.

1.4.4 Fetal behavioural states

Cerebral blood flow and electrocortical (ECoG) activity are closely linked; a 22% increase in cerebral blood flow occurs during low voltage (LV) activity when compared to high voltage

(HV). Increased cerebral temperature is also associated with HV activity (refer to Table 1.1; (Rankin *et al.*, 1987; Abrams *et al.*, 1990; Abrams *et al.*, 1991).
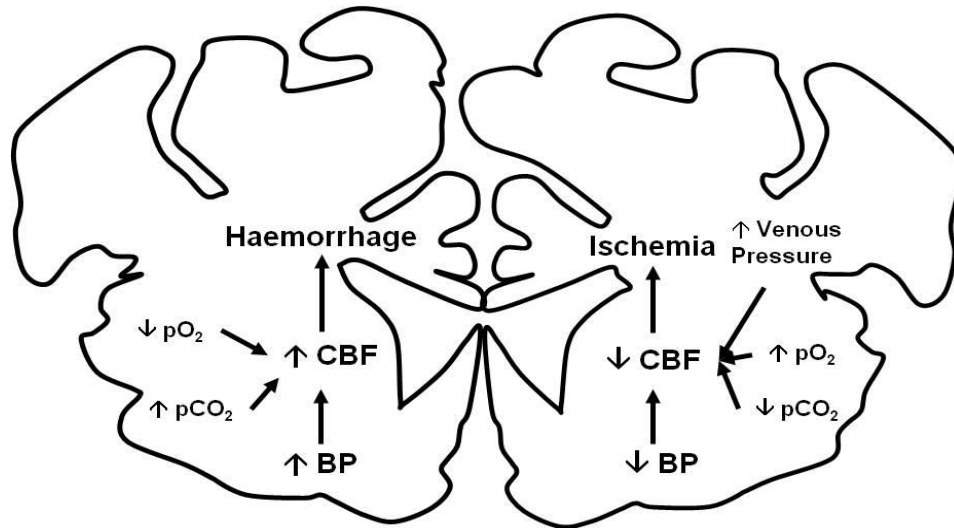
Figure 1.14: Schematic diagram of proposed contributing factors to cerebral haemorrhage and ischemia. Systemic hypoxia (decreased pO$_2$), hypercapnia (increased pCO$_2$) and hypertension contribute to increased cerebral blood flow (CBF), leading to haemorrhage. Increased venous pressure, hyperoxia (increased pO$_2$), hypocapnia (decreased pCO$_2$) and hypotension leading to decreased CBF result in ischemia. Adapted from (Wigglesworth & Pape, 1978). A Licence Agreement from the publisher (Elsevier) for permission to adapt this figure has been attained.

Fetal behavioural states describe the FBM, ECoG, electro-ocular (EOG) and postural (nuchal) muscle activity (EMG - nuchal) that develop during gestation. They are present before birth in species that have significant *in utero* brain development, such as humans, monkeys and sheep (Clewlow *et al.*, 1983; Lamblin *et al.*, 1999; Morrison *et al.*, 2005; Andre *et al.*, 2010). Electrocortical activity is electrophysiologically similar to rapid and non-rapid eye movement states characterised in the human (Morrison *et al.*, 2005). Much of the research into the understanding into the development and responses to *in utero* stressors of fetal behavioural states has been conducted in monkeys and chronically catheterised fetal sheep.

Clewlow *et al.,* (1983) investigated the maturational changes and relationship between these four parameters from 95 – 135 days GA (term is ~145 days) in fetal sheep. It was found that by 120 days ECoG activity was differentiated into HV and LV states. LV amplitude was also

associated with relaxation of nuchal muscles, rapid EOG and diaphragm activity (Jost *et al.*, 1972; Clewlow *et al.*, 1983). Table 1.1 summarises activity in each state.

Table 1.1: Fetal behavioural states. Comparison of LV/REM and HV/NREM in fetal sheep (Jost *et al.*, 1972; Clewlow *et al.*, 1983; Rankin *et al.*, 1987; Abrams *et al.*, 1990)

	Low-Voltage/REM	**High-Voltage/NREM**
ECoG – Amplitude	Low-Voltage	High-Voltage
ECoG - Frequency	Fast	Slow
EOG	Present	Absent
Nuchal Muscle	Atonia	Tone
FBM	Present	Absent
Cerebral Blood Flow	Increase	Decrease
Cerebral Metabolism	Increase	Decrease
Cerebral Temperature	Decrease	Increase
Mean Arterial Pressure	Low	High
Heart Rate	Low	High

During pregnancy numerous factors can influence ECoG activity and the incidence of fetal behavioural states including hypoxia (see Section 1.4.5) and hormones. Suppression of arousal occurs during increased maternal progesterone and increased expression of progesterone metabolites such as allopregnanolone, that works on the $GABA_A$ receptor (Crossley *et al.*, 1997; Nicol *et al.*, 1997; Yawno *et al.*, 2010).

1.4.4.1 Fetal breathing movements

Studies from the fetal sheep have shown that FBM readily occur in the presence of LV ECoG and ocular muscle activity (Table 1.1). With advancing gestation, FBM become episodic, vigorous and longer in duration, however no change in amplitude of breathes are seen. FBM are also seen to readily occur in the presence of LV ECoG and ocular muscle activity (Dawes *et al.*, 1972; Boddy *et al.*, 1974; Clewlow *et al.*, 1983; Baier *et al.*, 1992). Breathing activity is also

closely associated with increase fetal O_2 demand (Rurak & Gruber, 1983). Control of FBM occurs at the level of the brainstem, the upper pons is associated with controlling the incidence of FBM and co-ordinating with LV-ECoG (Dawes *et al.*, 1983).

1.4.5 Hypoxia and fetal behavioural states

From experiments in fetal sheep, severe hypoxia results in a suppression of ECoG activity following UCO (Kawagoe *et al.*, 1999a; Yan *et al.*, 2009). Reduction in uterine blood flow and hypercapnia also result in cessation of nuchal and ocular activity (Boddy *et al.*, 1974; Bocking & Harding, 1986). Hypoxia and hypoxemia also change the incidence and amplitude of FBM, which indicate possible injury in the brainstem regions that control FBM (Clewlow *et al.*, 1983; Dawes *et al.*, 1983; Bocking & Harding, 1986; Gluckman & Johnston, 1987; Bissonnette *et al.*, 1989). However the subsequent consequences of these alterations following birth have not been well investigated.

Fetal monitoring techniques are limited to assessing heart rate variability with fetal body and breathing movements (Bocking, 2003). Therefore investigating the fetal and newborn behavioural responses in late gestation unanaesthetised fetal sheep provides a functional assessment of the consequence of UCO; this is the aim for the studies detailed in Chapter 6.

1.5 SUMMARY

Many of the previous studies have focussed on the consequences of a focal ischemic insult (such as MCAO) on the cerebrovasculature of the adult. These studies have adequately detailed the complex but increasingly important influence of blood vessels, in particular the implications of VEGF, on the pathogenesis of injury following hypoxia-ischemia.

Currently the understanding of the pathogenesis of perinatal brain injury has concentrated on excitotoxicity, oxidative stress and the neuroinflammatory response, with the contribution of the vasculature being vastly overlooked. The response of the cerebrovasculature, including the expression of growth factors such as VEGF, changes in BBB permeability, angiogenesis and alterations in blood flow could explain both the reasons for regional susceptibility and the mechanisms that contribute to neuroprotection or injury. The response of cerebral blood vessels may also influence other cells such as neurons, astrocytes or oligodendrocytes. However, whether the developing fetal brain, which has an inherent regional vulnerability, responds in such a way, has not been well investigated. Importantly the studies in this thesis aim to investigate the response of the cerebrovasculature following a 'global' hypoxic insult and the consequences this may contribute to the incidence of brain injury in late gestation.

1.6 RATIONALE

In the term fetal brain cortical injury is more common than white matter injury, with the occurrence of haemorrhage presenting predominantly in subcortical regions, in comparison to intraventricular haemorrhage in the preterm neonate (Van den Broeck *et al.*, 2007). Clinical studies of full term infants have found that the perinatal period is the most important in contributing to the presentation of hypoxic-ischemic encephalopathy (p7, para 1). Obstetric complications that result in a global fetal hypoxia that may lead to fetal brain damage are difficult to detect, and the incidence of such *in utero* complications may be significantly

underestimated. Furthermore, the contribution of such complications to neonatal brain injury are not well understood.

Following hypoxia-ischemia in the adult brain, VEGF, a key hypoxia-responsive angiogenic factor, has been suggested to play a role in instigating cerebrovascular injury, as well as having possible neuroprotective actions. However, whether VEGF is important in the highly dynamic developing fetal brain following a hypoxic insult has not been well investigated (p14 para 2). Clinical evidence showing high VEGF expression in the foci of necrosis in neonates presenting with PVL (Arai *et al.*, 1998), and studies by Ballabh *et al.,* (2004a, b; 2010) in pre-term newborn humans and rabbits strongly suggest that understanding the response of cerebral blood vessels during development will increase our understanding of why there is a regional vulnerability of the brain to injury.

The use of mid gestation fetuses would be optimal to investigate preterm brain injury, however for this thesis the late gestation fetal sheep was chosen which has brain development comparable to the near term human fetal brain (p7). As mentioned above, the term infant is vulnerable to cortical injury and subcortical haemorrhage following hypoxia. Therefore, a model of global fetal hypoxia in pregnant sheep was also chosen, where a single bout of reversible umbilical cord occlusion (UCO) for 10 minutes results in a systemic response on the grounds that this is an event that can happen *in utero* in the third trimester. Previous studies using a single UCO for 10 minutes in late gestation fetal sheep have found significant alterations in cerebral blood flow, cerebral metabolite and lipid peroxidation production (Mallard *et al.*, 1994; Miller *et al.*, 2005; Yan *et al.*, 2009). Epo, a hypoxia sensitive gene was also seen to be up-regulated following UCO (Castillo-Melendez *et al.*, 2005), thereby continuing on from these findings we wanted to investigate the expression of another hypoxic sensitive gene, VEGF and the possible consequences it may also have in the near term brain. These previous studies were also relatively a short-term follow up (up to 48 h) following UCO. Therefore, some of the experiments in this thesis allowed for investigation of the impact this

may have had on the fetal brain (p36 para 1), up to term, and also investigated the effects on both fetal and postnatal behaviour (p47).

1.6.1 Aims

Specifically, it is the aims of this thesis to:

- Characterise changes in cerebral vascular morphology in the late gestation fetal sheep following UCO.

- Investigate the expression and distribution of VEGF in the fetal brain in the hours (24 h and 48 h) and days prior to birth following UCO.

- Determine if changes in VEGF expression in the near term fetal sheep brain are associated with an angiogenic response and/or alterations in the blood-brain barrier (BBB) permeability.

- Investigate whether a consequence of brief UCO has a profound or persisting effect on both fetal and postnatal behaviour.

1.6.2 Hypotheses

(1) From previous studies in the adult and neonatal rodent, it is hypothesized that following a global fetal hypoxia that cerebral blood vessels will show regionally-specific morphological changes and expression of key angiogenic proteins, that could better contribute to the understanding of the pathogenesis of perinatal brain injury.

(2) The effect of a brief global hypoxia on the fetal brain will be to significantly change CNS activity, and this will be revealed by changes in both fetal and neonatal behaviour.

Chapter 2

GENERAL METHODS

TABLE OF CONTENTS

To help understand the pathogenesis of clinical conditions in humans, animal models are widely used to overcome ethical and technical issues. Animal models are commonly used in fetal and neonatal physiology to understand normal brain development, and the mechanisms which underlie perinatal brain injury and these include mice, rats, rabbits, pigs, sheep and monkeys. Any animal one may choose for experiments has strengths and limitations, and is dependent on the question one aims to answer. Length of gestation, maternal and fetal body size, organ development and basic physiology all need to be taken into consideration.

The use of rodents in perinatal research allows for a large sample size and provides a wide availability of antibodies to be used; however mice and rats are "postnatal brain developers" (Dobbing & Sands, 1979) so the timing of insults is usually given after birth. Recently, rabbit kits have been used; utilising imaging and behavioural measurements to investigate brain injury that results in a cerebral palsy like condition (Derrick *et al.*, 2004). Larger animal models (pigs, sheep and llamas) are used as they have a long gestation and are perinatal brain developers (similar to humans), however smaller group sizes are usually obtained.

Chronically instrumented fetal sheep are a widely characterised and used model to study the developing fetus. The pregnant ewe tolerates surgery well, the fetus can be catheterised and implanted with blood flow probes and electrodes, and these allow for long term experiments to be conducted. Although there are anatomical and physiological differences with humans, fetal sheep allow for both insult (e.g. infection, hypoxia or growth restriction) and responses (e.g. blood pressure, blood flow and electrocortical activity) to be investigated *in utero.*

Brain development in the ovine fetus has been characterised as mature at birth (~146 days gestational age (GA); 0.65 GA and 0.9 GA are deemed equivalent to 24 – 26 weeks and 37 – 42 weeks in the human, respectively (McCrabb & Harding, 1995; Hagberg *et al.*, 2002; Back *et al.*, 2006). Fetal sheep also develop clear patterns of electrocortical activity late in gestation, similar to humans. For these reasons, the pregnant sheep model has been used in this thesis.

2.1 ETHICS CLEARANCE AND ANIMAL WELFARE

All animal experimentation obtained prior approval from the School of Biomedical Sciences Animal Ethics Committee. All animal handling, care and use of animals for experimentation followed the National Health and Medical Research Council (NHMRC) Australia Code of Practice for the Care and Use of Animals for Scientific Purposes. Procedures associated with minimum pain and/or distress were used. Any abnormal physical or physiological symptoms were inspected by a veterinary specialist and treated under specific instructions.

Time mated Merino/Border Leicester cross breed pregnant ewes (117 ± 3 days GA, term is ~146 ± 1 days) were obtained from an approved animal supplier and transported to the department animal housing facility (Department of Physiology, Monash University) a week before surgery. This allowed ewes time to adapt to the new environment. Each pregnant ewe was housed in individual metabolic cages, fed daily with ~ 1 kg of Lucerne-chaff mix and water provided *ad libitum*. Food intake and general wellbeing of animals were monitored and recorded daily. Ewes were kept under a constant environment of 22°C and 45 – 55% humidity with a 12-hour light/dark cycle (lights on at 0700 h, lights off at 1900 h).

Any ewe that did not make a rapid recovery following surgery, or showed signs of severe pain (such as tooth grinding or altered posture) received additional analgesics and was monitored closely for the next 24 – 48 h. Any ewe that failed to eat, was deteriorating in condition or not responding to treatment was assessed by a veterinary specialist and if necessary was humanely killed (Section 2.8.1). Since this project was designed to examine fetal responses late in gestation, all pregnant ewes were closely monitored for signs of labour (Section 0for details).

2.2 CATHETER PREPARATION

Polyvinyl tubing (Outer diameter (O.D.) 1.52 mm; Inner diameter (I.D.) 0.86 mm, Microtube Extrusions, Australia) were used as fetal catheters, and cut to 1.5 m length. At one end of the catheter, a 20 gauge blunt needle (Sherwood Davis and Geck, USA) was inserted after temporary expansion of the catheter with chloroform (Merck, Germany). Catheters for maternal vessels and to measure fetal tracheal and amniotic pressures were prepared the same way, but using a thicker polyvinyl tubing (O.D. 2.5 mm; I.D. 1.5 mm) and a 15 gauge blunt needle. All catheters were packaged into a heat sealed sterilisation bag and sterilised by Ethylene Oxide (EO; Steritech, Australia).

2.3 ELECTRODE PREPARATION

2.3.1 Electrocorticogram

Electrocorticogram (ECoG) electrodes were made prior to surgery and sterilised by EO. A single length (1 m) of polyvinyl tubing (O.D. 2.5 mm; I.D. 1.5 mm) was cut and threaded with three strands of insulted stainless steel wire (1.2 m, Cooner Wire Co., Chateworth, CA, USA). Approximately 5 cm of each length of wire was left extending from one end of tubing, and 15 cm at the other (Figure 2.1 A). The lengths of the wires were secured in the tubing by injecting silastic sealant (Silastic 732 RTV Sealant; Dow Corning Corporation, Midland, USA) using an 18 gauge needle with a 5 ml syringe. The silastic sealant was left to set overnight. The short end (5 cm) of each wire was stripped of ~1 cm of insulation using a soldering iron, and soldered into small gold pins (1 mm diameter; D Crimp pins; RS Components, Clayton, Australia). Two wires from the long end (15 cm) had a rubber disc (1 mm thick, 5 mm diameter) threaded ~ 2 cm, using an 18 gauge needle, and secured. The ends of these wires were exposed (~ 0.5 cm) using a soldering iron. The third wire, which was to serve as a 'common' electrode, also had ~ 1 cm section exposed so that it would be in contact with the tissue when sewn into the skin.

2.3.2 Electromyogram and Electro-oculogram

Two strands of insulated stainless steel wires were cut and threaded into the polyvinyl tubing as described above. The short ends were prepared with gold pins (as above) and the long ends of electromyogram (EMG) wires were prepared the same as the ground wire of the ECoG (Figure 2.1 B). Two, Two lead EMG electrodes were used to measure nuchal muscle activity and eye movements (electro-oculargram; EOG).

2.3.3 Piezoelectric ultrasonic probe

A piezoelectric ultrasonic probe (1mm x 1mm, Frequency: 20 mHz, Model: F, Iowa Doppler Products, Iowa, USA) were pre-made and ordered from Iowa Doppler Products. The probe was attached to two intertwined stainless steel wires, these were threaded into 1 m of polyvinyl tubing, and each end was secured with silastic sealant and left to dry overnight. The other end were prepared with gold pins (as ECoG and EMG electrodes; Figure 2.1 C).
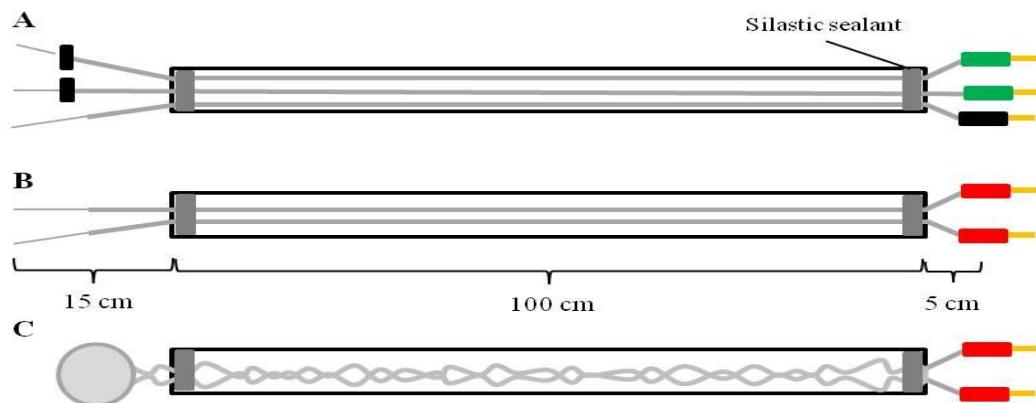
Figure 2.1: Schematic diagram of electrodes and doppler probe. Three wire ECoG (A), Two wire EMG (B) electrodes and piezoelectric ultrasonic doppler probe (C). All wires were inserted into polyvinyl tubing, both ends secured with silastic sealant and gold pins placed on one end to connect to amplifiers.

2.4 ANIMAL SURGERY

2.4.1 Surgical preparation

Surgery was performed under strict aseptic conditions. Fetal surgery occurred at 125 ± 1 days GA under aseptic conditions for the chronic implantation of catheters and electrodes. Ewes were fasted for approximately 24 hours prior to surgery, with unrestricted access to water.

Immediately prior to surgery, the ewe's right flank and underside neck region were shaved to skin using clippers and the ewe was given 1g of prophylactic antibiotics (Ampicillin sodium i.v.; Aspen Pharmcare Pty Ltd, Australia) in sterile water by injection into the jugular vein, to minimize the chance of infection. At surgery, both the ewe and fetus were anesthetized by a bolus injection (20 ml of thiopentone sodium dissolved in water (50 mg/ml, Pentothal, Jurox Pty Ltd., Australia) into the jugular vein of the ewe. Anesthetic was maintained throughout surgery using positive ventilation (8 breathes per min; 800 – 1000 ml per breath) of 1 - 2.5% isoflurane (Isoflow, Merial, Australia) in 70:30% oxygen-nitric oxide (BOC Gases, Australia) gas mixture using an automatic anesthetic ventilator (Campbell Anaesthetic Ventilator, UCLO Engineering, Australia). Following intubation with an endotracheal tube (Size 8-9, O.D. 10.9mm; I.D. 8.0mm, Portex Ltd., London), the ewe was ventilated mechanically in a closed circuit apparatus (CIG Midget 3 Medishield, Australia) for the duration of surgery.

While under anesthesia, the ewe was placed in a supine position and wool on the ventral abdominal and ventral neck were shorn. These areas were thoroughly cleaned with chlorohexadine antiseptic solution (1:10 dilution of 4% w/v chlorohexadine gluconate, Johnson & Johnson, Australia) in water, followed by 3 – 4 applications of Betadine Surgical Scrub (7.5% w/v povidone-iodine, Faulding Pharmaceuticals, Australia). All shorn areas were cleaned in a circular motion, beginning at the centre of the abdomen and extending outwards. The skin was then wiped clean and sprayed with Iodine antiseptic solution (10% povidone-iodine; Faulding Pharmaceuticals, Australia). The animal was then moved into the operating theatre and

placed on the operating table. Finally, the incision sites were wiped by a mixture of 10% Hibitane-Alcohol solution (Chlorhexidine gluconate 5% w/v, isopropyl alcohol 4% v/v; Hibitane, Zeneca Pharmaceuticals Australia Pty Ltd, Australia) just before the commencement of surgery.

All surgical instruments, drapes and gowns were sterilized prior to surgery by autoclaving. Maternal and fetal catheters, ECoG, EMG, EOG electrodes and a piezoelectric ultrasonic doppler probe to be used for measuring sagittal sinus blood flow velocity (SSbfv) were all previously sterilized by EO gas. An inflatable silastic cuff to be used for occluding the umbilical cord was sterilized by autoclaving. The hands and arms of each surgeon were thoroughly scrubbed with Hibiclens antiseptic solution (4% w/v chlorohexidine gluconate; 4% isopropyl alcohol; ICI Pharmaceuticals, Australia). Surgeons wore surgical caps, facemasks, sterile gowns and gloves (Ansell International, Australia) throughout surgery.

2.4.2 Fetal surgical procedure

Sterile plastic sheets and drapes were used to cover the ewe, except for the surgical incision site, leaving only the area immediately surrounding the incision site exposed. A longitudinal midline incision, approximately 15-20 cm long, was made on the skin of the ewe's abdomen, between the umbilicus extending to the udder. Care was taken to avoid superficial mammary and other major veins. A diathermy (LCC200, Erbe, Germany) was used to coagulate bleeding from small vessels. Subcutaneous tissue was moved aside and an incision was made on the *linea alba* and peritoneum to expose the uterus. The fetal head and position of the fetus was identified by palpation and part of the uterus with fetal head within, was brought out of the abdomen. On the uterus, a small incision was made using the diathermy, parallel to the uterine vessels, to expose the fetal head, carefully avoiding blood vessels and cotyledons. The fetal head and both front legs were brought out of the uterus through the incision site. Uterine muscle and the membranes (amnion and chorion) were clamped with Babcock clamps to minimize loss of amniotic fluid. Fetal skin was kept moist with sterile saline (0.9% NaCl, pH 7.4; Baxter, Australia).

2.4.2.1 Insertion of brachial catheter

An incision was made on the lateral anterior axilla at the level of the first rib to expose by blunt dissection the brachial artery of the right forelimb. Once identified, tissues were separated from the brachial artery for a length of 1 – 1.5 cm with care taken to avoid damage to adjacent vessels. Two silk sutures (Size 2.0; Dynek Pty. Ltd., Australia) were loosely tied around the vessel approximately 1cm apart; the artery was then occluded by securing the suture on the extremity side. A bulldog clip was placed distal to the suture on the brachial artery, a small incision was made on the arterial vessel wall and a small diameter (O.D. - 1.52mm and I.D. - 0.86mm; Critchley Electrical, NSW, Australia) fetal catheter filled with heparinised (50 000 IU/L; Heparin, Pharmacia, Australia) saline (0.9% NaCl, pH 7.4, Baxter, Australia), was inserted 3cm into the brachial artery, guided by forceps and secured into place by tying the suture outside the vessel and removing the bulldog clip. The catheter was tested for patency and flushed with heparinised saline to prevent the blood clotting. The skin incision was closed using a continuous suturing pattern with silk suture size 3.0 (Dynek Pty Ltd, Australia; Figure 2.2 A).

2.4.2.2 Insertion of tracheal and amniotic catheter

A large bore catheter (OD – 2.7 mm and ID – 1.5 mm; Critchley Electrical, NSW, Australia) was inserted into the fetal trachea (Figure 2.2 A) to measure pressure changes associated with fetal breathing movements (FBM). A large bore catheter filled with saline with a perforated end was attached to the fetal chest to measure amniotic pressure. This was electronically subtracted from fetal mean arterial blood pressure (MAP) and fetal tracheal pressure to correct for any pressure changes due to uterine activity and movement of the ewe.

2.4.2.3 Implantation of electrocorticogram and piezoelectric ultrasonic probe

The top of the fetal skull was exposed by a medial incision (~ 5 cm) using a diathermy. The underlying tissue was scraped clean from the bone by a scalpel blade, to expose the cranial and

sagittal sutures. Two holes (0.5 mm in diameter) were drilled in the skull with co-ordinates of 5mm forward of the coronal suture and 10 mm lateral of either side of the sagittal suture, into which the bare ends of the insulated wires were inserted to measure the bi-parietal ECoG (Clewlow *et al.*, 1983). The electrodes were inserted and secured with cyanoacrylate glue (Vetabond, 3M, St Paul MN, USA). A common (reference-earth) electrode was attached under the fetal skin. (Figure 2.2 B)

A small piece (2x5mm) of parietal bone was removed in the midline by surgical drill to expose the dura mater (Figure 2.2 C). The piezoelectric ultrasonic probe was placed on the dura mater directly above the sagittal sinus (Figure 2.2 D) to measure blood flow velocity using a Directional Pulsed Doppler Flowmeter (Bioengineering, University of Iowa, USA). The ultrasonic crystal was secured with Vetabond and covered with dental acrylic (Orthodontic Resin (Power and Liquid), LD Caulk Company, Milford, Delaware, USA) (Figure 2.2 E). The fetal skin was closed with silk suture.

2.4.2.4 Implantation of nuchal electromyogram and electro-oculogram

The nuchal muscles (located bilaterally of the midline of the neck) and the ocular muscles (located above and below the eye) were exposed (nuchal; ~5 cm. ocular; ~1 cm). A pair of insulated stainless steel EMG (2 lead) electrodes were sewn around two nuchal muscles, and another 2 lead EMG (will be referred to as EOG) were sewn around the ocular muscles, where the bared portion lay within the muscle. EMG electrodes were sewn under the skin and the skin incision was sutured closed with a silk tie (Figure 2.2 F, G).

2.4.2.5 Umbilical cord cuff

The fetus was gradually pulled out of the uterus until the umbilical cord was visible. A sterile inflatable vascular occlude cuff (outer circumference 16 HD; In Vivo Medical, Ukiah, CA, USA) was placed around the umbilical cord (Figure 2.2 H). The size of the occluder was carefully selected so it would cause complete cessation of umbilical flow when it was inflated

with 2 -3 ml of sterile water, but as to not impede blood flow when not in use. The occluder was secured to the fetal abdomen using silk suture to prevent any movement or obstruction of umbilical flow.

2.4.2.6 Exteriorising the fetal catheters and electrodes

Upon completion of instrumentation of the fetus, all catheters and electrodes were run to the back of the fetal neck and secured to the skin to prevent catheter tangling and blockage on the fetal body. The fetus was gently placed back into the uterus, avoiding loss of the amniotic fluid. The uterus and uterine membranes were closed using absorbable suture (Size 2.0; Chromic Surgical Gut, Dynek Pty Ltd, Australia) and interlocking stitches to prevent leakage of amniotic fluid. A second layer of Cushing pattern was applied to invert the incision within the uterus to avoid a raw edge being exposed. The uterus was placed back into the abdominal cavity and all the leads and catheters were placed into a sterile conical tipped tube. The tube was passed along the inside of the abdominal cavity to the right flank of the ewe, where a small incision was made. The tube was then passed out through the incision and all of the catheters and electrodes exteriorized. The small incision was closed with stitches between the catheters and electrodes, to prevent leaking of abdominal fluids. Sterile three-way stopcocks (Discofix-3, Braun, Germany) were attached to the exposed end of each of the three catheters and antibacterial spray (2 mg/g oxytetracyclin hydrochloride, Terramycin, Pfizer, Australia) was applied liberally.

The maternal abdominal *linea alba* was closed with individual stitches, approximately 1 cm apart, made with absorbable suture (Chromic gut 2, Dynek, Australia). Using a continuous stitch the subcutaneous tissue was closed. The skin of the abdomen and flank was closed with Vetafil Bengen synthetic suture (Clement Stansen, Nth Ryde, NSW, Australia).

2.4.2.7 End of surgery

At completion of surgery, anaesthetic gas was withdrawn from the ventilation gas to allow the ewe to recover from anesthetic. All incisions were sprayed with iodine (50 g/L

polyvinylpyrrolidone-iodine, Troy Laboratories Pty Ltd, Australia) and the midline incision was covered with a sterile cotton pad. The ewe was covered with elastic netting (Surgifix, size 7; Australian Home Healthcare, Australia) placed around the ewe's abdomen and chest. All catheters and electrodes were placed in self-seal plastic bags, tied securely on the ewes back, under the netting.

A self adhesive patch impregnated with the opioid analgesia fentanyl (7.5 mg, providing 75 μg/hr for 3 days, Duragesic, Janssencibig, NZ) was placed on the skin of the inner right leg of the ewe to provide post-surgical analgesia. Once the ewe's normal swallowing reflex and breathing had returned, the endotracheal tube was deflated and removed. The ewe was returned to their individual cage and monitored closely for the next 3 - 4 h. Food was provided for the ewe, and once muscle tone was apparent and the ewe was standing independently, water was also provided.

2.4.3 Maternal surgery

In the supine position, the maternal jugular vein could be palpated and an incision was made in the right jugular groove of the maternal neck. The surrounding adventitia was cleared from around the vessel using blunt dissection. The vein was occluded distal to the heart using a silk tie, similar to fetal catheterization. A small incision was made in the vessel wall and the polyvinyl catheter (O.D. 2.5 mm; I.D. 1.5 mm) was inserted 15 – 20 cm towards the heart and fixed in place using silk ties, and tested for patency. The skin incision was closed using a simple continuous stitch with silk suture.
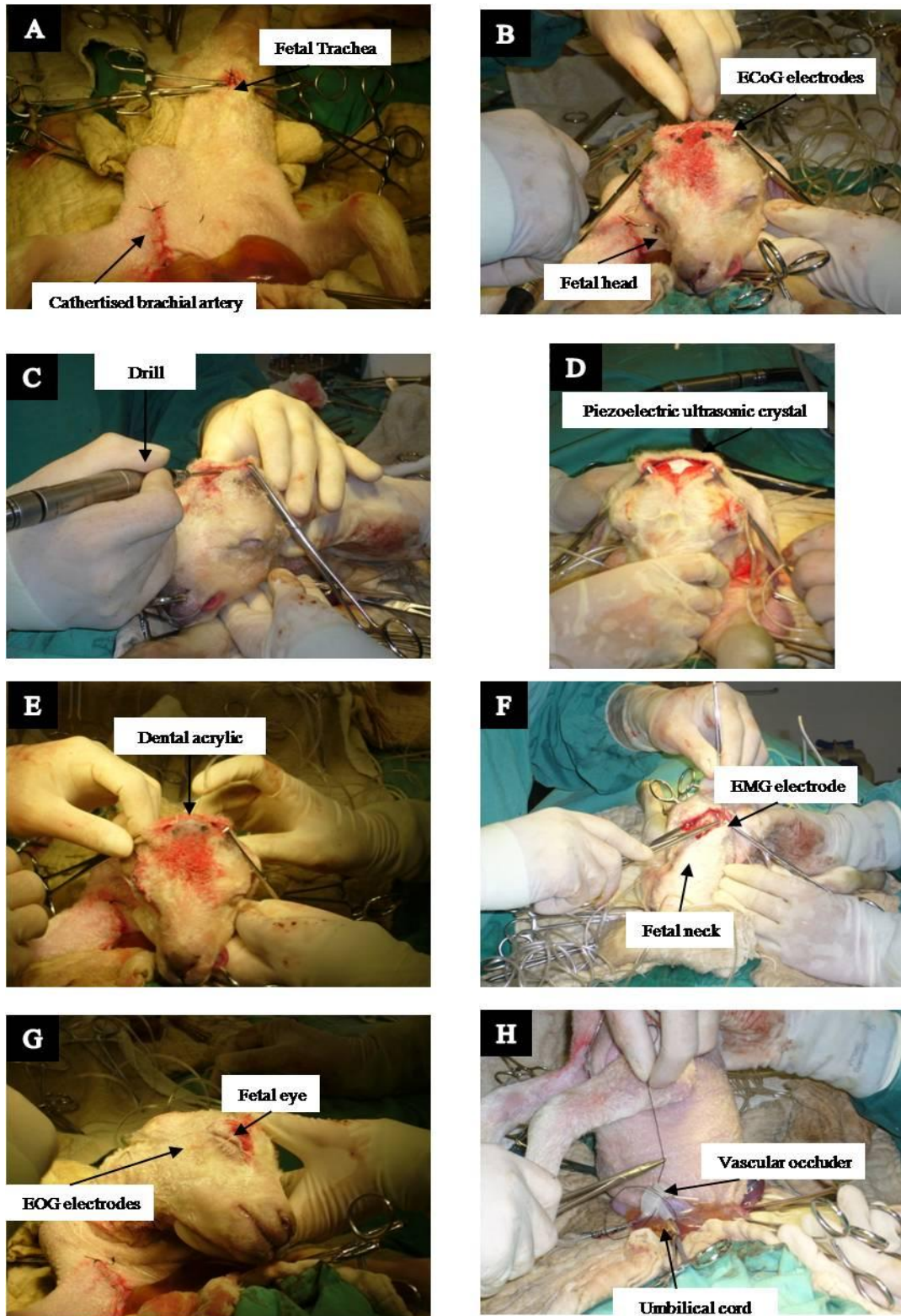
Figure 2.2: Photographs of late gestation fetal sheep surgery. 125 day GA fetus, catheterized brachial artery and trachea (A). The fetal skull was exposed to insert ECoG electrodes (B), drilled along coronal suture (C) to place ultrasonic doppler probe (D) and sealed with dental acrylic (E). The fetal neck and eye had two, two wire EMG leads placed around muscles (F & G). Finally a vascular occluder was placed around the umbilical cord (H).

All catheters were then sealed with sterile three-way stopcocks and flushed with sterile heparinised saline to ensure the catheter was free of blood.

2.4.4 Post-Operative care

For 3 days post-surgery 500 mg of powdered Ampicillin (Austrapen; CSL Ltd., Australia) suspended in 5ml of saline (25 IU/ml saline; Baxter, Australia) was administered to the fetus (via the amniotic catheter). The fetal brachial catheter was flushed daily with approximately 3-5 ml of heparinised saline. A 0.5 ml fetal blood sample was taken from a brachial artery catheter for blood gas measurements to asses fetal well being. Fetal blood gases (partial pressure of oxygen (pO_2), partial pressure of carbon dioxide (pCO_2), oxygen saturation (sO_2), pH, glucose and lactate were measured using an ABL 700 blood gas analyzer (Radiometer, Copenhagen). The parameters were corrected for the expected fetal body temperature of 39°C.

2.5 ANIMAL EXPERIMENTS

2.5.1 Recording of fetal parameters

Monitoring of fetal physiological parameters began a day prior to any of the experiments outlined in chapters. All analogue signals from were converted to digital signals by an analogue digital converter (Power Lab MKIII, ADInstruments, Australia). All data were recorded onto a computer hard disk by Chart 5 software (ADInstruments, Australia) and were continuously monitored, recorded and saved for the duration of the experiment (Figure 2.3).
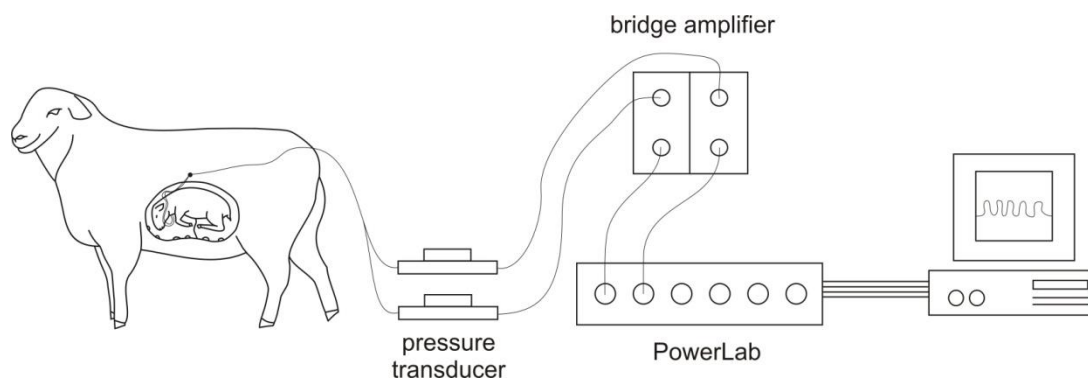
Figure 2.3: Sheep set-up. Schematic diagram of the set up used to record fetal sheep parameters. Image used courtesy of Dr. Edwin B. Yan (National Trauma Research Institute, Alfred Hospital, Melbourne, Australia).

2.5.1.1 Fetal blood pressure, breathing and heart rate records

Fetal catheters (brachial, tracheal and amniotic) were connected to solid state, disposable pressure transducers (Becton Dickinson and Co. USA) to measure MAP, fetal tracheal pressure and amniotic pressure. Pressure transducers were first sterilized by filling them with 2 % aqueous Hibitane for 30 min, followed by rinsing and filling with sterile saline, with care taken that no air bubble were present. The transducers were then connected to a multi-channel analogue pressure amplifier (Quad Bridge Amp, ML118, ADInstruments Pty Ltd., Australia). Catheters were then connected to a computer via an analogue to digital converter (PowerLab, ADInstruments, Australia). All data was then recorded on a computer utilizing Chart 5 computer software (ADInstruments, Australia) for further analysis.

The Bridge amplifier and PowerLab were calibrated by applying a known external pressure. Each pressure transducer was first opened to air to record atmospheric pressure at 0 mmHg, and then a pressure of 100 mmHg was applied using a sphygmometer to measure pressure (Sterilux, Japan). The signals correspond to 0 and 100 mmHg, entered into the BridgeAmp module in PowerLab, also calibrated to the same pressures. The transducers were secured on a rack and attached to the side of the metabolic cage and care was taken to ensure catheters had enough sufficient length to allow the ewe to move freely in her cage without applying tension to the catheters.

This setup results in alterations to hydrostatic pressure with the transducer because the position of the fetal heart could be either above or below the fixed position pressure transducers (depending on whether the ewe was standing or sitting). The real MAP was therefore calculated by electronically subtracting the amniotic pressure from the recorded brachial artery pressure. The real fetal tracheal pressure was also calculated as the recorded tracheal pressure minus the recorded amniotic pressure. This electronic subtraction was performed using the Chart 5 software; digital arithmetic function. Fetal heart rate (HR) was digitally calculated from the raw arterial blood pressure by Chart 5 software. Once setup was complete, the transducers were connected to the fetal catheters and MAP, HR, tracheal and amniotic pressure were continuously monitored, recorded (Figure 2.4) and saved to the hard disk until the completion of the experiment.

2.5.1.2 Monitoring of fetal electrocortical states

Fetal behavioural states in the late gestation fetal sheep are shown in Figure 2.5. Fetal electrocortical states were measured using ECoG, EMG – nuchal and EOG electrodes connected to a custom made recording lead (Department of Physiology, Monash University, Australia). Signals were then passed to a Polygraph (Model 79D, Grass Instruments Company, Quincy, Mass, USA), equipped with appropriate preamplifier modules. All channels on the Grass recorder used a 50 Hz notch filter to eliminate electrical interference from other appliances within the room.

A 100μV pulse was used to calibrate the ECoG signal. Fetal ECoG electrical activity was amplified by passing the signal through a Wide Band AC EEG Pre-Amplifier (Model 7P5B, Grass Instrument Co., MA, USA) with high input impedance. The fetal ECoG electrical activity was used to determine high voltage (HV) and low voltage (LV) electrical brain activity.
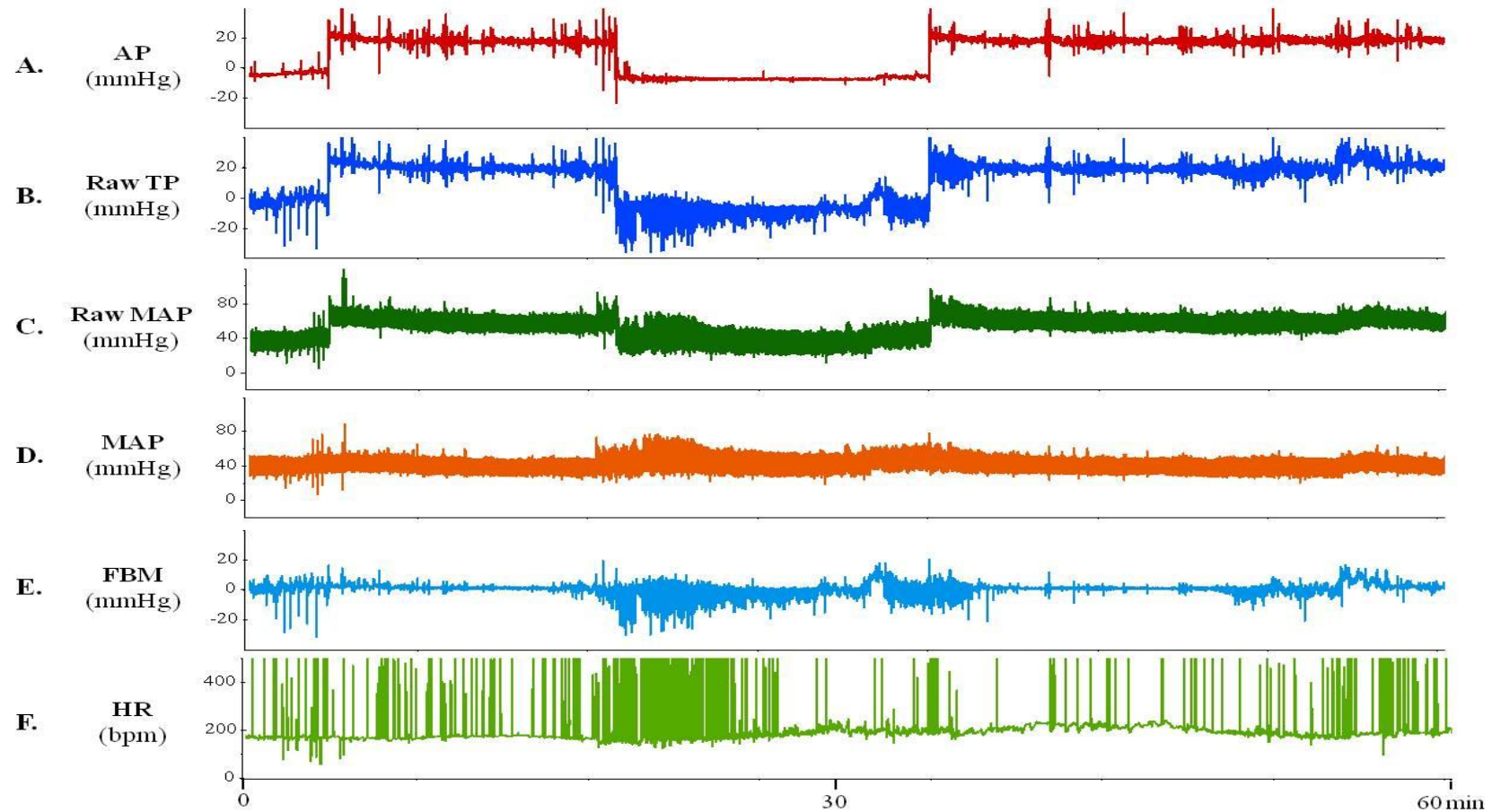
.**Figure 2.4: Fetal haemodynamic parameters recorded on PowerLab.** Raw amniotic pressure (AP; A), tracheal pressure (TP; B) and mean arterial pressure (MAP; C). Raw AP was subtracted from raw MAP for a true MAP recording (D). Raw AP was subtracted from raw TP for a real fetal breathing movement (FBM) pressure (E). Heart rate (HR; F) was calculated from raw MAP. From PowerLab recorded on Chart 5 Software.

Fetal nuchal muscle activity and the ocular movement signal were amplified by passing the signal through a Wide Band AC Pre-amplifier (Model 7P3B, Grass Instrument Co., MA, USA). The amplitude low frequency was set at 0.3 Hz and high frequency set at 15 Hz, a 200 μV was used to calibrate the signal.

2.5.1.3 Monitoring of Sagittal Sinus blood flow velocity

Methods of measuring and monitoring cerebral blood flow in the fetal sheep include the use of microspheres (coloured, fluorescent or radioactive labeled) (Ashwal *et al.*, 1980; McClure *et al.*, 2008; Yan *et al.*, 2009) and flow probes (Bennet *et al.*, 1998; Miller *et al.*, 2007). The benefits of the use of microspheres are that they allow for a quantitative measure of regional blood flow at given time points. The use of flow probes placed around the carotid artery give a continuous and quantifiable measure of cerebral blood flow, but gives no information on regional perfusion.

One of the requirements of the experimental protocol was to have a continuous but non-invasive measure of cerebral perfusion. For the studies detailed in Chapter 6 it was decided to use a piezoelectric ultrasonic crystal transducer, placed directly above the sagittal sinus to provide an indication of cortical perfusion, as done previously by us [see (Yan *et al.*, 2009)]. Although ultrasound techniques do not provide a quantitative measure of blood flow, we decided against using flow probes placed around the carotid arteries because of the risk that these might eventually mechanically interfere with blood flow to the fetal head, particularly since some of the fetuses were to remain *in utero* until the onset of labour. The ultrasonic transducers (and ECoG leads) are attached externally to the brain, and at post mortem they were easily removed without compromising fetal brain structure.

The piezoelectric ultrasonic crystal transducer was connected to a Directional Pulsed Doppler Flowmeter (545C-5, Bioengineering; The University of Iowa, Iowa City, IA). The signal derived from the piezoelectric ultrasonic crystal transducer is the maximum blood flow velocity, calculated from the shift of the ultrasound frequency which is directly proportional the mean

velocity of red blood corpuscles in the vessel being insonated. The Directional Pulsed Doppler Flowmeter used to receive the signal was calibrated (by the manufacturer) at 0.5 V/KHz of Doppler shift, and has a transmitter frequency of 20,000 KHz.

Ideally velocity (based on the sound) of blood flow (mm/sec) could be calculated using this system: $V = [(F_d*C)/(2*F_o*CosA)]$ where Fd = doppler shift frequency: 0.5 V/KHz, C = velocity of sound in blood (1,565,000 mm/sec), F_o = transmitter frequency (20,000 KHz) and A = angle between the sound beam and the transducer. For blood vessels that are approximately circular and where the diameter is known or measured, it is possible to derive the actual velocity of blood flow. However, this is not possible for the sagittal sinus due to its irregular shape; therefore this angle cannot be accurately determined hence a true 'velocity' measurements cannot be calculated.

The distance ('range') from the transducer that produced the maximum signal was calibrated from a voltage (V) to cm (0 cm = minimum range, 1 cm = maximum range) and adjusted to ensure that peak velocity (maximum output voltage) was always being measured. This signal was then averaged into 10 min epochs, and expressed as a percentage change from basal (-6 h to prior to UCO). The phasic and mean signals were also recorded (Figure 2.6).

2.5.1.4 Induction of fetal asphyxia – umbilical cord occlusion

Fetal asphyxia was induced by completely occluding the umbilical cord for ten minutes. This was achieved by injection of an appropriate amount (~2 – 3 ml) of sterile distilled water (dH$_2$O) into the cuff; this volume was determined at surgery, and was seen to produce complete occlusion of the vessels in the umbilical cord. MAP and HR were closely monitored, if MAP dropped below 20 mmHg, the sterile water was quickly withdrawn from the occluded cuff, to stop the occlusion immediately. Previous studies in our laboratory and by others have shown that the late gestation ovine fetus (~130 GA) can tolerate a maximum of 10 min complete UCO;

however when fetal MAP falls below 20 mmHg the fetus may not recover (Mallard *et al.*, 1994; Bennet *et al.*, 1998; Castillo-Melendez *et al.*, 2004).

Comment: The duration of 10 minutes of UCO was chosen as this is the longest the near term fetus can tolerate, recover and survive. Ligation of the fetal carotid artery or repeated UCO were possible also but not chosen, as we did not aim to investigate responses to a focal insult or aim to mimic 'labour' contractions.

2.5.2 Blood sampling

Fetal arterial blood samples (3 ml) were taken using sterile syringes; at -1 h, -5 min, +5 min, +9 min, +30 min, +1 h, +2 h +4 h, +6 h, +8 h, +10 h, +12 h (time 0 = start of UCO) and then daily until the ewe went into labour. A 5 ml syringe was connected to the fetal arterial catheter via a three-way stopcock to withdraw the heparinised saline from the catheter and a further 2 – 3 ml of fetal blood. A new 3 ml syringe was connected and 3 ml of blood sampled. The catheter was then cleared by pushing the blood back into the fetus in a pulsatile manner, from the original 5 ml syringe, and an additional 2 – 3 ml of heparinised saline was flushed into the catheter with a new syringe. After blood sampling, the syringe was capped to prevent contact of blood with air and kept on ice until further measurements could be performed.

Whole blood (95 µl) was used for the immediate analysis of blood gases pO_2 (mmHg), pCO_2 (mmHg), sO_2 (%), as well as pH, total haemoglobin (tHb; g/dL) and haematocrit (Hct; %) using an ABL 700 blood gas analyzer (Radiometer, Denmark). Fetal arterial glucose (mmol/L) and lactate (mmol/L) concentrations were also analysed in whole blood. Air bubbles were removed from the syringe to prevent inaccurate readings and to avoid further oxygenation of collected blood. Sample readings were corrected to the expected fetal body temperature of 39°C. The remaining blood was placed in EDTA tubes (Sarstedt, Australia) containing 50 µM indomethacin and centrifuged at 1500 g for 10 min at 4°C. The plasma was removed and
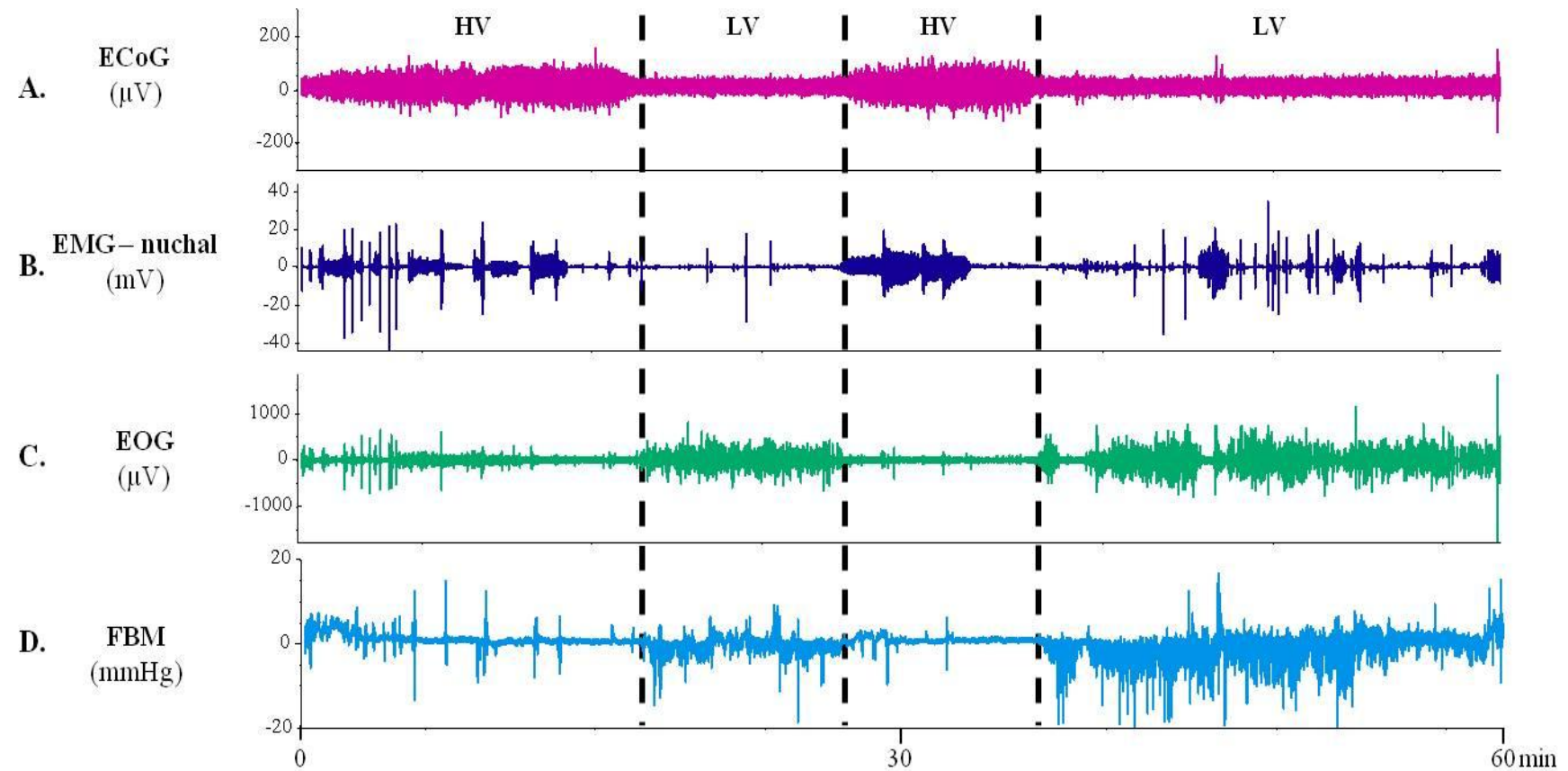
Figure 2.5: Fetal behavioural states in late gestation fetal sheep recorded on PowerLab. 130 day GA fetal behavioural recordings (ECoG (A), EMG-nuchal (B), EOG (C), FBM (D) from PowerLab recorded on Chart 5 Software. High voltage (HV) ECoG activity corresponds with EMG – nuchal activity, and no ocular muscle activity or fetal breathing movements (FBM). Low voltage (LV) ECoG activity corresponds with no EMG – nuchal activity but active EOG muscle activity an FBM.
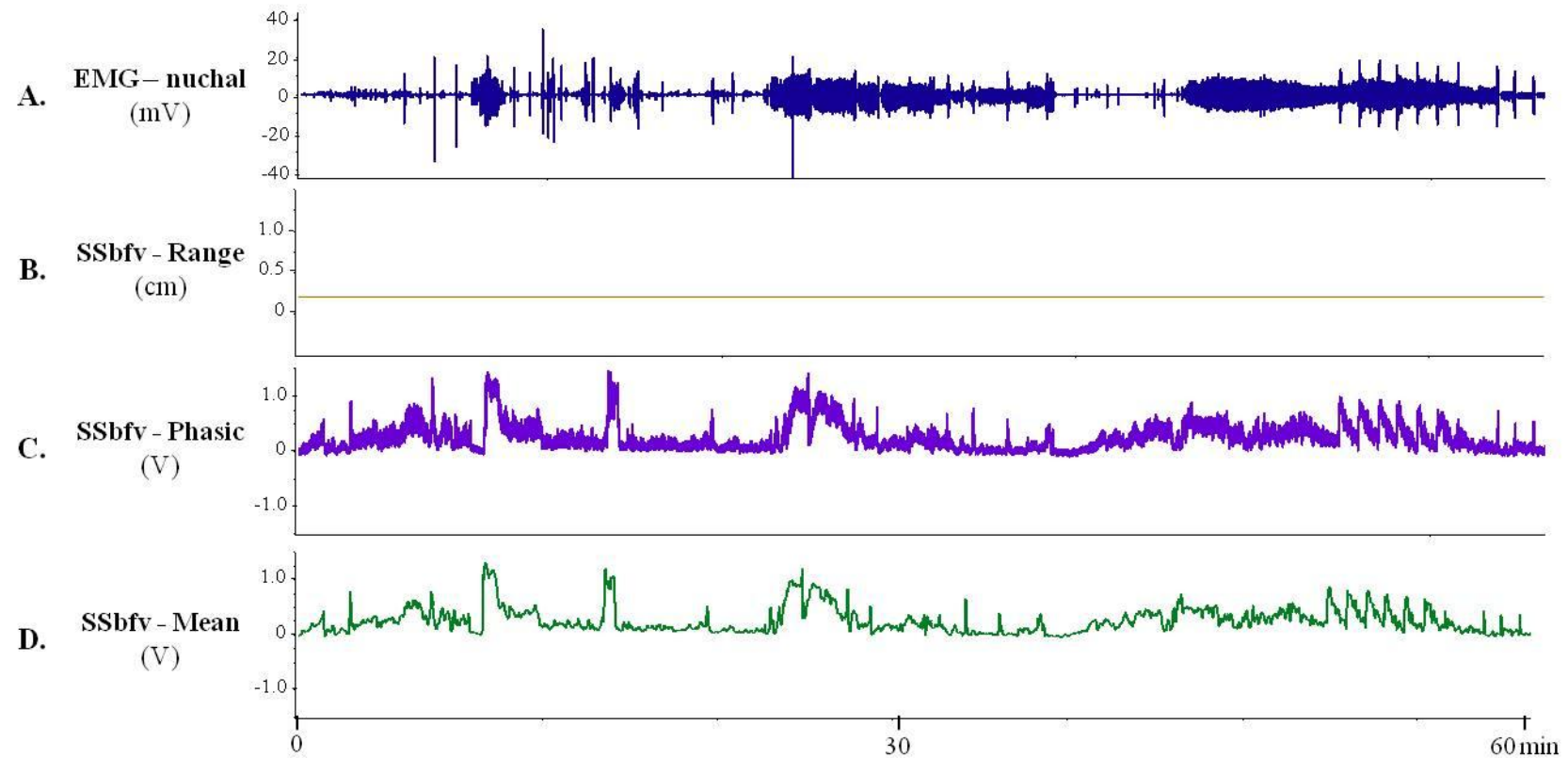
Figure 2.6: Sagittal sinus blood flow velocity recorded on PowerLab. 130 day GA fetal EMG-nuchal and sagittal sinus blood flow velocity (SSbfv) recordings (EMG-nuchal (A), SSbfv - Range (B), SSbfv - Phasic (C) and SSbfv – Mean (D) from PowerLab recorded on Chart 5 Software. SSbfv – Range was set at a constant for the duration for the experiment for each fetus. Peaks of SSbfv Phasic and Mean signals show increased EMG-nuchal signal.

divided into three aliquots (500 µl) placed in 1.5 ml eppendorf tubes, and stored at − 20°C until required for analysis of cortisol (Figure 2.7).

2.5.3 Signs of labour

The chronic monitoring of the fetus following a Sham UCO (control) or UCO concluded at 145 days GA or once the ewe was in labour. It was important to closely monitor and determine when the labour onset as the fetus was chronically instrumented we did not want the ewe to undergo parturition and deliver the fetus.

A few days prior to labour the ewe's vulva begins to change from light pink to dark pink and swollen, her udders also become larger (filling with colostrums). In the final 24 h (prior to labour) the ewe's behaviour also changes, she becomes restless, starts to dig a nest (for the lamb) and becomes disinterested in food and her surroundings. Once her water breaks (mucous secretions), under normal conditions, the front hooves of the lamb will come out first. In most cases we attempted to conduct a post mortem on the ewe once her water had broken.

We also used other indicators such as pressure changes (from the amniotic catheter which reflected uterine contractions; (Figure 2.7), and changes in fetal blood gases (decrease in sO$_2$). In sheep, the fetal hypothalamo-pituitary-adrenal-axis triggers the initiation of labour (Magyar et al., 1980; Unno et al., 1998); this is reflected with an increase in fetal plasma cortisol secretion in the days preceding labour (Bassett & Thorburn, 1969; Magyar et al., 1980; Challis & Brooks, 1989). Plasma cortisol concentrations were determined using a radioimmunoassay after the conclusion of the experiment (Figure 2.7), so were used to confirm onset of labour.
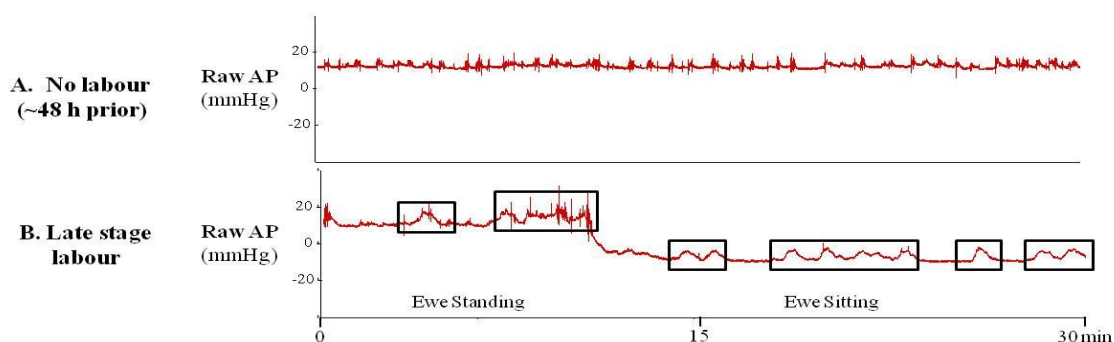
Figure 2.7: Amniotic pressure recording. Raw amniotic pressure (AP) trace during the absence (A) and presence (B) of labour contractions. The consistent peak and troughs in amplitude (B) is suggestive of contractions (shown in black boxes), regardless of the ewe's position (standing or sitting).

2.6 ANALYSIS OF FETAL HAEMODYNAMICS AND BEHAVIOUR

All parameters were recorded from the day prior to experimentation until the ewe went into labour. Time 0 represents that start of the Sham (Control) or actual UCO. All data were analysed in 10 min epochs starting from 6 h prior to UCO (or Sham UCO) until the end of the experiment using Chart 5 (v5.5.5, ADInstruments, Australia).

2.6.1 Fetal blood pressure and breathing movements

Analysis of fetal mean arterial blood pressure and heart rate were calculated by taking the mean values from each successive 10 min epoch. FBM were quantified by calculating the average amplitude and the incidence (minutes breathing/10 minute epoch) throughout the record.

2.6.2 Fetal behavioural states

The ECoG record was divided into epochs of high and low voltage activity (Boddy *et al.*, 1974; Clewlow *et al.*, 1983) using the mean amplitude for each type of activity obtained over at least 6 h of control (i.e., pre-UCO) recording. The results are expressed as the percentage of the time that each activity occurred during consecutive 2 h periods of the experiment. Very low amplitude ECoG activity (hereafter referred to as sub-low voltage) occurred after UCO in most

fetuses and was defined as an amplitude sustained for at least 1 min that was <25% of the amplitude of normal low-voltage ECoG activity (Yan *et al.*, 2009; Yawno *et al.*, 2010).

Both EOG and EMG-nuchal activity were also analysed in the same manner, the average amplitude for successive 10 minute epochs was determined. From the pre-UCO recordings (-6 h), the amplitude of activity (high amplitude) and no activity (low amplitude) were determined. This allowed for the determination of when nuchal or ocular muscle activity was present of absent. The percentage of time spent in each activity for 2 h consecutive periods was determined.

2.6.3 Sagittal sinus blood flow velocity

A mean value (phasic amplitude) of sagittal sinus blood flow velocity was obtained for successive 10 min epochs across the entire recording period of each experiment (i.e., - 6 h to end of experiment). The data for each fetus were then expressed as a percentage change from basal of the amplitude calculated for the 6-h period immediately prior to the time of UCO (or sham) to account for different signal levels between fetuses.

2.7 CORTISOL RADIOIMMUNOASSAY

2.7.1 Radioimmunoassay

Radioimmunoassay (RIA) is a technique widely used to determine concentrations of antigens (such as hormones) in blood, plasma and tissue. Yalow and Berson (1960), developed this specific and sensitive method to accurately measure hormones (insulin) levels in blood.

RIAs are a competitive assay and involve a radioactive labeled antigen (tracer), an antibody (antiserum) and the unknown concentration of antigen in blood, plasma or tissue (sample). The sample and tracer "compete" for binding sites on the antiserum. If concentrations in the sample

are high, more of the sample is bound to the antiserum, displacing the tracer. All bound (sample or tracer to antiserum) and unbound antigens are separated, and the remaining amount of radioactive tracer is measured (Figure 2.8). Using known standards a binding curve is constructed, allowing the concentration in unknown samples to be determined. Cortisol was measured in fetal plasma after extraction with dichloromethane as previously described (Bocking *et al.*, 1986). All reagents used for this assay are listed in Appendix 1.

2.7.2 Preparation of ^{3}H-cortisol tracer and standards

Cortisol tracer (250 µCi of [1,2,6,7 ^{3}H] cortisol (Amersham Biosciences, Australia) was made up in 5 ml of toluene-ethanol (9:1) and stored at -20°C until required. Approximately 30 µl of tracer was evaporated under air at 37°C and reconstituted in 10 ml of cortisol assay buffer (0.5M phosphate buffer (PB), pH 7.4). 100 µl was run on the β counter, ideal tracer counts was 10,000 cpm.

Cortisol standards (0 – 25 ng/ml) were produced by diluting cortisol stock solution (Hydrocortisone 5 µg/ml in 100% ethanol; Sigma Chemical Company, USA) in ethanol. In duplicate, 100 µl of each standard was aliquoted and mixed with 1 ml dichloromethane (CH$_2$Cl$_2$; Merck Damstadt, Germany) and evaporated under air at 37°C.

Maternal ovine plasma was used for recovery (no ^{3}H-cortisol) and total recovery (^{3}H-cortisol) samples. These were important to allow for an accurate calculation of the percentage of recovery that occurred in each assay.

In each RIA, two sets of quality controls were included; these were ovine plasma samples that contained a known concentration of cortisol. Blanks containing dH$_2$O and CH$_2$Cl$_2$ were also included in each assay.
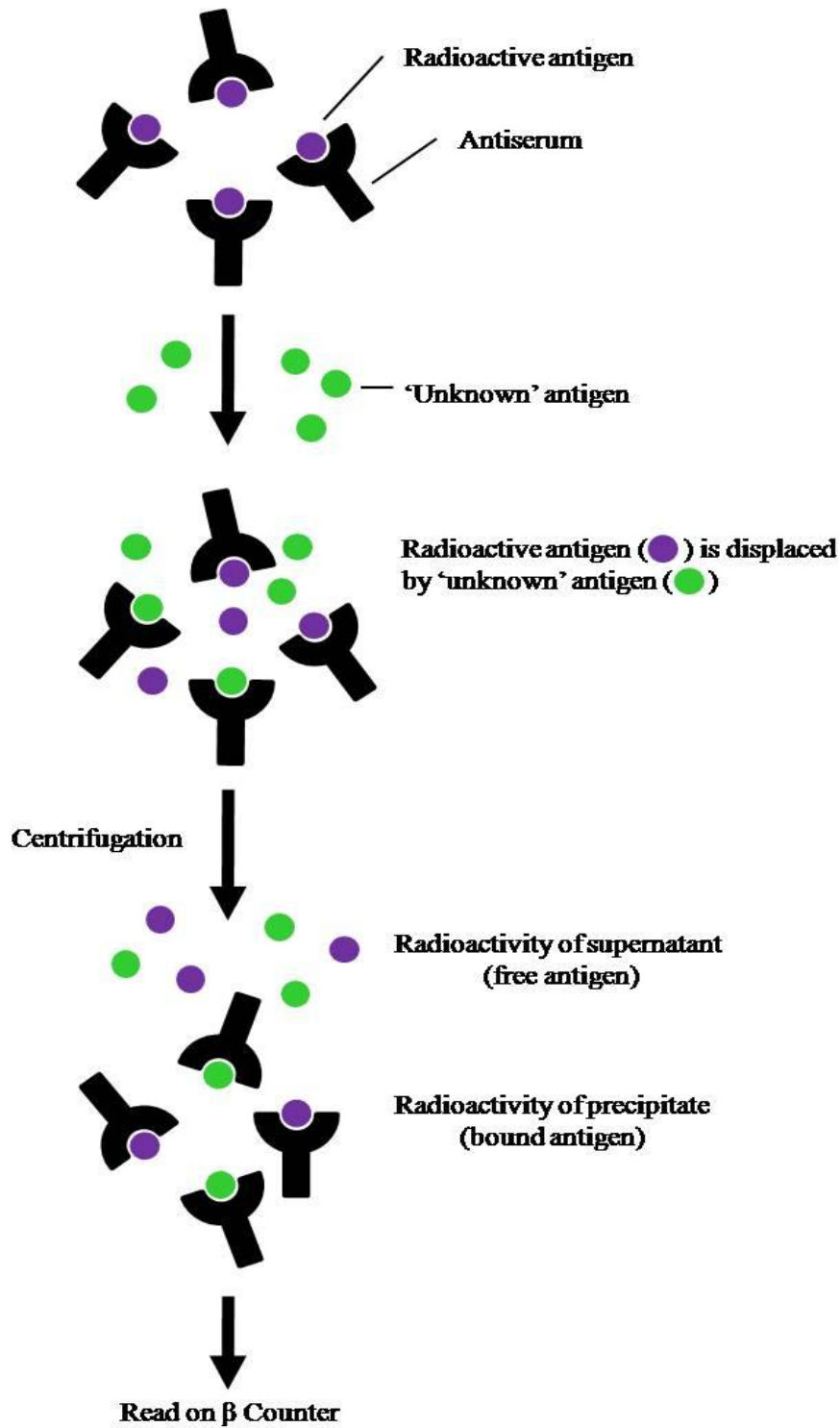
Figure 2.8: Illustration of radioimmunoassay. The radioactive and 'unknown' antigens compete for binding to the antiserum. As concentration of the unknown antigen (sample) increases, the radioactive antigen is displaced from the antiserum. Radioactivity measured is inversely proportional to the amount of 'unknown' antigen.

2.7.3 Extraction of cortisol

In glass tubes, cortisol was extracted from fetal plasma (100 μl in duplicate) with dH_2O (100 μl) and CH_2Cl_2 (2 ml). Plasma samples were vortexed thoroughly until two distinct layers were observed; the top layer was discarded, the lower (organic) layer (~1 ml) was transferred to plastic tubes and evaporated under air at 37°C.

2.7.4 Radioimmunoassay

Cortisol antiserum was raised in sheep (donated by Dr. R.I. Cox, Division of Animal Production CSIRO, Australia). Lyphilisied antiserum was reconstituted to 1:50 in 50% glycerol and stored at -20°C. The cross reactivities of the antiserum are represented in Table 2.2. Cortisol assay buffer (100 μl), antiserum (100 μl; working dilution; 1:5000), bovine γ-globulin (100 μl; at a concentration of 8 mg/ml; Calbiochem, Darmstedt, Germany) and ^{3}H-cortisol (100 μl) were added to all sample and standard tubes, vortexed, covered with paraffin and incubated overnight at 4°C. The following day, 1 ml of 22% polyethylene glycol (PEG) was added, vortexed and centrifuged (1800 g) for 15 min at 4°C to separate bound hormone from the unbound hormones. The supernatant was aspirated, the pellet was resuspended in cortisol assay buffer (200μl) and scintillation fluid (2 ml; Ultima Gold, Perkin Elmer, Australia) was added. Samples were vortexed, and placed in the β-counter (Beckman LS 3801, Beckman Instruments, USA) to determine radioactivity. Cortisol concentrations were calculated from the standard curve and a mean of duplicates was determined for each sample. The intra and inter-assay coefficient of variance were 15.4 and 24.6, the sensitivity of the assay was 0.43 ± 0.06 ng/ml and the average recovery was 91.9 ± 2.3 %.

Table 2.1: Cortisol antiserum and cross reactivity with closely related steroids. Adapted from (Bocking *et al.*, 1986).

Steroid compound	Cross reactivity (%)
Cortisol	100
Cortisone	20.5
17α-hydroxy progesterone	13.9
Corticosterone	1.00
Progesterone	0.57
Betamethasone	0.50
4-androsterone-3,17,dione	0.03
Testosterone	0.02
Dexamethasone	0.01

2.8 POST MORTEM AND TISSUE COLLECTION

2.8.1 Animal euthanasia and fetal delivery

For the fetal brains used in Chapter 3 and 4, these were collected 24 h and 48 h following UCO. For Chapter 5 and 6 the experiment endpoint was classified when the ewe went into labour or at 145 days GA. Both ewe and fetus were humanely killed according to the code of practice by intravenous injection of pentobarbitone sodium (Lethabarb, Virbac Pty Ltd, Australia) to the ewe. In the postnatal behavioural study detailed in Chapter 6, the ewe and lamb were euthanized approximately 24 h following birth. Ewes were examined for the absence of pupillary and somatic reflexes before proceeding further. The fetus was removed through an incision made along the abdomen and uterus of the ewe. A detailed description of any merconium staining, amount of amniotic fluid, as well as the condition and position of the umbilical cord were all noted. The umbilical cord was tied off and the fetus was immediately removed and weighed, crown – rump (nose tip to the end of the sacral spine [where tail begins]) length was measured, and the sex of the fetus was also noted.

2.8.2 Collection of the fetal brain

The fetal skull was exposed with a midline incision extending from between the eyes to cervical spine to allow for the fetal brain to be removed. Rongeurs were used to remove the top of the cranial vault. Once the dorsal surface of the brain was exposed, the spinal cord (at the level of cervical 1 or 2), olfactory bulb, optic chiasm and cranial nerves were cut; the brain was cleared of the dura, collected and weighed. The cerebellum was then removed and weighed separately.

The fetal brain was divided sagittally along the midline, the left hemisphere was further divided into major anatomical regions and quickly snap-frozen in liquid nitrogen and stored at -80°C for later analysis, (to use for rtPCR [Appendix 6], western blots or VEGF ELISA). The right hemisphere was cut coronally at distinct landmarks (beginning of lateral ventricle, beginning and end of thalamus/hypothalamus), cerebellum and brainstem (Figure 2.9 A). These were then immersion fixed in 4 % paraformaldehyde (PFA) solution for 48 h. The tissue blocks were then processed further for paraffin embedding and sectioning (Section 2.9).

The use of fresh frozen sections does preserve the antigens within the tissue; however the largest proportion of material for immunohistochemistry is formalin-fixed and paraffin-embedded. Paraffin sections do produce satisfactory results for the demonstration of majority of tissue antigens with the use of several different antigen retrieval techniques. Frozen brain sections were not trialed in this thesis when optimizing new immunohistochemistry protocols, as preliminary immunohistochemistry trials showed good vessel morphology (particularly laminin immunohistochemistry). Thus the use of paraffin tissue was chosen in these studies to help preserve tissue morphology. Additional to this project, the tissue sections were also sent to collaborators in Madrid, Spain (with paraffin embedded sections preferable to send internationally).
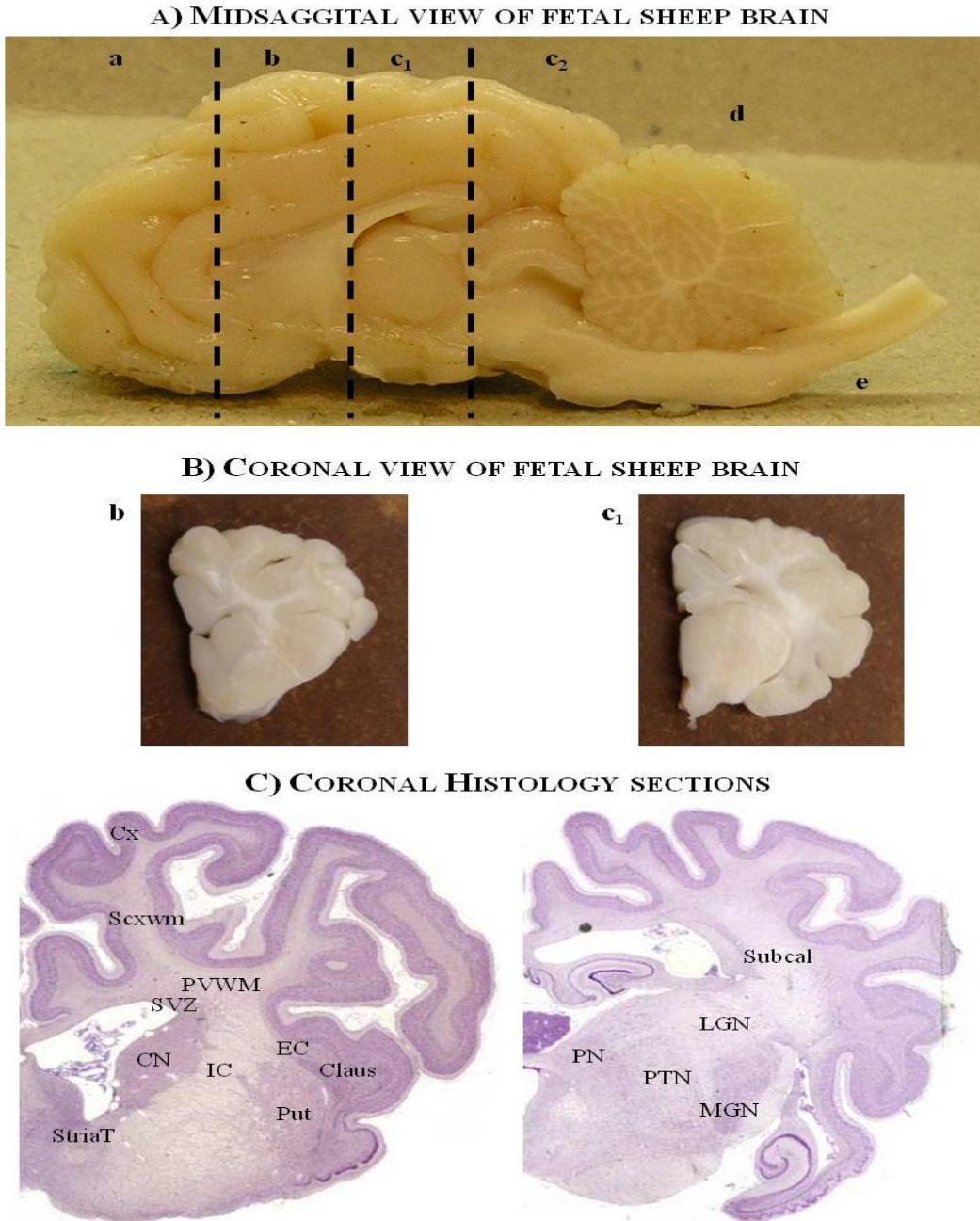
Figure 2.9: Fetal sheep brain dissection and histology. Midsagittal view of a near term fetal sheep brain (A). Dashed lines indicate cuts made to obtain various blocks (labelled a, b, c1, c2, d and e). Coronal sections of block b and c1 (B). Coronal histological sections of b and c1 indicate areas that were analysed. Block b; cortex (Cx), subcortical white matter (Scxwm), periventricular white matter (PVWM), subventricular zone (SVZ), stria-terminalus (StriaT), caudate nucleus (CN), internal capsule (IC), external capsule (EC), Claustrum (Claus) and putamen (Put). Block c1; Subcallosal bundle (SubCal), Lateral geniculate nucleus (LGN), medial geniculate nucleus (MGN), pretectal nucleus (PN) and posterior thalamic nuclear group (PTN). (C) Coronal histology sections have been reproduced and adapted with permission from http://www.brains.rad.msu.edu , supported by the US National Science Foundation.

2.8.3 Tissue collection

Once the brain was collected the fetal heart, lungs, liver, adrenals, brown fat and kidneys were dissected and weighed. The fetal heart, brown fat and one kidney and adrenal were snap frozen in liquid nitrogen. The other adrenal was fixed in 4% PFA for 48 h and processed for paraffin embedding with the brain.

2.9 BRAIN HISTOLOGY AND IMMUNOHISTOCHEMISTRY

2.9.1 Fixation of the fetal brain

The tissue blocks were placed in between biopsy pads and put into macro embedding cassettes (Tissue-Tek, Sakura Finetek, USA) and dehydrated in 70%, 90% and three repetitions of 100% ethanol (Chem Supply Pty Ltd, Australia) for at least 2 h in each solution. A longer cycle was chosen as blocks of tissue were thick and this allows for more time to adequately penetrate the whole tissue for even fixation. Dehydrated tissue blocks were then immersed twice into 100% cholorform and once in xylene (Merck and Co Inc, USA) for 2 h. The tissue was then placed into hot paraffin wax (Tissue-Tek, Sakura, USA) for 2 h under vacuum (Shandon Histocentre 3. Thermo Electron Corporation, USA). This processing was performed by Mr I. Boundy and Ms. S. Tombs at the Department of Anatomy and Cell Biology, Monash University.

2.9.2 Paraffin embedding and tissue sectioning

Tissues were manually embedded into paraffin wax. Using a rotary microtome, paraffin tissue was cut into 10 μm sections, placed on a warm water bath (~40 – 45 °C) to allow for tissue to expand and be mounted on Superfrost Plus slides (Mezel-Glaser, Germany) for examination of brain histology and immunohistochemistry.

2.9.3 Fundamentals of Immunohistochemistry

Immunohistochemistry is a technique used to visualise the location and distribution of specific antigens through antigen-antibody interactions. To achieve accurate and reliable results many factors must be considered and optimised for the species and tissue type of choice, as well as for the antibody of interest. There are two approaches to detecting antigens in tissue, a *direct* and *indirect* method. The *direct* method involves a labelled primary antibody that reacts directly with the antigen in the tissue. It is simple and quick and involves only one antibody; however this method is not sensitive enough.

The *indirect* method involves an unlabelled primary antibody which reacts with the tissue antigen. This is then labelled with a secondary antibody that is raised against the immunoglobulin G (IgG) species the primary antibody has been raised in. Normally the secondary antibody is biotinylated, this allows for it (biotin) to react and bond with a high affinity to streptavidin conjugated with horseradish peroxidise (Strep-HRP). This reaction is colourless, so the addition of diamino 3,3' diaminobenzadine (DAB) results in the biotin-Strep-HRP complex oxidising the DAB chromagen resulting in a brown stain (Figure 2.10). The *indirect* method is widely used as it amplifies the signal of the antigen-antibody complex leading to greater specificity of the staining (for more detail refer to Section 2.9.9). All reagents used for immunohistochemistry protocols are detailed in Appendix 2.
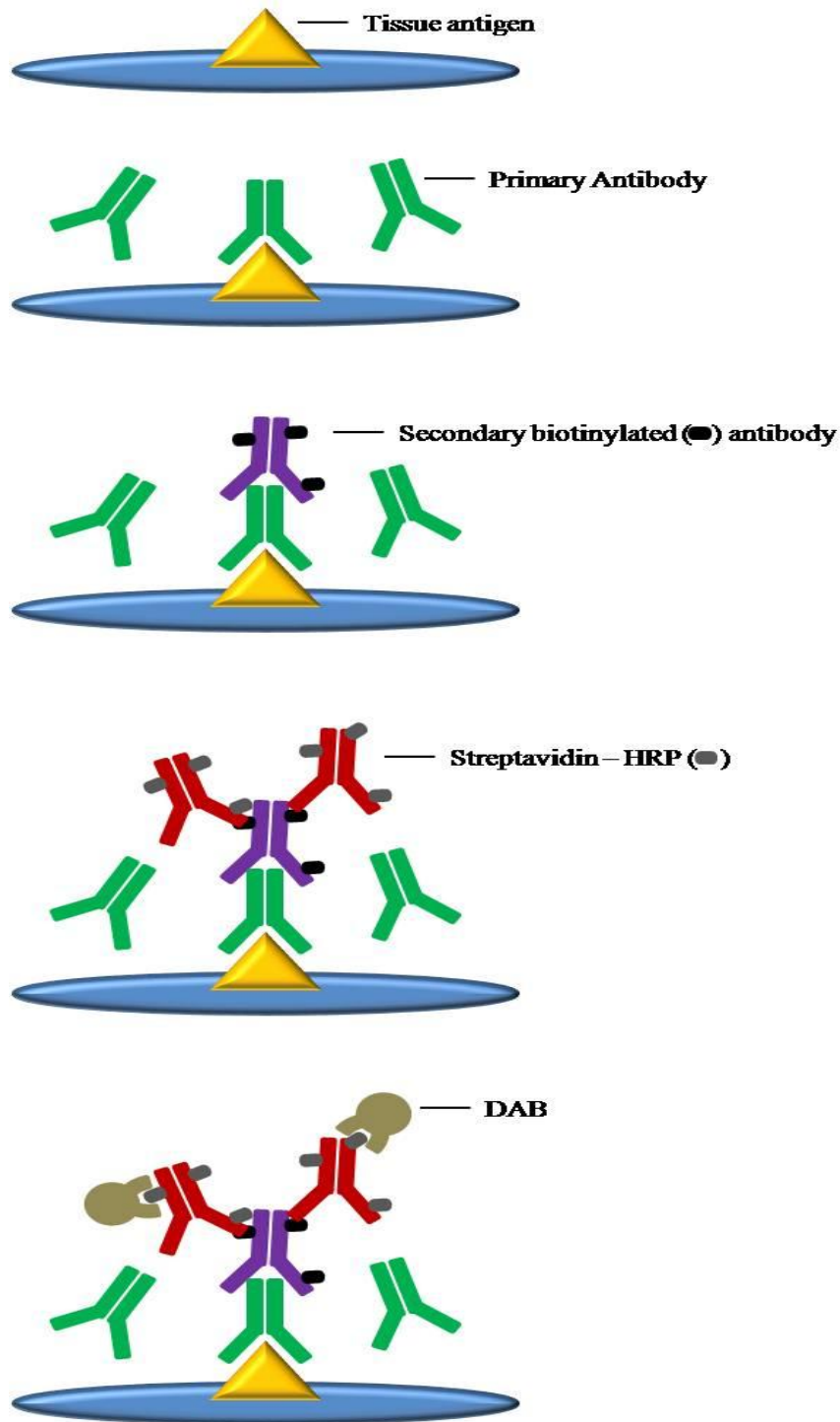
Figure 2.10: Illustration of *indirect method* of immunohistochemistry. Primary antibody is added to tissue (A, B), biotinylated secondary antibody binds to the primary (C), streptavidin-HRP binds to secondary antibody (D) and finally diamino3,3' diaminobenzadine (DAB) chromagen is added – amplifying the antibody-antigen complex.

2.9.4 Tissue fixation

As previously mentioned, the fetal sheep brain tissue in this thesis were immersion fixed in 4% PFA, a formalin based fixative. PFA is polymerised form of formaldehyde, when heated during preparation with 0.1M PB (pH 7.4) it depolymerises back to formalin. Adequate fixation, duration and fixative choice, is required to stabilize tissues from degradation and is vital for achieving good histology and immunohistochemistry staining. Fixation occurs by the formation of cross links between proteins in the tissue. PFA is a widely chosen fixative for brain tissue as it is well tolerated by tissue, provides good penetration (particularly for large tissue), allows for long term storage, maintains structural integrity of cells in tissue thereby providing optimal tissue preservation.

2.9.5 Antigen retrieval

The cross links formed during fixation with PFA can 'mask' antigen binding sites within the tissue. To overcome this problem, chemically treating the tissue with proteases or heat exposure by microwave radiation can be used to break bonds between antigens and surrounding proteins to free potential binding sites, resulting in increased reactivity and intensity in the signal (Shi *et al.*, 1991; von Wasielewski *et al.*, 1994).

In brief, *heat induced epitope retrieval* uses a microwave, water bath or autoclave to heat sections in buffer. Citric acid buffer (pH 6.0) is widely used and is suitable for most antibodies, tris buffered saline (TBS) can also be used when a higher pH is needed (9.0 or 10.0), generally heating sections between 5 – 30 min with an additional 30 min in the hot buffer is sufficient.

Proteolytic induced epitope retrieval uses proteases such as Proteinase K, trypsin and pepsin, normally heated to 37°C in an oven. This is effective for membrane antigens but can destroy tissue morphology. A combination of both retrieval methods maybe used particularly in double and triple labelling protocols. For both methods, care must be taken to assure tissue sections do

not dry out during antigen retrieval. In this thesis, both methods were done (based on cell type and antibody affinity).

2.9.6 Tissue permeability

Permeability of tissue is important, particularly in brain sections due to the high lipid content. The use of detergents such as Triton X-100 and Tween-20 (both purchased from Sigma Aldrich, USA) act to solubilise membrane lipids allowing for a greater number of antigen sites for the antibody to bind to. These detergents (one of) can be added to PBS when rehydrating sections, during rinses, serum blocking and in antibody diluent solution. Concentrations used vary between 0.1 – 3% and were optimised for each required antibody.

2.9.7 Blocking

Inadequate or delayed fixation of tissue can lead to false positive staining occurring, this can occur especially in the centre of large blocks where fixative has not entirely penetrated the block. Background staining due to specific or non-specific staining can commonly occur in immunohistochemistry. If tissues are made too permeable, non specific binding of Ig to proteins in the tissue, by hydrophobic and electrostatic forces, can also occur. To overcome these, a blocking step is included by adding a serum block from the species in which the secondary antibody is raised in. If a rabbit anti-mouse secondary antibody was used, normal rabbit serum (NRS) was included in the serum block, if goat anti-rabbit was the secondary antibody, normal goat serum (NGS) was used, these were both combined with serum bovine albumin (BSA).

Endogenous peroxidises can also be a problem and lead to a 'dirty' signal due to the use of HRP. Pre-treatment with hydrogen peroxide (H_2O_2) in methanol or dH_2O prior to primary antibody incubation will eliminate this.

Autofluorescence can also cause issues of non-specific background during fluorescent double labelling techniques. Reducing autofluorescence by pre-treating sections in sodium borohydride

(NaBH$_4$) overcomes this and is particularly beneficial for tissues fixed in PFA (Clancy & Cauller, 1998).

2.9.8 Antibody specificity

Primary antibodies used in immunohistochemistry protocols can be either monoclonal or polyclonal. Monoclonal antibodies are raised in a specific cell line so are designed to recognize only one epitope of the antigen of interest. They are highly specific for the antigen they are raised against and tend to result in less background, hence exhibit greater specificity. Polyclonal antibodies are raised in whole animals recognise a number of epitopes providing good antigen-antibody binding particularly when masking of the binding site may have occurred due to fixation. In this thesis, both types of antibodies were used, depending on availability, binding and specificity. Secondary antibodies used in this thesis were biotinylated and raised against the species the primary was raised in.

2.9.9 Immunohistochemical staining

2.9.9.1 Single label

As previously described (Section 2.9.3, Figure 2.10), the *indirect method* of immunohistochemistry is widely used and involves an amplification of the antigen-primary antibody binding. All single labelling immunohistochemistry in this thesis used this method. Following incubation with the biotinylated secondary antibody, an enzymatic reaction must occur to amplify the signal. Strep-HRP forms a strong bond with the biotin (Figure 2.10). An avidin-biotin complex may also be used; however this is less sensitive compared to the use of Strep-HRP.

To allow for visualisation of the antigen-antibody complex, the peroxidase is developed by the addition of the substrate chromagen. HRP requires an electron donor (from a chromagen) to form an enzyme-substrate complex. Biotin-Strep-HRP is reacted with DAB chromagen, an

electron donor, resulting in oxidation of DAB at sites that contain peroxidise activity, a brown colour formed (Figure 2.10 and 2.11). The use of DAB is known to be more sensitive, it is easy to prepare, insoluble to organic solvents such as ethanol (used in dehydrate process at the end of immunohistochemistry) and allows for a permanent counterstain (De Jong *et al.*, 1985).

2.9.9.2 Double label - Fluorescent

Double labelling techniques are widely used to identify which cell type is expressing the particular antigen/protein of interest. In this thesis, fluorescent labelled secondary antibodies (Alexa Fluor©, Invitrogen) were used in Chapter 4. Two primary antibodies that recognize various antigens of interest were used, with corresponding fluorescent-coupled secondary antibodies. The initial steps of immunohistochemistry (Figure 2.11) are the same; however blocking autofluorescence is required (Section 2.9.7). Ideally, both primary antibodies are raised in different species, allowing for both to be mixed into one solution and applied simultaneously in one step. If this was not possible, the first primary antibody was incubated, labelled with secondary antibody, and then repeated (Figure 2.11). Specific protocols and details of primary and secondary antibodies used are detailed in relevant chapters and in Appendix 3.

2.9.10   Optimisation

Optimisation was done for new antibodies used in this thesis (vascular endothelial growth factor (VEGF, VEGFR-2), angiopoietin (angpt) and laminin). Specifications from antibody data sheets were followed. However each antibody was optimised specifically with antigen retrieval (solution, time for heat and cool), permeabilsation, blocking concentration and antibody (primary and secondary) concentration and duration. Where possible, a positive control (Spiny Mouse placenta – kindly donated by Dr. Hayley Dickinson, The Ritchie Centre, Monash Institute of Medical Research) was run to identify positive and true staining.

2.9.11 Microscopy, cell counts and analysis

Sections were viewed at x400 magnification (unless otherwise stated) using light or fluorescent (red and green filters) microscopy (Model BX41; Fluorescent Burner Model U-RFL-T, both Olympus, Australia), equipped with a DP25 (Olympus, Japan) digital camera. Slides were blinded and three fields of view for each brain region were analysed in each section, for two adjacent sections of each brain region were examined. The average value for each brain region, for each fetus was obtained from the data of six fields of view and the results were averaged across all animals within the same treatment group.

2.9.12 Limitations

The use of immunohistochemistry is valuable in understanding changes in regional expression and localisation of specific protein within tissue; however quantification is obtained from two-dimensional 10 µm sections. Blood vessel structure and morphology can be examined using both 2D and 3D techniques, for this thesis (Chapter 3) we chose to use immunohistochemistry. Although electron microscopy techniques or stereology would accurately represent three-dimensional structure, the facilities required for both these techniques were not available for this thesis. The data in this thesis (Chapter 4 and 5) provides a relative measure of the cell number for a given region. We believe that this approach is acceptable since the important comparisons to be made are between treatments groups. The use of western blotting techniques would also allow for quantification of protein within tissue. However for this thesis, immunohistochemistry was chosen to allow for localisation and regional variation across groups to be compared.
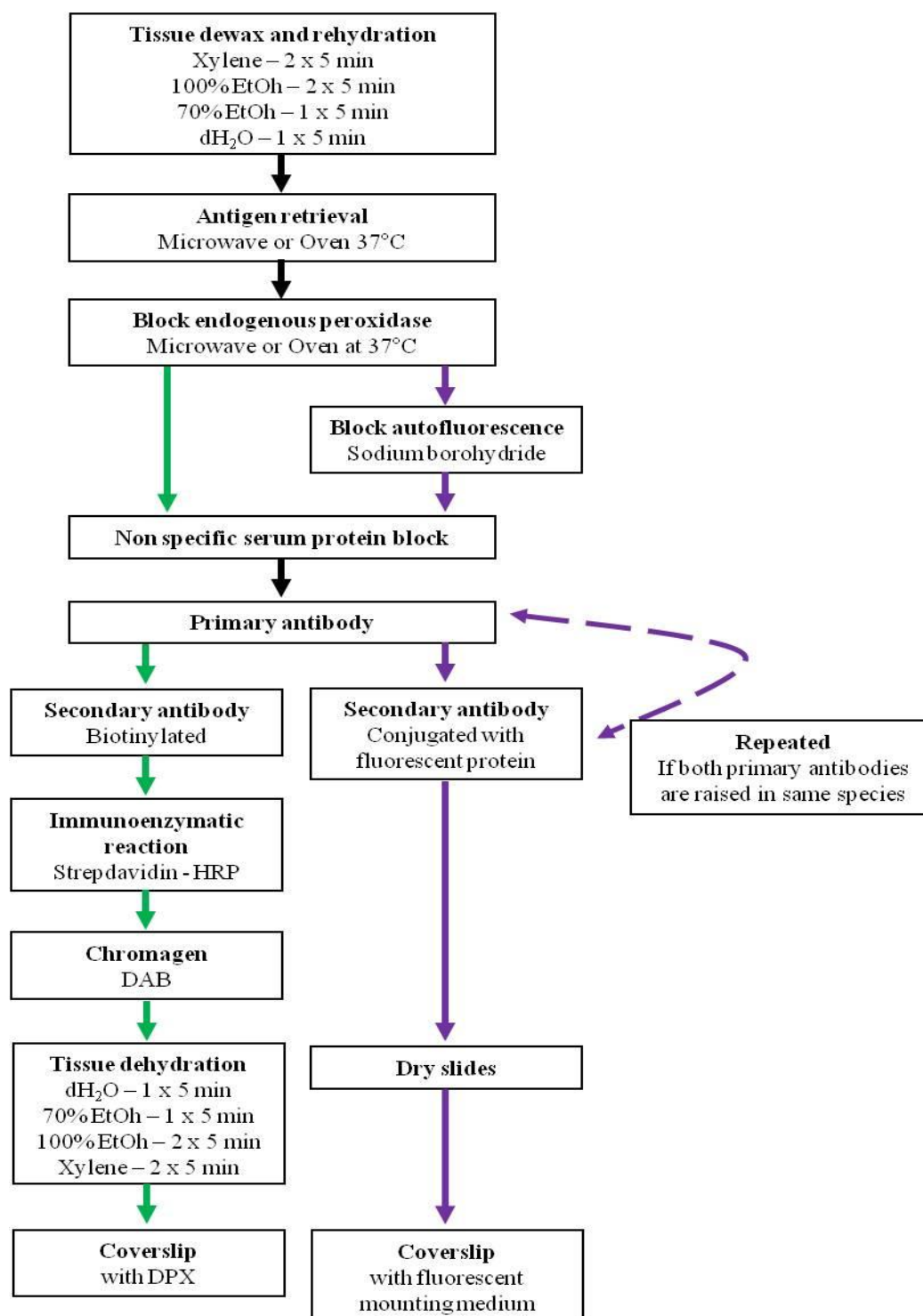
Figure 2.11: Immunohistochemistry protocol for single and double label techniques. General Immunohistochemistry protocol for single label (light microscopy, in green arrows) and double label (fluorescent microscopy, in purple arrows). Washes were done between each step, except between block and primary antibody incubation. Specific protocols are provided in each chapter.

2.10 STATISTICAL ANALYSIS

Data are presented as mean ± standard error of the mean (SEM). Firstly, a Shapiro-Wilks test for normality was conducted to see whether data was normally distributed ($p > 0.05$). If data met this assumption, a parametric test was run. If data was not normally distributed, data was then transformed (log_{10}, log_e and square root, if still failing normality a non-parametric equivalent test was conducted. A Levene's test for homogeneity of Variance ($p < 0.05$) was also conducted.

Immunohistochemistry data (Chapter 3, 4, 5), and fetal organ and body weight data (Chapter 5 and 6) were analysed using a One-Way analysis of variance (ANOVA), where significant, a Student Newman-Keuls post-hoc test was performed to see where significance existed. If normality was not reached, a non-parametric equivalent, Kruskal-Wallis test, with pairwise comparisons was conducted.

Fetal blood gases, cortisol, fetal behaviour (ECoG, EOG, EMG-nuchal, FBM) were all analysed using a Two-Way (Mixed Model) ANOVA for treatment (between groups) factor and time (within subject, repeated measure). If a significant interaction was obtain, further post-hoc analysis, a Bonferroni test was conducted to determine where statistical significance existed. Significance was always set at $p < 0.05$.

Statistical data were analysed using SPSS v18 for Windows, with significance set at $p < 0.05$. All graphs were made using GraphPad Prism Software for Windows (v5.03).

Chapter 3

CHANGES IN VASCULAR DENSITY AND

SMALL VESSEL MORPHOLOGY IN THE

LATE GESTATION FETAL SHEEP BRAIN

FOLLOWING UMBILICAL CORD

OCCLUSION.

TABLE OF CONTENTS

3.1 INTRODUCTION

Following an antepartum hypoxic event, devastating and permanent injuries that can occur in the fetal brain include germinal matrix-intraventricular haemorrhage (GM-IVH) and periventricular leukomalacia (PVL). The incidence of GM-IVH does not occur immediately but evolves over the first 24 to 48 h following birth (Tsiantos *et al.*, 1974; Kadri *et al.*, 2006). The presence of poorly perfused vessels and irregular capillary shape suggest a strong relationship between vascular supply and PVL (Takashima & Tanaka, 1978a). Late in gestation, hypoxia-ischemia predominantly results in injury of cortical gray matter, thalamic nuclei and subcortical haemorrhage (Cowan *et al.*, 2003; Van den Broeck *et al.*, 2007). The involvement and contribution of the vasculature to neonatal encephalopathy following hypoxia in the near term brain, has not been fully investigated.

Ballabh *et al.,* (2004a) highlighted the importance of understanding vascular changes such as vascular density and morphology in the human fetal brain and how this may contribute to the pathogenesis of periventricular white matter injury and GM-IVH. Their study focussed on investigating the anatomy of blood vessels in the germinal matrix, gray and white matter from mid-gestation to adulthood in the human brain. The main findings from this study were that the germinal matrix had a greater vascular density, possibly deeming it more susceptible to rupture. In contrast, white matter had the lowest blood vessel density which Ballabh *et al.,* (2004a) considered was a reason for some white matter regions (e.g. those near the ventricle) to develop leukomalacia and be vulnerable to ischemia-mediated injury.

Laminin is the major non-collagenous constituent of the basement membrane that separates endothelial cells from other brain cells. During the final stages of blood vessel development there is an up-regulation of laminin signalling (Timpl *et al.*, 1979; Risau & Lemmon, 1988; Milner & Campbell, 2002). As such, laminin has been widely used as a reliable marker of blood vessels to visualise and measure vascular density and morphology in many organs and tumours. Laminin immunohistochemistry is a simple technique that provides consistent staining with

minimal background (Eriksdotter-Nilsson *et al.*, 1986; Ballabh *et al.*, 2004a). Commonly two methods have been used to assess cerebral microvascular density; (i) densitometry assesses all positive staining (Eriksdotter-Nilsson *et al.*, 1986), and (ii) counting of microvessels, both automated and manual analysis (Fox *et al.*, 1995; Ballabh *et al.*, 2004a). Both techniques are widely used and validated, and will be used in this experimental chapter.

The assessment of the cerebral vasculature of late gestation fetal sheep has not been investigated before. Based on laminin as a marker of blood vessels, the first aim of this study was to provide a quantitative estimate of the vascular density in the fetal sheep brain. Secondly, the effects of umbilical cord occlusion (UCO) on the morphology of blood vessels in vulnerable brain regions following a single, severe bout of asphyxia in late gestation were investigated.

3.2 METHODOLOGY

The same fetal brains were used in both Chapter 3 and Chapter 4. Consideration was given to presenting all the data in one chapter however it was decided to separate these two chapters. This was done to allow a more detailed explanation of the assessment of vascular morphology techniques, analysis and laminin immunohistochemistry findings (Chapter 3), and the consequences of VEGF following UCO on cellular proliferation, alterations in blood brain barrier permeability and the possible influence of cortisol on the fetal brain (Chapter 4).

3.2.1 Animal surgery and experimentation

A detailed explanation of animal surgical procedures and experimentation is given in Chapter 2 (Section 2.4 and 2.5). Briefly, fourteen pregnant Border-Leicester ewes carrying a singleton fetus were used in this study. The use of these animals and all procedures had received prior approval from the School of Biomedical Science Animal Ethics Committee of Monash University. At 124-126 days gestational age (term is 146 days) surgery was performed under

aseptic conditions. An inflatable silastic cuff (type OC16, *In Vivo* Metric, Healdsburg, CA, U.S.A) was placed around the abdominal end of the umbilical cord, upon inflation this would cause complete cessation of blood flow in the cord (umbilical cord occlusion; UCO). The fetal femoral artery was catheterised to allow for blood sampling, fetal arterial blood pressure and heart rate measurements, and a large bore catheter was also placed in the amniotic sac to measure amniotic pressure.

On the day of the experiment, the umbilical cord was occluded completely for 10 min by inflating the cuff with 3 mL of sterile water (24 h post-UCO n=5, 48 h post-UCO n=4) or Control (sham UCO; n=5). Fetal haemodynamic responses were closely monitored, and if MAP dropped below 20 mmHg then UCO was stopped. Fetal arterial blood samples (0.5 mL) were taken before, during and after UCO to measure pO_2, pCO_2, O_2 saturation, pH and haematocrit using a Radiometer ABL5 analyser (Radiometer Medical A/S, Denmark), and blood glucose and lactate concentrations were measured by a YSI 2300 STAT Glucose and Lactate Analyser (YSI Life Sciences, USA).

At 24 h or 48 h after actual or sham UCO, the ewe and fetus were killed humanely by i.v. injection of pentobarbitone sodium (Lethabarb, Virbac Pty Ltd, Australia) given to the ewe. The fetal brain was transcardially perfused with 1L of sterile saline and then immediately with 4% paraformaldehyde (PFA; detailed explanation of post mortem procedures Chapter 2, Section 2.8).

3.2.2 Laminin immunohistochemistry

Immunohistochemistry was performed on 10 μm paraffin-embedded sections at two anatomical levels of the brain (Sheep Ovis Aries atlas sections 720 and 1080; Figure 3.1). A negative control slide was always included which was incubated without primary antibody, and when inspected no staining was present. All sections were placed on Superfrost plus glass slides (Mezel Glaser, Germany), de-waxed and re-hydrated through serial ethanols (100% and 70%).

A) MIDSAGGITAL VIEW OF FETAL SHEEP BRAIN
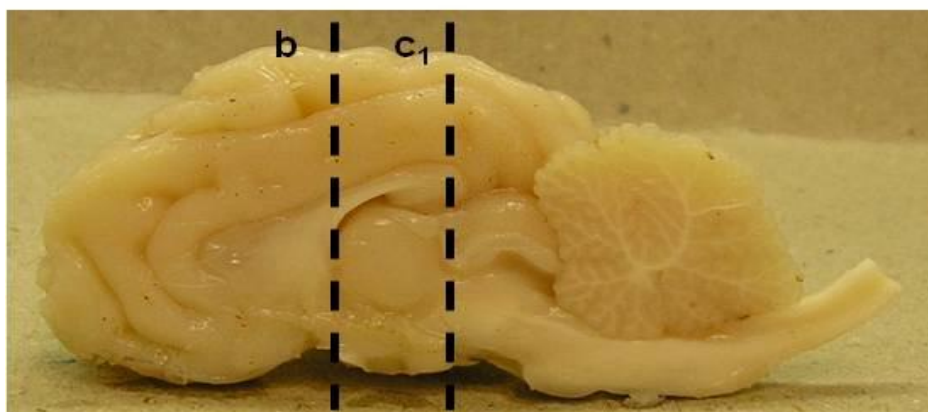
B) CORONAL HISTOLOGY SECTIONS
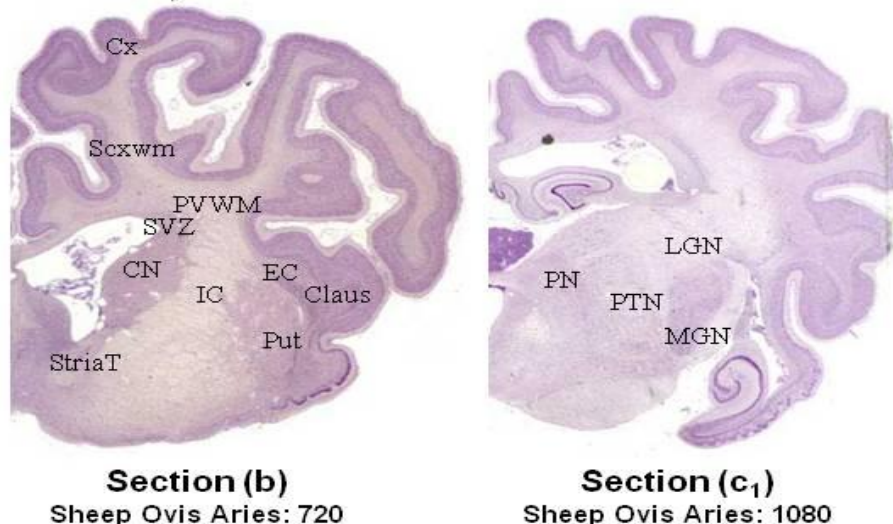
Section (b)
Sheep Ovis Aries: 720

Section (c_1)
Sheep Ovis Aries: 1080

Figure 3.1: Fetal sheep brain dissection and histology. Midsagittal view of anatomical levels a near term fetal sheep brain (A). Dashed lines indicate cuts made to obtain coronal sections of block b and c_1. Coronal histological sections of b and c_1 indicate areas that were analysed. Blocks b; cortex (Cx), subcortical white matter (Scxwm), periventricular white matter (PVWM), subventricular zone (SVZ), Stria-Terminalus (StriaT), caudate nucleus (CN), internal capsule (IC), external capsule (EC), Claustrum (Claus) and putamen (Put). Block c_1; Images from the lateral geniculate nucleus (LGN), medial geniculate nucleus (MGN), pretectal nucleus (PN) and posterior thalamic nuclear group (PTN) were used to analyse the thalamus. (B) Coronal histology sections have been reproduced and adapted with permission from http://www.brains.rad.msu.edu , supported by the US National Science Foundation.

Sections were rehydrated in 0.1M phosphate buffered saline (PBS) in 1% Triton-X 100 (Sigma, USA). Antigen retrieval was carried out on sections incubated with Proteinase K (40 µg/ml, Merck, USA) for 30 min at 37°C and cooled for 20 min at room temperature. Sections were then rinsed in PBS, incubated in 0.3% H_2O_2 (Merck, Australia) in 50% methanol for 15 min at

room temperature to block endogenous peroxidise activity, incubated with 2% normal goat serum blocking buffer in 0.1M PBS for 30 min at room temperature to block non-specific binding and then incubated overnight with anti-laminin rabbit polyclonal antibody (1:200; Novus Biologicas, USA). The sections were then washed incubated with a secondary biotinylated goat anti-rabbit (1:200; Vector Labs, USA) antibody for 45 min followed by 45 min incubation with streptavidin horseradish peroxidase (HRP; 1:200, Amersham Bioscience, USA). Staining was then visualised using metal-enhanced diaminobenzidine (DAB) and lightly counterstained with cresyl violet.

3.2.3 Assessment of microvascular density and morphology

The microvasculature is defined as blood vessels less than 100 μm in diameter (del Zoppo & Mabuchi, 2003) and because laminin immunohistochemistry doesn't differentiate between capillaries, arteries or veins all of these were included in the analysis. Images were taken using a light microscope (Model BX41, Olympus, Japan) at x100 magnification for all brain regions except the corpus callosum, which was taken at x200 magnification. Magnifications were chosen to allow for maximal regional specificity. Where possible, two or three fields of view were taken per brain section for the cortex, periventricular and subcortical white matter brain regions. All measurements (vascular density and morphology) were made using Metamorph Offline (v7.7., Molecular Devices, USA).

3.2.3.1 Microvascular density

Two methods, both widely validated, were used to measure microvascular density (Eriksdotter-Nilsson *et al.*, 1986; Ballabh *et al.*, 2004a), shown in Figure 3.2. Densitometry calculates the total number of positive staining in pixels to give the total percentage area occupied by blood vessels identified by laminin immunopositive staining. The total number of pixels that represented positive staining for each field of view was calculated and represented as a percentage of the total pixels of the image. The second method, counts all positively stained

blood vessels in the field of view; and the total number of blood vessels counted for each image, in each field of view was expressed relative to area (number of blood vessels/mm^2).
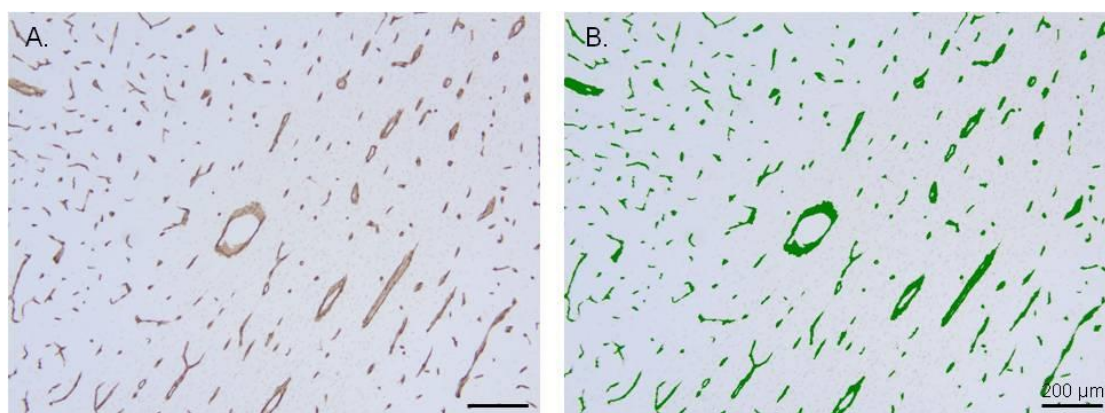
Figure 3.2: Microvascular density assessment of laminin immunohistochemistry in subcortical white matter. Image shows laminin immunohistochemistry photomicrograph (A), and details how Metamorph Offline software analysed vessel density (B). The threshold for 'positive staining' (B - green) was manually set by experimenter. Densitometry analysis; (positive staining in pixel number) and vessel density (blood vessels/mm^2); number of positive staining objects in field of view were calculated automatically by Metamorph Offline. Scale bar represents 200 μm.

3.2.3.2 Morphology measurement

All morphology analysis was conducted on Metamorph Offline. Each image was inspected and a threshold for the positive staining was set. Any positive staining region that occupied ≤ 5 pixels (equating to 3.4 μm or 2.3 μm^2) were considered non-specific and excluded from the analysis. All analysis was measured in pixels and later converted to μm (or μm^2 for area). Care was also taken to exclude staining artefacts and any positive staining of vessels that were not within the brain parenchyma (e.g. meninges are laminin positive structures (Eriksdotter-Nilsson *et al.*, 1986) or that were at the edge of regions of interest (cortex, corpus callosum, subventricular zone and stria terminalus). The parameters chosen to describe blood vessels size include perimeter, and several indices of vascular shape (length, breadth, radius and shape factor), defined by Metamorph Offline and described by Ballabh *et al.,* (2004a).

Mean surface area of blood vessel: The average surface area of positive staining of all blood vessels in a field of view.

Perimeter: The distance around the edge of the object, measuring from the midpoints of each pixel that defines the border (Figure 3.3 a).

Length: The span of the longest chord through the blood vessel (Figure 3.3 b).

Breadth: The calliper width of the blood vessel perpendicular to the length (longest chord; Figure 3.3 c)

Mean Radius: The average distance from the centroid to all points along the blood vessel edge (Figure 3.3 d).

Shape Factor: was calculated by the equation: $4\pi A / P^2$ where A = area and P = perimeter; a value of 0 indicates a flat (line) object, a value of 1 indicates a perfect circular object.
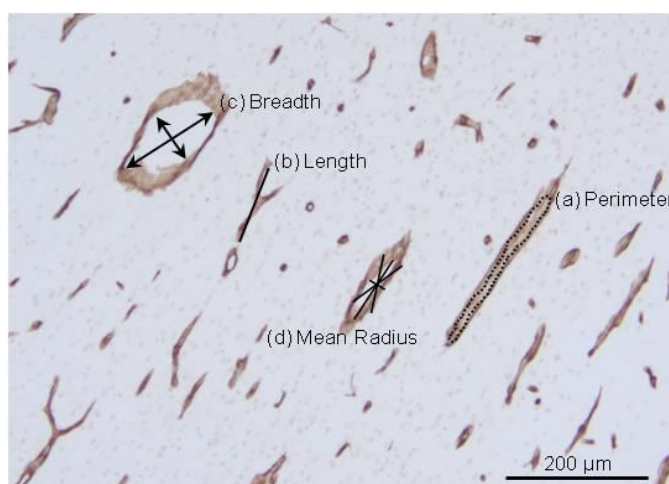
Figure 3.3: Blood vessel morphology assessment of laminin immunohistochemistry in subcortical white matter. Image details how each parameter; perimeter (a), length (b), breadth (c) and mean radius (d) were calculated by Metamorph Offline software. Scale bar represents 200 μm.

3.2.3.3 Distribution of blood vessel size

Perimeter data was used to define blood vessel size in a particular brain region, and a frequency distribution was calculated from this data set. Individual perimeter data was allotted to one of five categories (frequency intervals) of 3.4 – ≤10 μm (≤10 μm), >10 - 50 μm (≤ 50 μm), >50 – 100 μm (≤ 100 μm), >100 – 200 μm (≤ 200 μm) and >200 μm. Brain regions examined for this

analysis were the corpus callosum, cortex, subventricular zone, striatum (including the claustrum, caudate nucleus, putamen, external and internal capsule), thalamus, periventricular and subcortical white matter. All fields of view (and duplicates where possible) were included to achieve one frequency distribution for each brain region for each animal, these data were then averaged over all fetuses, for each group. When all percentage totals for 5 intervals were summed, this equalled 100% (of blood vessels from each field of view for a region).

3.2.4 Statistical Analysis

For vascular density and vessel morphology data a Kruskal-Wallis test (non-parametric ANOVA) was run to compare between control, 24 h and 48 h post-UCO groups. If significant, a Dunn's post-hoc was performed to compare where significance existed, as stated in Ballabh *et al.,* (2004a). For the Stria Terminalus, a Mann Whitney U test was used to compare control and 24 h post-UCO, as the in the 48 h post-UCO group only n=2 was attained so was excluded from analysis.

Two-Way (Mixed model) ANOVA tests were performed to compare the distribution of blood vessel size based on perimeter (within groups), 24 h and 48 h following UCO for brain regions (between groups). If a significant interaction was found, a Bonferroni post hoc test was conducted. All data are shown as mean ± standard error of the mean (SEM). For frequency distribution of blood vessel perimeter all data was expressed as mean ± SEM percentage frequency of total blood vessels per region. Statistical analysis was run on GraphPad Prism Software for Windows (v5.03). Statistical significance was set at $p < 0.05$.

3.3 RESULTS

3.3.1 Vascular density

The effect of UCO on vascular density in the corpus callosum, cortex, subventricular zone, stria terminalus, periventricular and subcortical white matter, striatal regions (caudate nucleus, claustrum, putamen, external and internal capsule) and thalamus are shown in Table 3.1. The number of blood vessels/mm^2 significantly decreased 48 h post-UCO (248.76 $\pm$ 63.43) compared to controls (583.26 $\pm$ 118.12, $p < 0.05$) in the caudate nucleus. A trend to a decrease in vascular density following UCO was seen in the cortex ($p = 0.08$) and subcortical white matter ($p = 0.0582$). No significant differences were seen in all other brain regions measured.

Densitometry analysis of the percentage area occupied by blood vessels was significantly different (decreased) in the caudate nucleus, cortex, thalamus ($p < 0.05$), but no other changes were seen in brain regions examined (Table 3.1).

Table 3.1: Blood vessel density measurements. The density of blood vessels in section that incorporated the corpus callosum, subventricular zone, stria terminalus, cortex, periventricular and subcortical white matter, striatal regions and thalamus in control, 24 h post-UCO and 48 h post-UCO fetal brains. N are stated for each region. Values expressed as mean $\pm$ SEM. * $p < 0.05$; ** $p < 0.01$ compared to control, $\dagger$ $p < 0.05$ compared to 24 h post-UCO. (On next page)

	Control	*24 h post-UCO*	*48 h post-UCO*
Corpus Callosum (n)	4	5	3
Vessel density (number/mm^2)	932.30 ± 247.00	954.78 ± 241.93	276.92 ± 88.07
Total Area (%)	5.96 ± 0.85	6.10 ± 1.02	3.59 ± 0.52
Subventricular Zone (n)	4	5	4
Vessel density (number/mm^2)	356.00 ± 59.82	415.85 ± 70.46	245.67 ± 64.45
Total Area (%)	7.27 ± 1.03	7.20 ± 0.83	5.26 ± 0.32
Periventricular White Matter (n)	4	5	4
Vessel density (number/mm^2)	446.49 ± 102.28	236.07 ± 41.33	209.26 ± 20.09
Total Area (%)	8.02 ± 0.59	6.98 ± 0.93	6.60 ± 0.41
Subcortical White Matter (n)	4	5	4
Vessel density (number/mm^2)	456.83 ± 33.88	300.39 ± 51.50	253.22 ± 16.98
Total Area (%)	7.79 ± 1.51	6.53 ± 0.69	5.75 ± 0.80
Cortex (n)	3	4	4
Vessel density (number/mm^2)	592.87 ± 42.20	355.41 ± 81.94	337.51 ± 28.89
*Total Area (%)**	8.34 ± 0.12	5.72 ± 0.99	5.30 ± 0.59
Caudate Nucleus (n)	3	4	4
*Vessel density (number/mm^2)**	583.26 ± 118.12	421.10 ± 51.24	248.76 ± 63.43*
*Total Area (%)**	7.62 ± 0.52	7.57 ± 0.91	4.81 ± 0.31* [†]
Putamen (n)	4	4	3
Vessel density (number/mm^2)	394.29 ± 100.64	583.82 ± 190.10	235.07 ± 53.17
Total Area (%)	7.73 ± 1.53	8.06 ± 2.09	4.84 ± 0.33
Claustrum (n)	4	4	3
Vessel density (number/mm^2)	485.41 ± 114.29	277.83 ± 84.85	341.18 ± 60.59
Total Area (%)	8.78 ± 2.59	5.83 ± 1.23	5.47 ± 0.54
External Capsule (n)	4	5	4
Vessel density (number/mm^2)	405.15 ± 82.66	322.35 ± 52.31	288.12 ± 44.71
Total Area (%)	8.38 ± 1.61	6.57 ± 0.37	4.90 ± 1.07
Internal Capsule (n)	4	5	4
Vessel density (number/mm^2)	461.71 ± 94.33	406.06 ± 51.14	319.63 ± 73.77
Total Area (%)	7.39 ± 1.52	9.12 ± 0.90	6.54 ± 1.32
Thalamus (n)	5	5	3
Vessel density (number/mm^2)	536.61 ± 46.65	437.24 ± 40.98	500.15 ± 77.42
*Total Area (%)**	12.92 ± 1.61	9.75 ± 0.98	8.60 ± 0.24*

3.3.2 Morphological assessment

3.3.2.1 Effect of umbilical cord occlusion on morphology of blood vessels

Morphology of blood vessels as assessed by mean area, perimeter, length, breadth, mean radius and shape factor was measured in the corpus callosum, cortex, subventricular zone, stria terminalus, periventricular and subcortical white mater (Table 3.2), striatal regions (caudate nucleus, claustrum, putamen, external and internal capsule) and thalamus (Table 3.3). UCO did not have a significant effect on any of the morphology parameters. A trend for an increase in the mean area of blood vessels was observed in the Stria Terminalus at 24 h post-UCO compared to controls ($p = 0.0571$). Due to n = 2 in the Stria Terminalus at 48 h post-UCO, no statistical comparisons were run and SEM could not be calculated (Table 3.2).

3.3.3 Regional comparison of vascular density and morphology

No significant regional differences in vascular density or percentage area occupied by blood vessels were seen in control brains between all regions. Comparing control values of all the parameters derived in the analysis (mean area, perimeter, length, breadth, mean radius and shape factor) also revealed no significant differences between all the brain regions examined (Table 3.1, 3.2, 3.3 – Control column).

Table 3.2: Blood vessel morphology measurements. Blood vessel morphology measurements in corpus callosum, subventricular zone, stria terminalus, cortex, periventricular and subcortical white matter in control, 24 h post-UCO and 48 h post-UCO fetuses. N are stated for each region. Values expressed as mean ± SEM. * $p < 0.05$; ** $p < 0.01$.

	Control	*24 h post-UCO*	*48 h post-UCO*
Corpus Callosum (n)	4	5	3
Mean Area (μm^2)	82.31 ± 17.67	88.07 ± 24.83	166.38 ± 62.46
Perimeter (μm)	35.97 ± 3.50	34.35 ± 5.89	53.27 ± 12.03
Length (μm)	12.07 ± 1.24	11.74 ± 1.84	18.85 ± 4.82
Breadth (μm)	5.67 ± 0.59	5.48 ± 0.84	8.05 ± 1.70
Mean Radius (μm)	3.57 ± 0.38	3.54 ± 0.58	5.72 ± 1.45
Shape Factor	0.63 ± 0.01	0.64 ± 0.03	0.60 ± 0.02
Subventricular Zone (n)	4	5	4
Mean Area (μm^2)	217.53 ± 18.45	239.85 ± 63.57	263.04 ± 50.23
Perimeter (μm)	60.36 ± 3.72	63.24 ± 10.28	70.26 ± 7.97
Length (μm)	21.24 ± 1.55	22.04 ± 3.30	24.97 ± 3.48
Breadth (μm)	11.12 ± 0.67	11.03 ± 1.60	12.79 ± 1.57
Mean Radius (μm)	6.66 ± 0.50	6.82 ± 1.06	7.93 ± 1.16
Shape Factor	0.65 ± 0.03	0.66 ± 0.03	0.62 ± 0.01
Stria Terminalus (n)	3	4	2
Mean Area (μm^2)	87.37 ± 24.45	208.10 ± 35.37	304.79 ±
Perimeter (μm)	40.62 ± 6.27	61.25 ± 5.53	86.62 ±
Length (μm)	14.47 ± 2.92	20.99 ± 1.55	29.25 ±
Breadth (μm)	7.26 ± 1.28	10.92 ± 0.96	13.51 ±
Mean Radius (μm)	4.30 ± 0.97	6.57 ± 0.52	8.83 ±
Shape Factor	0.64 ± 0.02	0.63 ± 0.03	0.58 ±
Cortex (n)	3	4	4
Mean Area (μm^2)	138.13 ± 8.21	172.37 ± 16.03	154.80 ± 6.88
Perimeter (μm)	51.59 ± 3.24	62.10 ± 4.15	55.75 ± 3.57
Length (μm)	18.18 ± 1.73	22.54 ± 1.77	19.84 ± 1.43
Breadth (μm)	9.65 ± 0.51	10.48 ± 0.61	9.95 ± 0.48
Mean Radius (μm)	5.61 ± 0.49	6.78 ± 0.53	6.09 ± 0.43
Shape Factor	0.63 ± 0.00	0.58 ± 0.01	0.62 ± 0.03

Table 3.2: Blood vessel morphology measurements. (Continued)

Periventricular White Matter (n)	4	5	4
Mean Area (μm^2)	241.47 ± 63.77	342.13 ± 70.72	335.20 ± 16.86
Perimeter (μm)	62.76 ± 12.51	81.53 ± 11.75	82.62 ± 2.94
Length (μm)	23.00 ± 4.97	29.76 ± 4.27	30.06 ± 1.39
Breadth (μm)	10.55 ± 1.88	13.43 ± 1.75	14.44 ± 0.43
Mean Radius (μm)	6.93 ± 1.52	9.10 ± 1.32	9.44 ± 0.36
Shape Factor	0.67 ± 0.03	0.63 ± 0.04	0.61 ± 0.03
Subcortical White Matter (n)	4	5	4
Mean Area (μm^2)	207.08 ± 52.57	262.91 ± 44.76	243.84 ± 41.51
Perimeter (μm)	57.90 ± 9.09	69.75 ± 8.26	68.06 ± 5.96
Length (μm)	20.57 ± 3.42	25.38 ± 2.94	24.63 ± 2.65
Breadth (μm)	9.58 ± 1.59	11.47 ± 1.12	12.08 ± 1.14
Mean Radius (μm)	6.15 ± 1.09	7.74 ± 0.90	7.74 ± 0.87
Shape Factor	0.65 ± 0.01	0.62 ± 0.03	0.61 ± 0.02

Table 3.3: Blood vessel morphology measurements in striatum and thalamus. Blood vessel morphology measurements in striatal regions: caudate nucleus, putamen, claustrum, external and internal capsule and thalamus in control, 24 h post-UCO and 48 h post-UCO fetuses. N are stated for each region. Values expressed as mean ± SEM. * $p < 0.05$; ** $p < 0.01$.

	Control	*24 h post-UCO*	*48 h post-UCO*
Caudate Nucleus (n)	3	4	4
Mean Area (μm^2)	148.82 ± 33.85	175.57 ± 32.74	243.50 ± 83.70
Perimeter (μm)	54.06 ± 7.32	62.99 ± 8.39	66.84 ± 14.45
Length (μm)	19.14 ± 2.78	21.82 ± 3.11	24.15 ± 5.82
Breadth (μm)	10.12 ± 1.06	10.85 ± 1.29	11.88 ± 2.24
Mean Radius (μm)	5.94 ± 0.86	6.61 ± 0.94	7.51 ± 1.84
Shape Factor	0.64 ± 0.02	0.59 ± 0.03	0.65 ± 0.01
Putamen (n)	4	4	3
Mean Area (μm^2)	227.94 ± 33.72	163.78 ± 32.17	236.29 ± 59.85
Perimeter (μm)	65.54 ± 3.52	56.09 ± 8.19	74.12 ± 14.58
Length (μm)	22.58 ± 1.55	20.43 ± 3.63	25.74 ± 5.69
Breadth (μm)	11.28 ± 0.40	10.02 ± 1.08	12.48 ± 1.98
Mean Radius (μm)	6.94 ± 0.41	6.22 ± 1.05	7.89 ± 1.62
Shape Factor	0.61 ± 0.01	0.63 ± 0.03	0.57 ± 0.01
Claustrum (n)	4	4	3
Mean Area (μm^2)	184.36 ± 13.67	233.09 ± 32.39	170.60 ± 21.13
Perimeter (μm)	61.23 ± 3.12	68.78 ± 7.55	59.14 ± 3.38
Length (μm)	20.40 ± 0.99	24.27 ± 3.22	21.95 ± 1.90
Breadth (μm)	10.63 ± 0.44	11.38 ± 1.09	11.01 ± 0.84
Mean Radius (μm)	6.30 ± 0.31	7.32 ± 0.94	6.84 ± 0.63
Shape Factor	0.62 ± 0.02	0.58 ± 0.01	0.62 ± 0.03
External Capsule (n)	4	5	4
Mean Area (μm^2)	225.86 ± 40.49	232.21 ± 38.40	170.78 ± 25.19
Perimeter (μm)	62.69 ± 6.75	67.61 ± 7.99	60.86 ± 5.98
Length (μm)	21.00 ± 2.43	24.69 ± 2.73	22.23 ± 2.72
Breadth (μm)	11.02 ± 0.87	11.43 ± 1.16	10.75 ± 0.76
Mean Radius (μm)	6.49 ± 0.72	7.49 ± 0.81	6.82 ± 0.78
Shape Factor	0.64 ± 0.01	0.62 ± 0.03	0.59 ± 0.02

Table 3.3: Blood vessel morphology measurements in striatum and thalamus. (Continued)

Internal Capsule (n)	4	5	4
Mean Area (μm^2)	175.68 ± 23.39	246.76 ± 41.02	278.58 ± 110.04
Perimeter (μm)	55.74 ± 4.29	71.56 ± 6.19	78.07 ± 19.32
Length (μm)	19.75 ± 1.90	25.05 ± 2.44	27.01 ± 7.24
Breadth (μm)	10.07 ± 0.71	12.62 ± 1.27	13.17 ± 2.80
Mean Radius (μm)	6.07 ± 0.58	7.80 ± 0.84	8.20 ± 2.13
Shape Factor	0.65 ± 0.02	0.61 ± 0.02	0.56 ± 0.01
Thalamus (n)	5	5	3
Mean Area (μm^2)	221.44 ± 39.11	197.85 ± 17.46	202.58 ± 42.88
Perimeter (μm)	72.53 ± 8.54	68.50 ± 5.92	73.93 ± 9.50
Length (μm)	24.83 ± 2.78	24.31 ± 2.25	25.67 ± 3.39
Breadth (μm)	12.50 ± 1.19	11.90 ± 0.96	12.30 ± 1.37
Mean Radius (μm)	7.58 ± 0.78	7.37 ± 0.67	7.72 ± 0.99
Shape Factor	0.57 ± 0.02	0.56 ± 0.01	0.54 ± 0.01

3.3.3.1 Change in size distribution of blood vessels.

Any particle smaller than 5 pixels was excluded from analysis, making the smallest vessel size detectable from 3.4 µm. For all brain regions, the greatest number of blood vessels in the control fetal brains was within the range of 10 – 50 µm. Following UCO in periventricular (Figure 3.4 A, B, C) and subcortical white matter a significant difference was seen in the frequency distribution of blood vessel perimeter. In periventricular white matter (Figure 3.4 D), at 48 h post-UCO (Figure 3.4 C) there was a significant decrease in the relative number of blood vessels $\leq$ 10 µm (29.5 $\pm$ 4.8% vs. 13.4 $\pm$ 3.8%; $p < 0.01$) and a corresponding significant increase in blood vessels $\leq$ 100 µm (16.5 $\pm$ 4.2% vs. 30.6 $\pm$ 1.3%; $p < 0.05$) compared to controls (Figure 3.4 A). In subcortical white matter, the percentage of blood vessels $\leq$ 10µm significantly decreased at 24 h (16.4 $\pm$ 2.9%; $p < 0.05$) and 48 h post-UCO (13.7 $\pm$ 1.7%; $p < 0.01$) compared to controls (27.1 $\pm$ 5.5%). At 48 h post-UCO 26.6 $\pm$ 2.1% blood vessels were $\leq$ 100 µm, which was significantly greater than controls (14.8 $\pm$ 3.3%; $p < 0.05$) (Figure 3.4 E). In the corpus callosum, there was a significant decrease at 48 h post-UCO (29.5 $\pm$ 5.9%) seen in blood vessels $\leq$ 50 µm compared to controls (49.4 $\pm$ 2.9%; $p < 0.01$) and 24 h post-UCO (46.6 $\pm$ 5.1%; $p < 0.01$) (Figure 3.5 A).

No significant differences in the distributions of blood vessels perimeter size were seen at 24 h and 48 h following UCO for the subventricular zone, striatum, thalamus, cortex or stria terminalus (48 h post- UCO, n=2) (Figure 3.5 B - F).
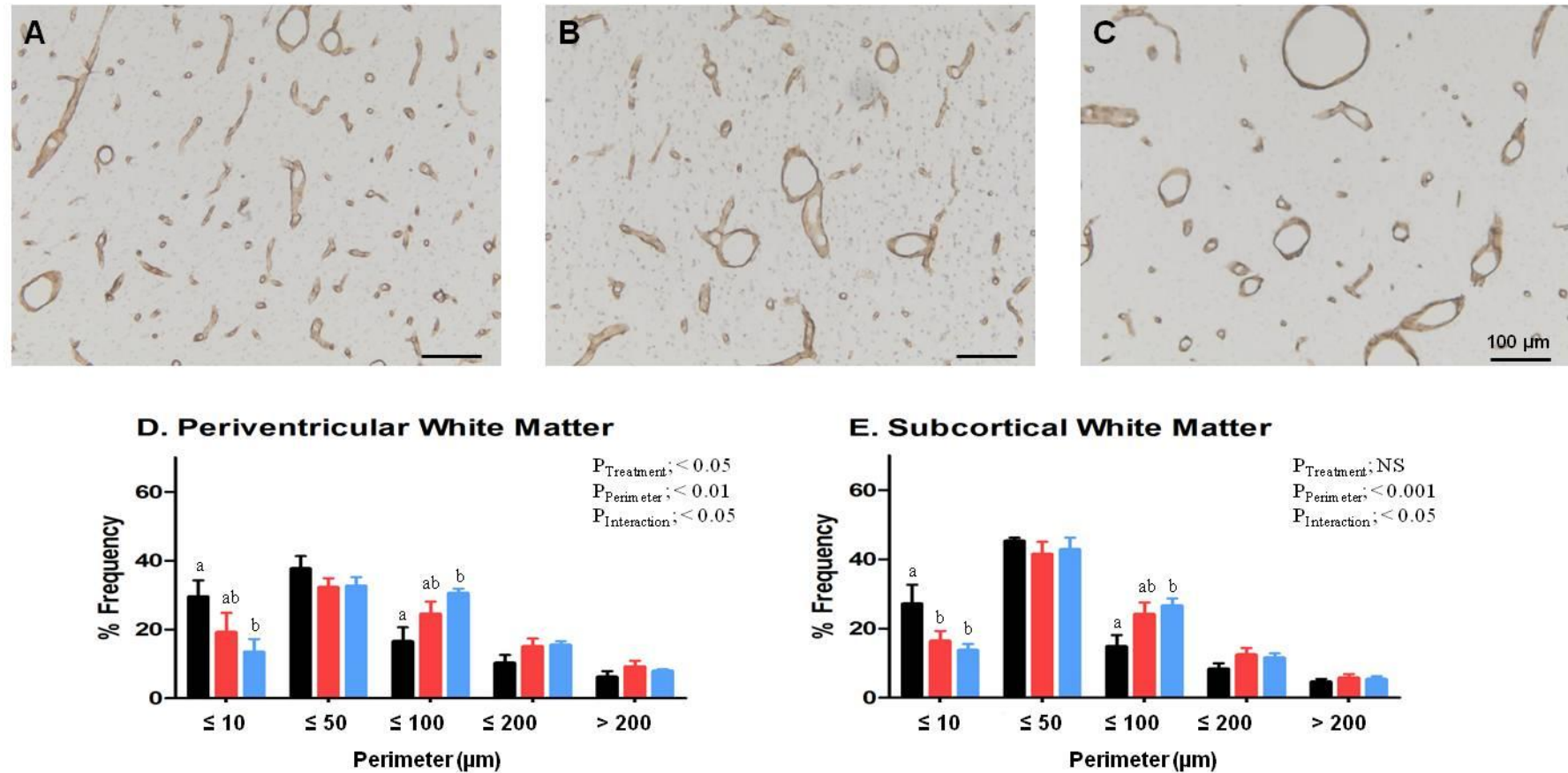
Figure 3.4: Size distribution of blood vessels in white matter. Photomicrographs of laminin immunohistochemistry in periventricular white matter from Control (A), 24 h post-UCO (B) and 48 h post-UCO (C). Percentage frequency histograms of the perimeter of blood vessels in periventricular (D) and subcortical (E) white matter in control (black), 24 h (red) and 48 h post-UCO (blue) in fetal sheep brains. Scale bar represents 100 µm. $p < 0.05$. Mean $\pm$ SEM. Not significant (NS)
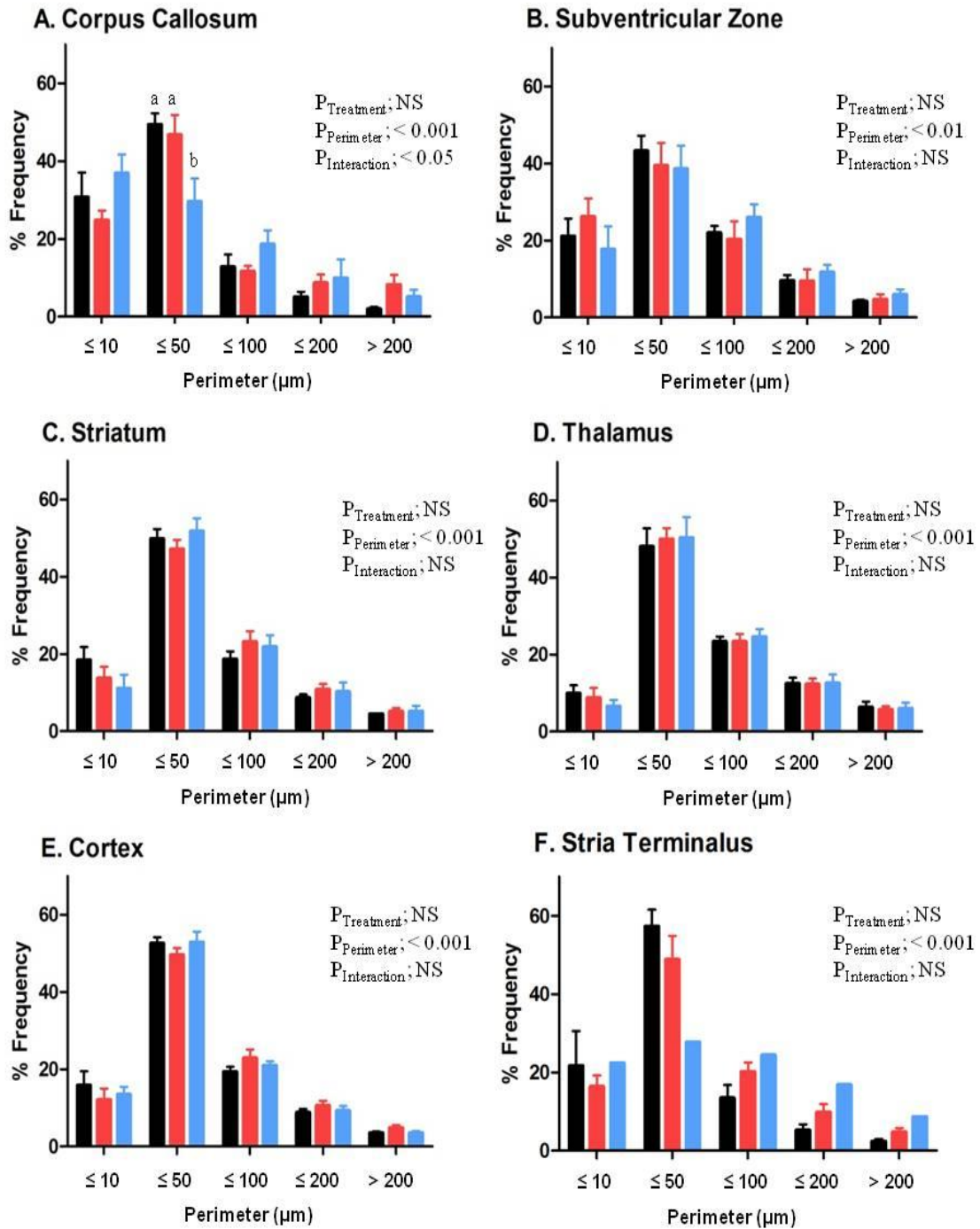
Figure 3.5: Size distribution of blood vessels in brain regions from fetal sheep. Percentage frequency histograms of the perimeter of blood vessels in corpus callosum (A), subventricular zone (B), striatum (C), thalamus (D), cortex (E) and stria terminalus (F) in control (black), 24 h (red) and 48 h post-UCO (blue) in fetal sheep brains. $p < 0.05$. Mean ± SEM. Not significant (NS).

3.4 DISCUSSION

This study assessed changes in vascular density and morphology using laminin immunohistochemistry in the late gestation fetal sheep brain following UCO. Vascular density measurements in control late gestation fetal sheep were comparable to human studies (Miyawaki *et al.*, 1998) The most striking finding of this study was that in periventricular and subcortical white matter, at 48 h following UCO, there was a significant decrease in the relative frequency of smaller (≤ 10 µm) blood vessels and an increase in the percentage frequency of larger blood vessels (≤ 100 µm). This shift in frequency indicates that one of the consequences of UCO is dilation of small blood vessels, at least in the short term. Thus, these results show for the first time a predilection for the prolonged vascular changes in fetal white matter but not in grey matter.

The significant decrease in vascular density seen in the caudate nucleus 48 h following UCO and the trend to a decrease in vascular density seen in the cortex and white matter may be attributed to morphological changes, i.e. larger vessels occupy more of the field of view. However, decreased vascular density has also been closely correlated with blood brain barrier (BBB) damage (albumin extravasation) resulting in oedema formation up to between 24 to 72 h following subarachnoid haemorrhage in rats (Scholler *et al.*, 2007). Contrary to this study, decreased microvascular density has been reported in the cortex of angiopoietin like-1 (angptl-1) protein transgenic mice and was associated with a paradoxical *decrease* in BBB breakdown and oedema formation (Lai *et al.*, 2008). Angiopoietin like proteins are similar to the angiopoietins, but do not bind to the Tie receptor. Angpt like proteins are suggested to be important in modulating angiogenesis and in stabilizing endothelial cells (Oike *et al.*, 2004; Lai *et al.*, 2008). However in our study the decreased vascular density in the caudate, thalamus and cortex were not associated with an increase in vessel size.

In studies of human white matter, Altman and colleagues (1988) described lower cerebral blood flow in white matter in preterm and term neonates using positron emission tomography (PET).

Lower vascular density (mid to late gestation) could also explain lower blood flow in white matter in the human fetus (Ballabh *et al.*, 2004a). In contrast, we did not observe any significant difference between grey and white matter regions in near term animals with respect to vascular density, but simply that there was a difference in the effect of UCO in these regions.

Following hypoxic and/or ischemic insults (middle cerebral artery occlusion (MCAO) or hypobaric hypoxia), increased capillary density has been widely reported in adult rats and mice, from 1 to 8 weeks following the insult (Lin *et al.*, 2000; Kanaan *et al.*, 2006; Milner *et al.*, 2008; Pan *et al.*, 2010). Hypoxic preconditioning followed by a hypoxic-ischemic insult in the immature rat brain also results in increased vascular density (Gustavsson *et al.*, 2007). Hypoxia induced angiogenesis occurs due to increased expression of hypoxia inducible factor-1α (HIF-1α) up-regulating expression of vascular endothelial growth factor (VEGF), a potent regulator of angiogenesis. The activation of hypoxia inducible genes and subsequent formation of new blood vessels following permanent ischemia occurs within the first 48 to 72 h in the adult (Marti *et al.*, 2000b), but it is not clear if new blood vessels contribute to perfusion at this stage. In adult mice the formation of new blood vessels is first visible from 4 to 12 days following administration with VEGF (Dellian *et al.*, 1996). Whether the developing brain responds in the same way to a severe but transient systemic insult (UCO) remains to be investigated and is discussed further in Chapter 4 and Chapter 5, although at 48 h no significant increase in vascular density would indicate this is too soon to occur in our model.

The striking difference in response to hypoxia of blood vessels of white matter (periventricular and subcortical) compared to other brain regions is an important finding that needs to be investigated further. Increased vessel perimeter could be indicative of increased nitric oxide (NO)- induced vasodilation, and endothelial nitric oxide synthase (eNOS) expression, which has a fundamental role in regulating cerebral blood flow, which has been shown to occur following hypoxia-ischemia (Bolanos & Almeida, 1999; Rodrigo *et al.*, 2005; Kaur & Ling, 2009).

In premature infants, increased cerebral blood flow is correlated with vulnerability to haemorrhage (Milligan, 1980; Ment *et al.*, 1991). However, Meek *et al.,* (1999) attributes low global cerebral blood flow within the first 24 h of birth to an increase in the incidence of severe GM-IVH, suggesting that cerebral ischemia may predispose the brain to haemorrhage. Inherent vulnerability of white matter to injury could also be attributed to vascular end zones, where basal penetrators (major arteries) end in subcortical and periventricular regions (De Reuck, 1971; Takashima & Tanaka, 1978a; Volpe, 1998). However, McClure *et al.,* (2008) do not attribute vascular end zones in white matter to ischemia-reperfusion injury in the preterm fetal sheep despite basal blood flow being lower in white matter compared to cortical and subcortical gray matter. Instead McClure *et al.,* (2008) argue that cellular immaturity (i.e. pre-oligodendrocytes) may be more responsible for white matter vulnerability, resulting in brain injury.

Previously, we have shown increased global cerebral blood flow during 10 min UCO, followed by 10 h of hypoperfusion, and a return to basal blood flow by 24 h post-UCO (Yan *et al.*, 2009). Expansion of blood vessels, as shown by increased perimeter, may be indicative of vascular dilation at 48 h post-UCO, which would increase oxygen and glucose supply to white matter. However, high blood flow through large diameter conduits does not necessarily increase oxygen or nutrient delivery, particularly when the vessel is large enough to permit laminar flow to develop, based on Poiseuille's equation. Vogel and colleagues (2003) transfected VEGF, a potent stimulator of angiogenesis, into rat brains and found that large (< 650 μm diameter from vessel cross sections) blood vessels actually had decreased local cerebral blood flow. They suggested that areas of high vascular density, with medium sized vessels (> 43 μm) were the regions that showed increased blood flow. This study highlighted an importance in differing regional flow patterns being attributed to the growth of new vessels and vessel size.

Following hypoxia, changes in vessel size have also been seen to occur in the cortex of the neonatal rat brain observed as an increase in vessel diameter (Ogunshola *et al.*, 2000), this is

contrast to our study where we only saw significant differences in white matter. In adult rats following cerebral ischemia, increased vessel perimeter of the ipsilateral hemisphere has also been observed (Zhang *et al.*, 2002a). Chen *et al.,* (2005) found that treatment with statins following stroke also produced a significant increase in vascular perimeter. Although the exact consequence of this response is not well understood, this study also found enhanced angiogenesis shown by increased numbers of BrdU labelled endothelial cells from 1 to 14 days following the induction of stroke. The increase in proportion of vessels ($\leq$100 μm) only occurring in white matter up to 48 h following UCO late in gestation could be indicative of increased expression of vasodilators, vasodilation and angiogenesis which is consistent with other studies from both the neonatal and adult brain (Ogunshola *et al.*, 2000; Zhang *et al.*, 2002a). Further analysis of vascular structure or discrimination of arteries or veins could help explore the significance of these findings.

Mito *et al.,* (1991) also suggested that proportionally large vascular diameter is associated with angiogenesis in both the cortex and white matter of the fetal human brain from mid to late gestation. Subsequently, smaller diameter vessels (<10 μm) occur throughout gestation, with larger vessels (>20 μm) appearing prominently from 35 weeks gestational age. During normal development of the human fetal brain, as gestational age increases so does vascular density in the germinal matrix and cortex. White matter has a smaller increase across gestation, and the lowest blood vascular density compared to the above brain regions (Gould & Howard, 1988; Ballabh *et al.*, 2004a). However, Mito *et al.,* (1991) manually counted vessels and noted no significant difference in white matter vascular density in the human fetal brain (from 14 to 38 weeks gestation). In contrast to no significant differences in vascular density between brain regions of late gestation control fetal sheep were observed. Vascular density in control brains was consistent with human studies (Eriksdotter-Nilsson *et al.*, 1986; Miyawaki *et al.*, 1998). The vascular morphology measurements of gray and white matter in control late gestation fetal brains were marginally smaller than the human (Ballabh *et al.*, 2004a).

It is interesting to note that there was a significant shift in the proportion of blood vessel perimeter in white matter but not in an overall difference when 'mean' vessel perimeters were compared (Table 3.2). There was a trend to an increase in vessel perimeter following UCO in white matter (periventricular and subcortical), but this was not significant. The statistical analysis chosen for this comparison was based on Ballabh *et al.,* (2004a) who did a similar analysis of blood vessels. The significance of these finding highlights that 24 and 48 h following UCO it is small (<10 µm) to medium (<100 µm) sized blood vessels in white matter that may be more vulnerable to hypoxia. This could be indicative of either changes in cerebral blood flow to these regions (discussed above) or angiogenic responses, whereby vascular expansion occurs early during blood vessel formation (Mito *et al.*, 1991).

Many antigens have been used in immunohistochemistry to label blood vessels, including constituents of the basal lamina (such as collagen IV and laminin), and endothelial cell markers (CD31, CD34, CD105 (endoglin), eNOS, von Willebrand factor [Factor VIII]), and lectin (Eriksdotter-Nilsson *et al.*, 1986; Hamann *et al.*, 1995; Vermeulen *et al.*, 1996; Brewer *et al.*, 2000; Simon *et al.*, 2008). Inconsistent results have been noted when comparing different endothelial markers (Brewer *et al.*, 2000; Simon *et al.*, 2008). Using collagen IV or laminin, both of which are expressed equally in the basement membrane, produces a consistent, reliable stain that also allows for densitometry analysis (Laurie *et al.*, 1980; Ment *et al.*, 1991; Mito *et al.*, 1991). The use of laminin immunohistochemistry to label and visualise blood vessels has been widely validated and proven to be a simple, accurate and specific method with minimal background (Eriksdotter-Nilsson *et al.*, 1986), and was therefore used in our study. A limitation of using basement membrane proteins such as laminin or collagen IV is that staining does not discriminate between capillaries, arterioles, arteries or veins.

Ment *et al.,* (1991) suggested that basement membrane proteins (laminin and collagen IV) are important in providing structural integrity to blood vessels, particularly in the germinal matrix (subventricular zone) to prevent rupture. Ultrastructural analysis using electron microscopy to measure morphology of germinal matrix blood vessels have found that immature vessels tend to

have a greater endothelial area and thinner basement membrane in comparison to cortical areas during 25 – 32 weeks gestational age (Trommer *et al.*, 1987; Grunnet, 1989). Grunnett (1989) and Trommer *et al.,* (1987) suggest that a large area of vascular lumen and large radius with a consistent pressure contribute to greater tension on the vascular wall and possibly lead to rupture of blood vessels, as described by LaPlace's law; $T = Pr/\alpha$ (T = circumferential tension, P = pressure, r = radius and α = thickness of wall). Whether blood vessels of the subventricular zone or white matter in the fetal sheep brain also respond this way still remains to be elucidated.

Degradation of laminin is consistent with disruptions of the BBB and can contribute to oedema formation and haemorrhage (del Zoppo & Mabuchi, 2003; Veltkamp *et al.,* 2006). Normally laminin expression is confined to the basement membrane. Xu *et al.,* (2008) measured laminin $\alpha1$, $\alpha4$ and $\alpha5$ isoforms in germinal matrix, gray and white matter of both human fetal (16 weeks to 40 weeks gestation) tissue and from rabbit pups and found developmental regulation of expression for each isoforms and greater $\alpha1$ expression in the germinal matrix. The primary antibody used for laminin immunohistochemistry in our study recognised all isoforms. However during development, laminin expression is induced by precursors of neurons and glia, and in response to injury is expressed by reactive astrocytes (Liesi *et al.*, 1984; Liesi, 1985).

Following hypoxia-ischemia matrix metalloproteinase-9 (MMP-9) is up-regulated, and laminin being a substrate, it is thought to correlate with laminin degradation (Zalewska *et al.*, 2002). Laminin degradation is also correlated with loss of pyramidal neurons in the hippocampus following excitotoxic injury, and following injury reactive astrocytes also express laminin (Chen & Strickland, 1997). The response of laminin isoforms and the possible degradation that may occur following hypoxia-ischemia could identify regional vulnerabilities of the basement membrane and other cell types. We saw no evidence of cellular laminin expression and it was beyond the scope of this study to assess laminin degradation; however using immunohistochemistry densitometry may provide an indication of degradation of laminin, but analysis of protein by western blot would be the most accurate. Veltkamp *et al.,* (2006) used

densitometry analysis of laminin positive staining and found degradation of laminin 24 h following MCAO. However, without an assessment of morphology or additional analysis of protein concentration using Western Blot techniques it is difficult to determine the significance of this finding.

When measuring vascular density it is important to consider morphological changes of the blood vessels, particularly in brain regions that contain vessels with a more circular form (shape factor closer to 1). Shape factor may be over-estimated in our study and influenced by perfusion of PFA during fixation of tissue. Trommer *et al.,* (1987) suggests differences in perfusion pressure and other fixation protocols may lead to distended vessels leading to discrepancies between studies measuring capillary luminal diameter using electron microscopy. Grunnet (1989) also saw this as an issue, so used immersion fixed brain tissue for analysis. While perfusion fixation may alter the true vessel shape, it is unlikely this could have produced the difference seen between the UCO and sham-UCO brains unless a pre-existing difference in vascular structure was present.

Comparison and validation of methods used to measure vascular density have been mostly done in regards to tumour angiogenesis. The Chalkley count method has been widely used in which "hot spots" of high vessel growth are recognised and counted using a 25-point graticule (Weidner *et al.*, 1991; Fox *et al.*, 1995). However, for analysis of vascular density across larger regions, this may not be accurate due to the variability of vascular density of brain regions and morphology of blood vessels. Manual and computerised methods have both been utilized to measure vascular density. Counting of blood vessels and densitometry image analysis of total positive staining (of pixels) in a field of view have also been widely used (Mito *et al.*, 1991; Hamann *et al.*, 1995; Cavaglia *et al.*, 2001; Veltkamp *et al.*, 2006). Ballabh *et al.,* (2004a) used a computerised method of quantification that allowed for a consistent, quick and unbias evaluation of vessel number and related individual size parameters. In our study, our findings

suggest that either densitometry or counting of vessels is accurate but morphological assessment must also be done to accurately represent microvascular density.

It could be argued that a limitation of this study was that we didn't measure diameter of vessels, as other studies have. However, the vessel would need to be a perfect circle for this to be an accurate measure. The difference we saw was a shift in frequency of vascular perimeter following UCO. Possibly analysing radius, length and breadth of blood vessels as a frequency distribution would indicate the shape changes occurring, although perimeter measurements do take into account changes in these parameters, thereby accurately measuring vessel size. Large variation occurred (particularly for perimeter) as blood vessel perimeters ranged from < 10 μm to > 200 μm which included a mixture of both oblong and circular vessels.

Large SEM values may account for the trend, but no significant difference, between groups when assessing 'mean' vessel perimeter (and other morphological parameters). This may exist due to the large range of vessel perimeters, ≤ 10 μm to > 200 μm, and that there was between 1000 to 2000 positive stained blood vessels (objects) per field of view. This observation highlights that the differences in vessel perimeter were subtle and a more specific analysis may be required. A close assessment of all blood vessels being represented as a frequency distribution appears to be a more accurate representation and method for closely assessing changes in vessels morphology.

In summary this study has found that cerebral blood vessels in white matter have a different response compared to other brain regions, including gray matter, following global hypoxia caused by UCO late in gestation. While the observations made here are still relatively short term (i.e. 48 h following UCO); it is apparent that the cerebrovasculature is significantly affected by a brief (10 min) period of severe hypoxia, even though the systemic cardiovascular and metabolic status of the fetus to return to normal within hours of the insult.

Chapter 4

VEGF EXPRESSION IN THE LATE GESTATION FETAL OVINE BRAIN FOLLOWING UMBILICAL CORD OCCLUSION.

TABLE OF CONTENTS

4.1 INTRODUCTION

Perinatal hypoxia-ischemia can have severe, acute consequences such as germinal matrix and intraventricular haemorrhage (GM-IVH), brain oedema in the fetal brain, followed by more chronic effects including periventricular leukomalacia (PVL), cerebral palsy and other neurological deficits (Abraham *et al.*, 1999). However the pathogenesis of brain injury following a severe hypoxic event is not well understood. The actions of hypoxia sensitive genes such as hypoxia inducible factor (HIF) and vascular endothelial growth factor (VEGF) which are robustly up-regulated following hypoxia have been shown to have both protective and damaging consequences. Mostly from studies in the adult brain, there is limited explanation about the implication of their findings for the fetal and neonatal brain.

VEGF is an important regulator of vasculogenesis (new vessel formation), angiogenesis (sprouting of blood vessels from pre-existing ones), endothelial cell differentiation and neurogenesis (neuronal growth) during embryonic and fetal development (Breier *et al.*, 1992; Breier & Risau, 1996; Ogunshola *et al.*, 2000; Sun *et al.*, 2003), with hypoxia being a key regulator of VEGF expression (Forsythe *et al.*, 1996). VEGF has homologous family members (VEGF-A, placental growth factor (PIGF) VEGF-B, VEGF-C, VEGF-D and VEGF-E) and three high affinity tyrosine receptors (VEGFR-1 (Flt-1), VEGFR-2 (Flt-2/KDR) and VEGFR-3 (Flt-4) (Breier, 2000).

Following a hypoxic event, transcriptional factor HIF-1α is robustly upregulated resulting in increased expression of hypoxia responsive genes including erythropoietin (Epo) and VEGF (Mu *et al.*, 2003; Kaur *et al.*, 2006a). Increased VEGF expression results in an angiogenic response, and in ischemic tissue this leads to increased perfusion (Breier *et al.*, 1992; Breier & Risau, 1996; Ment *et al.*, 1997; Nag *et al.*, 1997; Zhang *et al.*, 2000; Sun *et al.*, 2003). However, VEGF expression can also lead to increased vascular permeability and leakage of plasma proteins into the extravascular space (Schoch *et al.*, 2002). This response has been widely studied in tumour growth (Kim *et al.*, 1993; Breier & Risau, 1996; Banerjee *et al.*, 1997; Breier,

2000), wound healing (Bates & Jones, 2003; Otrock *et al.*, 2007), adult stroke (Zhang *et al.*, 2000; del Zoppo & Mabuchi, 2003) and even the fetal retina (Alon *et al.*, 1995). Aly *et al.,* (2009) found increased circulating VEGF from the cord blood of human infants who had experienced perinatal asphyxia, many of whom continued on to develop hypoxic-ischemic encephalopathy. Two neonatal rodent models have also found increased VEGF following hypoxia (Ment *et al.*, 1997; Mu *et al.*, 2003; Kaur *et al.*, 2006a). However whether up-regulation of VEGF occurs in the fetal sheep brain after global hypoxia, and the implications of this for the physiological status of the cerebral circulation have not been fully investigated.

It is well established following hypoxia-ischemia the neonatal brain responds with fluctuations in cerebral haemodynamics and blood flow in association with the onset of excitotoxicity, oxidative stress, inflammation and subsequent brain injury (McLean & Ferriero, 2004). For the fetus, umbilical cord complications, particularly near term are common and severe hypoxia can result in devastating brain injury. In some instances term fetuses appear to be more vulnerable to occlusion of the umbilical cord than the mid gestation fetuses (Mallard *et al.*, 1994).

In previous studies using fetal sheep it has been shown that, a single 10 minute period of umbilical cord occlusion (UCO) in late gestation resulted in increased hydroxyl radical production, increased lipid peroxidation and seizure activity for up to 10 h (Mallard *et al.*, 1994; Miller *et al.*, 2005; Yan *et al.*, 2009). This hypoxic stress was also associated with increased expression of Epo (a hypoxia sensitive gene) and Epo-receptor following one or two bouts of UCO (Castillo-Melendez *et al.*, 2005), which might be an adaptive response, as Epo treatment has been shown to be neuroprotective following neonatal stroke in rats (Chang *et al.*, 2005; Iwai *et al.*, 2007).

In this study we aimed to determine the effects of UCO on expression of VEGF, another hypoxia-inducible gene, in the major regions of the fetal sheep brain together with effects on cell proliferation and blood brain barrier (BBB) permeability changes at 24 and 48 h following this single but severe asphyxic event. It is hypothesised fetuses subjected to UCO will be

stressed (increased cortisol) and that up-regulation of VEGF in the fetal sheep brain following UCO could have the benefits of inducing angiogenesis, but also have the detrimental consequences forming fragile vessels and increasing BBB permeability, similar to those seen in adult hypoxia-ischemia.

4.2 METHODOLOGY

The animal surgery and experimental protocols are given in detail in Chapter 2, Section 2.4, and 2.5. Although generally the same animal surgery and experimental procedures were conducted, the animals used in Chapter 4 and Chapter 5 were different groups of animals, so the methods sections are repeated as they detail different protocols.

4.2.1 Animal surgery and experimentation

Fourteen pregnant Border-Leicester ewes carrying a singleton fetus were used in this study. The use of these animals and all procedures had received prior approval from the School of Biomedical Science Animal Ethics Committee of Monash University. As previously described by Castillo-Melendez *et al.,* (2005) and Yan *et al.,* (2009), the surgery was performed under general anaesthesia at 124-126 days gestational age (GA; term is 146 days), which was induced by an intravenous injection of 1 g sodium thiopentone (50 mg/ml; Pentothal, Boehringer Ingelheim Pty Ltd, Australia) in 20 mL sterile water and maintained for the duration of surgery using 1.5-2% isoflurane (Isoflo, Abbott Australasia Pty Ltd, Kurnell, Australia). Under aseptic conditions the fetal hindlimbs were exposed through abdominal and uterine incisions. A polyvinyl catheter filled with heparinised saline was inserted into a femoral artery to obtain blood samples and measure arterial pressure. A second saline-filled catheter was filled was placed in the amniotic sac for a pressure reference. An inflatable silastic cuff (type OC-16, *In Vivo* Metric, Healdsburg, CA, U.S.A) was placed around the abdominal end of the umbilical cord, which on inflation results in complete cessation of blood flow in the cord. The fetus was

then returned to the uterus and the incision closed. All catheters was exteriorised through a maternal flank incision, and the maternal abdominal incision was closed.

Experiments were performed 4-5 days after surgery. Fetal blood pressure and amniotic pressure were measured using solid state pressure transducers, and fetal arterial pressure calculated by electronic subtraction of amniotic pressure. Fetal heart rate was calculated online from the blood pressure pulse. All data was recorded continuously on the hard disk of a computer via an analogue-digital converter and Chart software (PowerLab, ADInstruments, NSW, Australia).

On the day of the experiment, in 9 fetuses the umbilical cord was occluded completely for 10 min by inflating the cuff with 3mL of sterile water; in 5 fetuses a sham UCO procedure was performed. Fetal arterial blood samples (0.5 mL) were taken at -1 h, -5 min, +5 min, +9 min, 30 min, 1, 2, 4, 6, 8, 10, 12 and 24 h relative to the start of the occlusion (time=0). Blood samples were used immediately to measure pO_2, pCO_2, O_2 saturation, pH and haematocrit using a Radiometer ABL5 analyser (Radiometer Medical A/S, Denmark), and blood glucose and lactate concentrations were measured by a YSI 2300 STAT Glucose and Lactate Analyser (YSI Life Sciences, USA).

At 24 h (n=5) or 48 h (n=4) after the actual or sham UCO (n=5; 24 h [5]) , the ewe and fetus were humanely euthanized by i.v. injection of pentobarbitone sodium (Lethabarb, Virbac Pty Ltd, Australia) to the ewe. The fetal brain was transcardially perfused with 1L of sterile saline and then immediately with 4% paraformaldehyde (PFA). (Detailed explanation of post mortem procedures Chapter 2, Section 2.8)

4.2.2 Cortisol radioimmunoassay

For a detailed protocol please refer to Chapter 2, Section 2.7.

Cortisol was extracted from plasma samples using dicholoromethane as previously described by Bocking *et al.,* (1986). Briefly, following extraction Cortisol assay buffer (100 μl), antiserum

(100 µl; working dilution; 1:5000), bovine γ-globulin (100 µl; at a concentration of 8 mg/ml; Calbiochem, Darmstedt, Germany) and ^{3}H-cortisol (100 µl) were added to all sample and standard tubes, vortexed, covered with paraffin and incubated overnight at 4°C. The following day, 1 ml of 22% polyethylene glycol (PEG) was added, vortexed and centrifuged (1800 g) for 15 min at 4°C to separate bound hormone from the unbound hormones. The supernatant was aspirated, the pellet was resuspended in cortisol assay buffer (200 µl) and scintillation fluid (2 ml; Ultima Gold, Perkin Elmer, Australia) was added. Samples were vortexed, and placed in the β-counter (Beckman LS 3801, Beckman Instruments, USA) to determine radioactivity. Cortisol concentrations were calculated from the standard curve and a mean of duplicates was determined for each sample. The intra-assay and inter-assay co-efficient of the assays were 15.4 and 24.6 respectively.

4.2.3 Immunohistochemistry

4.2.3.1 Single label

Immunohistochemistry was performed on 10 µm paraffin-embedded sections at two anatomical levels of the brain (Sheep Ovis Aries atlas sections 720 and 1080; Chapter 2, Figure 2.8). A negative control slide was always included which primary antibody was not included, and when inspected no staining was present. All sections were placed on Superfrost plus glass slides (Mezel Glaser, Germany), de-waxed and re-hydrated through serial ethanols (100% and 70%).

VEGF: Sections were rehydrated in 0.1M PBS in 1% Triton-X 100. Antigen retrieval was carried out with 0.05M tris buffered saline (TBS; pH 10) for 3 x 10 min in a microwave oven and cooled for 30 min. Sections were then rinsed in 0.1M PBS with 1% Triton X-100, incubated in 0.3% hydrogen peroxide (H_2O_2) for 10 min at room temperature to block endogenous peroxidise activity, incubated with 2% normal rabbit serum (Vector Laboratories, USA) blocking buffer in 0.1M PBS for 45 min at room temperature to block non-specific binding and then incubated overnight at 4°C with anti-VEGF mouse monoclonal antibody (1:300; Novus

Biologicas, USA) made up in True Vision (Sapphire Bioscience, Australia). The sections were then washed three times and incubated with a secondary biotinylated rabbit anti-mouse (1:200, DAKO, USA) antibody for 1 h followed by 1 h incubation with Streptavidin horseradish peroxidise (HRP; 1:200 Amersham Bioscience, UK). Staining was then visualised using metal-enhanced diaminobenzidine (DAB, Pierce Biotechnology Inc., Illinois, USA).

Comment: The anti-VEGF antibody used (Novus Biologicas, Cat Number: NB100-648) predominantly stains for the VEGF-A isoform (Immunogen VEGF183), which is the isoform that is most important for vascular development. It was also chosen because antibodies to some other VEGF isoforms do not work well in sheep tissue.

Ki67: Antigen retrieval was carried out with 0.01M citric acid buffer (pH 6) using a microwave oven (3 x 10 min). Sections were then rinsed in 0.1M PBS with 1% Triton X-100 (Sigma Aldrich), incubated in 3% H_2O_2 for 10 min at room temperature to block endogenous peroxidise activity, incubated with 5% normal goat serum and 2% bovine serum albumin in 0.1M PBS for 45 min at room temperature to block non-specific binding and then incubated overnight with Ki67 rabbit monoclonal antibody (1:100, Thermo Scientific, USA) made up in 0.1M PBS. The sections were then washed three times with PBS and incubated with a secondary biotinylated goat anti-rabbit (1:200, Vector Laboratories, USA) antibody for 45 min followed by a 45 min incubation with streptavidin HRP (1:200). Staining was then visualised using DAB.

Albumin: Sections (10 μm) were stained for endogenous albumin. The staining procedures were performed as described above except: (a) no antigen retrieval step was used; (b) to block non-specific binding DAKO protein block (DAKO, USA) was used; (c) sheep anti-albumin (1:1000, Accurate Chemical & Scientific Corporation, USA) was made up in DAKO Real Antibody Diluent (DAKO, USA) and incubated overnight at 4°C. The sections were then washed three times, incubated with a secondary biotinylated goat anti-rabbit (1:500) antibody for 60 min, followed by 30 min incubation with streptavidin HRP (1:200). Staining was then visualised using DAB.

4.2.3.2 Double label

Sections were incubated with either monoclonal anti-GFAP (1:100; Sigma, USA), or anti-MAP2 (1:200; NeoMarkers, Calif., USA) to identify astrocytes, and neurons respectively, and mouse monoclonal antibody to identify VEGF (1:200). Immunoreactivity was visualized with Alexa Fluor® 594 goat anti-mouse (1:1,000; Invitrogen, Australia) for GFAP or MAP2 and Alexa Fluor® 488 goat anti-mouse (1:1,000; Invitrogen, Australia) for VEGF.

4.2.3.3 Quantification

All slides were coded and counting and other estimates were done with the examiner blinded to the source of the material. Images were taken under light microscopy (Olympus BX41; x400 magnification; DP25 Camera, Olympus, Japan). The number of Ki67 and VEGF-immunopositive cells were counted using Image J (v1.6.0 for Windows, National Institute of Health (NIH), USA). For each region the results of three fields of view per section, for two adjacent (duplicate) sections were averaged for each animal, and then the results averaged for all animals in each group (Control [n=5], 24 h post-UCO [n=5], 48 h post-UCO [n=4]). The number of blood vessels expressing either Ki67 or VEGF were counted and expressed as a percentage of the total number of blood vessels per field of view. Double label fluorescent images were assessed with fluorescence (red and green filters) microscopy using an Olympus BX41 (Olympus, Australia)

Albumin immunohistochemistry was assessed for the presence of intracellular albumin (Hutton *et al.*, 2007), blood vessels that contained and exhibited extravasation of albumin (Yan *et al.*, 2004). Images were taken at x200 magnification.

4.2.4 Statistical analysis

Data are shown as mean ± SEM. A Shapiro-Wilks test for normality was conducted, if passed ($p > 0.05$), and then a parametric test was run. A Two-Way mixed model ANOVA for time (within

subjects) and treatment (between subjected) was used to analyse cortisol data with a Bonferroni post-hoc.

Cell counts in each brain region of the sham controls, 24 h post-UCO and 48 h post-UCO groups were compared using a One-Way ANOVA, if significant; a Student-Neuman-Keul post hoc analysis was done. If data were not normally distributed, transformations (Log_{10}, exponential and square root) were conducted, failing to achieve normality, a non-parametric Kruskal Wallis test was conducted with pairwise comparisons. All statistical data were analysed using SPSS v18 for Windows, with significance set at $p < 0.05$. All graphs were made using GraphPad Prism Software for Windows (v5.03).

4.3 RESULTS

4.3.1 *In utero* umbilical cord occlusion - blood gases

It has previously been shown that UCO caused significant hypoxia, hypercapnia and academia in both (24 and 48 h) groups that were subjected to UCO (Castillo-Melendez *et al.*, 2005; Yan *et al.*, 2009). UCO also resulted in an initial hypertension and corresponding bradycardia. Arterial blood pressure then decreased and became hypotension and tachycardia resulted. All fetuses survived the cord occlusion and by 2 – 3 h following UCO blood gases (pO_2, pCO_2 and pH) and cardiovascular parameters were not different from control values.

4.3.2 Plasma cortisol

Following a 10 min UCO, plasma cortisol concentrations were significantly increased at 30 and 60 min and at 2 h, 4 h when compared to controls (Figure 4.1). Plasma cortisol then decreased reaching a nadir at 10 h when concentrations were not statistically different from control values. However in the UCO fetuses there was a second increase of plasma cortisol with concentrations

reaching 38.36 ± 8.85 ng/ml at 24 h, significantly higher than control values and not significantly different from values reaches at 30 – 120 min after UCO.
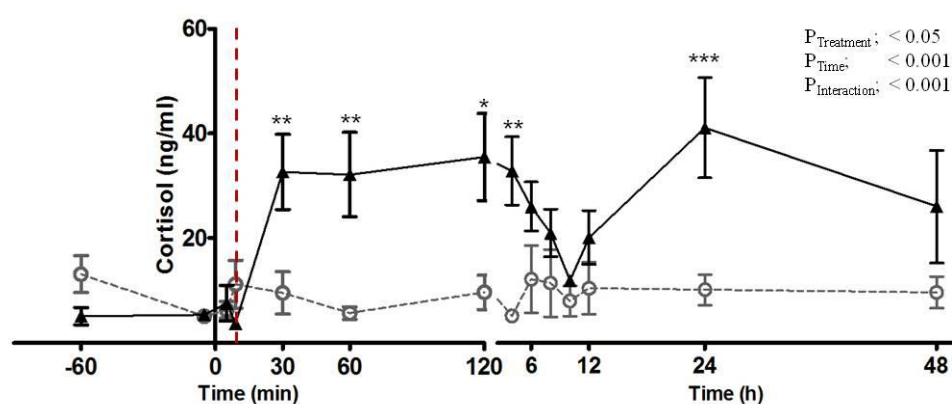
Figure 4.1: Plasma cortisol concentration (ng/ml) in response to UCO. Plasma cortisol concentration was measured in Control (n = 7; open grey circles) and fetuses that had experienced a 10 min UCO (n = 6; closed black triangle). Dashed red line indicates end of UCO. * indicates $p < 0.05$, ** indicates $p < 0.01$, *** indicates $p < 0.001$ compared to control. Mean $\pm$ SEM. Note x axis scale changes from min to hours.

4.3.3 VEGF immunohistochemistry

4.3.3.1 Single label – overall cell counts

VEGF immunostaining (Figure 4.2 A, B) was quantified by manual cell counting. At 48 h post-UCO a significant increase in the number of VEGF-immunopositive cells occurred in the external (455.5 ± 137.4 vs. 1038.8 ± 169.9, $p < 0.05$) and internal capsule (444.8 ± 137.4 vs. 1009.4 ± 58.2, $p < 0.05$) and in the striatum (516.8 ± 63.9 vs. 981.2 ± 170.4, $p < 0.05$; all striatal regions were combined) as shown in Table 4.1. The claustrum and putamen showed a trend to increased VEGF expression, however this was not significant ($p = 0.091$, $p = 0.078$ respectively). No significant differences of VEGF expression at 24 or 48 h following UCO were seen in the corpus callosum, cortex, subventricular zone, stria terminalus, thalamus, periventricular and subcortical white matter (Table 4.1).

Table 4.1: VEGF immunopositive cells. Number of immunopositive cells for VEGF (cells/mm^2) in brain regions of Control (n=5), 24 h post-UCO (n=5) and 48 h post-UCO (n=4) fetal sheep. Values expressed as mean ± SEM. * p < 0.05; ** p < 0.01 compared to control.

Brain Region	Control	24 h post-UCO	48 h post-UCO
Corpus Callosum	741.1 ± 103.5	836. 8 ± 64.0	954.3 ± 241.3
Subventricular Zone	1979.9 ± 172.8	1775.8 ± 92.8	2089.7 ± 351.2
Stria Terminalus	1617.9 ± 136.7	1999.0 ± 147.2	2009.3 ± 351.1
Periventricular White Matter	617.6 ± 35.0	960.9 ± 214.3	1286.1 ± 406.0
Subcortical White Matter	678.4 ± 98.5	985.5 ± 143.6	948.5 ± 203.2
Cortex	783.3 ± 128.5	1006.7 ± 148.1	1301.8 ± 283.0
*Striatum***:**	516.8 ± 63.9	806.2 ± 79.9	981.2 ± 170.4*
- **Caudate Nucleus**	522.1 ± 73.2	833.5 ± 86.9	1079.0 ± 277.0
- **Putamen**	608.7 ± 62.2	895.6 ± 84.0	973.5 ± 147.4
- **Internal Capsule**	444.8 ± 137.4	691.7 ± 129.3	1009.4 ± 58.2* (n=3)
- **External Capsule**	455.5 ± 137.4	719.9 ± 92.0	1038.8 ± 169.9* (n=3)
- **Claustrum**	522.1 ± 73.2	833.5 ± 86.9	1021.7 ± 258.8
Thalamus(combined):	782.9 ± 114.2	776.8 ± 95.5	895.1 ± 168.8
- **Lateral Geniculate Nucleus**	891.1 ± 120.4	755.4 ± 84.3	924.6 ± 174.7
- **Medial Geniculate Nucleus**	750.7 ± 111.8	821.8 ± 90.5	951.2 ± 154.4
- **Posterior Thalamic Nucleus**	770.4 ± 124.1	784.9 ± 170.4	857.7 ± 306.9
- **Pretectal Nucleus**	719.2 ± 110.8	743.9 ± 149.4	911.7 ± 132.9

4.3.3.2 VEGF immunopositive staining associated with blood vessels

The relative number (%) of blood vessels associated with expression of VEGF (Figure 4.2 D) was increased significantly ($p < 0.05$) in the subventricular zone, periventricular and subcortical white matter and the cortex at both 24 and 48 h after UCO (Figure 4.3 B-E). The corpus callosum (Figure 4.3 A) and medial geniculate nucleus of the thalamus (Figure 4.4 B) showed significantly increased expression at 48 h post UCO. The external capsule (Figure 4.5 C) showed a trend for an increase, but this did not reach significance ($p = 0.083$). The stria terminalus (Figure 4.3 F) and all regions examined within the striatum (caudate nucleus, putamen, claustrum, internal and external capsule) showed no significant change at 24 or 48 h compared to controls (Figure 4.5 A-F).
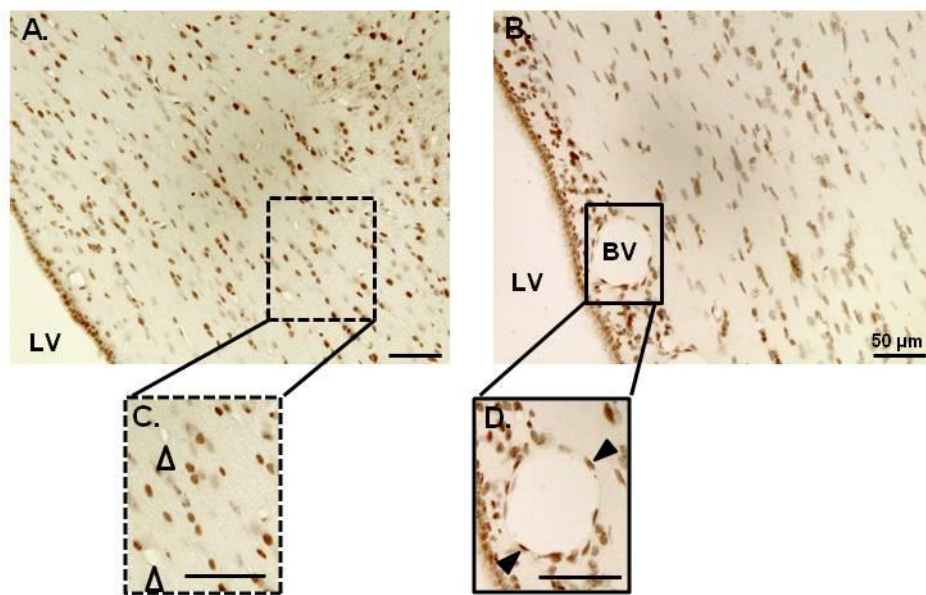
Figure 4.2: VEGF immunohistochemistry in fetal sheep brain. Photomicrographs show VEGF immunohistochemistry from control (A, C) and 48 h post-UCO (B, D) in the corpus callosum. Closed arrow head indicates positive staining associated with blood vessel (D), and open arrow head indicate no positive staining associated with blood vessel (C). Scale bar represents 50 µm. Lateral Ventricle (LV), blood vessel (BV).
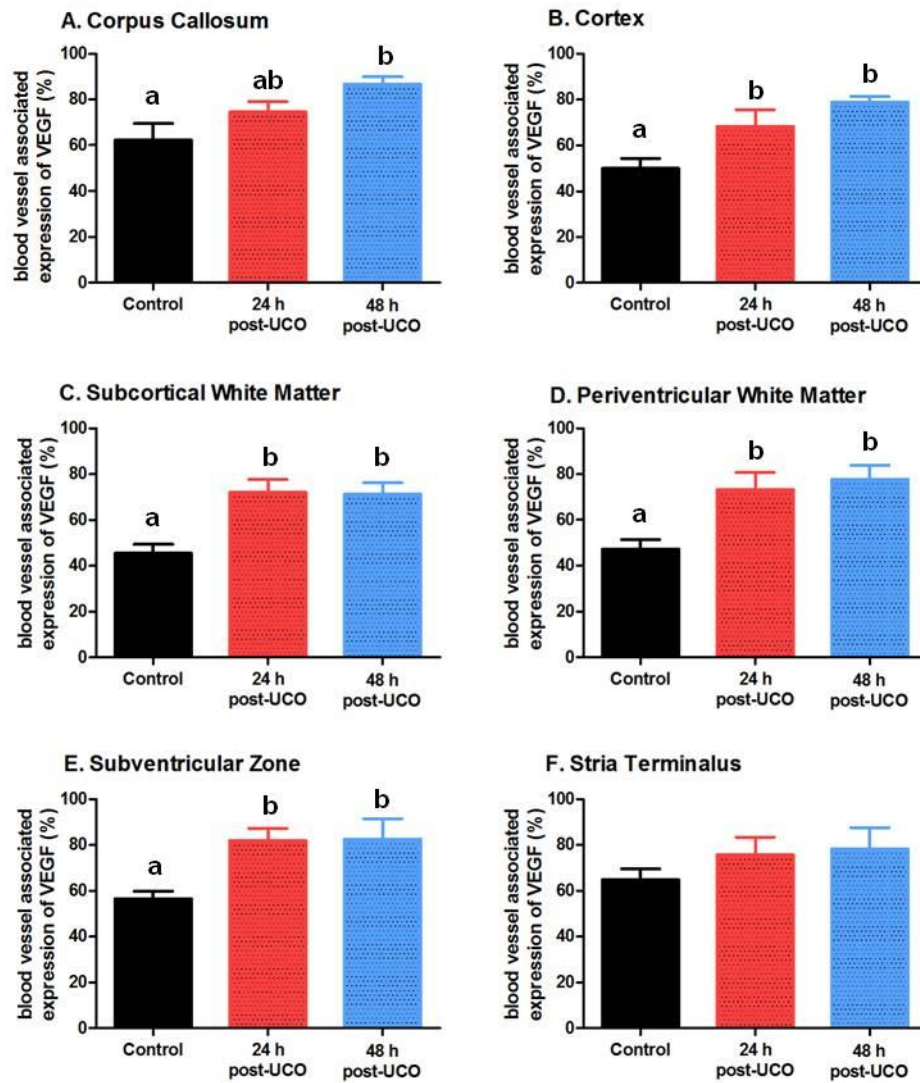
Figure 4.3: VEGF associated expression with blood vessels in the cortex, white matter, subventricular zone and stria terminalus. Graphs show the percentage of blood vessel associated expression of VEGF (A – F) in the corpus callosum (A), cortex (B), subcortical white matter (C), periventricular white matter (D), subventricular zone (E) and stria terminalus (F) for control (black), 24 h post-UCO (red) and 48 h post-UCO (blue). Significance $p < 0.05$. Mean ± SEM.
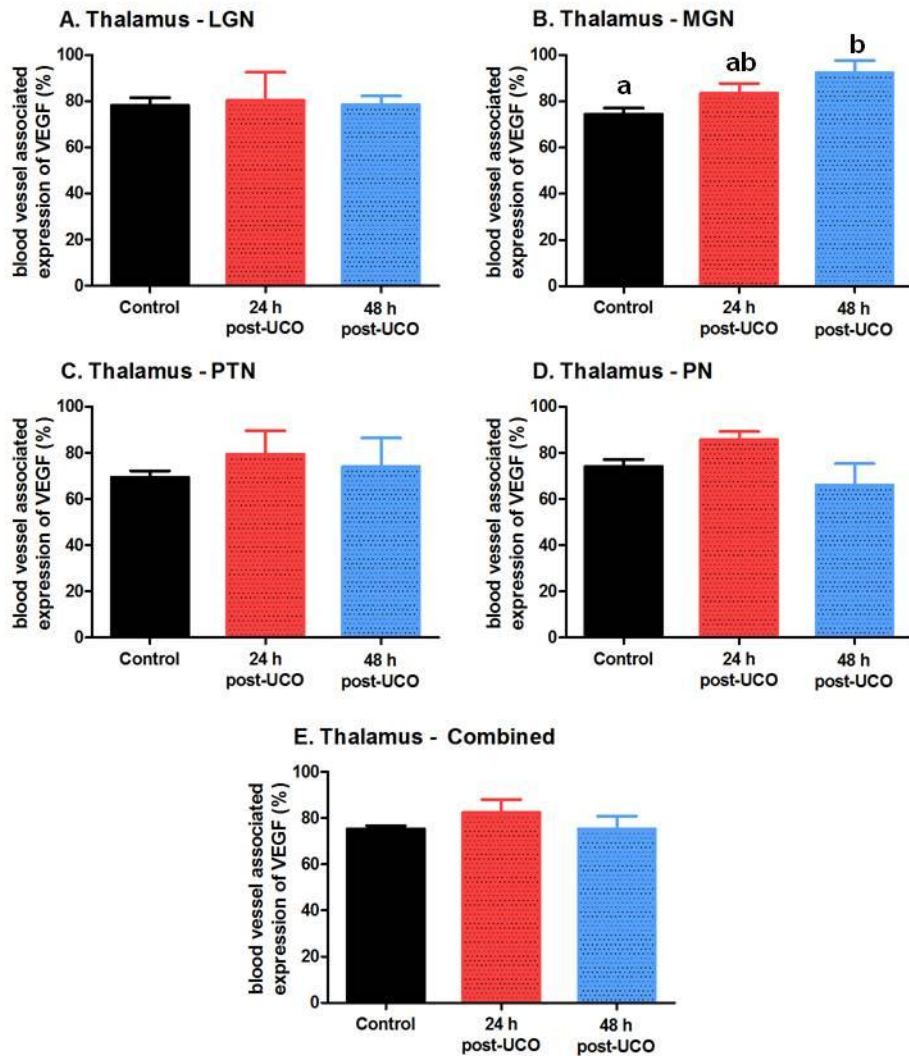
Figure 4.4: VEGF associated expression with blood vessels in the thalamus. Graphs show the percentage of blood vessel associated expression of VEGF (A –E) in thalamic nuclei; lateral geniculate nucleus (LGN; E) medial geniculate nucleus (MGN; F), posterior thalamic nuclei (PTN; C), pretectal nuclei (D) and all thalamic regions combined (E) for control (black), 24 h post-UCO (red) and 48 h post-UCO (blue). Significance $p < 0.05$. Mean ± SEM.
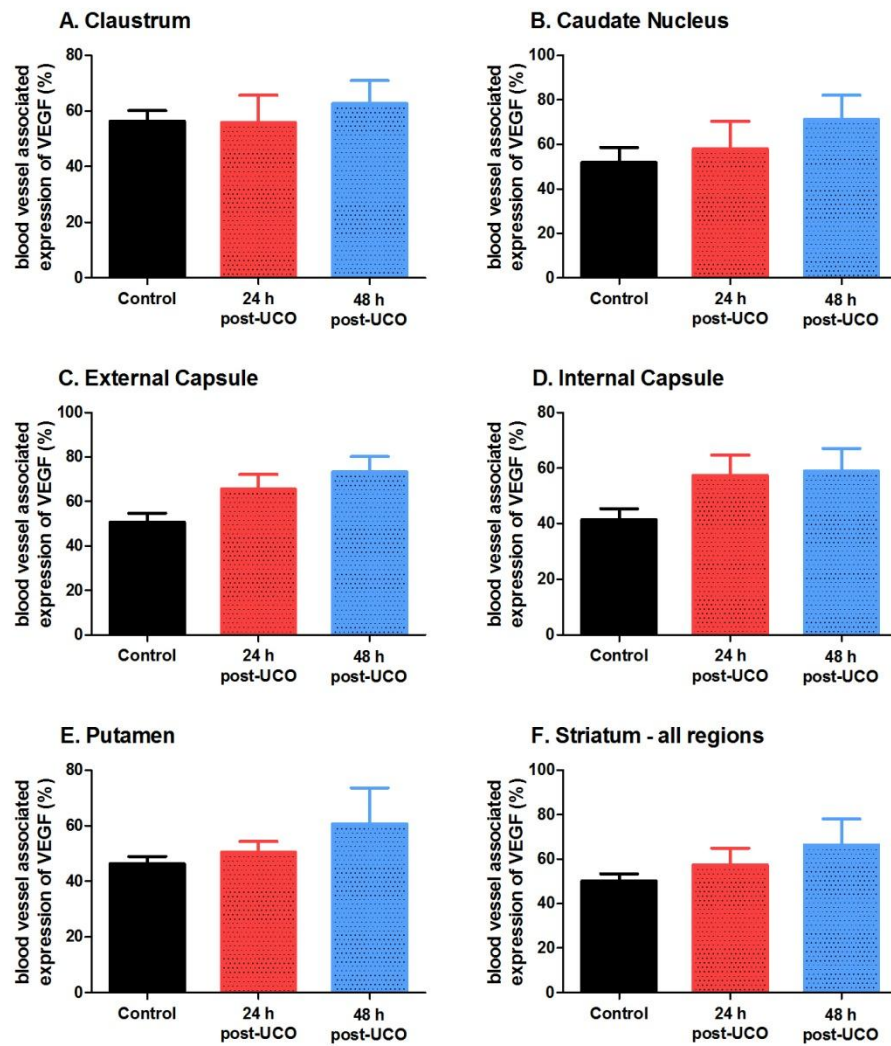
Figure 4.5: VEGF associated expression with blood vessels in the striatum. Graphs show the percentage of blood vessel associated expression of VEGF (A –F) in striatal regions including the Claustrum (A), Caudate Nucleus (B), external capsule (C), internal capsule (D), putamen (E) and striatal regions combined (F) for control (black), 24 h post-UCO (red) and 48 h post-UCO (blue). Significance *p* <0.05. Mean ± SEM.

4.3.3.3 Double label immunocytochemistry

Strong MAP-2 (mature neurons) and VEGF co-expression (Figure 4.6 A-C) was seen in the cortex (Figure 4.6 C), and striatal regions (caudate nucleus and putamen), with as expected, low to moderate expression in white matter. No co-localisation of VEGF and MAP-2 was seen in the corpus callosum. No apparent change in co-expression with MAP-2 was seen in any brain region examined following UCO. VEGF co-localisation with GFAP (astrocytes; Figure 4.6 D - G) proved to be low in all brain regions examined; this included the corpus callosum, cortex (Figure 4.6 F), striatum and white matter, and there was no apparent change in expression following UCO.
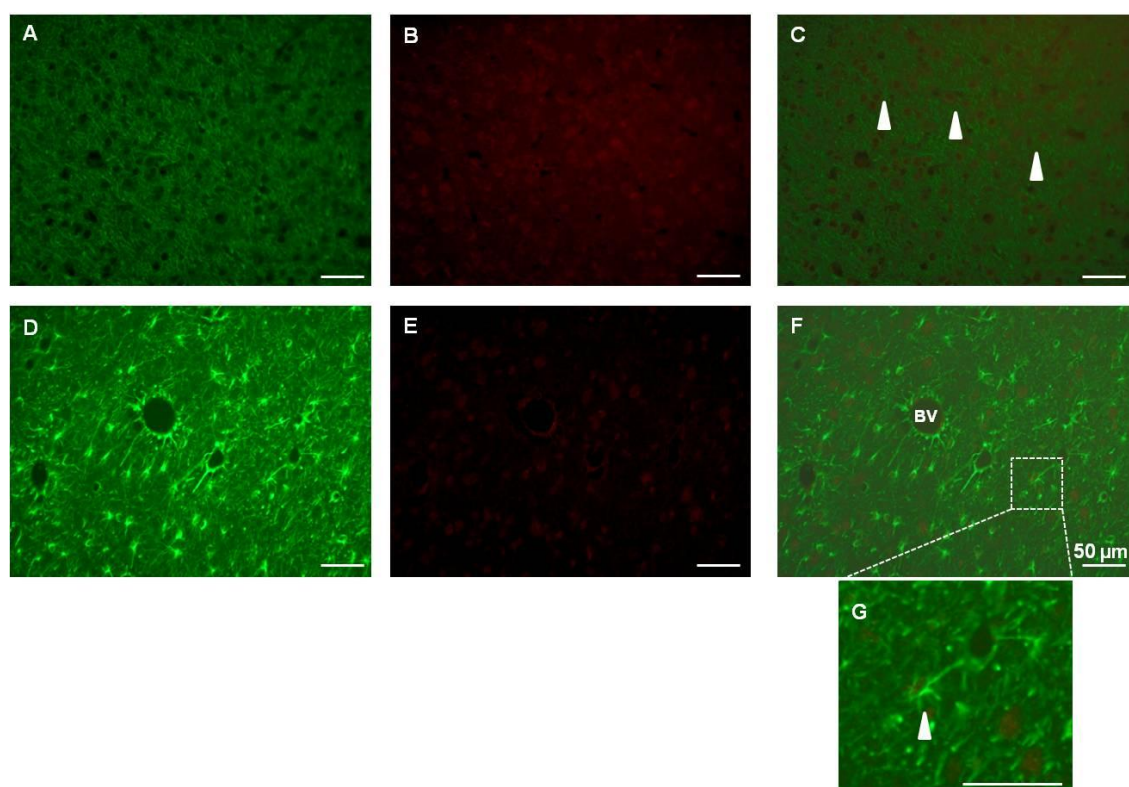
Figure 4.6: Immunofluorescent double labelling in fetal sheep brain. Photomicrographs of MAP-2 (A; green, marker for mature neurons) and VEGF (B; red) in the cortex. High co-localisation was seen between MAP-2 and VEGF (C). GFAP (D; green, marker for astrocytes) and VEGF (E; red) in the cortex. Low co-localisation was seen between GFAP and VEGF (F). Dashed box is shown at a higher magnification (G). White arrow heads indicate double labelling. Scale bar represents 50 μm. Blood vessel (BV).

4.3.4 Ki67 immunohistochemistry

Proliferating cells were quantified by manually counting Ki67 immunopositive cells (Figure 4.7). In general, there was no significant change in overall Ki67 expression (immunopositive cells) in all brain regions examined at 24 h or 48 h following 10 min UCO compared with control brains (Table 4.2), there was a trend to significance in the thalamus - combined (p = 0.065).

However, there was a significant increase in the percentage of blood vessels associated with Ki67 immunopositive cells in the subventricular zone at 24 h (13.5 ± 2.1 %) compared to control (1.7 ± 0.6 %; $p < 0.05$) and 48 h (4.6 ± 3.0; $p < 0.05$). By 48 h there was no difference compared to controls (Table 4.3) In the striatum, there was a trend for an increase of the number of blood vessels containing positive Ki67 cells at both 24 and 48 h following UCO (One-Way ANOVA; p = 0.095). There was no significant differences between groups (control, 24 h and 48 h post-UCO) for other brain regions examined (corpus callosum, white matter; periventricular, subcortical, cortex, stria terminalus, thalamus).
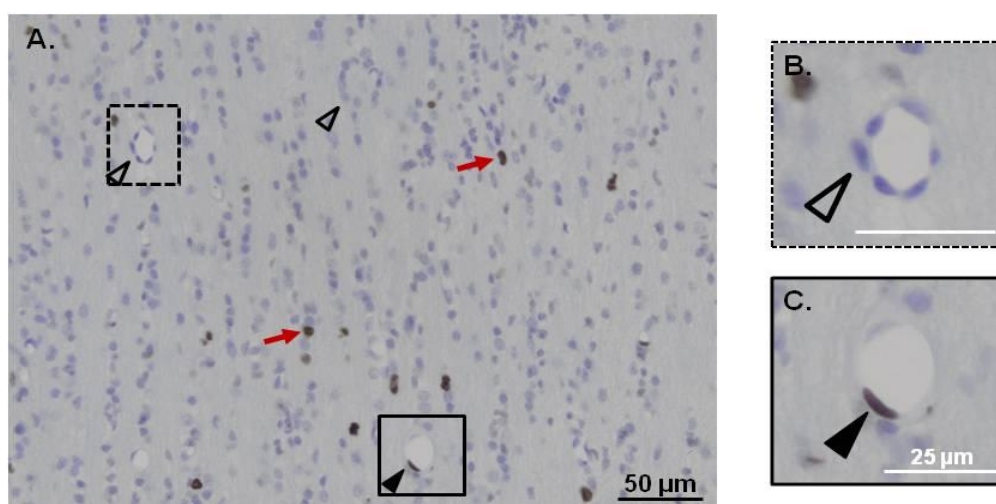
Figure 4.7: Photomicrograph of Ki67 immunohistochemistry in fetal sheep brain. Ki67 immunopositive staining (red arrow) in periventricular white matter 48 h post-UCO. Open arrow head indicates no Ki67 staining associated with blood vessel (B), and closed arrow head indicate positive Ki67 staining associated with blood vessel (C). Black scale bar represents 50 μm and white scale bar represents 25 μm.

Table 4.2: Ki67 immunopositive cells. Number of immunopositive cells for Ki67 (cells/mm^2) in brain regions of Control (n=4), 24 h post-UCO (n=4) and 48 h post-UCO (n=4) fetal sheep. Values expressed as mean ± SEM. * p < 0.05; ** p < 0.01 compared to control.

Brain Region	Control	24 h post-UCO	48 h post-UCO
Corpus Callosum	50.7 ± 12.6	72.2 ± 16.2	60.2 ± 10.3
Subventricular Zone	363.7 ± 48.4	506.6 ± 105.8	349.5 ± 140.0
Stria Terminalus	327.6 ± 128.1	697.8 ± 250.0	526.1 ± 215.3
Periventricular White Matter	42.4 ± 9.2	83.3 ± 13.6	90.1 ± 23.1
Subcortical White Matter	42.8 ± 17.5	81.0 ± 17.2	83.0 ± 38.3
Cortex	23.8 ± 8.5	57.5 ± 8.7	35.8 ± 16.7
*Striatum***:**	42.7 ± 4.8	63.0 ± 6.7	64.1 ± 10.6
- Caudate Nucleus	23.5 ± 2.9	53.1 ± 7.3	53.2 ± 17.8
- Putamen	42.8 ± 10.2	55.9 ± 4.4	66.1 ± 10.1
- Internal Capsule	46.6 ± 6.7	82.1 ± 10.5	84.5 ± 18.2
- External Capsule	56.9 ± 9.5	70.4 ± 11.0	59.8 ± 3.8
- Claustrum	43.7 ± 8.6	53.7 ± 11.5	56.7 ± 9.9
Thalamus(combined):	81.4 ± 14.8	74.1 ± 12.9	125.7 ± 16.1
- Lateral Geniculate Nucleus	96.8 ± 26.8	84.2 ± 14.0	147.2 ± 22.5
- Medial Geniculate Nucleus	77.7 ± 16.5	68.5 ± 16.5	114.4 ± 20.8
- Posterior Thalamic Nucleus	77.6 ± 8.4	76.1 ± 15.0	116.7 ± 20.8
- Pretectal Nucleus	73.2 ± 14.4	67.7 ± 18.8	128.3 ± 32.3

Table 4.3: Ki67 expression associated with blood vessels. Percentage of blood vessels immunopositive for Ki67 in brain regions of Control (n=4), 24 h post-UCO (n=4) and 48 h post-UCO (n=4) fetuses. Values expressed as mean ± SEM. * $p < 0.05$; ** $p < 0.01$ compared to control, [†] $p < 0.05$ compared to 48 h post-UCO.

Brain Region	*Control*	*24 h post-UCO*	*48 h post-UCO*
Corpus Callosum	2.5 ± 1.2	8.6 ± 3.6	4.8 ± 2.6
Subventricular Zone	1.7 ± 0.6	13.5 ± 2.1*[†]	4.6 ± 3.0
Stria Terminalus	4.3 ± 1.5	20.5 ± 8.0	16.1 ± 7.1
Periventricular White Matter	3.7 ± 1.5	10.1 ± 2.8	8.7 ± 5.0
Subcortical White Matter	2.4 ± 1.9	8.9 ± 3.5	5.3 ± 2.9
Cortex	0.9 ± 0.9	13.2 ± 2.8	7.3 ± 4.9
***Striatum*:**	2.7 ± 0.2	9.3 ± 1.9	10.1 ± 4.3
- Caudate Nucleus	2.2 ± 0.3	9.9 ± 3.0	11.2 ± 6.1
- Putamen	4.0 ± 0.9	10.9 ± 4.3	13.7 ± 6.3
- Internal Capsule	1.4 ± 0.6	12.7 ± 3.0*	8.8 ± 4.8
- External Capsule	2.7 ± 0.4	6.0 ± 1.8	6.1 ± 3.3
- Claustrum	4.2 ± 1.8	6.7 ± 1.7	10.8 ± 3.5
***Thalamus(combined)*:**	6.1 ± 1.4	5.8 ± 1.8	6.0 ± 2.3
- Lateral Geniculate Nucleus	6.2 ± 2.0	4.8 ± 1.7	8.3 ± 2.8
- Medial Geniculate Nucleus	5.8 ± 1.9	5.0 ± 1.4	3.8 ± 1.4
- Posterior Thalamic Nucleus	7.2 ± 1.7	7.8 ± 3.0	7.0 ± 3.0
- Pretectal Nucleus	5.0 ± 1.9	6.0 ± 2.8	6.5 ± 2.6

4.3.5 Albumin immunohistochemistry

Extravasation of albumin into the brain parenchyma associated with blood vessels, seen as intense albumin staining, was observed in white matter (periventricular and subcortical) of most fetuses and in the subventricular zone at 48 h following UCO (Figure 4.8, Table 4.4). Albumin immunopositive cells were identified in all control and UCO fetal brains in the corpus callosum, periventricular and subcortical white matter (Table 4.4). In the cortex and subventricular zone most fetal brains showed intracellular albumin staining whereas the striatum showed no albumin immunopositive cells. Only the LGN of the thalamus appeared to increase cellular expression of albumin 24 h following UCO, however by 48 h post-UCO no albumin positive staining was seen. The basement membrane of some blood vessels appeared to also be albumin positive (Figure 4.8 B, D); however no difference was seen following UCO (Table 4.4).
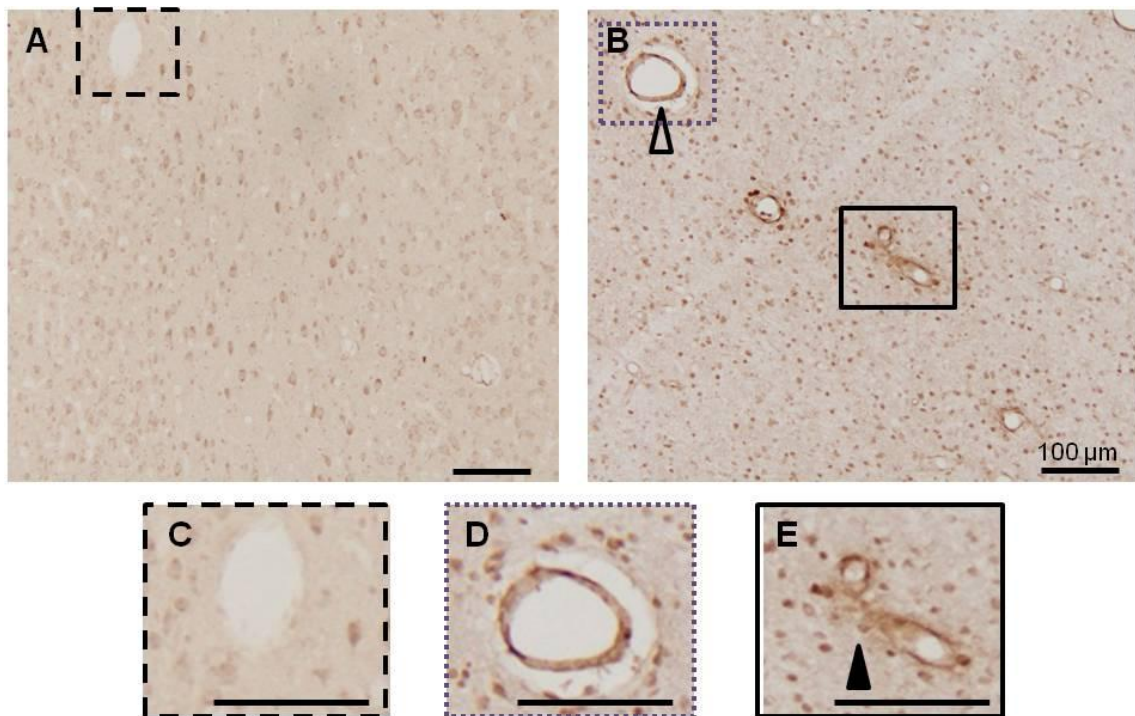
Figure 4.8: Albumin immunohistochemistry in white matter of fetal sheep. Albumin immunohistochemistry in periventricular white matter (A, B) in control (A, C), 24 h (B, D, E) post-UCO. Some blood vessels appeared to have albumin lining the vessel wall (open arrow head, D) and other blood vessels did not (C). Black arrowheads indicate albumin extravasation (E). Scale bar represents 100 μm.

Table 4.4: Summary of incidence of albumin in fetal sheep brains following UCO. Indicates the incidence of intracellular albumin expression, albumin contained to blood vessels and the occurrence of albumin extravased from blood vessels in control (n=5), 24 h (n=5) and 48 h (n=3) post-UCO. Brain regions examined included the corpus callosum, cortex, white matter (periventricular and subcortical), striatum, thalamus and subventricular zone.

Brain Region	Intracellular expression of albumin			Albumin contained to blood vessel wall			Extravasation of albumin associated with blood vessels		
	Control	*24 h post-UCO*	*48 h post-UCO*	*Control*	*24 h post-UCO*	*48 h post-UCO*	*Control*	*24 h post-UCO*	*48 h post-UCO*
Corpus Callosum	5/5	5/5	3/3	3/5	2/5	0/3	0/5	0/5	0/3
Cortex	4/5	4/5	3/3	2/5	1/5	0/3	0/5	0/5	0/3
Periventricular White Matter	5/5	5/5	3/3	5/5	5/5	3/3	3/5	4/5	3/3
Subcortical White Matter	5/5	5/5	3/3	3/5	5/5	3/3	1/5	5/5	3/3
Striatum	0/5	0/5	0/3	0/5	0/5	0/3	0/5	0/5	0/3
Subventricular Zone	4/5	5/5	3/3	4/5	5/5	3/3	0/5	0/5	2/3
Thalamus - LGN	0/5	3/5	0/4	1/5	2/5	2/4	0/5	0/5	0/4
Thalamus – PN	0/5	0/5	1/4	0/5	1/5	0/4	0/5	0/5	0/4

4.4 DISCUSSION

This is the first study to determine the distribution and expression of VEGF, Ki67 (a marker of proliferation) and albumin in the late gestation fetal sheep brain at 24 and 48 h following *in utero* UCO. In response to UCO fetal sheep were stressed as expected, and this was shown by the increase of plasma cortisol. The significant increase in VEGF expression associated with the vasculature of the subventricular zone, cortex, corpus callosum, medial geniculate nucleus and white matter following UCO is the key finding of this study. A trend to significant changes in proliferation associated with blood vessels were observed, up-regulation of VEGF appeared to have other consequences. Upon analysis of control fetal brains, it is interesting to also note that late in gestation the thalamic nuclei had the greatest percentage of proliferating blood vessels.

VEGF is an endothelial-specific mitogen, important for endothelial cell survival (Alon *et al.*, 1995). Increased VEGF expression associated with blood vessels as seen in white matter, cortex, subventricular zone and MGN (thalamus) could be indicative of endothelial cell activation, as VEGF is extremely important in inducing and regulating angiogenesis (Leung *et al.*, 1989; Breier, 2000). In white matter of PVL brains, endothelial expression of VEGF was seen to correlate with neovascularisation in the foci of necrosis (Arai *et al.*, 1998). Following neonatal stroke in rats, VEGF expression associated in blood vessels also peaked at 24 h (Mu *et al.*, 2003). During normoxia in the retina, Alon *et al.*, (1995) suggest the presence of VEGF preserves existing blood vessels by protecting endothelial cells from apoptotic death. Following hypoxia, up-regulation of VEGF initiates angiogenesis and vascular remodelling (Alon *et al.*, 1995).

It is important to also recognise the regionally different response of the fetal sheep brain to UCO, as shown in this study. The significant increase of VEGF associated with blood vessels in white matter and cortex could highlight regions that are particularly sensitive to hypoxia, where there was an increase in VEGF expression at both 24 and 48 h. The incidence of serum protein

albumin that had released from blood vessels, predominantly seen in white matter (periventricular and subcortical) and the subventricular zone, is consistent with the increased permeability often associated with VEGF. Also known as vascular permeability factor, increased VEGF expression is closely correlated with increased BBB permeability following hypoxia (Zhang *et al.*, 2000; Kaur *et al.*, 2006b), and dilation of cerebral microcirculation (Mayhan, 1999). This is consistent with our findings presented in this study and in Chapter 3.

Kumar *et al.,* (2008) found increased BBB permeability was correlated with increased malondialdehyde (a marker of lipid peroxidation) and nitrate/nitrite levels in term human neonates following perinatal asphyxia. These newborns also developed hypoxic-ischemic encephalopathy. In an adult model of focal cerebral ischemia, (24 h middle cerebral artery embolism) acute up-regulation of VEGF also correlated with increased BBB leakage of Evans blue dye and FITC-dextran at 4 h following embolism (Zhang *et al.*, 2002b). A similar response is also seen following traumatic brain injury in adult rats, with alterations in BBB permeability peaking at 2 – 4 days which also correlated with increased vascular VEGF expression (Nag *et al.*, 1997). Following inflammation, increased permeability in white matter of fetal sheep (Yan *et al.*, 2004) and in newborn rats (Stolp *et al.*, 2005) has been reported.

The exact mechanisms that result in increased BBB permeability after cerebral hypoxia or ischemia are not well understood. Tight junctions exist between endothelial cells and are functionally important in controlling paracellular permeability and following hypoxia-ischemia, disruptions to those tight junctions can occur. *In vitro* studies have shown that increased permeability in brain microvessel endothelial cells following hypoxia resulted in VEGF mediated disorganisation and reduced expression of key tight junctional proteins such as occludin and zona occludin-1 (Wang *et al.*, 2001; Fischer *et al.*, 2002).

Interestingly, treatment with human serum albumin 2 h, but not immediately, after middle cerebral artery occlusion (MCAO) in adult rats has protective actions. Yao *et al.,* (2010) found treatment with albumin resulted in decreased VEGF expression only at 6 and 24 h post-MCAO.

This correlated with decreased oedema (brain water content) and improvement of neurologic scores seen at 24 h following MCAO. The beneficial actions of albumin administration following adult stroke are thought to occur by providing energy for neuronal metabolism, and albumin having both antioxidant and anti-apoptotic actions (Zoellner *et al.*, 1996; Remmers *et al.*, 1999). Although the exact mechanisms of action have not been elucidated, the initial down regulation of VEGF 6 to 24 h hours following ischemia suggest that this time frame, up to 24 h following ischemia (when VEGF is now robustly up-regulated), could be the most detrimental resulting in brain injury. Consistent with this, treatment with recombinant human VEGF 1 h following ischemia (MCAO) resulted in increased BBB permeability, haemorrhagic transformation and ischemic cell death. However, treatment 48 h following MCAO improved functional outcome in adult rats (Zhang *et al.*, 2000).

VEGF has direct actions on endothelial cells and pericytes stimulating proliferation and causing hyper-permeability (Hippenstiel *et al.*, 1998; Yamagishi *et al.*, 1999; Thanabalasundaram *et al.*, 2010). We did not see any significant change in the percentage of blood vessels expression Ki67. Pericytes have been suggested to be the first cells to respond to hypoxia and express VEGF; they are part of the basement membrane and communicate with endothelial cells (Yamagishi *et al.*, 1999; Gonul *et al.*, 2002; Al Ahmad *et al.*, 2009). The severity of oxygen deprivation contributes to the rate of BBB function loss; during acute hypoxic exposure pericytes exacerbate disruption of the BBB (Al Ahmad *et al.*, 2009). Pericyte-mediated barrier regulation and opening of the BBB is also correlated with increased matrix metalloproteinase (MMP) 2 and 9 activity.

MMPs play an important role in basal lamina degradation following hypoxia (Valable *et al.*, 2005; Thanabalasundaram *et al.*, 2010). Down-regulation of angiopoietin-1, important for blood vessel stabilisation and potentiating neovascularisation, is closely correlated with increased BBB leakage (Zhang *et al.*, 2002b; Valable *et al.*, 2005). Synthesis and release of soluble guanylate cyclase, nitric oxide and prostaglandins and increased calcium influx also contribute

to changes in vascular permeability (Bates & Curry, 1997; Murohara *et al.*, 1998; Fischer *et al.*, 1999; Mayhan, 1999).

Disruptions in BBB permeability, elevation in mean arterial blood pressure and subsequent accumulation of water in the brain parenchyma all contribute to the formation of vasogenic oedema (Kuroiwa *et al.*, 1985; Klatzo, 1987). Following hypoxia and brain (trauma) injury, BBB leakage triggers the activation of astrocytes, corresponding with an increase in expression of aquaporin 4 (AQ4; the astrogilal water channel which facilitates water movement in and out of the brain), this response would also contribute to formation of oedema (Papavassiliou *et al.*, 1997; Kaur *et al.*, 2006b). Although an absence of astrocytes can also contribute to vascular leakage, BBB permeability has also been shown to be restored in the absence of astrocytes (Willis *et al.*, 2004).

In the present study we found low co-localisation of VEGF with astrocytes but strong co-expression with neurons particularly in the cortex and striatum. Increased VEGF cellular expression was only seen at 48 h post-UCO in the external and internal capsule, with no significant change in blood vessel associated expression. Although the implications of this have not been further investigated, this finding may be indicative of a neurogenic response, as strong co-localisation was seen between MAP-2 and VEGF staining, and VEGF has been shown to be an important regulator of neurogenesis (Sun *et al.*, 2003). In neonatal and adult studies following hypoxia and/or ischemia, VEGF expression has been co-localised not only with endothelial cells but neurons, astrocytes, pericytes, microglia and macrophages (Arai *et al.*, 1998; Plate *et al.*, 1999; Jin *et al.*, 2000b; Mu *et al.*, 2003; Al Ahmad *et al.*, 2009). In white matter of neonates who had PVL, endothelial cells and reactive astrocytes expressed VEGF which correlated with neovascularisation around the foci of necrosis (Arai *et al.*, 1998). The presence of VEGF is also important in proliferation and survival of astrocytes following injury (Schmid-Brunclik *et al.*, 2008).

Sentilhes *et al.,* (2010) characterised VEGF expression in developing human brain tissue, and found VEGF was expressed by neurons, neurite processes, astrocytes and blood vessels from mid (24 weeks) to late (34 weeks) gestation in the telencephalon and also by oligodendrocytes in the cerebellum. In the developing rat cortex, neuronal expression of VEGF provides the initial signal for angiogenesis, and subsequently glial expression of VEGF coincides with end-feet investing blood vessels and the maintenance of the vasculature (Alon *et al.*, 1995; Ogunshola *et al.*, 2000). These studies highlight the importance of VEGF during cerebral development, although no changes were noted in co-expression following UCO, high VEGF expression in the fetal brain is suggestive of ongoing neurogenesis.

During development and following hypoxia, HIF-1α is upregulated and one of its target genes is VEGF. In periventricular white matter of postnatal rats, Kaur *et al.,* (2006a) saw peak HIF-1α gene expression at 3 h post hypoxia (2 h of hypobaric exposure), with VEGF expression highest at 7 d when HIF-1α was significantly reduced. Mu *et al.,* (2003) also found peak gene expression of HIF-1α and VEGF at 8 h following neonatal stroke (focal ischemia; 1.5 h of MCAO). These studies highlight that HIF-1α is up-regulated within the first few hours following hypoxia, and then quickly returns to basal levels. Schmid-Brunclik and colleagues (2008) found *in vitro*, that VEGF protein was still induced in astrocytes following severe hypoxia in the absence of HIF-1α (by knockdown of HIF-1α in siRNA *in vitro* experiments).

Two important aspects must be taken into consideration when understanding hypoxia-induced VEGF expression. Firstly the time course of the VEGF and HIF-1α response is dependent on severity and duration of the hypoxic insult; and secondly, several other factors such as hormones (particularly in ovary and adrenal gland), can regulate VEGF expression (Shweiki *et al.*, 1993). Other factors seen to be important in the regulation of VEGF expression during development include cortisol, which parallels increased VEGF expression in the fetal sheep intestine in late gestation (Holmes *et al.*, 2008). From our data we saw a significant increase in plasma cortisol at 24 h post-UCO, and although we did not see a significant increase of VEGF

expression in fetal sheep brains following UCO, circulating VEGF concentration from plasma samples was not measured. Increased VEGF from cord blood has been seen to be significantly higher in infants who experienced perinatal asphyxia and subsequently developed encephalopathy (Aly *et al.*, 2009). Increased circulating VEGF could be regulated by increased cortisol following asphyxia, which could be a possible clinical measure at birth for at risk infants.

Interestingly, another study found that transcriptional co-activator, PGC-1α (peroxisome-proliferator-activated receptor-γ coactivator-1α) was a powerful regulator of VEGF following nutrient and oxygen deprivation, and most importantly, this was independent of HIF (Arany *et al.*, 2008). PGC-1α co-activates the oestrogen related receptor-α (ERR-α) and is important in linking the regulation of oxygen consumption by the mitochondria to the delivery of oxygen and nutrients. Although it is not essential for embryonic vasculogenesis, PGC-1α knockdown mice do show behavioural abnormalities and progressive vacuolisation in brain regions, particularly the striatum and white matter (Lin *et al.*, 2004; St-Pierre *et al.*, 2006; Cowell *et al.*, 2007). PGC-1α KO mice were also seen to be more vulnerable to oxidative stress in the brain. PGC-1α is important for the induction of two key antioxidant enzymes, superoxide dismutase 2 (SOD2) and GPx1 highlighting it as a powerful regulator of reactive oxygen species (ROS) metabolism (St-Pierre *et al.*, 2006; Arany *et al.*, 2008). In the developing rat brain, PGC-1α is also a key regulator of neuronal and GABAergic signalling (Cowell *et al.*, 2007). These findings highlight that PGC-1α could be highly active in the striatum and white matter, and could be an important therapeutic target following hypoxia.

One of the main limitations in our study is that we were unable to optimize an accurate marker of endothelial cells and pericytes in the fetal sheep brain. This would enable us to better understand the cerebrovascular expression of VEGF. Albumin immunohistochemistry was used to indicate alterations in BBB permeability, however a more accurate method could involve the injection of FITC or Indian ink prior to post mortem to better visualise sites of vascular leakage.

VEGF does have both neurotoxic and neuroprotective actions, although the present study suggests within the first 48 h following a 10 min episode of severe hypoxia, VEGF is associated with increasing blood vessel permeability. However increased capillary associated expression of VEGF has also been shown to decrease apoptotic death in endothelial cells (Alon *et al.*, 1995), which needs to be further investigated in our study.

Depending on severity and duration of hypoxia, age and animal species, hypoxia-mediated VEGF expression clearly has complex effects (Mu *et al.*, 2003). Blocking the actions of VEGF prevents hypoxia-induced vascular leakage and BBB permeability changes (Schoch *et al.*, 2002; Kaur *et al.*, 2006b). We also saw the presence of intracellular expression of albumin in most brain regions of both control and cord occluded fetal sheep brains. The preferential uptake of albumin by astrocytes is TGF- β receptor mediated, and neuronal uptake of albumin has been previously noted in the cerebellum (Hutton *et al.*, 2007; Ivens *et al.*, 2007). In our study we need to further investigate the reasons for the presence of intracellular albumin and how increased BBB permeability in white matter may contribute to vasogenic oedema.

Although the neonatal brain may be more vulnerable to VEGF-mediated BBB permeability changes, this could prove to be beneficial allowing the transport of large molecules (possible therapeutic and neuroprotective agents) into the brain aiding in repair mechanisms (Young *et al.*, 2004). Administration of human serum albumin 2 h following ischemia in the adult, results in decreased brain oedema and improvement of neurological scores, at least short term (24 h) (Yao *et al.*, 2010). Treatment with HIF-1α, PGC-1α or VEGF during re-oxygenation following hypoxia has also been shown to be protective, by inhibiting apoptosis, stimulating neurogenesis and reducing the extent of brain injury in both neonatal and adult studies (Ogunshola *et al.*, 2000; Zhang *et al.*, 2000; Baranova *et al.*, 2007; Feng *et al.*, 2008; Sheldon *et al.*, 2009).

There is a significant up-regulation of VEGF associated with blood vessels which could explain the increased incidence of BBB permeability seen in white matter. However as permeability changes were only seen in white matter, VEGF could have regionally different (protective or

damaging) actions. A trend but not a significant change in endothelial cell proliferation could suggest angiogenic responses may occur after 48 h in an attempt to protect the neonatal brain following hypoxia. Adult rodent studies have shown that following cerebral ischemia, early, acute (up to 24 h) up-regulation of VEGF has detrimental consequences (increased BBB permeability), however increased expression of VEGF following this (after 48 h) has a beneficial outcome. Whether this also occurs in the developing fetal sheep brain, following a transient systemic hypoxic event will be discussed in the next chapter. Further investigation will highlight the potential actions and implications of VEGF for the neonatal brain.

Chapter 5

AN IMMUNOHISTOCHEMICAL

INVESTIGATION OF CEREBROVASCULAR

RESPONSES FOLLOWING BRIEF GLOBAL

HYPOXIA IN LATE GESTATION FETAL

SHEEP.

TABLE OF CONTENTS

5.1 INTRODUCTION

Clinical studies of the full term infant suggest that a period preceding birth, is a time when brain physiology may be disturbed, leading to changes that result in neonatal encephalopathy and brain injury, with timing and gestational age (GA) of the insult contributing to the pattern of injury (Badawi *et al.*, 1998; Cowan *et al.*, 2003; Van den Broeck *et al.*, 2007; Foran *et al.*, 2009). Term neonates who experience hypoxia-ischemia in late gestation tend to have injuries such as haemorrhage and wide spread cell death in the hippocampus, thalamus and cortical regions (Wigglesworth & Pape, 1978; Inder & Volpe, 2000; McLean & Ferriero, 2004; Perlman, 2004). Antepartum events such as placental abruption or interference with umbilical blood flow result in severe hypoxia or asphyxia, but these are difficult to detect clinically, and therefore may significantly contribute to a great proportion of the injury seen in term infants.

Following hypoxia, angiogenesis (sprouting of blood vessels from pre-existing ones) occurs as a response that increases vascularisation and increases oxygen delivery to oxygen-deprived tissue (Shweiki *et al.*, 1993). In the brain, this angiogenic response is also suggested to improve neuronal survival following ischemia (Krupinski *et al.*, 1994). Key mediators of this tightly regulated process are hypoxia inducible factor-1α (HIF-1α), vascular endothelial growth factor (VEGF) and one of its' tyrosine kinase receptors VEGFR-2, all of which are up-regulated following hypoxia (Marti *et al.*, 2000b). Increased expression of VEGF in the hours and days following hypoxia is associated with increased blood brain barrier (BBB) permeability, and this has been shown to occur in both neonatal (Kaur *et al.*, 2006a) and adult rat (Zhang *et al.*, 2000; Zhang *et al.*, 2002b) models. We have also seen increased VEGF associated with the increased incidence of BBB permeability 48 h following umbilical cord occlusion (UCO) in the late gestation fetal sheep brain (Chapter 4).

Increased expression of VEGF and/or VEGFR-2 over many days or weeks is suggested to be a neuroprotective response in the brain. In addition to promoting vascularisation, increased VEGF expression is also associated with increased survival of endothelial cells and astrocytes, and

inhibition of apoptosis (Gora-Kupilas & Josko, 2005; Schmid-Brunclik *et al.*, 2008). Treatment with VEGF following hypoxia has been shown to reduce brain injury and apoptosis (Feng *et al.*, 2008) whereas inhibition of VEGFR-2 activity in a neonatal model of stroke resulted in increased brain injury and cell death (Shimotake *et al.*, 2010). Like VEGF and its receptors, the angiopoietins (angpt-1 and -2) and their receptor (Tie-2) are important for stimulating vessel growth and remodeling (Dumont *et al.*, 1993; Yancopoulos *et al.*, 2000). Expression is also affected by hypoxia, where angpt-1 *down-regulation* is correlated with increased BBB leakage (Zhang *et al.*, 2002b).

In late gestation, reduced uterine or umbilical blood flow results in severe fetal hypoxia, leading to significant neuronal injury, lipid peroxidation, inflammation and cell death in the brain over for at least 72 h after the insult (Gunn *et al.*, 1992; Mallard *et al.*, 1992; Mallard *et al.*, 1994; Castillo-Melendez *et al.*, 2004; Duncan *et al.*, 2004). However, adaptive mechanisms are also triggered following hypoxia/ischemia which may be responses that limit further cell death and brain damage. In particular, brain-derived erythropoietin (Epo) - another HIF-1α induced protein - has been implicated in neuroprotection by direct and indirect mechanisms including inhibition of hypoxia-ischemia induced apoptosis, and vessel growth and neovascularisation. We have previously shown increased neuronal and astrocytic expression of Epo and Epo-receptor 48 h following umbilical cord occlusion (UCO) in the late gestation fetal sheep brain (Castillo-Melendez *et al.*, 2005).

Few studies have assessed the consequences of asphyxia on the fetal sheep brain beyond the 48 to 72 h time frame when such adaptive processes, particularly increased expression of VEGF and VEGFR-2, might be very important. Therefore it was important that this study assessed the consequence of UCO (mild or severe) in late gestation on VEGF and VEGFR-2 expressions over days leading up to birth. The expression of Epo and a key vascular marker (angpt-1) was also assessed, to understand the extent of the vascular response to UCO in late gestation fetal sheep.

Of interest was the finding that the immediate response to UCO was different between fetuses, making it was possible to distinguish between 'mild' and 'severe' changes in blood gases and metabolic status. Therefore the long term effect of these different responses on the brain, particularly in relation to the expression of the hypoxia-sensitive genes discussed above, has also been examined.

5.2 METHODOLOGY

The animal surgery and experimental protocols are the same as those given in detail in Chapter 2. The same fetuses were also used for the fetal behavioural experiments detailed in Chapter 6. These fetuses were catheterized and underwent implantation of a sagittal sinus transducer and electrodes, these surgical details are mentioned in Section 6.2.1.

5.2.1 Animal surgery and experimentation

Fourteen pregnant Border-Leicester ewes carrying a singleton fetus were used in this study. The use of these animals and all procedures had received prior approval from the School of Biomedical Science Animal Ethics Committee of Monash University. At 124-126 days GA (term is 146 days), the surgery was performed under general anaesthesia, induced by an intravenous injection of 1 g sodium thiopentone (50 mg/ml; Pentothal, Boehringer Ingelheim Pty Ltd, Australia) in 20 mL sterile water and maintained for the duration of surgery using 1.5-2% isoflurane (Isoflo, Abbott Australasia Pty Ltd, Kurnell, Australia). Under aseptic conditions the fetal head and both front legs were brought out of the uterus through the incision site. A polyvinyl catheter (0.86 mm ID × 1.52 mm OD) filled with heparinised saline was inserted into a brachial artery to obtain blood samples and measure arterial pressure. A second saline-filled catheter was filled was placed in the amniotic sac for a pressure reference. An inflatable silastic cuff (type OC16, *In Vivo* Metric, Healdsburg, CA, U.S.A) was placed around the abdominal end of the umbilical cord, on inflation; this would cause complete cessation of blood flow in the

cord. The fetus was then returned to the uterus and the incision closed. All catheters was exteriorised through a maternal flank incision, and the maternal abdominal incision was closed.

Experiments were performed 4-5 days after surgery. Fetal blood pressure and amniotic pressure were measured using solid state pressure transducers, and fetal arterial pressure was calculated by electronic subtraction of amniotic pressure. Fetal heart rate was calculated online from the blood pressure pulse. All data was recorded continuously on the hard disk of a computer via an analogue-digital converter and Chart software (PowerLab, ADInstruments, NSW, Australia).

On the day of the experiment (130–132 days GA) the umbilical cord was occluded completely for 10 min by inflating the cuff with 3mL of sterile water. Fetal arterial blood samples (3 mL) were taken at -1 h, -5 min, +5 min, +9 min, 30 min, 1, 2, 4, 6, 8, 10, 12 and daily after that, relative to the start of the occlusion (time = 0). Arterial blood samples were used immediately to measure pO_2, pCO_2, O_2 saturation, pH, glucose and lactate, using a Radiometer ABL700 analyser (Radiometer Medical A/S, Denmark). In addition to the Control (sham UCO; n=5) group, on the basis of the changes in blood gases at the end of the UCO period, fetuses were allocated retrospectively to one of the following two groups: severe-UCO (n = 5), or mild-UCO (n=4) (see Results Section 5.3.1, Table 5.1 for details).

All pregnancies were allowed to continue until such time when labour had spontaneously commenced - this was between 5 and 14 days following UCO or sham UCO (see Results 5.3.3). When the ewe was deemed to be in early stage labour, based on observation of rupture of membranes, vaginal loss of amniotic fluid, presentation of a fetal part, or signs of abdominal straining by the ewe, the ewe and fetus were humanely euthanized by i.v. injection of pentobarbitone sodium (Lethabarb, Virbac Pty Ltd, Australia) given to the ewe.

The fetal brain was then removed as soon as possible, weighed, cut sagittally into left and right half and further sectioned coronally into 3mm blocks. The blocks from one half of the brain were snap frozen in liquid N_2 and stored at -80°C, and blocks of the other half were immersion-

fixed in 4% paraformaldehyde (PFA) for 48 h at 4°C and then placed into macro-cassettes. Macro cassettes were then immersed in 70% ethanol for 3 to 4 hours, cleared in sulphur-free xylene and infiltrated with paraffin wax at 58°C (Department of Anatomy, Monash University). (Detailed explanation of these post mortem procedures has been given in Chapter 2, Section 2.8)

5.2.2 Immunohistochemistry

Immunohistochemistry was performed on 10 μm paraffin-embedded sections at two anatomical target regions of the brain, which contained brain areas previously identified to be vulnerable to hypoxia (Sheep Ovis Aries atlas Section 720 and 1080 – Chapter 2, Figure 2.9). All sections were placed on Superfrost plus glass slides (Mezel Glaser, Germany), de-waxed and re-hydrated through serial ethanols (100% and 70%). A negative control slide was always run which was not incubated with primary antibody, and when inspected, no immune-specific staining was present.

Vascular Endothelial Growth Factor (VEGF)

Sections were rehydrated in 0.1M PBS in 1% Triton-X 100 (Tx-100). Antigen retrieval was carried out in 0.05M tris buffered saline (TBS; pH 10) for 3 x 10 min in a microwave oven and cooled for 30 min at room temperature. Sections were then rinsed in 0.1M PBS with 1% Triton X-100, incubated in 0.3% H_2O_2 for 10 min at room temperature to block endogenous peroxidise activity, incubated with 2% normal rabbit serum (Vector Laboratories, USA) blocking buffer in 0.1M phosphate buffered saline (PBS) for 45 min at room temperature to block non-specific binding and then incubated overnight at 4°C with anti-VEGF mouse monoclonal antibody (1:200; Novus Biologicas, USA) made up in True Vision (Sapphire Bioscience, Australia). The sections were then washed and incubated with a secondary biotinylated rabbit anti-mouse (1:200, DAKO, USA) antibody for 1 h followed by 1 h incubation with streptavidin horseradish

peroxidise (HRP; 1:200 Amersham Bioscience, UK). Immunostaining was then visualised using metal-enhanced diaminobenzidine (DAB, Pierce Biotechnology Inc., Illonois, USA).

VEGFR-2

Antigen retrieval was carried out in 0.01M citric acid buffer (pH 6.0) for 3 x 5 min in a microwave oven and cooled for 30 min at room temperature. Sections were then rinsed in 0.1% Tx-100 and 0.1M PBS, incubated in 3% H_2O_2 in 50% methanol for 10 min, incubated with 5% normal goat serum (NGS) and 2% bovine serum albumin (BSA, Sigma, Australia) in PBS for 60 min. Sections were then incubated overnight at 4°C with polyclonal rabbit anti-VEGFR-2 (1:200, Abcam, USA) made up in DAKO Real diluent (DAKO, USA). Sections were rinsed and incubated with a biotinylated secondary goat anti-rabbit (1:200, Vector Laboratories, USA), rinsed and incubated with strep-HRP (1:200) for 60 min at room temperature. Sections were the visualised with DAB.

Epo

The immunohistochemistry protocol is as for VEGFR-2 except: (a), antigen retrieval occurred for 2 x 5 min: and (b), incubation with primary antibodies polyclonal rabbit anti-Epo (1:200, Santa Cruz, USA) occurred for 48 h at 4°C.

Angpt-1

The immunohistochemistry protocol is as for VEGFR-2 except: (a), antigen retrieval occurred for 2 x 5 min; (b), incubation with primary antibodies polyclonal rabbit anti-angiopoietin-1 (1:200, Abcam, USA) in True Vision (Sapphire Bioscience, USA) primary antibody diluent occurred for 60 min at room temperature, then overnight at 4°C.

Laminin

Sections were rehydrated in 0.1M PBS in 1% Triton-X 100. Antigen retrieval was carried out on sections incubated with Proteinase K (40μg/ml) for 30 min at 37°C and cooled for 20 min at

room temperature. Sections were then rinsed in PBS, incubated in 0.3% H_2O_2 in 50% methanol for 15 min at room temperature to block endogenous peroxidise activity, incubated with 2% normal goat serum blocking buffer in 0.1M PBS for 30 min at room temperature to block non-specific binding and then incubated overnight with anti-laminin rabbit polyclonal antibody (1:200; Novus Biologicas, USA). The sections were then washed incubated with a secondary biotinylated goat anti-rabbit (1:200; Vector Labs, USA) antibody for 45 min followed by 45 min incubation with strep-HRP (1:200). Immunopositive vessels were then visualised using DAB.

5.2.3 Quantification

Digital colour images were taken under light microscopy (Olympus BX41; x400 magnification) using a DP25 Camera (Olympus, Japan). Duplicate sections of each brain region per animal were coded and then examined so that the source of the section (fetus, treatment) was unknown. Images were taken of the corpus callosum, cortex (between layers II to V), and subventricular zone, periventricular and subcortical white matter at the level of the lateral ventricle (Sheep Ovis aries – Section 720) and subcallosal bundle and thalamus (Sheep Ovis Aries – Section 1080 – 1160).

VEGF and VEGFR-2 immunopositive cell counts were manually completed using ImageJ (Java v1.6.0 for Windows, NIH, USA). For Epo immunopositive cell counting was done automatically using Metamorph Offline (v7.7., Molecular Devices, USA). A range for the intensity of positive staining, and a filter for the particle size (in pixels) was set to allow for accurate analysis. In the subventricular zone, densitometric analysis was done using Scion Image (v4.03, National Institute of Health (NIH), USA) because of the large number of VEGF, VEGFR-2 and Epo-positive cells present in this region. The total positive staining (above threshold) in pixels was calculated to give the total percentage area occupied by positive cells. The total number of pixels that represented positive staining for each field of view was calculated and represented as a percentage of the total pixels of the image.

The number of blood vessels expressing VEGF, VEGFR-2, Epo and angpt-1 were counted and expressed as a percentage of the total number of blood vessels per field of view. All analysis was quantified from 3 fields of view for each brain region on 2 brain sections per animal, and the average from these 6 fields of view were calculated for each animal in each group (Control (n=5), Mild UCO (n=4), Severe UCO (n=5)).

Images for laminin immunohistochemistry were taken using a light microscope (Model BX41, Olympus, Japan) at x200 magnification for all brain regions examined, for duplicate sections where possible. Vessel density, morphology and size distribution analysis were done as detailed in Chapter 3.

5.2.4 Statistical analysis

Data are shown as mean ± SEM. A Shapiro-Wilks test for normality was conducted, and if passed ($p > 0.05$), a parametric test for comparison of means was then used. A Two-Way mixed model ANOVA for time (within subjects) and treatment (between subjected) was used to analyse fetal systemic blood gases, if a significant interaction was achieved, a Bonferroni post-hoc was conducted.

Cell counts in each brain region of the controls (sham UCO), Mild UCO and Severe UCO groups were compared using a One-Way ANOVA; if significant, a Student-Neuman-Keul post hoc analysis was done. If data were not normally distributed, transformations (Log_{10}, exponential and square root) were conducted, failing to achieve normality, a non-parametric Kruskal Wallis test was conducted with pair-wise comparisons. Laminin immunohistochemistry was analysed using a Mann Whitney-U between groups (Control and Severe UCO) for vessel density and morphology analysis (as in Chapter 3). Two-Way (Mixed model) ANOVA tests were performed to compare the distribution of blood vessel size based on perimeter (within groups; Severe UCO and Control), for brain regions (between groups). If a significant interaction was found, a Bonferroni post hoc test was conducted. All statistical data were

analysed using SPSS v18 for Windows, with significance set at $p < 0.05$. All graphs were made using GraphPad Prism Software for Windows (v5.03).

5.3 RESULTS

Fetuses were initially randomly assigned to either a control or UCO group (animals were always run in pairs and random assignment occurred prior to surgery); however it appeared that there was a range of hypoxic insults caused by UCO which subsequently resulted in a range of fetal responses. Figure 6.2 (A – F) shows the response of all fetuses to UCO compared with Control values for arterial blood gases, O_2 saturation, pH, ABE and blood lactate. This strongly suggests that some fetuses became more hypoxic than others. It is possible that the UCO was incomplete in some fetuses, although the intention was always to completely occlude blood flow by fully inflating the cuff around the umbilical cord. However as umbilical blood flow was not measured sub-division of groups into 'partial' or 'complete' UCO cannot be accurately done.

The Control (n=5) and UCO (n=11) group data are presented in Appendix 7. Appendix 7 shows that all fetuses that were subjected to UCO became significantly hypoxic, hypercapnic and experienced metabolic acidosis. The primary outcome of these studies (Chapter 5 and 6) was to determine the effect of UCO (brief, global hypoxia) in late gestation on VEGF expression in the fetal brain and whether there are any consequences on fetal behaviour, until the onset of labor. However, there were considerable differences in the degree of hypoxia and hypercapnia produced by the UCO between fetuses (Figure 6.2), and sub-classification of fetuses into 'mild' or 'severe' was done to allow for further examination of the outcome measures.

The benefit of using the sheep model is that systemic parameters such as blood gases, MAP and HR can be measured during UCO, which allows for an accurate representation of the <u>degree</u> of hypoxia or response to hypoxia. This is in contrast to, for example, rodent hypoxia-ischemia

models which have limited capacities to measure these parameters, and there is an assumption that the hypoxic challenge was the same or where the degrees of hypoxia are so varied that they do not completely reveal the true nature of findings. The discussions in these Chapters (5, 6 and 7) address the important point of whether the different outcomes were due to a specific degree of hypoxia (Mild or Severe), or occurred regardless of the degree of hypoxia (i.e both UCO groups were significantly different to Controls).

5.3.1 Severity of UCO

As the same animals were used for the experiments detailed in Chapter 5 and Chapter 6 the details for the sub divisions into 'Mild UCO' and 'Severe UCO' are stated in Section 6.3.1 Severity of UCO (Figure 6.2, Table 6.2). The response of the fetuses to UCO; blood gases (Section 6.3.2.1, Figure 6.3) and physiological responses (MAP, BP; Section 6.3.2.1 and Section 6.3.2.2, Figure 6.4). The outcome of pregnancy is detailed in Section 6.3.3 and Figure 6.7. Finally the Post Mortem details are listed in Section 6.3.3.2 and Table 6.3.

5.3.2 Immunohistochemistry – total cell counts

Immunohistochemical analysis in fetal sheep brains were examined in Control (n=5), Mild UCO (n=4), Severe UCO (n=5). Not all animals yielded brain samples that were suitable for immunohistochemical assessment, as some of the tissues collected were damaged by over-processing.

Due to a harsh antigen retrieval procedures required for the VEGF immunohistochemistry, some tissues lifted from the slides and did not produce reliable results (Control [n=3]; mild UCO [n=3]; severe UCO [n=4]), and therefore were not included in the analysis.

5.3.2.1 VEGF and VEGFR-2

Quantification of the overall number of VEGF and VEGFR-2 immunopositive cells was done for the corpus callosum, cortex (layers II – V), periventricular and subcortical white matter,

subcallosal bundle and thalamus (Table 5.1). No significant difference ($p > 0.05$) was seen between the Control, mild UCO or severe UCO groups for these brain regions. Using densitometry to quantify the percentage of positive VEGF staining above threshold in the subventricular zone, no significant difference was seen between groups (Table 5.1).

No significant effect of UCO on VEGFR-2 expression was seen in the corpus callosum, cortex or subcortical white matter (Table 5.1), but a near-significant increase occurred in the periventricular white matter ($p = 0.053$). Densitometry analysis of the VEGFR-2 immunopositive staining in the subventricular zone showed a significant increased in severe UCO group (22.43 $\pm$ 1.66 %) compared to mild UCO (15.83 $\pm$ 2.09 %) and Control (17.14 $\pm$ 0.24 %) groups of fetuses (Table 5.1).

Table 5.1: VEGF and VEGFR-2 immunopositive cells. Number of immunopositive cells for VEGF and VEGFR-2 (cells/mm^2) from Control, Mild UCO and Severe UCO fetal brains. Values expressed as mean ± SEM. * p < 0.05 compared to control; # p < 0.05 compared to mild UCO.

Brain Region	Control	Mild UCO	Severe UCO
VEGF (cells/mm^2)	(n = 3)	(n = 3)	(n = 4)
Corpus Callosum	1764.66 ± 139.20	1902.19 ± 109.03	1727.44 ± 197.01
Periventricular White Matter	1960.20 ± 227.53	2036.85 ± 277.67	1736.17 ± 144.03
Subcortical White Matter	1560.69 ± 187.32	1616.81 ± 377.28	1346.66 ± 98.45
Cortex	1221.80 ± 107.01	1353.99 ± 99.28	1153.94 ± 154.47
Subcallosal Bundle	2040.76 ± 135.95	2466.87 ± (n = 2)	2140.69 ± 188.87
Thalamus	1649.66 ± 59.23	1724.75 ± (n=2)	1811.19 ± 216.96
VEGFR-2 (cells/mm^2)	(n = 5)	(n = 4)	(n = 5)
Corpus Callosum	1414.36 ± 140.11	1477.62 ± 120.90	1308.29 ± 123.60
Periventricular White Matter $^{(p = 0.053)}$	1300.31 ± 117.93	2009.47 ± 74.64	1959.18 ± 238.43
Subcortical White Matter	1459.82 ± 112.25	1696.59 ± 111.07	1565.18 ± 167.55
Cortex	1189.49 ± 179.93	1131.06 ± 139.62	1074.04 ± 100.51
Subcallosal Bundle	2714.14 ± 245.63	3128.41 ± 354.05	2771.63 ± 117.29
Thalamus	2294.10 ± 152.95	2175.50 ± 74.59	2365.08 ± 150.58
Densitometry (% above threshold)			
VEGF – Subventricular Zone	16.99 ± 3.03	18.98 ± 2.62	19.03 ± 1.77
VEGFR-2 – Subventricular Zone	17.14 ± 0.24	15.83 ± 2.09	22.43 ± 1.66*#

5.3.2.2 Epo

UCO had no significant effect on the over-all number of Epo immunopositive cells observed in the corpus callosum, white matter (periventricular and subcortical), cortex, subcallosal bundle and thalamus (Table 5.2). Similarly, when densitometry was used to quantify the percentage of positive staining above threshold in the subventricular zone, no significant difference was seen between groups.

Table 5.2: Epo immunopositive cells. Number of immunopositive cells for Epo (cells/mm^2) in brain regions of Control (n=5), Mild UCO (n=4) and Severe UCO (n=5) fetal brains. Values expressed as mean ± SEM. * p < 0.05; ** p < 0.01 compared to control.

Brain Region	Control	Mild UCO	Severe UCO
Epo (cells/mm^2)	(n = 5)	(n = 4)	(n = 4)
Corpus Callosum	1686.35 ± 268.77	1498.25 ± 369.77	1450.64 ± 370.07
Periventricular White Matter	1644.68 ± 280.75	1953.55 ± 206.13	1998.43 ± 416.06
Subcortical White Matter	2011.51 ± 129.22	2192.61 ± 289.26	2097.86 ± 209.87
Cortex	1870.36 ± 115.85	1884.03 ± 136.06	2023.36 ± 106.58
Subcallosal Bundle	1717.71 ± 88.87	1624.44 ± (n=2)	1746.46 ± 246.45
Thalamus	1212.61 ± 173.66	1043.26 ± 54.20	1147.34 ± 141.11
Densitometry (% above threshold)			
VEGF – Subventricular Zone	20.01 ± 1.65	24.67 ± 2.26	26.04 ± 2.51

5.3.3 Immunohistochemistry – blood vessel associated expression

5.3.3.1 VEGF and VEGFR-2

Figure 5.1 shows the percentage of blood vessels in a field of view with expression of VEGF (panels A – F) or VEGFR-2 (panels G- L) in the cortex, corpus callosum, white matter (periventricular and subcortical), subcallosal bundle and thalamus respectively. Analysis of the subcallosal bundle and thalamus was possible for only 2 fetal brains in the mild UCO group, so comparison was only made between the control and severe UCO groups, between which, for VEGF immunopositive staining, no significant differences were seen in any brain region examined. There was also no significant difference of VEGFR-2 expression for any brain region, except for subcortical white matter, where expression was significantly greater in the severe UCO group (64.87 ± 1.95 %) compared to mild UCO (54.62 ± 3.74 %) and controls (53.22 ± 3.40 %).
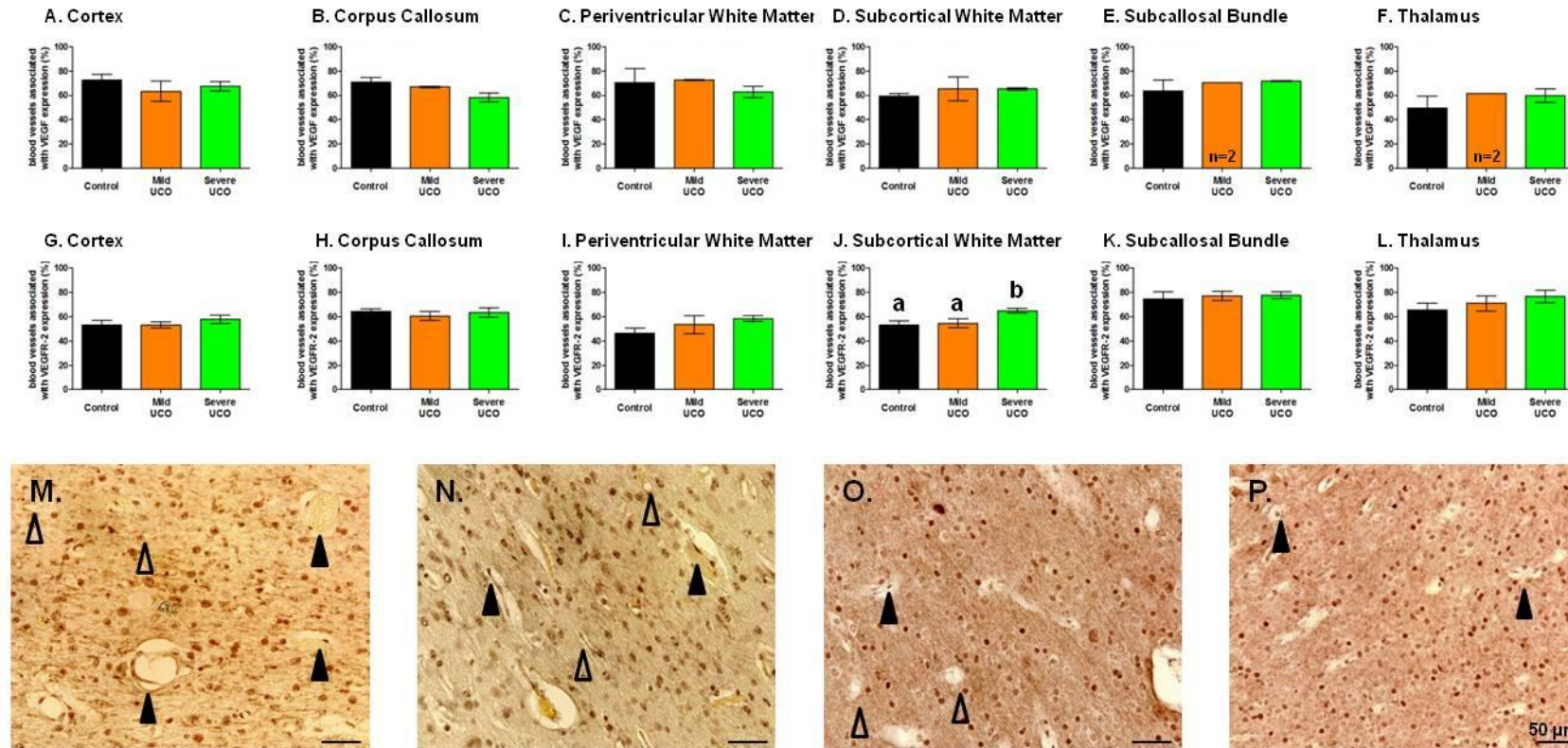
Figure 5.1: VEGF and VEGFR-2 associated expression with blood vessels. Graphs showing the percentage blood vessel associated expression of VEGF (A –F) and VEGFR-2 (G-L) in the cortex (A, G) corpus callosum (B, H), periventricular (C, I), subcortical white matter (D, J), Subcallosal bundle (E, K) and thalamus (F, L) for control (black), mild UCO (orange) and severe UCO (green). Significance $p < 0.05$. Mean ± SEM. Photomicrographs show VEGF (M, N) and VEGFR-2 (O, P) in subcortical white matter of Control (M, O) and severe UCO (N, P) fetal sheep brain. Closed arrow heads shows blood vessels with positive staining for VEGF or VEGFR-2; closed arrow heads indicate blood vessels with no positive associated expression.

5.3.3.2 Epo

Epo immunopositive staining associated with blood vessels was quantified in the cortex and periventricular and subcortical white matter. A trend to significance was seen in the cortex (p = 0.074), but no significant differences were present between groups in white matter (Figure 5.2).
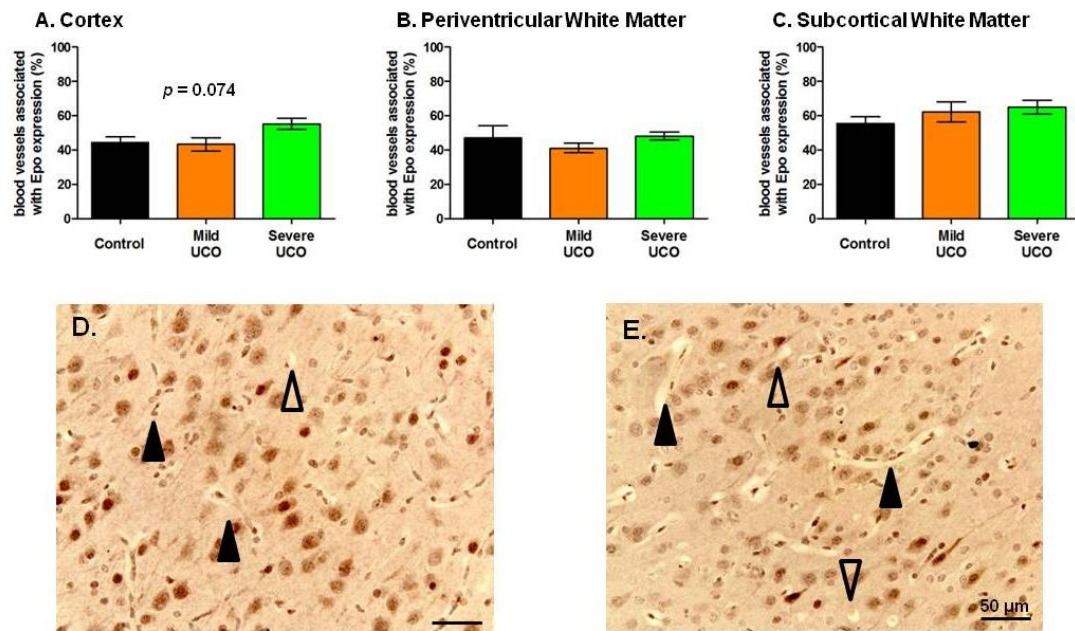
Figure 5.2: Epo expression associated with blood vessels. Graphs showing the percentage blood vessel associated expression of Epo in the cortex (A), periventricular (B) and subcortical white matter (C) for control (black), mild UCO (orange) and severe UCO (green). Significance p < 0.05. Mean ± SEM. Photomicrographs showing Epo immunoreactivity in the cortex of control (D) and severe UCO (E) in fetal sheep brain. Closed arrow head indicates positive staining associated with blood vessel, and open arrow indicate no positive staining associated with blood vessel (G). Scale bar represents 50 µm.

5.3.3.3 Angpt-1

The percentage of blood vessels associated with angpt-1 positive immunostaining in the cortex, periventricular and subcortical white matter is shown in Figure 5.3. In the periventricular white matter (panel B), expression was significantly decreased in both the mild UCO (35.39 ± 2.83 %) and severe UCO (39.77 ± 3.46 %) groups compared to the control group (60.99 ± 4.53 %). No significant change was seen in the cortex (panel A) or subcortical white matter (panel C) between groups.
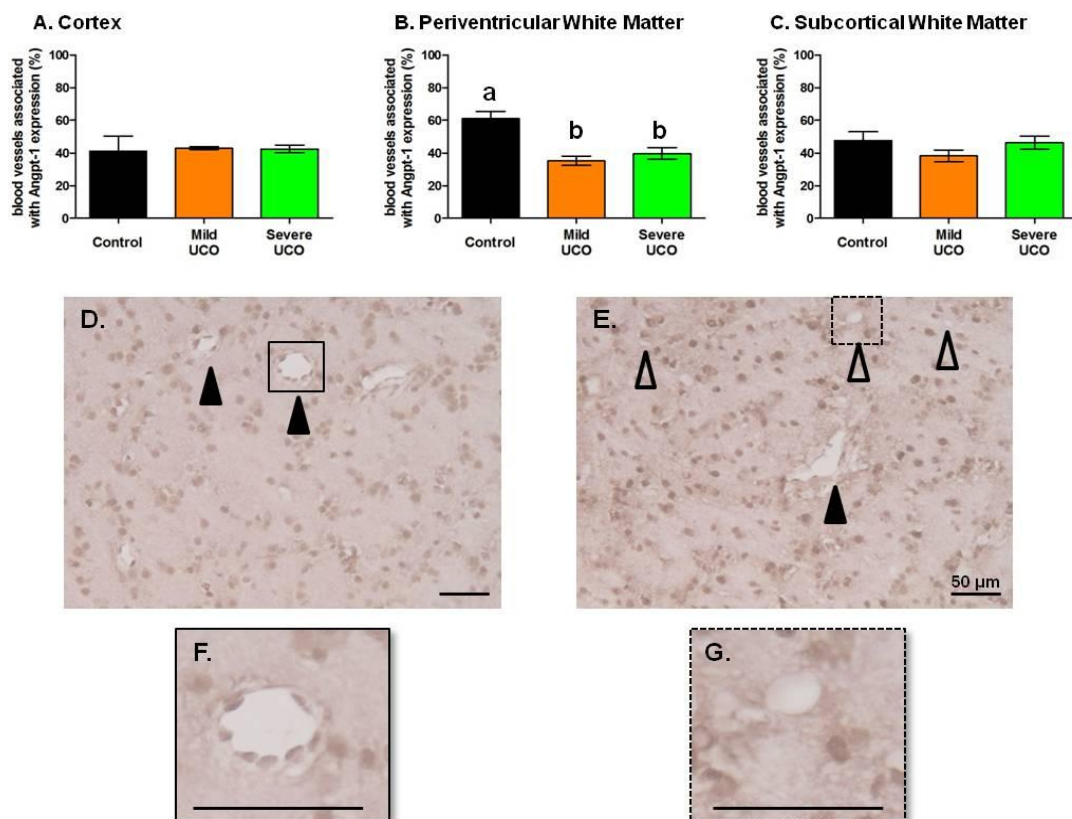
Figure 5.3: Angiopoietin-1 expression associated with blood vessels. Graphs showing the percentage blood vessel associated expression of angpt-1 in the cortex (A), periventricular (B) and subcortical white matter (C) for control (black), mild UCO (orange) and severe UCO (green). Significance $p < 0.05$. Mean $\pm$ SEM. Photomicrographs showing angpt-1 immunoreactivity in the periventricular white matter of control (D, F) and severe UCO (E, G) in fetal sheep brain. Closed arrow head indicates positive staining associated with blood vessel (F), and open arrow indicate no positive staining associated with blood vessel (G). Scale bar represents 50 µm.

5.3.4 Laminin

As discussed in Chapter 3, laminin was used to identify blood vessels, and determine mean vessel size and vascular density (Figure 5.3). Some animals (Control n=2, Mild UCO n=3, Severe UCO n=1) were excluded from analysis due inconsistent staining, so that statistical comparison was possible only between the control and severe UCO groups. There was no significant differences seen in vascular density, size or morphology in the cortex or white matter (periventricular or subcortical) between control and severe UCO groups (Figure 5.3). Figure 5.4 shows the percentage frequency of blood vessel perimeter in the cortex (A), periventricular (B) or subcortical (C) white matter.
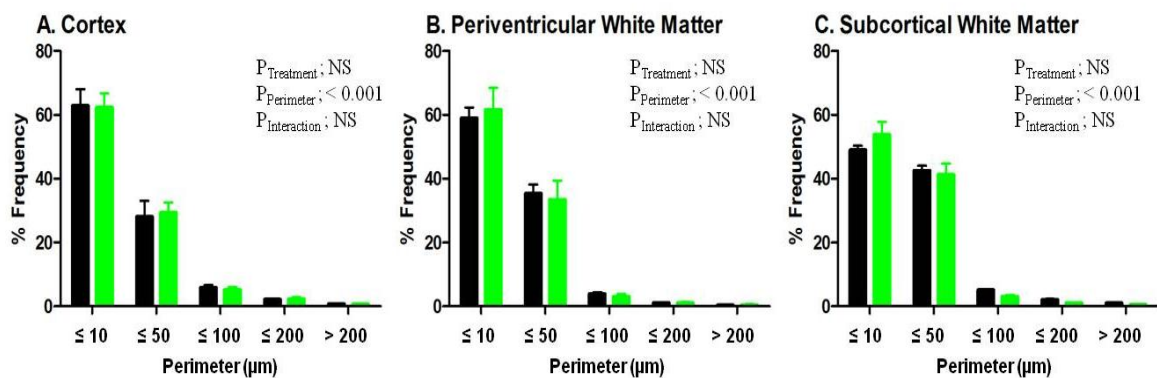
Figure 5.4: Size distribution of blood vessels in brain regions from fetal sheep. Percentage frequency histograms of the perimeter of blood vessels in the cortex (A), periventricular (B) and subcortical (C) white matter in control (black) and severe-UCO (green) fetal sheep brains. Significance $p < 0.05$. Mean ± SEM. Not significant (NS).

Table 5.3: Blood vessel density and morphology. Vessel density and morphology measurements in cortex, periventricular and subcortical white matter, in control and severe-UCO fetal brains. N are stated for each region. Values expressed as mean ± SEM. * $p < 0.05$; ** $p < 0.01$ compared to control.

	Control	*Severe UCO*
Cortex (n)	3	4
Vessel density (number/mm^2)	2382.86 ± 786.53	1969.75 ± 479.64
Total Area (%)	5.23 ± 1.82	3.40 ± 0.38
Mean Area (μm^2)	24.38 ± 4.45	23.72 ± 9.35
Perimeter (μm)	20.99 ± 1.04	20.42 ± 4.27
Length (μm)	7.21 ± 0.44	7.36 ± 1.58
Breadth (μm)	3.36 ± 0.21	3.31 ± 0.61
Mean Radius (μm)	2.06 ± 0.15	2.09 ± 0.48
Shape Factor	0.65 ± 0.01	0.65 ± 0.02
Periventricular White Matter (n)	3	4
Vessel density (number/mm^2)	2003.26 ± 87.70	1852.31 ± 246.13
Total Area (%)	6.13 ± 1.89	4.25 ± 1.37
Mean Area (μm^2)	24.30 ± 1.94	17.11 ± 4.69
Perimeter (μm)	16.52 ± 0.36	15.60 ± 2.30
Length (μm)	5.91 ± 0.12	5.37 ± 0.77
Breadth (μm)	3.45 ± 0.09	2.98 ± 0.38
Mean Radius (μm)	1.84 ± 0.05	1.59 ± 0.25
Shape Factor	0.71 ± 0.01	0.67 ± 0.02
Subcortical White Matter (n)	3	3
Vessel density (number/mm^2)	1736.95 ± 243.34	3021.65 ± 601.24
Total Area (%)	8.94 ± 2.76	5.85 ± 1.09
Mean Area (μm^2)	43.34 ± 13.05	20.50 ± 6.82
Perimeter (μm)	24.27 ± 3.64	17.23 ± 2.08
Length (μm)	8.60 ± 1.59	6.16 ± 0.85
Breadth (μm)	3.99 ± 0.17	3.30 ± 0.35
Mean Radius (μm)	2.55 ± 0.42	1.84 ± 0.27
Shape Factor	0.67 ± 0.01	0.70 ± 0.01

5.4 DISCUSSION

The most important finding of this study was that 5 – 10 days following a single, short bout of fetal hypoxia and hypercapnia (10 mins UCO) in late gestation, the fetal sheep brain showed a regionally-selective vascular response between white and gray matter. VEGFR-2 expression associated with blood vessels was significantly *increased* in the subcortical white matter of fetuses when the effect of the UCO had been 'severe'. However, periventricular white matter showed a significant *decrease* of angpt-1, a marker of vessel maturity, following mild or severe UCO. A significant increase in overall cellular expression of VEGFR-2 was seen in periventricular white matter and the subventricular zone. There was no effect of UCO on the expression of VEGF 5 – 10 days following the insult.

The increased expression of VEGFR-2 (total cell number), despite no change in VEGF expression itself in periventricular white matter and the subventricular zone at 5 – 10 days following a severe response to UCO, is consistent with the focal ischemia studies in the adult brain (Lennmyr *et al.*, 1998; Marti *et al.*, 2000b). These studies suggest that early up-regulation of VEGFR-2 following hypoxia-ischemia occurs in ischemic cells. Kilic *et al.,* (2006) found that as early as 24 h following focal cerebral ischemia (middle cerebral artery occlusion, MCAO) VEGFR-2 was activated (via phosphorylation) by VEGF and up-regulated in both **ischemic** neurons and astrocytes. Increased glial and endothelial VEGFR-2 expression has also been reported to occur following MCAO in the adult rat although Lennmyr *et al.,* (1998) found no change in neuronal expression 1 to 3 days following permanent or transient MCAO. Our results could suggest that following an antepartum hypoxic event both the subventricular zone and periventricular white matter are ischemic, due to up-regulation of VEGFR-2 by cell types such as neurons and astrocytes, and thereby possibly vulnerable to injury.

In the current study we found increased VEGFR-2 expression despite no change in VEGF cell number which is also consistent with adult ischemia studies. Marti *et al.,* (2000b) found up-regulation of VEGFR-2 expression in the border of the infarct by 48 h, peaking at 72 h

following MCAO in adult rats. This was despite VEGF mRNA expression increasing much earlier, 6 h following MCAO in the adult mouse, and VEGF protein expression peaking at 12 and 48 h post MCAO. Increased VEGFR-2 expression 24 h to 7 days following MCAO was also seen in the hippocampus, a 'remote region' in relation to the infarct area. Cellular expression was thought to be neuronal, and this study suggests that the neuronal expression of the VEGF/VEGFR system could be neuroprotective, occurring prior to neovascularisation (Marti *et al.*, 2000b). This study showed a persistent up-regulation of VEGFR-2 after VEGF expression has declined occurring in adult mice, and now we have also found this in periventricular white matter of the late gestation fetal sheep brain.

Elevated VEGFR-2 expression has also been suggested to be neuroprotective. Providing further evidence for the neuroprotective actions of VEGF/VEGFR-2, inhibition of VEGFR-2 both *in vivo* and *in vitro* has been trialled in two neonatal stroke models and been shown to result in worse neurological outcome. Shimotake *et al.,* (2010) have investigated this by inhibiting of VEGFR-2 *in vivo*, 2 days following MCAO in the neonatal rat. They found that 7 days following MCAO, injury had worsened (increased infarct size), increased cell death, and decreased endothelial cell proliferation despite increased VEGFR-2 expression 5 days following injury. This could occur as *in vitro* inhibition of VEGFR-2 was seen to reduce the protective effect of VEGF-A (Lee *et al.*, 2010).

However, prenatal treatment with ZD6474 an anti-angiogenic drug, that inhibits VGEFR-2 expression, was shown to reduce the incidence of glycerol induced germinal matrix haemorrhage in rabbit pups (Ballabh *et al.*, 2007). This study concluded that elevated VEGF-A and angpt-2 (important in vascular remodelling) experiments were detrimental, suggesting enhanced endothelial proliferation and angiogenesis in the germinal matrix may predispose this region to haemorrhage, hence inhibition of VEGFR-2 (and subsequent angiogenesis) could be protective. It is important to note that this study only targeted the vascular effects of VEGFR-2, and did not take into account the possible neuroprotective benefits. Secondly, prenatal treatment

with an anti-angiogenic drug could be incredibly harmful to the brain of the preterm or term neonate.

In vivo and *in vitro* studies have shown that treatment with VEGF stimulates neurogenesis, and is mediated by VEGFR-2 (Jin *et al.*, 2000a; Jin *et al.*, 2002). The neuroprotective actions of VEGF and VEGFR-2 are suggested to occur via phosphorylation of cAMP response element binding protein (CREB)/Akt/ERK-1 pathways (Wick *et al.*, 2002; Kilic *et al.*, 2006; Lee *et al.*, 2010). From *in vitro* and *in vivo* analysis, it was found that in P7 rat pups following hypoxia-ischemia, VEGF-A activated the VEGFR-2, which in turn phosphorylated CREB in endothelial cells and neurons, and so protected them from hypoxic-ischemic and oxygen-glucose deprivation injury (Lee *et al.*, 2010). Phosphorylation of Akt/PKB and ERK-1 occur following focal cerebral ischemia or hypoxic preconditioning in the adult also resulting in enhanced neuronal survival, although increased BBB permeability is a consequence of those effects of hypoxia-ischemia (Wick *et al.*, 2002; Kilic *et al.*, 2006).

Numerous studies have evaluated the response of VEGF and to a lesser degree VEGFR-2, following global and focal ischemia, particularly in the adult. However, there is less understanding of the importance of *vascular* VEGFR-2 expression following hypoxia-ischemia *in vivo*. We found a significant increase of VEGFR-2 expression associated with blood vessels in subcortical white matter. This finding suggests that blood vessels in the subcortical matter respond differently to UCO, compared to other brain regions examined (periventricular white matter and cortex). It also highlights that blood vessels, and in particular vascular cells (such as endothelial cells and pericytes) in subcortical white matter may be more sensitive to UCO than other cell types in this region, as no significant change was seen in cell number. Marti *et al.,* (2000b) suggests that increased VEGFR-2 expression occurs prior to neovascularisation.

VEGF and VEGFR-2 activation promotes neuronal growth, migration, maturation, survival as well as axonal and dendritic outgrowth (Hermann & Zechariah, 2009; Sentilhes *et al.*, 2010). The high expression of both VEGF and VEGFR-2 seen prior to birth in both control and UCO

(mild and severe) fetal sheep brains suggest that key developmental processes, such as angiogenesis and neurogenesis are occurring during late in gestation. Studies from the human (Sentilhes *et al.*, 2010) and rodent brain (Nico *et al.*, 2002; Yang *et al.*, 2003) of VEGFR-2 expression highlight the importance of VEGFR-2 during brain development. In the human, neurons, astrocytes and endothelial cells express VEGFR-2 from 20 weeks gestation until at least 5 months postnatally (Sentilhes *et al.*, 2010). By 34 weeks gestation, VEGF expression had declined in blood vessels while VEGFR-2 expression was still high, suggesting the rate of angiogenesis may slightly decline toward the end of gestation (Sentilhes *et al.*, 2010). Studies in the rodent also show high neuronal and endothelial expression of VEGFR-2 well into adulthood (Yang *et al.*, 2003). Sentilhes *et al.,* (2010) also suggest that astrocytic generation and maturation may also be another important role of the VEGF/VEGFR-2 system.

In our study we saw a high VEGFR-2 (and VEGF) expression, both cellular and associated with blood vessels in all groups (Control and UCO), so the question must be asked as to what could be regulating their expression. Although it is widely accepted that hypoxia up-regulates VEGF, and subsequently VEGFR-2 at a protein level (Waltenberger *et al.*, 1996; Kremer *et al.*, 1997), *in vitro* studies suggest hypoxia may **not** be the key regulator of VEGFR-2 gene expression (Gerber *et al.*, 1997). Following systemic hypoxia in the adult mouse, VEGFR-2 expression was not modulated by hypoxia, although VEGFR-1 was (Marti & Risau, 1998). *In vitro* studies have shown that HIF-2, but not HIF-1, regulate mRNA transcription of VEGFR-2 although this was not see in the brain (Gerber *et al.*, 1997; Kappel *et al.*, 1999; Marti *et al.*, 2000b). As well as hypoxia, expression of VEGFR-2 in endothelial cells can be also modulated by external factors including glucose deprivation and in the presence of cytokines and basic fibroblast growth factor (Pepper & Mandriota, 1998).

To further investigate whether the increased expression of VEGFR-2 is possibly neuroprotective, the expression of Epo, another key hypoxia sensitive gene with neuroprotective actions, was examined. Following hypoxia, Epo is up-regulated (Bernaudin *et al.*, 1999; Yeo *et*

al., 2008; Fan *et al.*, 2009) and suggested to be neuroprotective by increasing expression of anti-apoptotic genes and promoting survival of oligodendrocytes, neurons, astrocytes and microglia (Bernaudin *et al.*, 1999; Marti *et al.*, 2000a; Marti, 2004; Chang *et al.*, 2005; Iwai *et al.*, 2007; Fan *et al.*, 2009). Epo can also stimulate the expression of VEGF and its' receptor on endothelial cells (Iwai *et al.*, 2007; Hermann & Zechariah, 2009). Increased expression of Epo and Epo-R has been seen 48 h following UCO in late gestation fetal sheep (Castillo-Melendez *et al.*, 2005). In the present study, we assessed the number of cells expressing Epo and found there was no significant difference in control, mild or severe UCO groups of the brain regions examined. However, we did see a trend to a significant increase of blood vessel associated expression of Epo in the cortex, which could help explain a regional 'protection' of the cortical vasculature. *In vitro*, Epo can modulate angiogenesis by stimulating endothelial cell migration and proliferation (Anagnostou *et al.*, 1990; Yamaji *et al.*, 1996).

Studies of permanent focal cerebral ischemia in adult mice found that the cellular expression pattern of Epo and Epo-R was modulated by the evolution of the infarct. Post-ischemic cellular expression of Epo occurs initially in endothelial cells (1 day), inflammatory cells (3 days) and then reactive astrocytes (7 days) (Bernaudin *et al.*, 1999). Although Bernaudin and colleagues (1999) did not elucidate the sequence of cellular change in Epo expression, it could be speculated that endothelial cells are the first to be protected, due to Epo's anti-apoptotic actions. However if this were the case in our study, it could be suggested that endothelial cells in white matter, in comparison to the gray matter (cortex) are less able to be protected. Studies using recombinant human Epo (rhEpo) as a neuroprotective treatment following neonatal stroke have seen enhanced vascular remodelling promoting neurogenesis (Iwai *et al.*, 2007). Increased revascularisation and neurogenesis, amelioration of tissue loss and improve functional sensorimotor outcome also occur when rhEpo treatment was administered in neonatal rats following hypoxia-ischemia (Chang *et al.*, 2005; Iwai *et al.*, 2007).

The finding that there was no significant difference across groups with respect to blood vessel associated expression of VEGF may suggest that 5 − 10 days following *in utero* hypoxia there is not a greater capacity of hypoxia induced angiogenesis. In Chapter 4, endothelial cell proliferation was assessed as a result of the significant increase in vessel-associated VEGF expression that had occurred 24 and 48 h after UCO. In the present study this was not done as no differences in VEGF expression were seen at 5 − 10 days following UCO. We also saw no significant change in vascular density in brain regions, although only a few fetal brains could be analysed. High VEGF expression was still seen in all groups suggesting that angiogenesis is still ongoing at this late stage of gestation in fetal sheep.

At 10 days following UCO it might be possible to assess the **maturity** of blood vessels. To investigate whether hypoxia had had an effect on vessel maturation, the expression of angpt-1 associated with blood vessels in grey matter (cortex) and white matter (periventricular and subcortical) was assessed. Angiopoietins, most importantly angpt-1 and angpt-2, work in close association with VEGF in stimulating angiogenesis. They are an important family of protein growth factors that are also up-regulated following hypoxia (Beck *et al.*, 2000; Lin *et al.*, 2000; Yancopoulos *et al.*, 2000). Angpt-1 is important for stimulating vessel growth, branching, maintenance and stabilisation of the vasculature (Yancopoulos *et al.*, 2000; Carmeliet, 2003; Kim *et al.*, 2008). Angpt-2, important in initiating vascular remodelling, has both agonistic and antagonistic actions to angpt-1. When binding to Tie-2 angpt-2 is involved in both the initiation of angiogenesis as well as destabilisation of capillaries (Maisonpierre *et al.*, 1997; Yancopoulos *et al.*, 2000; Gale *et al.*, 2002). Unlike VEGF which is upregulated within hours following hypoxia-ischemia, angpt-1 and angpt-2 exert their functions in the later stages to produce further vascular change and remodelling, sometimes referred to as 'vascular maturation' (Plate *et al.*, 1999; Beck *et al.*, 2000).

The most novel finding of this study was that UCO significantly decreased blood vessel associated expression of angpt-1 in periventricular white matter. Angpt-1 also promotes the

"tightening" of vessels by increasing expression of tight junctional proteins thereby resulting in decreased permeability of vessels (Thurston *et al.*, 1999; Thurston *et al.*, 2000; Valable *et al.*, 2005; Hansen *et al.*, 2008). Although we did not see a significant change of vascular VEGF or VEGFR-2 in periventricular white matter, decreased angpt-1 protein expression could also be indicative of decreased structural support, as increased angpt-1 expression is implicated in enhancing the interaction between endothelial cells and the recruitment of pericytes (Suri *et al.*, 1996). Following focal cerebral ischemia, increased VEGF mRNA expression and decreased angpt-1 mRNA expression has been correlated with a significant increase in BBB permeability (Zhang *et al.*, 2002b). Our findings that UCO results in a persistent decrease of angpt-1 expression in periventricular white matter could be indicative of vascular leakage or a compromised BBB in this brain region at 5 – 10 days following UCO.

Further to our findings, although only blood vessels associated expression was analysed, angpt-1 immunoreactivity was also observed; astrocytes and pericytes (Yancopoulos *et al.*, 2000; Carmeliet, 2003; Ballabh *et al.*, 2007; Kim *et al.*, 2008). Interestingly, angpt-1 may have neuroprotective potential as *in vitro* studies have found ischemic neurons were **protected** from apoptosis and necrotic death in the presence of angpt-1 occurring via the activation of PIK-3 pathway. Further quantification of the cellular expression of angpt-1 in our study could help explain the significance of increased VEGFR-2 expression, also important for neurogenesis, which was increased in periventricular white matter.

We did attempt to assess angpt-2 expression in fetal brains, however a clear signal could not be obtained so further investigation of the role of angpt-2 is also required. The vascular permeability effects of VEGF that may have resulted in the increased incidence of BBB permeability seen at 24 and 48 h following UCO (Chapter 4), suggests changes in BBB permeability are transient and an early response to asphyxia. This is consistent with neonatal and adult focal cerebral ischemia studies in the rat (Zhang *et al.*, 2000; Zhang *et al.*, 2002b; Kaur & Ling, 2008; Al Ahmad *et al.*, 2010). However, although VEGF associated with blood

vessels was not significantly increased in this study, but decreased angpt-1 was seen in periventricular white matter assessment of the tight junctions such as claudin and occludin could reveal the consequence of these changes in expression. Implications of decreased angpt-1 expression could also be explained by assessment of the expression of pericytes; as pericyte migration occurs following hypoxia-ischemia (Takahashi *et al.*, 1997; Gonul *et al.*, 2002), which contributes to an immature and destabilised vasculature.

It was a limitation of the study that fetuses in both UCO groups went into labour between 136 – 144 days gestational age. However, as there was a significant difference in VEGFR-2 and angpt-1 in groups despite this range of gestational ages as an end point, it suggests that hypoxia and not gestational age resulted in the significant differences. Subsequent studies could help delineate the time course of the alterations in expression of these proteins.

This study highlights that regional responses of the vasculature in the fetal brain persists after a single short hypoxic challenge, and suggests some of the predilection to periventricular white matter injury may have a vascular origin. Interestingly, following UCO it is apparent that there are regionally differing responses of cellular and vascular expression of VEGFR-2 also. In periventricular white matter we saw increased cellular VEGFR-2 expression and no change in the vascular expression, a region that also showed decreased angpt-1 expression associated with blood vessels. In contrast, subcortical white matter showed increased vascular VEGFR-2 expression and no change in total expression, suggesting that in this brain region, blood vessels could be protected while neurons, astrocytes and pericytes could be the cell types that are susceptible to ischemic injury. Strengthening the argument that white matter is more vulnerable to injury, gray matter (cortex) was relatively unaffected over the 5 – 10 days following UCO, except for a trend to an increase in Epo expression associated with blood vessels.

UCO did not affect vessel density, morphology or size distribution, however only low numbers were available for this analysis. The increased expression of VEGFR-2, but not VEGF, is consistent with adult brain focal ischemia studies. Angpt-1, a key angiogenic protein important

for vascular development and maturation, was *decreased* only in periventricular white matter, a region known to be susceptible to ischemic injury. Periventricular white matter following *in utero* UCO may show greater permeability, due to significant decreased expression of angpt-1, whereas as subcortical white matter may be protected due to increased VEGFR-2 expression associated with blood vessels following UCO, severe or mild. The predilection of the perinatal brain to white matter lesions may be explained, in part, by these regionally-selective vascular responses to transient global hypoxia.

Chapter 6

IN UTERO AND POSTNATAL

BEHAVIOURAL CONSEQUENCES

FOLLOWING UMBILICAL CORD

OCCLUSION IN LATE GESTATION FETAL

SHEEP.

TABLE OF CONTENTS

6.1 INTRODUCTION

The Australian Cerebral Palsy Foundation states that over the last 40 years the incidence of Cerebral Palsy (approximately 1 in 400 live births) has remained relatively unchanged (Alcorn & Shean, 1995; Stanley *et al.*, 1995, Cerebral Palsy Australia, 2010). It is commonly thought that hypoxia-ischemia occurring during pregnancy or at birth significantly contributes to the cognitive impairment, developmental delay, motor deficits and epilepsy all of which can be associated with Cerebral Palsy and manifest themselves after birth. However, the pathogenesis of the injury to the brain is not well understood.

Numerous clinical studies have attributed timing and gestational age to determining the pattern of injury (Sims *et al.*, 1985; Badawi *et al.*, 1998; Cowan *et al.*, 2003; Van den Broeck *et al.*, 2007; Foran *et al.*, 2009). Antepartum events such as complications of the umbilical cord or placental abruption resulting in severe hypoxia or asphyxia are difficult to detect, but may be the sentinel event that causes a great proportion of the injury not seen until after birth. All forms of fetal monitoring remain limited in being able to detect fetal brain injury per se, although heart rate variability and fetal body and breathing movements can provide measures of fetal distress *in utero (Bocking, 2003).* For example, Low *et al.,* (1989) noted a case of antepartum asphyxia resulting in reduced fetal movement a week prior to labour.

Fetal sheep provide a good model to assess complications and behavioural responses *in utero*. By 120 days gestational age (GA; term 146 days), electrocortical (ECoG) activity is differentiated into high voltage (HV) and low voltage (LV) states, and fetal behaviour shows cyclical changes with time, as for the human fetus (Clewlow *et al.*, 1983; Lamblin *et al.*, 1999; Vanhatalo & Kaila, 2006; Andre *et al.*, 2010). LV ECoG activity is also associated with eye movements and diaphragm and fetal breathing movements (FBM) (Jost *et al.*, 1972; Clewlow *et al.*, 1983), with the suggestion that this is the fetal equivalent of postnatal rapid eye movement (REM), or 'active' sleep.

Many studies have assessed both fetal behaviour (Kawagoe *et al.*, 1999a; Yan *et al.*, 2009) and neuropathology (Mallard *et al.*, 1992; Mallard *et al.*, 1994; Ikeda *et al.*, 1998a; Ikeda *et al.*, 1998b; Duncan *et al.*, 2004) up to 72 h following partial or complete umbilical cord occlusion (UCO) in late gestation fetal sheep. We have previously shown suppression of fetal ECoG activity, increased amplitude of FBMs and increased extracellular glycerol and pyruvate in the brain suggesting a loss of membrane integrity in the hours following UCO (Yan *et al.*, 2009). However, whether the changes in fetal behaviour that have been seen at 24 − 72 h persist, recover or worsen after this period of time has not been determined.

In addition, limited data is available on the postnatal behavioural outcomes following *in utero* complications that are known to damage the fetal brain. Many studies of postnatal behaviour in smaller animal models has been widely used (e.g. mouse, rats, spiny mice, rabbit) that allow for the assessment of fine motor skills and cognitive impairments following an hypoxic event (Derrick *et al.*, 2004; Fan *et al.*, 2005; Hutton *et al.*, 2009; Ireland *et al.*, 2009). The use of larger animal models to monitor postnatal behavioural outcome is limited.

The experiments described in this chapter were designed to investigate how the near term sheep fetus responds to a single severe bout of hypoxia produced by occlusion of the umbilical cord. Firstly, this study aimed to assess the effect on fetal behaviour parameters such as ECoG, postural muscle (nuchal) activity, eye movements and FBM. Following this, a separate set of experiments was designed to create an assessment scale for the newborn lamb to determine the consequence of this *in utero* hypoxic event on key developmental milestones on postnatal recovery at birth. We adapted a behavioural testing method, based on the assessment criteria described by the Scottish Agricultural College and Dwyer and colleagues (1996), for assessing the ability of newly-born lambs to resuscitate themselves and reach the important behavioural 'milestones' such as gaining posture, locomotion, and success at suckling. These milestones were used to determine the effects of a brief asphyxic insult on lamb survival and behaviour.

Comment: Most studies only monitor fetuses up to 72 h following UCO; fetuses in this study were kept alive until labour or 24 h post-birth. It was the aim of this study to monitor them intensively to determine if, and how, their physiological and behavioural status differed from Control fetuses for this longer duration. It was not intended that behavioural alterations could be correlated or attributed to the vascular responses that were found in previous chapters.

6.2 METHODOLOGY

Specifically for this study two different sets of experiments were conducted. Firstly for fetal behavioural assessment 16 pregnant ewes carrying singleton fetuses, underwent surgery for chronic catheterisation (brachial artery and tracheal) and implantation of sagittal sinus blood flow velocity and electrodes to measure ECoG, EMG-nuchal activity, EOG and FBM.

A second set of experiments to monitor postnatal behavioural consequences required 14 pregnant ewes. These fetuses only had a femoral artery catheter and silastic umbilical cuff inserted during surgery. The following sections detail the experiments for each set of studies separately.

6.2.1 Animal surgery

A detailed explanation of animal surgical procedures and experimentation is detailed in Chapter 2 (Section 2.4 and 2.5). Briefly, pregnant Border-Leicester ewes carrying a singleton fetus were used in both studies. The use of these animals and all procedures had received prior approval from the School of Biomedical Science Animal Ethics Committee of Monash University. At 124-126 days gestational age surgery was performed under aseptic conditions. An inflatable silastic cuff (type OC16, *In Vivo* Metric, Healdsburg, CA, U.S.A) was placed around the abdominal end of the umbilical cord, upon inflation; of which complete cessation of blood flow in the cord (UCO) was achieved.

6.2.1.1 Fetal behavioural experiments

Catheterisation

The fetal brachial artery was catheterised to allow for blood sampling, fetal mean arterial blood pressure and heart rate measurements, and a large bore catheter was also placed in the amniotic sac to measure amniotic pressure. The trachea was also catheterised, pressure changes allow for the measurement of fetal breathing movements (See Section 2.4.2.1 and 2.4.2.2 for details).

Electrocorticogram and piezoelectric ultrasonic probe

Two wires of the ECoG lead were inserted bi-parietally, with the third electrode attached under the fetal skin (Clewlow *et al.*, 1983). A piezoelectric ultrasonic probe was inserted through a burr hole onto the dura mater directly above the sagittal sinus to measure blood flow velocity using a Directional Pulsed Doppler Flowmeter (Bioengineering, University of Iowa, USA). (See Section 2.4.2.3 for details).

Electromyogram-nuchal and electro-oculargram

Two lead EMG wires were sewn into the posterior nuchal muscle, and another two lead wire electrode was sewn under the skin above and below the orbit of the eye, electro-oculargram (EOG). These wires allowed for the measurement of postural muscle and eye muscle activity (See Section 2.4.2.4. for details).

6.2.1.2 Newborn lamb behaviour experiments

These experiments were designed so the ewe would deliver lambs naturally, with minimal interference. Therefore the fetal femoral artery was chosen to be catheterised to allow for blood sampling, fetal mean arterial blood pressure and heart rate measurements. A large bore catheter was also placed in the amniotic sac to measure amniotic pressure. A silastic cuff was also placed around the umbilical cord of fetuses.

6.2.2 Animal experiments

On the day of the experiment, the umbilical cord was occluded completely for 10 min by inflating the cuff with 3mL of sterile water (Fetal behaviour study UCO; n = 11, postnatal behaviour n=5) or sham UCO (Control fetal behaviour study n=5, postnatal behaviour study n=6). Fetal haemodynamic responses were closely monitored; if MAP dropped below 20mmHg then UCO was stopped. Fetal arterial blood samples (0.5 mL) were taken before, during and after UCO to measure pO_2, pCO_2, O_2 saturation, pH and haematocrit using a Radiometer ABL5 analyser (Radiometer Medical A/S, Denmark), and blood glucose and lactate concentrations were measured by a YSI 2300 STAT Glucose and Lactate Analyser (YSI Life Sciences, USA).

For the *in utero* study, fetal behaviour was recorded continually until 145 days gestation or until the ewe went into labour. The onset of labour was closely monitored by visual inspection for vaginal secretions, and alterations in amniotic pressure. A detailed explanation is given in Chapter 2, Section 2.5.3). The ewe and fetus were then humanely killed by i.v. injection of pentobarbitone sodium (Lethabarb, Virbac Pty Ltd, Australia) given to the ewe. The fetal brain was removed from the skull and immersion fixed for 48 h with 4% paraformaldehyde (PFA; for a detailed explanation of post mortem procedures Chapter 2, Section 2.8). The analysis of the brains from these animals is detailed in Chapter 5.

6.2.3 Measurement of fetal physiological parameters and fetal behaviour

All analog signals were converted into digitalized at 100 Hz continuously from the 3rd postoperative day and the data stored on the hard disk of a computer using chart software (PowerLab, ADInstruments, Castle Hill, NSW, Australia).

6.2.3.1 Fetal blood pressure, tracheal pressure and heart rate

Fetal blood pressure, tracheal pressure and amniotic pressure were measured using solid state pressure transducers (DTXPlus, B-D Medical Systems) attached to the side of the cage, and fetal arterial pressure was calculated by electronic subtraction of amniotic pressure. Fetal tracheal pressure, used to indicate the presence of FBM, was also calculated after subtraction of amniotic pressure also, this was used to indicate FBM. Fetal heart rate was calculated online from the blood pressure pulse.

6.2.3.2 Sagittal sinus blood flow velocity

Sagittal sinus blood flow velocity (SSbfv) was measured using a directional pulsed Doppler flowmeter (545C-5, Bioengineering; The University of Iowa, Iowa City, IA), with the depth (range) of the reflected signal adjusted if necessary to ensure that the peak velocity was always being recorded.

6.2.3.3 Fetal behaviour - ECoG, EOG, EMG-nuchal

ECoG, EOG, EMG-nuchal was recorded using high common mode rejection amplifiers, and the signal recorded after low-pass filtering (approximately 30 Hz, but calibrated for each animal).

6.2.4 Newborn lamb behaviour assessment

6.2.4.1 Induction of premature labour

Because occlusion of the umbilical cord resulted in significantly early delivery in 3 of the 5 UCO lambs compared to the sham-occluded group (see Figure 6.14 in Results), a further group of 5 ewes was introduced to the study where labour was induced by intramuscular injection of betamethasone (5.7mg, Celestone Chronodose; Schering Plough, Australia) at 12:00 h, followed by Epostane (Sanofi-Synthlabo Research, Malvern, PA, USA; 50 mg in 2 ml ethanol, i.v.) at 17:00 h on day 136 of gestation. This led to the onset of premature labour after 36-48 h following the Epostane injection (Silver & Fowden, 1991; De Matteo *et al.*, 2008). If labour had

not commenced after 48 h (i.e., by 138 days gestation), a further injection of Epostane (50 mg) was given at 17:00 h on that day, however this was not required.

6.2.4.2 Video observation of parturition and lamb resuscitation

Ewes were placed in a large pen (1.8 m x 1.2 m) from 48 h following UCO, where they remain until the onset of labour and parturition. A video record of the birth and the lamb's behaviour was made until 24 h after birth using an over-head camera system. Four closed-circuit cameras (SW224-MDN, Swann Security Products) with infrared night vision were mounted on the ceiling directly above the lambing pen; brackets allowed the viewing angles to be adjusted to obtain the best view of the ewe and its lamb.

At the onset of labour, at least two investigators were present to assist the ewe if necessary, to cut and secure the catheters when the lamb delivered and to remove the umbilical cuff immediately after the lamb was completely clear of the birth canal. This was the only interference over the time period of behavioural assessment, with the exception of when lambs failed to feed 4 hours after birth.

At approximately 24 h after birth each lamb was euthanized by i.v injection of sodium pentobarbital, the lamb weighed and physical dimensions recorded. The brain was removed and placed in 4% PFA for 48 hours before paraffin embedding and processing for immunohistochemistry (the brain analysis from these postnatal experiments are not included in this thesis).

6.2.4.3 Scoring of lamb behaviour

We adapted a neuro-behavioural assessment protocol based on observations previously conducted in sheep to monitor their well-being following birth (Dwyer *et al.*, 1996). The time taken to reach certain behavioural 'milestones' immediately after birth (head lift and shake; first use of hind limbs; first use of four legs; standing; finding the udder, suckling) were assessed

with time '0' being the time at which all parts of the lamb had completely cleared the birth canal (Figure 6.1 A) and the behaviours are detailed in Table 6.1.

The video record was then reviewed to determine the time taken to reach each behavioural milestone. If a lamb did not achieve the first four behaviours in the first 2 h after birth, or find the udder and suckle within the first 4 h, this was noted as 'failed', as it was expected that lambs should have performed these important behaviours within that time frame based on previous research (Dwyer *et al.*, 1996; Dwyer *et al.*, 1999; Dwyer & Lawrence, 2000) and in comparison to the full-term control lambs in the present study.

Table 6.1: Lambing behavioural milestones. Key behavioural milestones from the time of birth (time 0). These include head shake, use of hindlimbs, four legs, attain a stable standing position, find the udder and successfully suckle. The time taken to attain these was also monitored.

Behaviour	Description	Time
Head shake	Lambs lifts and shakes head	< 5 min
Hindlimbs	First attempt to use hindlimbs (Figure 6.1 B)	< 2 h
Four legs	First attempt to use and stand on four legs	< 2 h
Stable standing	Lamb independently is standing on all four legs for a minimum of 5 seconds. (Figure 6.1 C)	< 2 h
Find udder	Lamb finds and begins to nudge ewe's udder, attempting to suckle	< 4 h
Successfully suckle	Lamb's head is in an appropriate position, suckling from ewe's udder for min 5 seconds, with associated head movements to indicate swallow. Lambs tail may also move. (Figure 6.1 D)	< 4 h
Rest-Active	Time spent active (standing, walking and exploring pen) compared to time spent at rest (legs folded underneath body)	4 h to 23 h

If the lamb had failed to suckle after the first 4 h, the lamb was then fed by bottle. The amount of time each lamb spent at rest (legs folded underneath body) compared to the time spent standing, walking, and exploring the confines of the lambing pen was determined from the video record from 4 to 23 h after birth; 4 h was chosen for the start of this analysis because the

presence of the investigators from birth until this time was likely to influence some of the ewe and lamb behaviours.
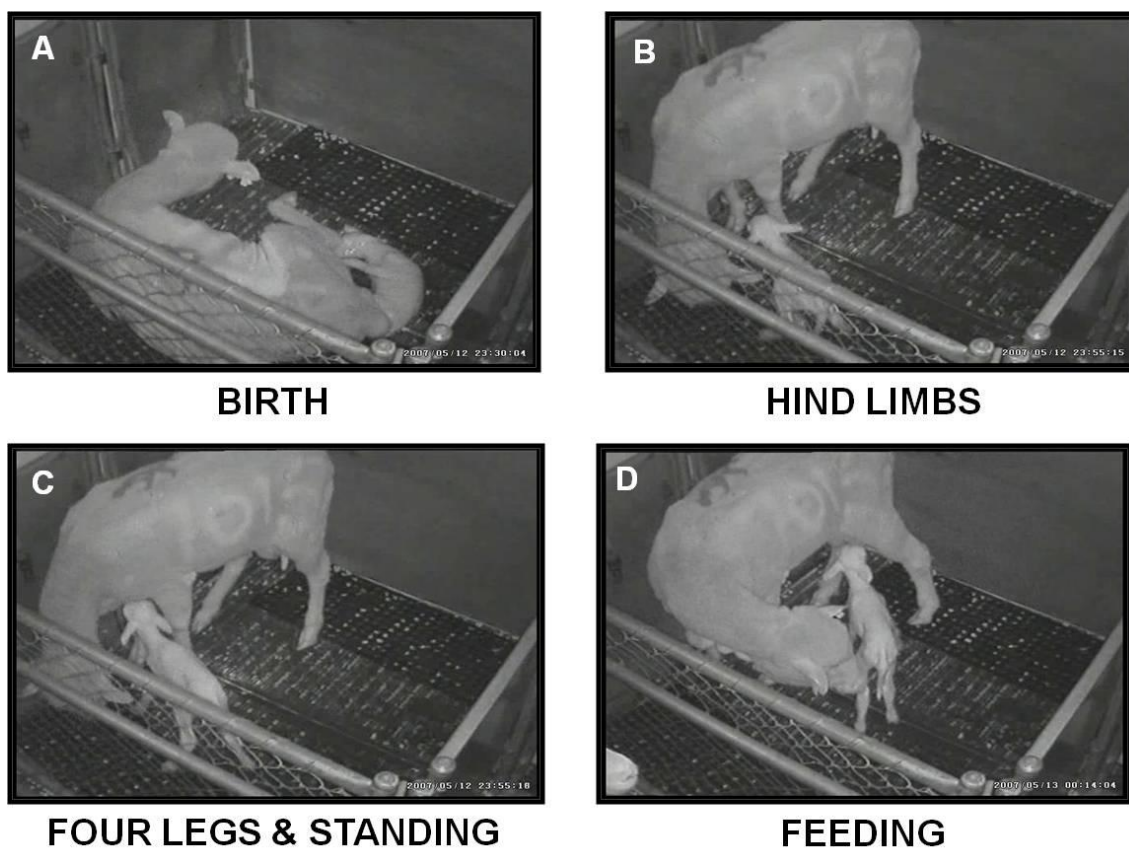
Figure 6.1: Photographic stills of lambing behaviour video monitoring set up. The time taken to achieve key behavioural milestones from birth (A; when the lamb has completely cleared the birth canal; time 0). The time taken for the newborn lamb to use hindlimbs (B), use four legs and attain a stable standing position (C) and successfully suckle (D) from the ewe were measured.

6.2.5 Data analysis

A mean value of the phasic amplitude of SSbfv was obtained for successive 10 min epochs across the entire recording period of each experiment (i.e., - from 6 h before UCO until the onset of labour, or until 145 days gestation). The data for each fetus were then expressed as a percentage change from basal of the amplitude calculated for the 6 h period immediately prior to the time of UCO (or sham) to account for different signal levels between fetuses.

The ECoG record was divided into successive 10 min epochs of high and low voltage activity (Boddy *et al.*, 1974; Clewlow *et al.*, 1983) using the mean amplitude for each type of activity obtained over at 6 h of control (i.e., pre-UCO) recording, and the results are expressed as the percentage of the time that each activity occurred during consecutive 2 h periods of the experiment. Very low amplitude ECoG activity (hereafter referred to as sub-low voltage) occurred after severe UCO in most fetuses and was defined as an amplitude sustained for at least 1 min that was <25% of the amplitude of normal low-voltage ECoG activity (Yan *et al.*, 2009; Yawno *et al.*, 2010).

Both EOG and EMG-nuchal activity were also analysed in the same manner, the average amplitude for successive 10 min epochs was determined. From the pre-UCO recordings (-6 h), the presence or absence of nuchal and eye movement activities was determined from the presence or absence of high and low amplitude signal, respectively. The percentage of time spent in each activity for 2 h consecutive periods was then determined.

FBM were quantified by calculating the average amplitude, and the incidence throughout the record, for continuous 10 min epochs. A negative deflection of tracheal pressure >2 mmHg (minus amniotic pressure) was classified as a breathing movement (Clewlow *et al.*, 1983), and the incidence of FBM (min/h) was then calculated.

The assessment of fetal behaviour was conducted by looking at the incidence of EMG- nuchal activity during LV-ECoG, and EOG activity during HV-ECoG for continuous 10 minute averages, when these two behaviours were present. The occurrence of both of these behaviours would indicate a "disorganization" of fetal behaviour.

6.2.6 Cortisol radioimmunoassay

For a detailed protocol please refer to Chapter 2, Section 2.7.

Cortisol was extracted from plasma samples using dicholoromethane as previously described by Bocking *et al.,* (1986). Briefly, following extraction cortisol assay buffer (100 µl), antiserum (100 µl; working dilution; 1:5000), bovine γ-globulin (100 µl; at a concentration of 8 mg/ml; Calbiochem, Darmstedt, Germany) and ^{3}H-cortisol (100 µl) were added to all sample and standard tubes, vortexed, covered with paraffin and incubated overnight at 4°C. The following day, 1 ml of 22% polyethylene glycol (PEG) was added, vortexed and centrifuged (1800 g) for 15 min at 4°C to separate bound hormone from the unbound hormones. The supernatant was aspirated, the pellet was resuspended in cortisol assay buffer (200 µl) and scintillation fluid (2 ml; Ultima Gold, Perkin Elmer, Australia) was added. Samples were vortexed, and placed in the β-counter (Beckman LS 3801, Beckman Instruments, USA) to determine radioactivity. Cortisol concentrations were calculated from the standard curve and a mean of duplicates was determined for each sample. The intra-assay and inter-assay co-efficient of the assays were 15.4 % and 24.6 % respectively.

6.2.7 Statistical analysis

All data are presented as mean ± standard error of the mean (SEM) unless otherwise stated. For the parameters in the fetal behaviour study (blood gases, cortisol, fetal behaviour and blood flow) all data are shown. Information from some fetuses was lost, or some ewes went into labour during the monitoring period that followed UCO, thus statistical analysis was only run when group numbers were 3 or more. After this, data were not analysed. This was done as ewes went into labour at different days following UCO, discussed in Results Section 6.3.3. The post UCO classification of fetuses into 'mild' and 'severe' groups explained in Chapter 5 has been retained throughout the analysis of results in this chapter.

A Shapiro-Wilks test for normality was conducted, if passed ($p > 0.05$) then a parametric test was run. Fetal blood gases, cortisol, fetal behaviour (ECoG, EOG, EMG-nuchal, FBM) were all analysed using a Two-Way (Mixed Model) ANOVA for treatment factor (between groups) and time (within subject, repeated measure). If a significant interaction was obtain, further post-hoc

analysis, a Bonferroni test, was conducted to determine where statistical significance existed. SSbfv was analysed using a One-Way Repeated Measures ANOVA where, if a significant interaction was detected, a Dunns post hoc was conducted to analyse statistical difference between basal (pre-UCO) and post-UCO values. For the postnatal behaviour analysis a One-Way ANOVA was conducted, and if significant, a Student Newman Keuls post hoc was also done. Statistical data were analysed using SPSS v18 for Windows, with significance set at $p <$ 0.05. All graphs were made using GraphPad Prism Software for Windows (v5.03).

6.3 RESULTS – FETAL BEHAVIOUR

Physiological and fetal behavioural measurements were analysed in Control (n=5), Mild UCO (n=5), Severe UCO (n=6). Below the systemic blood gases and outcome of pregnancy are detailed for all the animals used in this study.

6.3.1 Severity of UCO

Fetuses were randomly assigned to either a control or UCO group, however it appeared that there was a range of hypoxic insults caused by UCO which subsequently resulted in a range of fetal responses. Appendix 7 details the Control and UCO data. Figure 6.2 shows a scatter plot each fetuses arterial blood gases, O_2 saturation, pH, acid base excess (ABE) and lactate at 9 min after the start of UCO. Fetuses that were initially randomly assigned to the UCO group ([n=11], Figure 6.2 A – F), but were then sub-classified into either a 'mild' UCO (n=5) or 'severe' UCO (n=6) group based on the changes that occurred with respect to blood gases (Figure 6.2 G – L). The classification of mild or severe UCO was based on heart rate at 5 min, and arterial blood gases, pH and O_2 saturation values at 9 min during UCO, as summarized in Table 6.2. The change from basal values (obtained at -5 min) for each fetus is also shown in Figure 6.2 (M – R). Duration of UCO was not different between mild or severe UCO.
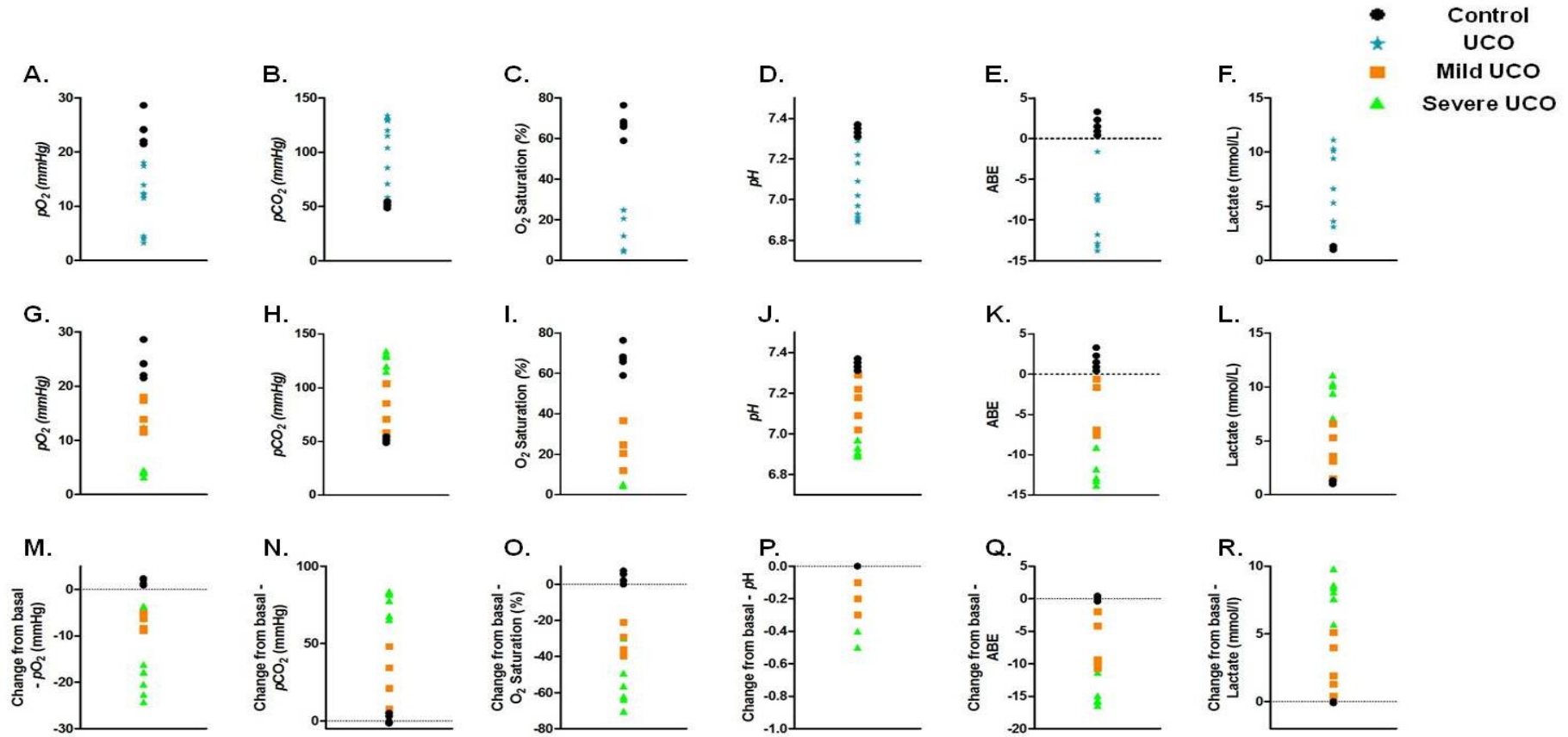
Figure 6.2: Scatter plots showing arterial blood gases, O$_2$ saturation, pH, ABE and blood lactate at 9 min during UCO. Initially fetuses were assigned to control (n=5; black circles) or UCO (n=11; blue stars) groups (A – F). Following UCO, it was apparent that fetuses that experienced UCO had a 'mild' (n=5; orange square) or 'severe' (n=6; green triangle) response (G – L). The absolute change from pre-UCO (-5 min) at 9 min during UCO is also shown (M – R).

Table 6.2: Classification of responses to UCO. Fetal haemodynamic (HR) and blood gas values (pO_2, pCO_2, pH, O_2 Sat, Lactate*)* were used to group severity of UCO into mild or severe.

	Control	*Mild UCO*	*Severe UCO*
pO_2 (mmHg)	>20	10 – 20	<10
pCO_2 (mmHg)	>50	50 – 110	>110
pH	>7.30	7.00 – 7.30	<7.00
O_2 Saturation (%)	>50	10 – 50	<10
Lactate (mmol/L)	< 2	2 – 6	>6
HR (BPM; at 5 min)	~ 150	< 150	>180
ECoG	HV/LV	HV/LV	>50% incidence of isoelectric activity

6.3.2 Response to UCO

6.3.2.1 Blood gases

Fetuses that experienced UCO and were then classified as either mild UCO (n=5) or severe UCO (n=6) experienced hypoxia, hypercapnia and acidosis during UCO (Figure 6.3 A, B, C, D) when compared to controls (n=5). Irrespective of whether the effect ***during*** UCO was 'mild' or 'severe', the arterial blood pO_2, pCO_2 and oxygen saturation had returned to pre-UCO values by 30 mins after the end of UCO (Figure 6.3 A, B and D). 'Mild' UCO showed a persistent arterial acidosis until 30 min post-UCO (7.29 ± 0.02) and 'severe' UCO was elevated until 1 h post-UCO; 7.29 ± 0.02).

Blood glucose concentration (Figure 6.3 E) significantly increased in the mild UCO fetuses at 9 (2.10 ± 0.49 mmol/L) and 30 min (1.52 ± 0.23 mmol/L) when compared to controls (0.84 ± 0.10 mmol/L, 0.84 ± 0.13 mmol/L respectively). When compared to controls, fetuses that experienced a severe UCO response had significantly increased blood glucose from 30 min (1.83 ± 0.12 vs. 0.84 ± 0.10 mmol/L) following UCO that was sustained until 6 h post-UCO

(1.53 ± 0.14 mmol/L vs. 0.96 ± 0.11). During the UCO itself, blood glucose increased significantly more in the mild UCO group (2.10 ± 0.49 mmol/L) compared to severe UCO group (1.38 ± 0.28 mmol/L).

Blood lactate (Figure 6.3 F) was significantly increased in fetuses that experienced a mild UCO from 5 mins (3.28 ± 0.73 mmol/L) until 1 h (3.46 ± 0.80 mmol/L) post-UCO, compared to the control fetuses (1.28 ± 0.04 mmol/L, 1.32 ± 0.10 mmol/L). Fetuses classed in the severe UCO group had a significantly increased blood lactate from 5 mins (7.03 ± 0.67 mmol/L), peaking at 9 min during UCO (9.57 ± 0.56 mmol/L), but remaining significantly increased until 6 h following UCO, when compared to the control group (5 min; 1.28 ± 0.04 mmol/L, 9 min; 1.22 ± 0.06 mmol/L 6 h; 1.38 ± 0.09 mmol/L), and to the mild UCO group at 6 h (1.86 ± 0.27 mmol/L).

Following this no significant differences were seen between groups for the duration of the experiment (i.e., until 145 days, or when the ewe came into labour). All blood gas values are listed in Appendix 4.

6.3.2.2 Mean Arterial Blood Pressure

During the experiment the patency of the fetal brachial arterial catheter used to measure MAP and HR did not allow for a continuous measurement in beyond 24 h in the control (n=5), and UCO (mild [n=5], severe [n=6]) fetuses. The fetal brachial artery catheter was also extremely sensitive to fetal movements. Therefore calculating these continuous cardiovascular parameters was not possible.

A severe response to UCO resulted in initial significant hypertension peaking at 2 min following the start of cord occlusion in fetuses (60.79 ± 8.90 mmHg vs. 42.37 ± 0.56 mmHg). Mild UCO resulted in significant hypertension for the duration of UCO, peaking 3 min in (61.29 ± 4.74 mmHg) compared to the MAP in the control fetuses (41.74 ± 0.96 mmHg).
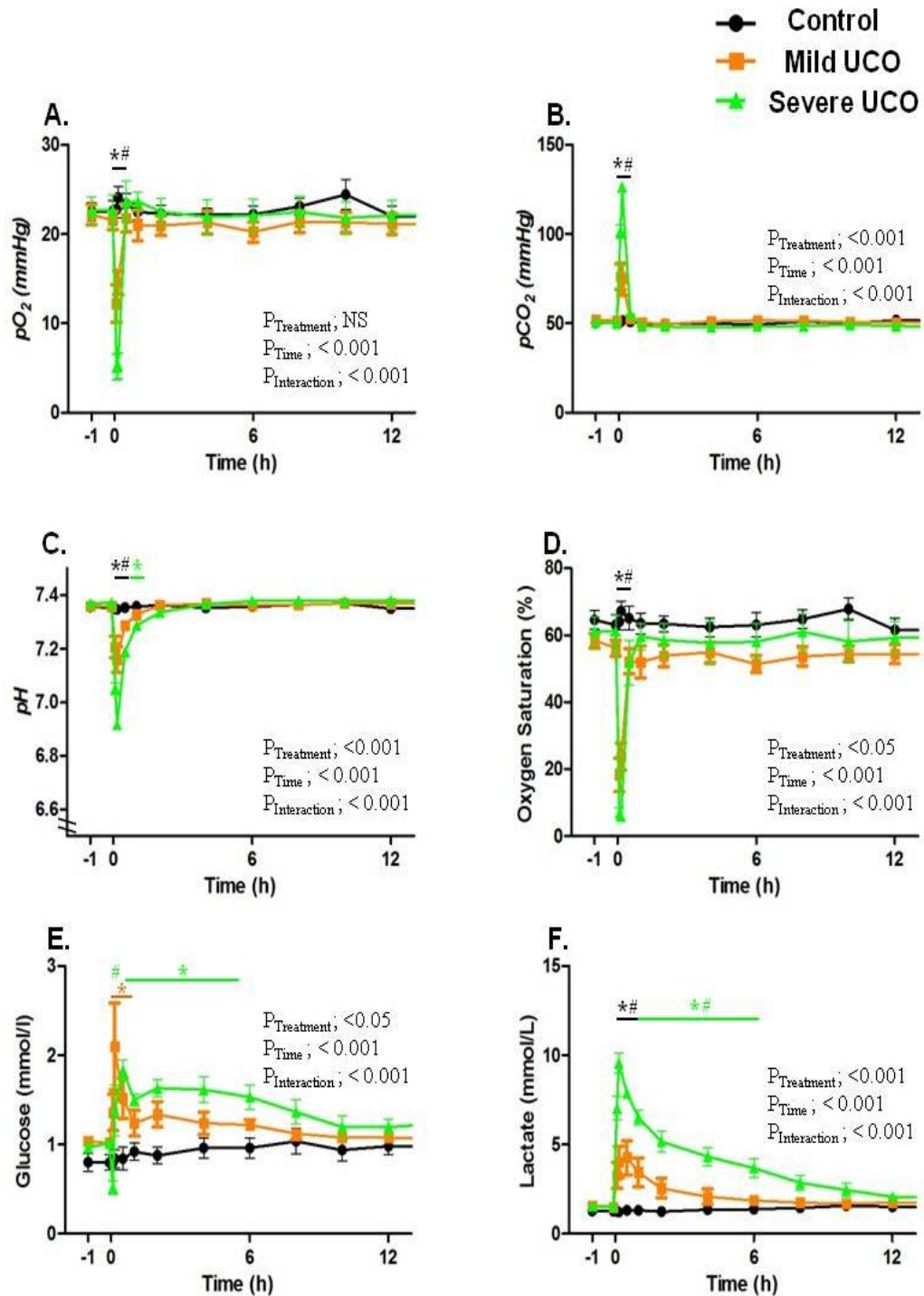
Figure 6.3: Fetal systemic blood gases in response to Sham or 10 min UCO. Fetuses subjected to a sham UCO (Control; black, n=5), mild UCO (orange, n=5) or severe UCO (green, n=6) responses to pO_2 (A), pCO_2 (B), pH (C), O_2 saturation (D), plasma glucose (E) and plasma lactate (F) from -1 h to +12 h. Time 0 indicates start of UCO (or Sham UCO). * indicates significant ($p < 0.05$) differences compared to controls (black; both mild UCO and severe UCO, orange; mild UCO only, green; severe UCO only), # indicates significant ($p < 0.05$) difference between severe UCO and mild UCO. Mean ± SEM.

MAP of the mild UCO fetuses was significantly increased compared to severe UCO at 7 min (55.54 ± 2.06 mmHg vs. 41.35 ± 4.03 mmHg respectively) and 8 min (54.81 ± 2.21 mmHg vs. 37.68 ± 4.56 mmHg) during UCO. On release of the umbilical cord cuff, fetuses that experienced a mild UCO returned to pre-UCO values. MAP in the severe UCO group significantly increased again at 13 min (53.99 ± 2.94 mmHg), following this MAP returned to pre-UCO values and by 15 min after UCO, after which there was no significant differences between groups (Figure 6.4 A).

6.3.2.3 Heart Rate

Initially during UCO, both 'mild' and 'severe' groups responded with a significant bradycardia. Then upon release of the cuff, only the group of fetuses classified in the 'severe' group experienced tachycardia, this did not happen in the mild UCO group.

A significant decrease in fetal heart rate at 1 min during severe UCO (119.51 ± 13.39 bpm) compared to controls (179.81 ± 16.23 bpm). At the end of severe UCO, heart rate significantly increased at 10 min (258.04 ± 37.80 bpm vs. 157.35 ± 6.29 bpm), 24 min (216.66 ± 14.63 182.58 ± 22.25 bpm), 28 min (204.43 ± 11.29 bpm vs. 155.59 ± 8.71 bpm) and 36 min (231.72 ± 23.83 bpm vs. 165.14 ± 13.57 bpm). Fetuses that experienced a mild UCO had a significantly lower heart rate at 2 min during UCO (104.26 ± 14.62 vs. 167.44 ± 15.67 bpm) (Figure 6.4 B).
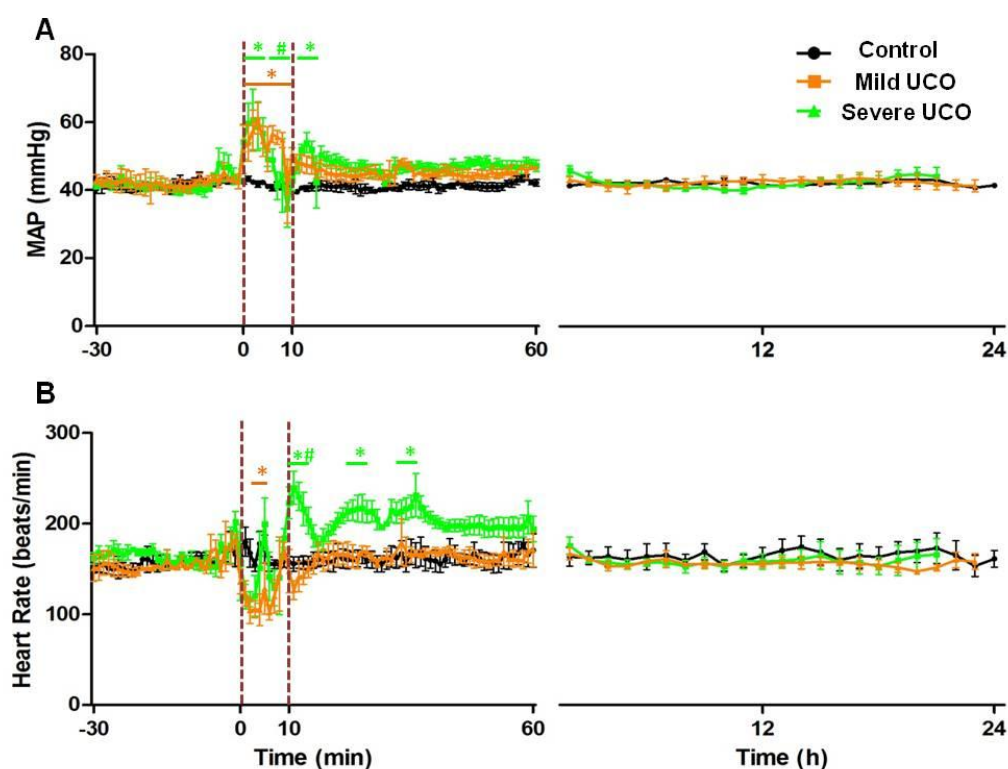
Figure 6.4: Fetal physiological responses to UCO. Mean arterial blood pressure (MAP; A) and heart rate (HR; B) monitored from -30 min to 24 h post-UCO. Time 0 indicates start of UCO (or Sham UCO). * indicates significant ($p < 0.05$) differences compared to controls (black; both mild UCO and severe UCO, orange; mild UCO only, green; severe UCO only), # indicates significant ($p < 0.05$) difference between severe UCO and mild UCO. Mean ± SEM. Note x axis scales from minutes to hours.

6.3.2.4 Plasma cortisol

Plasma cortisol was determined using plasma samples taken from control (n=5) and the UCO fetuses (mild [n=5], severe [n=6]). Following a 10 min UCO, in the fetuses grouped into the 'mild' category UCO resulted in significantly increased plasma cortisol from 5 min (during UCO) until 1 hour post-UCO compared to controls. In contrast, fetuses in the 'severe' UCO group had significantly increased plasma cortisol at 1, 4 and 24 h following UCO (Figure 6.5). The severe UCO group when compared to mild response to UCO had a significantly elevated plasma cortisol at 5, 9 minutes during UCO, and at 30 mins, and 1 and 4 h post-UCO (Figure 6.5). From 6 hours following UCO there were no significant differences between groups. No significant interaction was reached from 3 days post-UCO, however a significant time effect

was achieved. All plasma cortisol values for the duration of the experiment are detailed in Appendix 4.
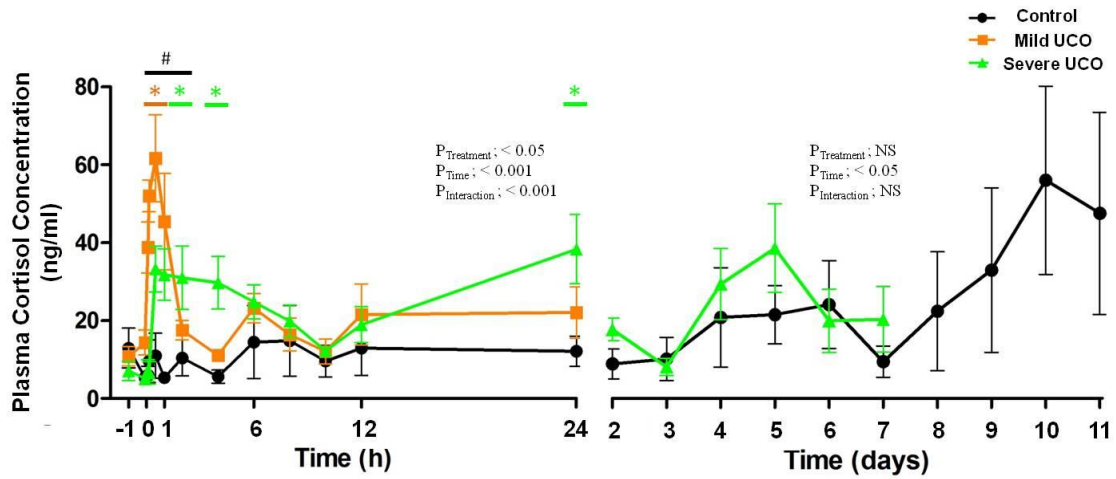
Figure 6.5: Plasma cortisol concentration (ng/ml) in response to UCO. Plasma cortisol was measured using RIA in Control (n = 5; black) and fetuses that had experienced a 10 min Mild UCO (n = 5; orange) or severe UCO (n=6; green) from -1 h to + 11 days. Time 0 indicates start of UCO. * indicates significant ($p < 0.05$) differences compared to controls (black; both mild UCO and severe UCO, orange; mild UCO only, green; severe UCO only), # indicates significant ($p < 0.05$) difference between severe UCO and mild UCO. Mean ± SEM. Note x axis scales from hours to days.

Increased plasma cortisol was seen to occur up to 3 days prior to labour onset, shown in Figure

6.6 for all groups (these values were removed from the previous Figure 6.5). No significant

treatment of interaction was seen between groups, but a significant time effect was noted.
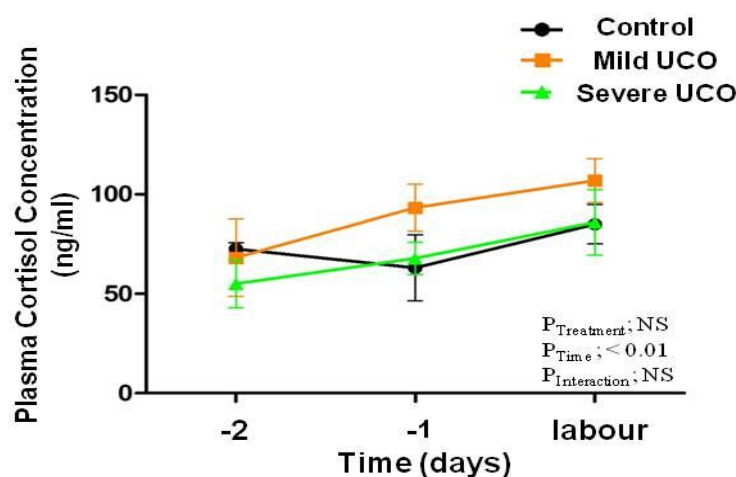
Figure 6.6: Plasma cortisol concentration (ng/ml) prior to labour. Plasma cortisol was measured using RIA in Control (n = 5; black) and fetuses that had experienced a 10 min Mild UCO (n = 5; orange) or severe UCO (n=6; green) from -2 days to day in labour. Time 0 indicates start of UCO. * indicates significant ($p < 0.05$) differences compared to controls (black; both mild UCO and severe UCO, orange; mild UCO only, green; severe UCO only), # indicates significant ($p < 0.05$) difference between severe UCO and mild UCO. Mean ± SEM.

6.3.3 Outcome of UCO

6.3.3.1 Gestational age in labour

Following UCO (or Sham UCO), on day 0 (130 – 132 days gestation), all fetuses were allowed

to recover and continue to develop *in utero* to the end of pregnancy. Figure 6.7 shows the

survival plot for the GA that ewes were in labour. Ewes whose fetuses were subjected to a mild

UCO (139.2 ± 1.8 days) or a severe UCO (139.7 ± 1.2 days) went into labour significantly

earlier than full-term controls (144.0 ± 1 days; Table 6.3). One control ewe went into labour at

140 days GA; the fetus appeared healthy so was included in the analysis. The remaining 4

control fetuses continued to develop till 145 days (n=2 in labour, n=2 post mortem at 145 days).

Shown in Figure 6.7, ewe's whose fetuses experienced a severe UCO went into labour earlier

than 145 days gestation (137; n=2, 138; n=1, 140; n=1, 142; n=1, 144;n=1). All of these fetuses were alive prior to post mortem. Ewe's whose fetuses experienced a mild UCO also went into labour prior to 145 days gestation. One of these fetuses died while the ewe was in early stage labour, this was at 136 days, the remainder of the fetuses were alive prior to post mortem and were in labour at 136 days; n=1, 137 days; n=1, 143 days; n=1, 144 days; n=1 (Figure 6.7).

As fetuses that were subjected to UCO did not continue till 145 days gestation, all the physiological and behavioural data in this chapter are shown for each group from the beginning of the experiment until all groups are n =3, after this data are not shown and statistical analysis was not run.
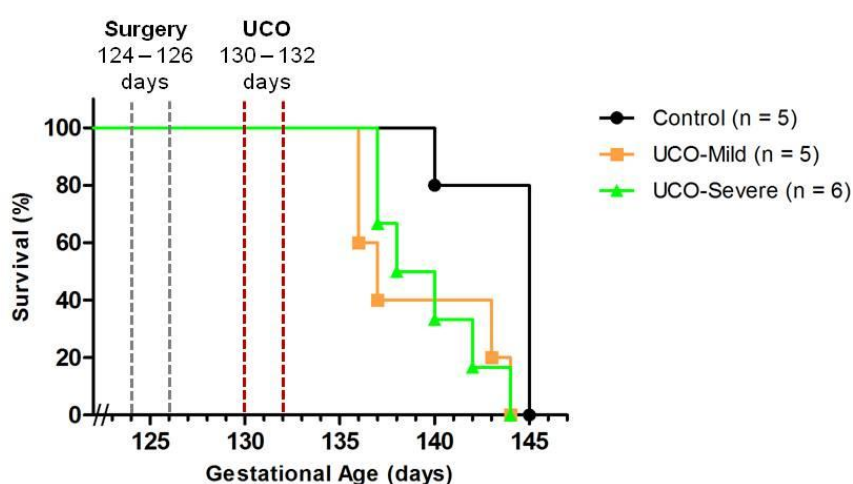
Figure 6.7: Survival plot showing gestational age ewes' went into labour – fetal behaviour study. Fetal sheep surgery was done between 124 – 126 days GA, 10 min UCO (or Sham) occurred between 130 – 132 days GA for Control (n=5; black), mild UCO (n=5; orange) and severe UCO (n=6; green) groups.

6.3.3.2 Post mortem

The full term control group of fetuses consisted of 3 males and 2 females; mild response to UCO fetuses had 2 male and 3 female, and the severe UCO group had 2 males and 4 females (Table 6.3). No significant differences were seen in fetal body weight or organ:body weight ratio between groups for the brain, heart, liver, brown fat, adrenals (both left and right combined for each fetus) and kidneys (both left and right combined for each fetus; Table 6.3).

Table 6.3: Outcome of pregnancy. GA in labour, birth weight, male:female ratio, nose-rump length and organ to body weight ratios for Control (n=5), mild UCO (n=5) and severe UCO (n=6). * $p < 0.05$ difference compared to controls. Mean ± SEM.

	Control (n = 5)	*Mild UCO* (n = 5)	*Severe UCO* (n = 6)
GA in labour (days) - Range	140 - 145	136 – 144	137 - 144
GA in labour (days) - Median	145	137	139
GA in labour (days) - Mean	144 ± 1.0	139.2 ± 1.8*	139.7 ± 1.2*
Birth weight (kg)	5.59 ± 0.40	5.13 ± 0.34	4.48 ± 0.50
Male / Female Ratio	3 / 2	2 / 3	2 / 4
Nose-rump length (cm)	65.50 ± 2.36 (n=3)	61. 80 ± 1.56	61.58 ± 2.34
Organ (g):body weight (kg) ratio			
Brain	9.31 ± 0.55	10.22 ± 0.42	11.05 ± 0.95
Lungs	30.26 ± 0.94	24. 60 ± 5.27	23.62 ± 2.84
Heart	7.06 ± 0.35	6.36 ± 0.23	7.56 ± 0.67
Liver	27.28 ± 2.26	29.94 ± 2.55	32.54 ± 3.59
Brown Fat	3.60 ± 0.60	4.94 ± 0.26	5.00 ± 0.29
Kidneys	5.14 ± 0.32	5.56 ± 0.18	5.37 ± 0.49
Adrenal Glands	0.18 ± 0.02	0.17 ± 0.02	0.22 ± 0.04

6.3.4 Fetal behavioural response to UCO

Figure 6.8 shows the response of a fetus from the 'severe' group from 30 mins before until 30 mins after the UCO. Prior to the onset of UCO, regular episodes of ECoG activity with either low amplitude (LV) or high amplitude (HV) were always observed, with EOG and FBM activities associated with LV and nuchal EMG activity associated with HV. It can be seen that during UCO, ECoG (Figure 6.8 A) became isoelectric and this persisted after UCO. While the fetal ECoG showed this near isoelectric activity, there was increased nuchal EMG and EOG activity during and after UCO (Figure 6.8 B, C), and there was no evidence of LV and HV ECoG states. An increase in sagittal sinus blood flow (Figure 6.8 D) during UCO also occurred. Finally, 'gasping' FBM occurred during and after UCO, as shown by the strong negative pressure deflections in the FBM trace (Figure 6.8 E).
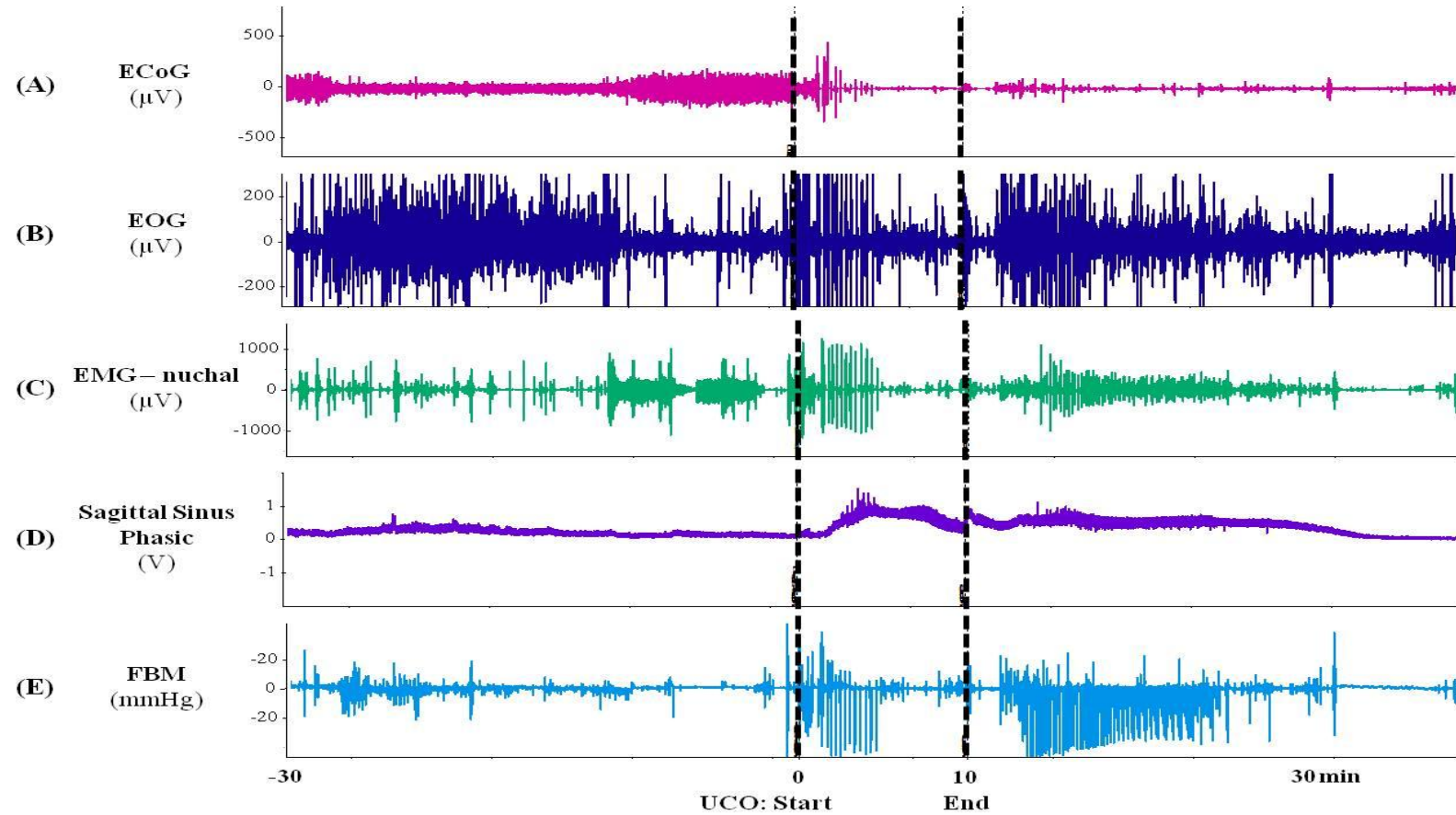
Figure 6.8: Response to severe UCO in late gestation fetal sheep - Chart recording. Chart recording of fetal behavioural responses before (-30 min), during and after (+30 min) severe UCO. Time 0 indicates start of UCO and ends at 10 min. Prior to UCO, low voltage (LV) and high voltage (HV) ECoG (A), during and following UCO this becomes isoelectric. Increased electro-ocular (EOG; B) and EMY- nuchal (C) activity. Increased sagittal sinus phasic (D) also occurs during UCO. Before UCO, Fetal breathing movements (FBM; E) are episodic with LV ECoG. During and following UCO, there are deep, gasping breathing movements.

6.3.5 Sagittal sinus blood flow velocity

Due to high noise to signal ratio and a change in manufacturer's production of the sagittal sinus doppler probe, we were only able to analyse SSbfv from 3 control, 4 mild UCO and 5 severe UCO fetuses. Due to noise, some of the time intervals in the control group were excluded (n < 3). To allow for accurate statistical analysis, both UCO groups were compared to their own pre-UCO values (-6 h to 0 h were calculated as basal), instead of comparison to the control group.

A significant increase in the amplitude of SSbfv occurred from 13 min to 17 min in the group of fetuses that experienced a severe UCO (Figure 6.9), peaking at 14 min (71.93 ± 31.88 % compared to basal -0.51 ± 0.82 %). Following this SSbfv significantly decreased in the UCO severe group to approximately 45% below basal, from 36 min to 60 min post UCO. A significant ANOVA was seen until 12 h post-UCO; although there appeared to be an increase from 12 – 84 h no significant differences were detected. No differences were also seen in the mild UCO group of fetuses (Figure 6.9). From 5 days, there were less than n=3 for the mild UCO group, so data are only shown for the severe UCO group.
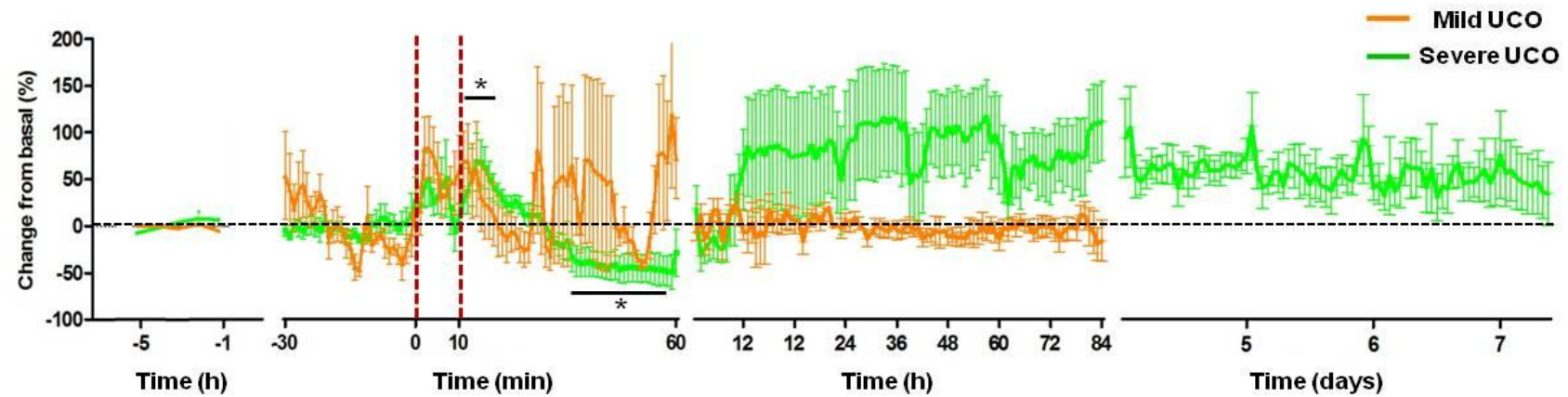
Figure 6.9: Fetal sagittal sinus blood flow doppler velocity. Percentage change from basal (-6 h to 0) sagittal sinus blood flow velocity in mild UCO (orange) and severe UCO (green). Red dashed lines indicate start (0) and end (10 min) of UCO. Blacked dashed line indicates no change from basal (0). * indicates significant ($p < 0.05$) differences compared to basal. Mean ± SEM. Note x axis scales from hours, minutes, hours to days.

6.3.6 Electrocortical Activity

Electrocortical activity was measured from fetuses that were subjected to no UCO (control n=5), a mild UCO (n=5), or a severe UCO (n=6); activity was analysed from 6 h prior to UCO until the end of the experiment. A Chart record of a severe response to UCO, with respect to ECoG is shown in Figure 6.8 A. Figure 6.10 compared the ECoG response to UCO between fetuses that were classified as either mild (B) and severe (C). Mild UCO did not result in isoelectric activity in any of the fetuses, where as severe UCO did so in 5 of the 6 fetuses in this group (Table 6.2).
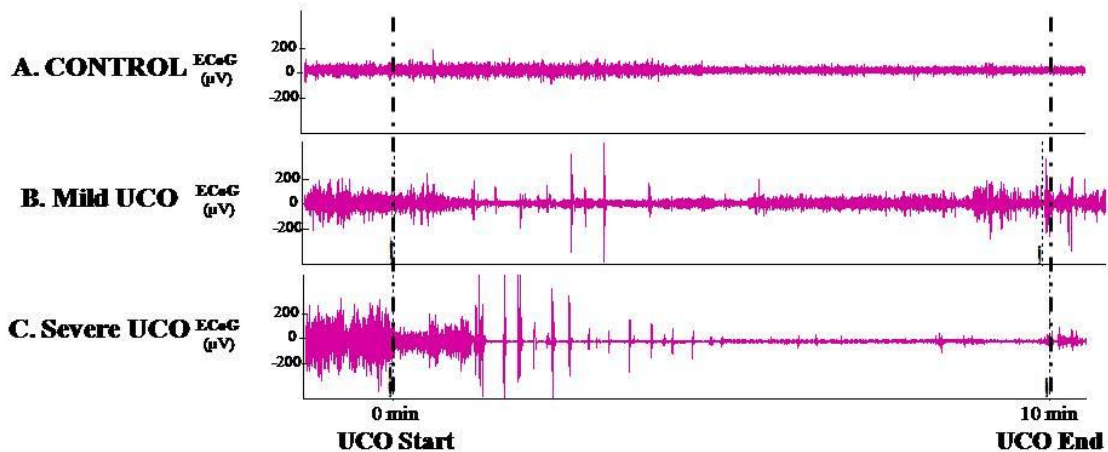
Figure 6.10: ECoG recording during 10 min UCO and Sham UCO – UCO Severity. In Control (A) and Mild UCO (B) fetuses, ECoG cycle between high voltage (HV) and low voltage (LV) activity, but during severe UCO (C) the fetus has a sub-low voltage activity (also referred to as isoelectric).

Figure 6.11 shows the percentage of time per 2 h epoch spent in high voltage (Figure 6.11 A), low voltage (Figure 6.11 B) and sub-low (<25% of normal low voltage) voltage (Figure 6.11 C). Fetuses who were subjected to a severe UCO had a significantly greater occurrence of sub-low ECoG activity than compared to Control and mild UCO fetuses.
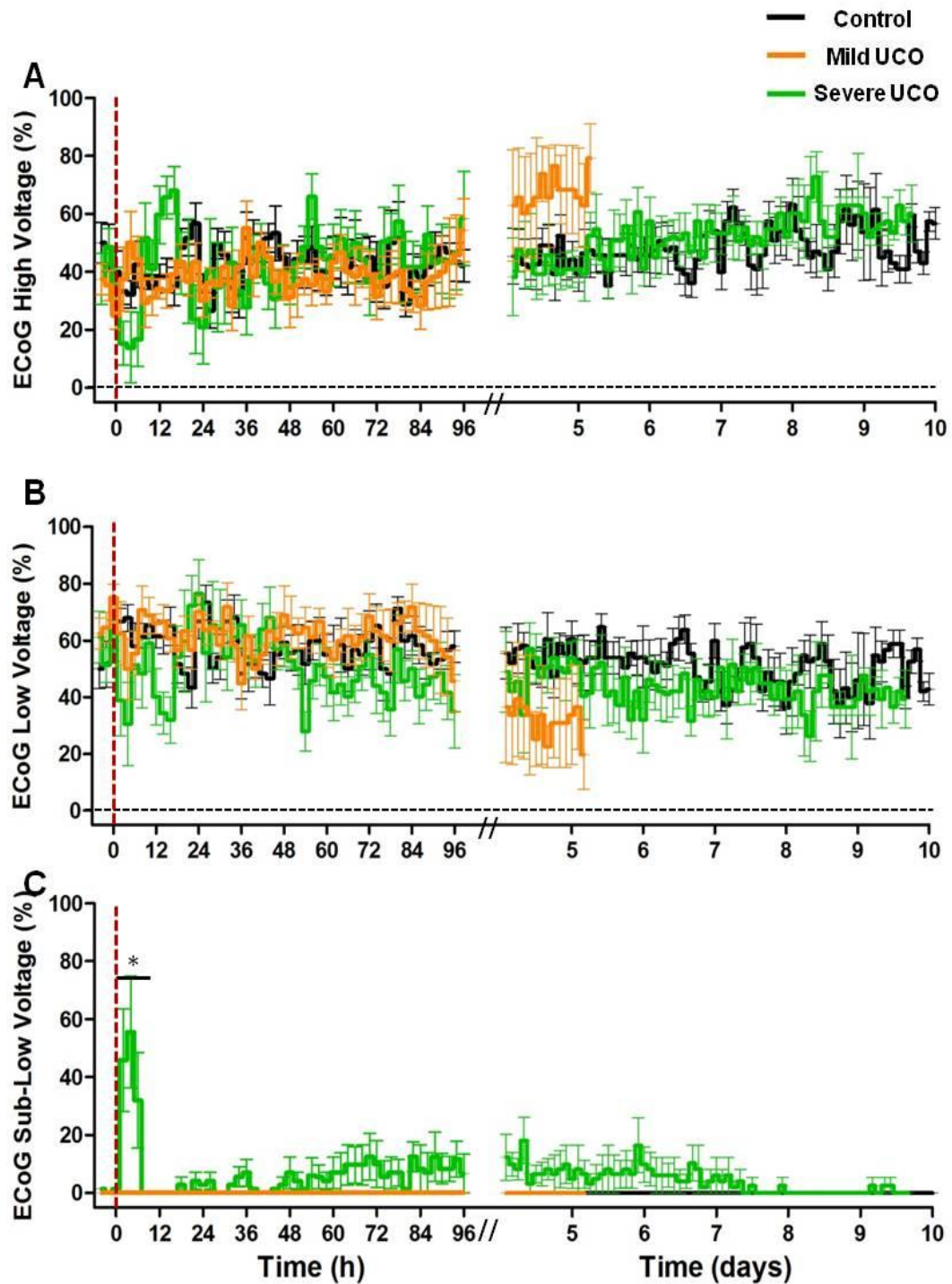
Figure 6.11: Electrocortical (ECoG) states in late gestation fetal sheep. The percentage of time spent in high voltage (HV; A), Low voltage (LV; B) and sub-low voltage (C) activity in fetuses subjected to (sham) control (black), mild UCO (orange) or severe UCO (green) prior to UCO to 10 days post-UCO. Red dashed line indicates UCO. * indicates significant ($p < 0.05$) differences compared to control. Mean $\pm$ SEM. Note x axis scales from hours to days.

6.3.7 Electromyogram – Nuchal and Eye Movement

The presence of eye movements (EOG; Figure 6.11 A) and nuchal muscle activity (EMG; Figure 6.12 B) were measured from -6 h until the ewes went into labour in control (n=5), mild UCO (EOG n=4, EMG-nuchal n=5) and severe UCO (n=6) groups. High amplitude or low amplitude signals were measured for successive 10 min blocks; the percentage incidence was calculated for every 2 h epoch (Figure 6.12). No significant interaction between time and treatment was seen for EOG activity. Although a significant time effect and treatment effect was seen between 16 and 124 h. No significant interaction, time or treatment effect was seen for nuchal muscle EMG.

6.3.8 Fetal breathing movements

The change in tracheal pressure was used to measure FBM in control (n=5), Mild UCO (n=5) and Severe UCO (n=5) fetuses. The incidence of FBM following UCO resulted in a significant interaction between groups until 14 h post UCO and between severe UCO and control groups between 196 h and 232 h (Day 7 – 8). A significant time effect was seen to occur from the start of the experiment (-6 h) until 125 h (Figure 6.13 A).

Amplitude of FBM was significantly increased in fetuses that experienced a severe UCO compared to controls and mild UCO groups from 18 h to 26 h post-UCO (Figure 6.13 B). Peak amplitude was seen in UCO severe group at 20 h (11.37 ± 2.74 mmHg) compared to controls (2.41 ± 0.34 mmHg) and mild UCO (2.21 ± 0.25 mmHg). Significant time effect occurred until 178 h post –UCO.

6.3.9 Fetal behavioural states

The effect of UCO on the organisation of fetal ECoG into LV and HV episodes is shown in Figure 6.14, for up to 7 days following UCO. This analysis specifically included the paradoxical association of LV with nuchal EMG (LV + EMG; Figure 6.14 A), and HV with EOG (HV + EOG; Figure 6.14 B) for control (n=4), mild UCO (n=4), severe UCO (n=4).

No significant interaction was seen between time and treatment with the percentage incidence of normal association of LV ECoG with EMG nuchal activity. Severe UCO did result in a significant increase in the incidence of EOG activity occurring during HV-ECoG (Figure 6.14 B), during day 1 (12 – 16 h), day 3 (52 – 56 h), day 7 (148 – 160 h).
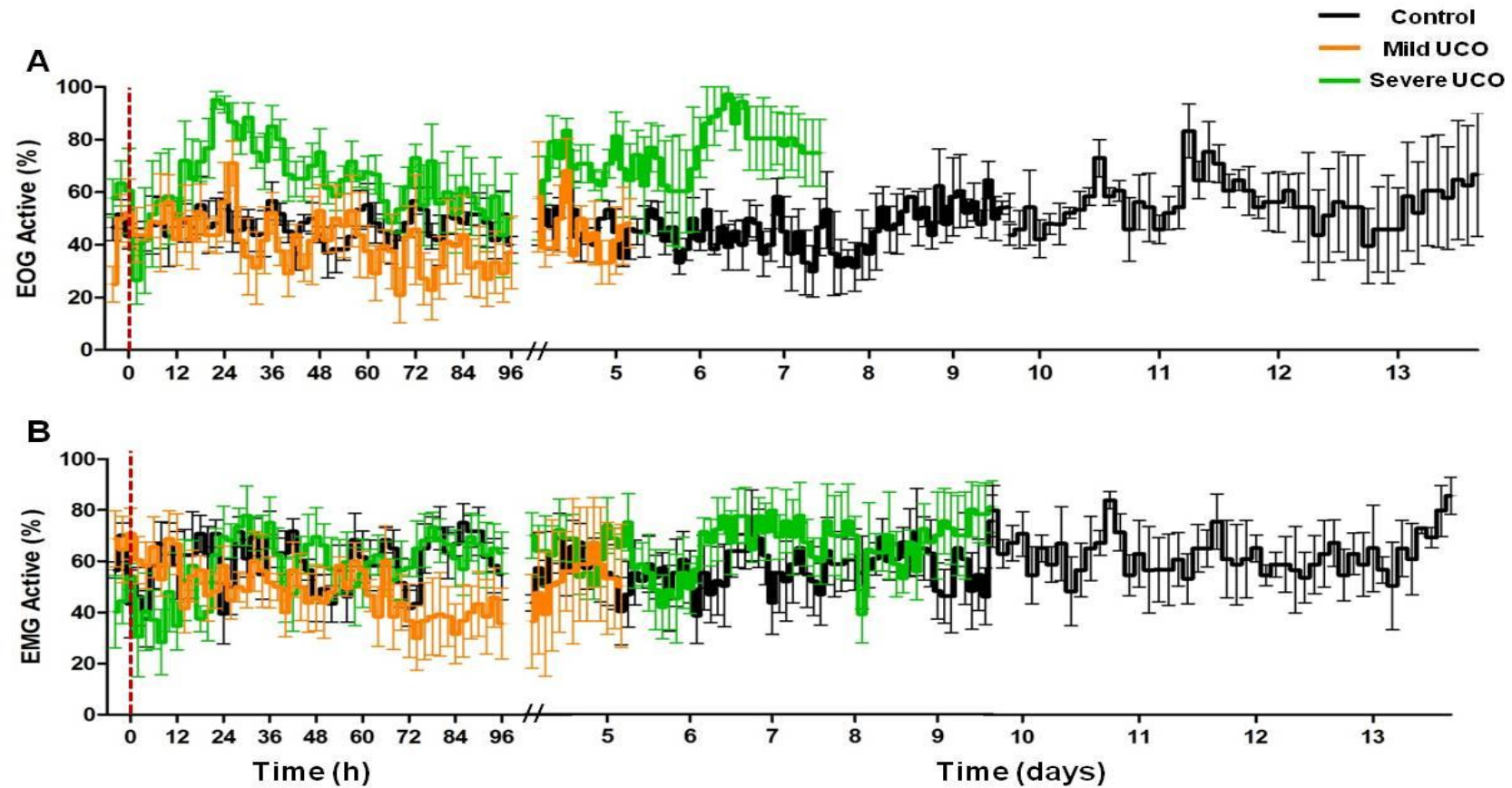
Figure 6.12: Electro-ocular (EOG) and EMG - nuchal activity in late gestation fetal sheep. The percentage of time spent with ocular muscle (EOG; A) and EMG-nuchal muscle (B) active in fetuses subjected to (sham) control (black), mild UCO (orange) or severe UCO (green) prior to UCO to 13 days post-UCO. Red dashed line indicates UCO. * indicates significant ($p < 0.05$) differences compared to control. Mean ± SEM. Note x axis scales from hours to days. Mean ± SEM.
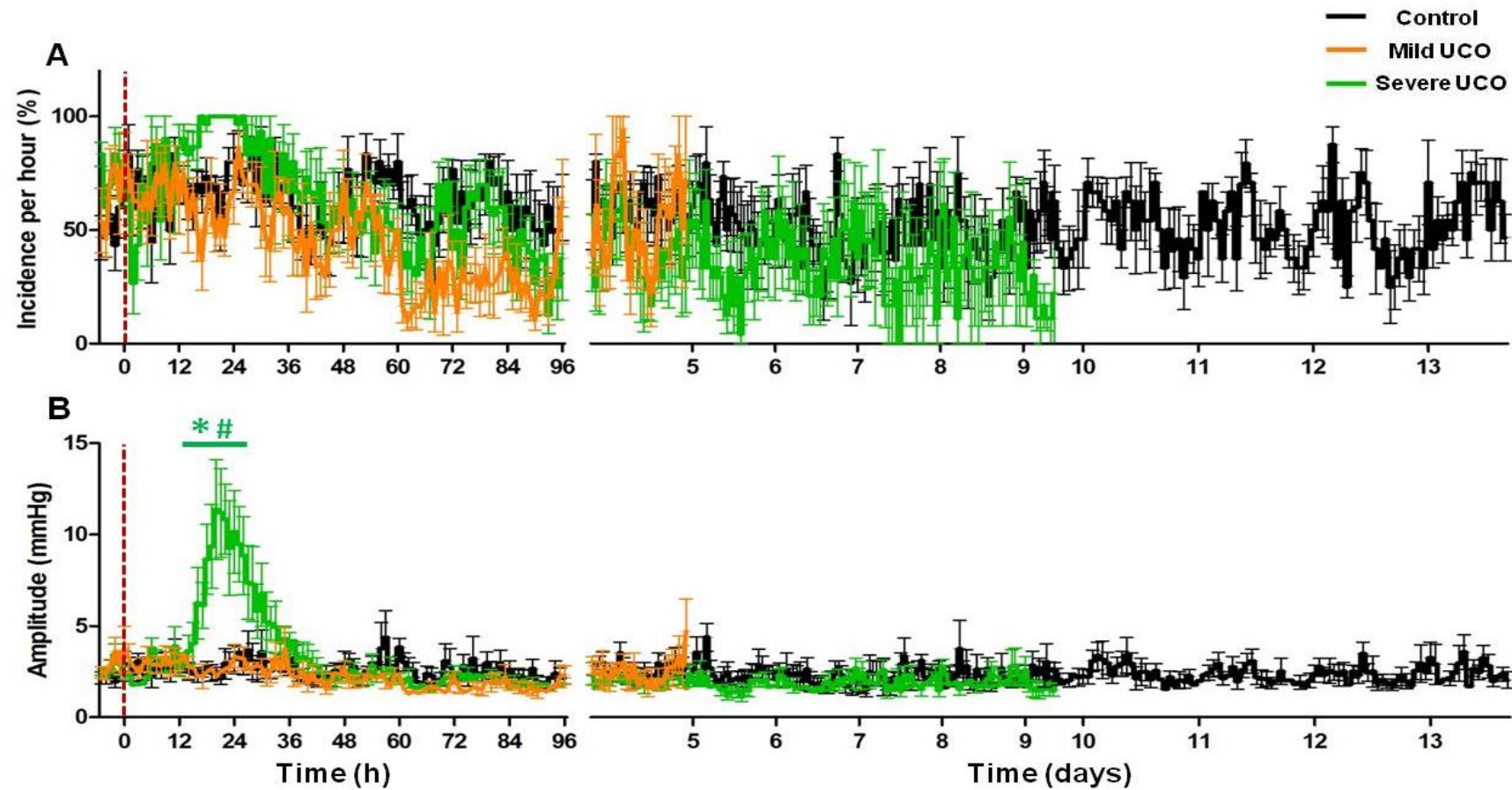
Figure 6.13: Incidence and amplitude of fetal breathing movements (FBM) in late gestation fetal sheep. The incidence (A) and amplitude (B) of FBM in fetuses subjected to (sham) control (black), mild UCO (orange) or severe UCO (green) prior to UCO until 13 days post-UCO. Red dashed line indicates UCO. * indicates significant ($p < 0.05$) differences compared to control, # indicates significant ($p < 0.05$) differences to mild UCO (green; severe UCO only). Mean ± SEM. Notes x axis scales from hours to days. Mean ± SEM.
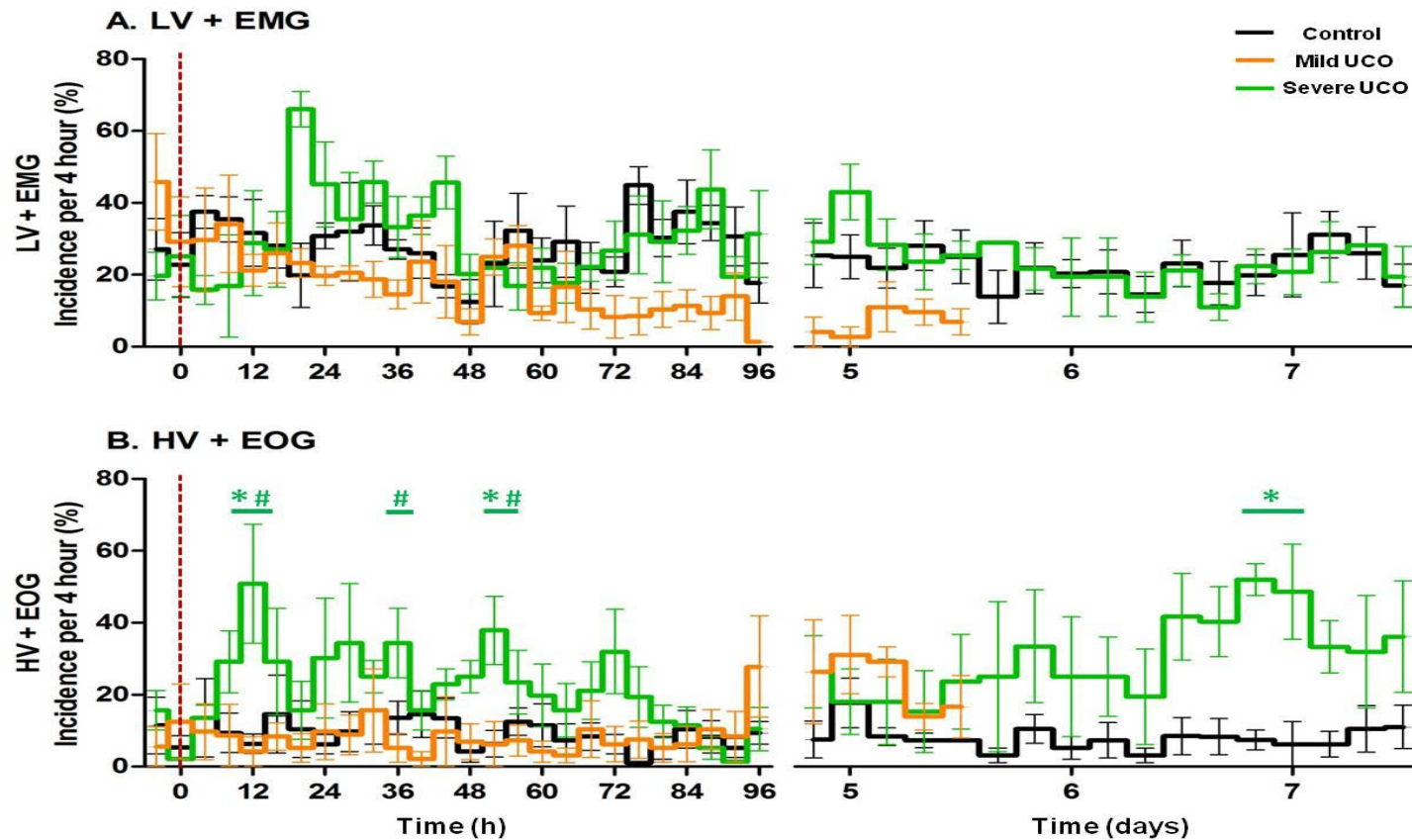
Figure 6.14: Disorganisation of fetal behaviour in late gestation fetal sheep. Percentage incidence (per 4 h) of the occurrence of EMG-nuchal activity with LV ECoG (A) and EOG activity during HV ECoG (B) in control (black, n=4), mild UCO (orange, n=4) and severe UCO (green, n=4) fetal sheep. Red dashed line indicates UCO. * indicates significant ($p < 0.05$) differences compared to control, # indicates significant ($p < 0.05$) differences to mild UCO (green; severe UCO only). Mean ± SEM. Notes x axis scales from hours to days. Mean ± SEM.

6.4 RESULTS – POSTNATAL BEHAVIOUR

6.4.1 Severity of UCO

Occluding the umbilical cord for up to 10 minutes resulted in acute hypoxemia (decreased pO_2), hypercapnia (increased pCO_2) and acidosis (decreased pH) which all recovered, and returned to pre-UCO values by 1 hour (Table 6.4). Metabolic acidosis, as shown by increased plasma lactate was significantly increased until 2 hours after UCO, when it then decreased to be not different from pre-UCO values. One fetus had a 'mild' response to UCO (pH > 7.0, Table 6.5), however in this study (postnatal behaviour), fetuses that were subjected to UCO were not further sub-classified into 'mild' or 'severe' due to low numbers of animals.

6.4.2 Outcome of pregnancy after UCO

Fetuses that were subjected to 10 min UCO between 130 to 134 days gestation were born significantly earlier (139.7 ± 2.23 days) than Sham UCO controls (148.67 ± 0.56 days; Figure 6.15, Table 6.6). In the UCO group, fetuses were born as early as 134 days gestation (n=1), 136 days (n=1), 138 days (n=1), 146 days (n=1) and 147 days (n=1). The control fetuses were born at 147 days (n=1), 148 days (n=2), 149 (n=2), 151 (n=1).
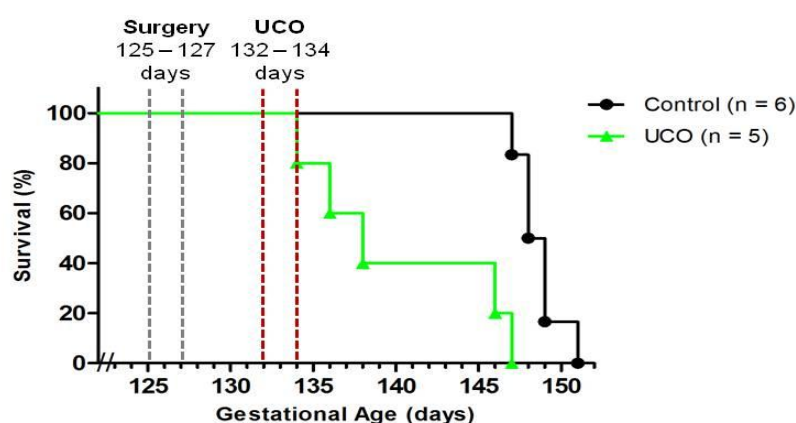
Figure 6.15: Survival plot showing gestational age (GA) lambs were born – postnatal behaviour study. Fetal sheep surgery was done between 125 – 127 days GA, 10 min UCO (or Sham) occurred between 132 – 134 days GA for Control (n=6; black), and UCO (n=5; green) groups.

Table 6.4: Fetal arterial blood gases in response to UCO – postnatal behaviour study. Blood gas parameters (pO_2, pCO_2, O_2 Saturation, pH and plasma lactate) were measured from -1 h to + 8 h in fetuses subjected to UCO. * indicates significance ($p < 0.05$) compared to pre-UCO (-1 h). Mean ± SEM.

Time relative to onset of UCO	-1 h	+10 mins	+1 h	+2 h	+4 h	+8 h
pO_2 (mmHg)	20.20 ± 0.60	4.88 ± 1.46*	21.18 ± 0.54	20.36 ± 0.50	18.58 ± 1.36	18.16 ± 1.01
pCO_2 (mmHg)	55.44 ± 0.95	126.6 ± 12.85*	53.48 ± 0.85	51.36 ± 0.89	52.18 ± 1.11	53.80 ± 0.57
O_2 saturation (%)	48.48 ± 2.96	4.96 ± 2.16*	47.64 ± 2.50	48.32 ± 2.13	44.14 ± 5.03	41.20 ± 4.08
pH	7.35 ± 0.01	6.95 ± 0.06*	7.28 ± 0.02	7.33 ± 0.01	7.35 ± 0.01	7.35 ± 0.01
Plasma lactate (mmol/L)	1.56 ± 0.17	8.90 ± 1.50*	6.58 ± 1.08*	4.64 ± 0.72*	3.50 ± 0.67	2.82 ± 0.71

6.4.3 Attainment of key milestones

Continuous video records were attained from the time of birth. Six control lambs, five pre-term controls (induction of labour by Epostane) and five lambs that were subjected to UCO were included in the analysis. Pre-term controls were included as occlusion of the umbilical cord resulted in significantly early delivery in 3 of the 5 UCO lambs compared to the sham-occluded group (see Figure 6.14). The time taken to attain each "milestone" is shown in Figure 6.16, whilst the individual times taken by UCO lambs are shown in Table 6.5. No significant difference was seen across groups in the time taken for lambs to shake their head (Figure 6.16 A) or use their hindlimbs (Figure 6.16 B). Lambs subjected to UCO took significantly longer (28.14 ± 4.28 min; n = 4) to stand on all four legs, when compared to full term controls (10.96 ± 1.34 min) and pre-term controls (15.16 ± 2.14 min), one UCO lamb took 169 minutes, to stand on four legs and subsequently failed (i.e., longer than 120 minute) to achieve this 'milestone' (Figure 6.16 C, Table 6.5).

Pre-term controls took significantly longer to find the udder (107.97 ± 17.21 min) and successfully suckle (130.26 ± 5.38 min) from the ewe, compared to full term (30.94 ± 4.71 min and, 41.10 ± 6.25 min) and UCO lambs (44.97 ± 3.20 min, 75.12 ± 12.42 min). However, 2 lambs that were subjected to UCO took longer than 4 hours to find the udder and successfully feed, so were noted as "failing" these milestones as experimenter intervention was required (Figure 6.16 E,F, Table 6.5). Pre-term lambs spent significantly less time active (255.94 ± 23.58 min) compared to full term controls (588.77 ± 8.30 min) and UCO lambs (372.74 ± 115.80 min; Figure 6.16 G). Only 3 pre-term lambs, four UCO lambs were include in measure due to inadequate video footage for analysis.
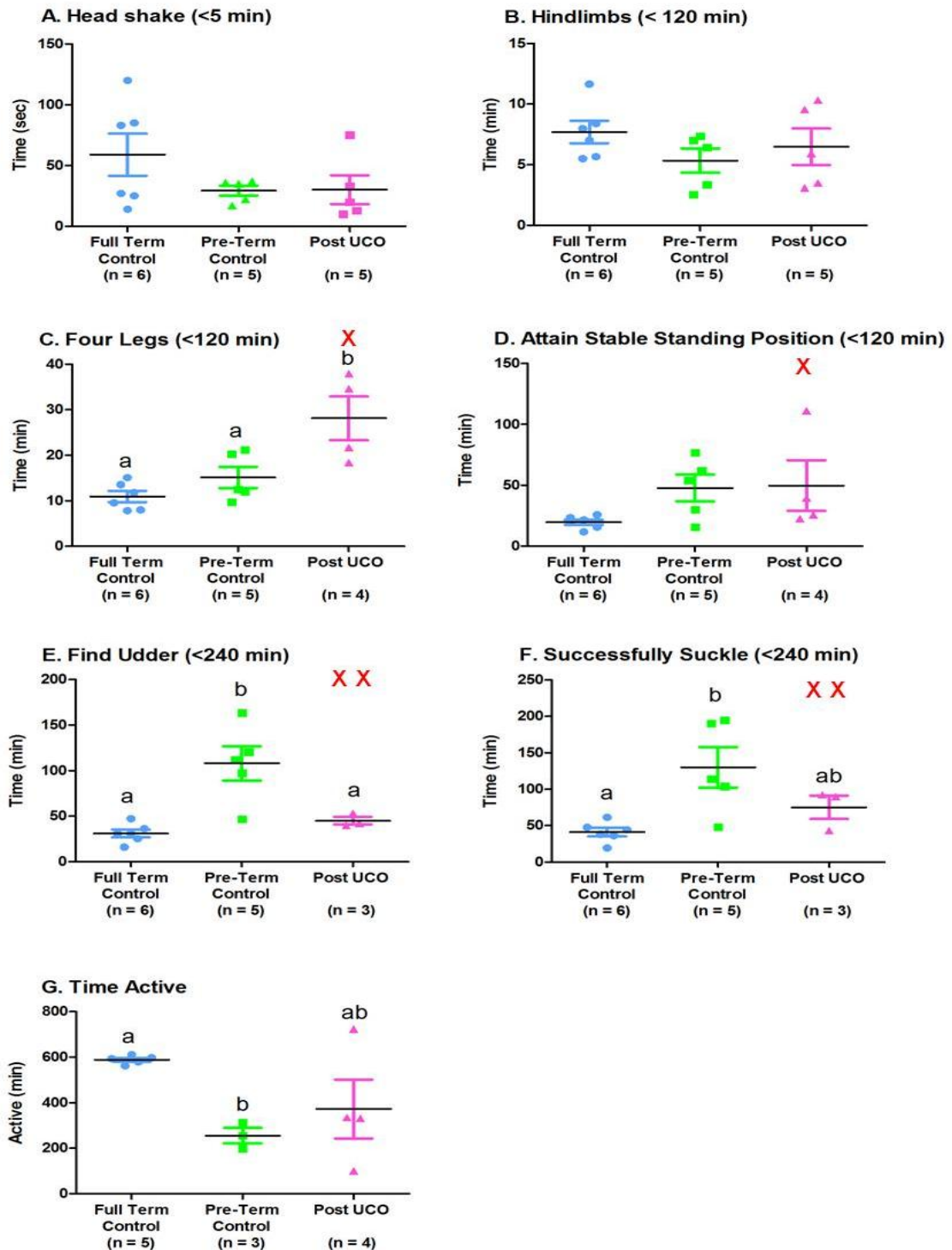
Figure 6.16: Attainment of key behavioural milestones from birth. Mean values and the range of times associated with each key behaviour; head shake (A), use of hindlimbs (B), use of four legs (C), stable standing position (D), finding udder (E), successfully suckle (F) and time spent active (G) for full term control (blue), pre-term control (green) and post-UCO (pink) lambs. N are stated for each milestone. Significance ($p < 0.05$). Red crosses indicate lambs that failed to achieve the milestone in the time stated in brackets.

Table 6.5 gives the individual details and outcomes of lambs that were subjected to an *in utero* UCO. UCO severity (measured by drop in pH), UCO duration, gestational age born, sex and whether assistance was required during delivery or to feed are shown (Individual times taken to achieve 'milestones' are also shown). Of note, the two lambs that responded to UCO with the most severe drop in pH (animal number 7108 and 7137; 6.832, 6.866 respectively) were the two lambs that failed to achieve all 'milestones'. No direct correlation was seen between pH during UCO and time to stand (Figure 6.17 A), attain a stable standing position (Figure 6.17 B) or time spent active (Figure 6.17 C).

6.4.4 Postnatal outcome

Control ewes gave birth between 147 to 151 days gestational age, whereas as ewes carrying fetuses subjected to UCO gave birth between 134 to 147 days gestation (Table 6.6). Pre-term controls (138.4 ± 0.2 days; 3.74 ± 0.16 kg) and UCO lambs (139.7 ± 2.2 days; 3.51 ± 0.32 kg) were born significantly earlier and were significantly smaller than full-term controls (148.7 ± 0.6 days; 5.14 ± 0.34kg). The full term control group of lambs consisted of 2 males and 4 females, pre-term lambs has 2 male and 3 females and the UCO lamb group had 2 males and 4 females (Table 6.6). No significant differences were seen in organ:body weight ratio between groups for the brain, heart, liver, brown fat, adrenals (both left and right combined) and kidneys (both left and right combined; Table 6.6).

Table 6.5: Individual outcome of lambs that experienced UCO. Details of each lamb (Animal #) that experienced UCO; pH at end of UCO, UCO duration, GA born, sex of lamb, Any assistance required during delivery or feeding and individual times to attain milestones, time spent active and brain:body weight ratio.

Animal #	UCO Severity pH	UCO Duration (min)	GA Born (days)	Sex	Assisted Delivery	Assisted Feeding	Head Shake (sec)	Hindlimbs (min.sec)	Four Legs (min.sec)	Stable Standing (min.sec)	Find Udder (min.sec)	Successful Suckle (min.sec)	Rest Activity (%)	Brain(g): Body Weight (kg)
7065	6.924	10	146	F	N	N	20	9m 33s	18m 22s	22m 20s	39m 43s	89m 57s	50.32	12.49
7080	6.901	8m20s	147	M	N	N	13	5m 59s	21m 41s	25m 46s	42m 4s	43m 4s	23.27	10.82
7108	6.832	10	134	M	N	Y	75	10m 20s	169m	350m	**Fail**	**Fail**	6.98	15.58
7137	6.866	10	136	M	N	Y	33	3m 6s	37m 55s	111m 9s	551m 44s	**Fail**	22.97	16.88
7212	7.224	10	138	F	N	Y	10	3m 30s	34m 35s	39m 37s	53m 7s	92m 20s	-	11.98
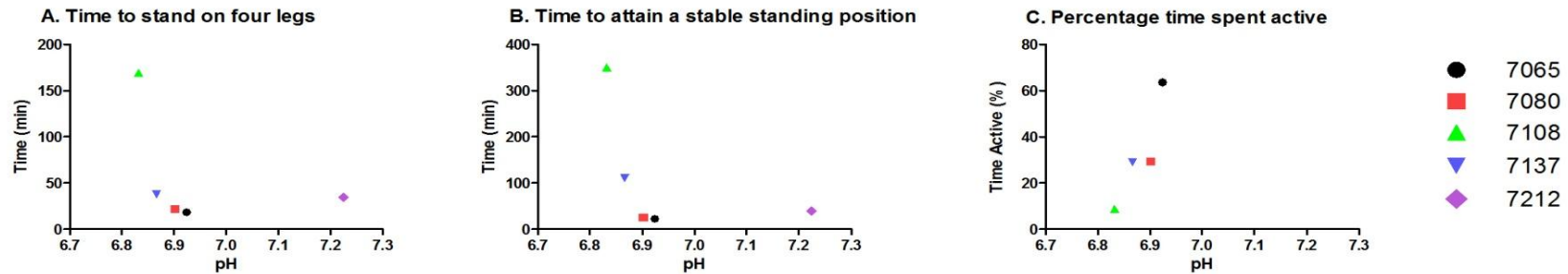
Figure 6.17: Scatter plot of pH and behaviours at birth for lambs that experienced UCO. Scatter plot of pH during UCO and time to stand on four legs (A), attain a stable standing position (B) and percentage of time spent active (C).

Table 6.6: Outcome of pregnancy – 24 h old lambs. GA in labour, birth weight, male:female ratio. Nose-rump length and organ to body weight ratios were recorded at time of post mortem, 24 h after birth for full term control (n=6), pre-term control (n=5) and post-UCO lambs (n=5). * $p < 0.05$ difference compared to controls. Mean ± SEM.

	Full-term Control lambs **(n=6)**	*Pre-term Control lambs* **(n=5)**	*Post-UCO Lambs* **(n=5)**
GA at delivery (days) - Range	147 - 151	138 - 139	134 - 147
GA at delivery (days) - Median	148	138	138
GA at delivery (days) - Mean	148.7 ± 0.6	138.4 ± 0.2*	139.7 ± 2.2*
Post mortem weight (kg)	5.14 ± 0.34	3.74 ± 0.16*	3.51 ± 0.32*
Male/female Ratio	2 / 4	2 / 3	2 / 4
Nose-rump length (cm)	66.1 (n=2)	61.1 ± 1.73	59 ± 3.12 (n=4)
Organ (g):body weight (kg) ratio			
Brain	10.99 ± 0.71	12.82 ± 0.63	13.35 ± 1.07
Heart (*p* = 0.056)	8.23 ± 0.32	10.95 ± 1.09	10.81 ± 1.11
Liver	27.85 ± 0.95	24.75 ± 1.69	31.55 ± 3.30
Brown Fat	6.24 ± 0.44	3.57 ± 0.80	5.50 ± 1.13
Kidneys	7.19 ± 0.87	6.41 ± 0.06	7.11 ± 0.59
Adrenal Glands	0.17 ± 0.01	0.18 ± 0.01	0.23 ± 0.02

6.5 DISCUSSION

This study has shown that a single occlusion of the umbilical cord in late gestation results in significant and persistent effects on fetal and postnatal behavioural outcome, despite fetal blood gases and cardiovascular haemodynamics returning to pre-UCO levels soon after (< 6 h) the UCO. However, fetuses that experienced a severe UCO showed more persistent disturbances in fetal behaviour. Interestingly, UCO of either severe or mild response (based on blood gas parameters) resulted in ewes going into labour earlier and lambs being born earlier.

We used fetal plasma to measure cortisol as an indicator of stress. Fetuses that experienced mild occlusion of the umbilical cord responded with a rapid increase of plasma cortisol during UCO,

which only returned to basal levels by 2 h (Figure 6.6). Severe UCO did also result in peak cortisol secretion, however this peak occurred at 30 min following UCO and was markedly reduced in comparison the mild UCO groups' peak at 9 min. Cortisol secretion in response to hypoxia, hypoxemia and decreased uterine blood flow, both chronic and acute, has been seen to occur in fetal sheep, piglets and goats (Bocking *et al.*, 1986; Giussani *et al.*, 1994; Unno *et al.*, 1997; Roelfsema *et al.*, 2005; Fujimori *et al.*, 2008; Harris *et al.*, 2009). The secondary peak of serum cortisol concentration at 24 h following severe UCO has also been seen in the preterm sheep fetus following UCO (Roelfsema *et al.*, 2005).

Increased cortisol secretion is suggested to mediate the increase of MAP following asphyxia, which has been seen to occur in preterm fetal sheep (Roelfsema *et al.*, 2005), however in our study increased cortisol occurred when MAP was not different to controls. In near term fetal sheep, carotid chemoreflexes and the release of catecholamines (such as noradrenaline) from the adrenal medulla are important and involved in the cardiovascular responses to hypoxia (Giussani *et al.*, 1993; Giussani *et al.*, 1994), but the implication of this interaction in near-term fetal sheep needs to be further investigated in our study.

Possible mechanisms that may contribute to the differing response of cortisol following a mild or severe hypoxia could be explained by the production of adenosine, known to increase during hypoxia and asphyxia and act as a potent vasodilator (Chau *et al.*, 1999; Blood *et al.*, 2003). Infusion of adenosine receptor antagonists has been shown to suppress cortisol production during cord occlusion in late gestation fetal sheep (Chau *et al.*, 1999; Jensen *et al.*, 2010). From our study, increased cortisol production during (9 min) a mild UCO and immediately following (30 min) severe UCO could be due to increased adenosine production.

Cortisol production and secretion is also suggested to also be mediated by prostaglandin (PG) production. Experiments conducted in late gestation fetal sheep showed that injection of PGE_2 increased secretion of adrenocorticotropic hormone (ACTH) and plasma cortisol (Hollingworth *et al.*, 1995; Knutson & Wood, 2010). Conversely, when PG production is blocked by

nimesulide (a PG-H$_2$ synthase inhibitor), decreased secretion of ACTH and cortisol occur (Unno *et al.*, 1998; Knutson & Wood, 2010). Whether UCO results in increased PG production, possibly mediating increased cortisol in response to UCO needs to be investigated further. PGs may also be implicated in the high plasma lactate (metabolic acidosis) seen up to 8 h following severe UCO. In response to hypoxemia in fetal sheep, inhibition of prostaglandin synthesis also resulted in severe metabolic acidosis (Hooper *et al.*, 1992).

Cortisol production during and following hypoxia has also been suggested to be an indicator of neurological outcome, although findings are conflicting. Increased cortisol during the end of hypoxia has been associated with a positive neurological outcome (measured by cerebral function, ECoG, cerebral impendence and MAP-2 immunohistochemistry) in newborn piglets (Harris *et al.*, 2009). However the use of metyraprone, known to suppress glucocorticoid synthesis, was closely associated with a reduction in brain injury and excitotoxic seizure activity following global or focal ischemia in adult rats, and this was correlated with a reduction in corticosterone concentration (Smith-Swintosky *et al.*, 1996; Krugers *et al.*, 1998).

These studies suggest that increased cortisol following severe UCO could be responsible for the increased incidence of seizure activity. We have previously shown suppression of ECoG activity for up to 4 h after UCO in last gestation fetal sheep (Yan *et al.*, 2009). The current study found similar results, and there was tendency for isoelectric activity continuing for several days. Previous studies suggest that fetal electrocortical activity changes following metabolic acidosis (Bocking, 1992; Richardson *et al.*, 1992), which in our study occurred in fetuses that experienced the 'severe' reaction to UCO. Studies from near term fetal sheep subjected to repeated episodes of UCO suggest that during ECoG suppression there is increased cerebral blood flow and increase cerebral glucose delivery, suggesting a shift to anaerobic metabolism and a lack of adequate oxygen uptake by the post-hypoxic fetal brain (Kawagoe *et al.*, 1999b; Kaneko *et al.*, 2003).

To some extent our sagittal sinus doppler flow data supports this concept. For the fetuses that had a 'severe' reaction to UCO there was a significant decrease in blood flow velocity for up to 1 h post-UCO, but after this there was a trend to increases in SSbfv; however, there was a great degree of variability between animals. Taken together with the trend to an increase in the incidence of sub-low activity (Figure 6.11 C), cerebral hyper-perfusion, seen as increased SSbfv (see Figure 6.10), could be indicative of changes in both blood flow regulation and electrocortical activity that persist for days after a single hypoxic (albeit, severe) event for the fetus, *in utero*.

Increased regional cerebral blood flow and cerebral metabolism occur during LV ECoG and REM (ocular muscle activity; EOG), during which FBM also readily occur (Dawes *et al.*, 1972; Boddy *et al.*, 1974; Clewlow *et al.*, 1983; Richardson *et al.*, 1985; Abrams *et al.*, 1990; Abrams *et al.*, 1991; Baier *et al.*, 1992). Breathing activity is also closely associated with increased fetal oxygen demand (Rurak & Gruber, 1983). Studies from fetal sheep have shown that with advancing gestation FBM become episodic, vigorous and longer in duration. In response to single or repeated asphyxia, hypoxia, or reduced uterine blood flow in fetal sheep, a decreased incidence of FBM and increase in the incidence of gasping activity has been observed (Clewlow *et al.*, 1983; Bocking & Harding, 1986; Bissonnette *et al.*, 1989; Bocking, 1992; Kawagoe *et al.*, 1999a). The incidence of fetal gasping (single, deep breathes) that occurred during and shortly after UCO (Figure 6.8 E) was not measured for the duration of the study, and perhaps should be investigated further, as this breathing activity may be indicative of brainstem hypoxia.

Importantly the observations of changes in FBM suggest that control centres in the brainstem may be significantly affected by UCO, since it was mainly amplitude and not the incidence of FBM that was affected by UCO. To delineate the mechanisms, it may be necessary to determine if UCO alters descending inhibition at the level of the pons, resulting in an increase in the amplitude of breathing activity in the fetuses that had a more severe reaction to UCO (Walker, 1995; Breen *et al.*, 1997; Nitsos & Walker, 1999).

During UCO, a cessation of eye movement and reduction of nuchal-EMG activity occurred (Figure 6.8), consistent with the observations of previous studies of responses to hypercapnia and reduction of uterine blood flow (Boddy *et al.*, 1974; Bocking & Harding, 1986). Although we did not see a significant difference in the **incidence** of nuchal or ocular activity (Figure 6.12) following UCO, it was important to investigate the occurrence of this activity in association with particular ECoG activity such as HV and LV. Importantly the incidence of EMG-nuchal activity during LV ECoG, and EOG activity during HV ECoG, was done to assess whether UCO significantly affected the occurrence of 'typical' fetal behaviour which could reveal injury to the neural pathways that modulate fetal behaviour. Motor control is suggested to be dependent on the functional maturation of the mid-brain (Clewlow *et al.*, 1983; Dawes *et al.*, 1983).

On analysis we did find a higher than expected (approximately 30 %) occurrence of LV + EMG activity in the control group (Figure 6.14 A) however this was consistent across all groups. It was found that following UCO profound and persistent changes occurred in the occurrence of disorganised behavioural states. The observation of a significant increase in the incidence of EOG activity occurring during HV-ECoG suggests a persistent dissociation of activity, as EOG activity generally occurs only during LV ECoG. This finding suggests disturbances of fetal behaviour occurring in response to a 10 minute severe UCO could be due to possible injury to the neural pathways above and including the mid-brain (Clewlow *et al.*, 1983), possibly responsible for the co-ordination of fetal behaviour.

In fetal sheep, both PGE_2 and cortisol secretion increase at the end of gestation (Bassett & Thorburn, 1969; Challis *et al.*, 1976; Magyar *et al.*, 1980; Challis & Brooks, 1989). In our study there was no difference between groups in the cortisol increase that occurs prior to labour, despite the observation that in pregnancies where fetuses had undergone UCO (either mild or severe response) labour was found to occur earlier than in the control fetuses. The change of fetal behaviour pattern in the hours preceding and during labour is an important adaptation for

the fetus. It has been shown that 7 to 4 h prior to labour a greater incidence and duration of time are spent in a HV ECoG state (Shinozuka & Nathanielsz, 1998). During labour, there is also a decrease in the incidence of FBM (Boddy *et al.*, 1974). Increased maternal progesterone secretion at the end of pregnancy in sheep also results in a suppression of arousal fetal EOG activity (Nicol *et al.*, 1997). From the animals that went in to labour significantly earlier (fetuses subject to UCO; mild or severe) it was difficult to accurately assess whether there were changes in fetal behaviour responses to labour. It was also difficult to determine whether a change in fetal behaviour occurred during the perinatal period, particularly ECoG activity. This may serve as a predictor highlighting infants that are at greater risk of developing neonatal seizures.

The strong association between hypoxia and increased incidence of neonatal seizures has been observed to occur both clinically (de Vries *et al.*, 1997; Miller *et al.*, 2002) and experimentally (Gonzalez *et al.*, 2005; Harris *et al.*, 2009; Yan *et al.*, 2009; Bjorkman *et al.*, 2010). Clinically the increased incidence of neonatal seizures has been associated with worse neurodevelopmental outcome (Glass *et al.*, 2009). During seizure activity in near term fetal sheep a mismatch between cerebral blood flow and cerebral metabolism occurs, generally leading to cerebral deoxygenation (Gonzalez *et al.*, 2005). In our current study the incidence of 'spiking' or seizure activity during or after UCO was not measured. Postnatally, no observable 'seizure-like' behaviour occurred in lambs whom had experienced *in utero* UCO.

Postnatal behaviour following *in utero* UCO in late gestation resulted in a variable but significant delay, or even failure, to adequately use four legs, find the udder and successfully feed from the ewe within the first four hours of life. Lambs that experienced UCO were also born significantly earlier than compared to full term controls. Although we did not measure the duration of labour, no apparent correlation was present between treatment and parturition. The introduction of a group of ewes induced to deliver fetuses earlier (138 – 139 days GA) also allowed us to delineate which behavioural delays were possibly attributed to *in utero* hypoxia or could be a result of being born preterm. Our findings suggest that just being born 7 – 10 days

prior to term can result in delays of feeding and less activity in the first day of life. More importantly, lambs found to have experienced a more severe fall in pH (< 6.9) during the UCO, were those who failed to attain behavioural milestones, particularly feeding.

Clinically the use of the APGAR (**A**ppearance, **P**ulse, **G**rimace, **A**ctivity, **R**espiration) Scale allows for a quick and reproducible assessment of the newborn which gives a score suggestive of the risk of the development of neurological damage. In this study we also chose to closely measure behaviours such as time taken to stand and to feed, which in sheep, are considered to be imperative for survival immediately following birth (Dwyer & Lawrence, 2000). Newborn lambs lift and shake their heads almost immediately after clearing the birth canal allowing for the clearance of amniotic fluid and lung liquid from the nose and mouth to allow for breathing to occur. Once able to stand, the lamb can begin to walk to find the ewe, and suckle. No lamb showed difficulty in the early stages of auto-resuscitating, and were able to begin spontaneous breathing without any experimenter intervention. However, in the later stages following birth it appeared as though fetuses that experienced *in utero* hypoxia were delayed in being able to use their four legs. Two of the 5 UCO lambs also failed to feed from the ewe. The development of sucking activity within the first few hours of life provides positive reinforcement for the lamb and strengthens its' bond with its mother (Nowak *et al.*, 1996). The more colostrum ingested also strengthens the maternal bond with her lamb (Val-Laillet *et al.*, 2004).

Occlusion of the umbilical cord in monkeys has also resulted in delays in feeding, seizure activity and contributed to the development of hypoxic-ischemic brain injury (Juul *et al.*, 2007). In sheep, Camm *et al.,* (2000) set up a battery of tests to assess learning ability and behaviour for up to 6 weeks postnatal age. This study by Camm and colleagues highlights that sheep can be used for long term behavioural outcome assessments, and could be used to further evaluate the effect of *in utero* UCO on lamb recovery and behaviour.

Interestingly there was a greater degree of variability in time to attain 'milestones' in both the pre-term control group and the UCO lambs compared to controls. This could be further

attributed to the variability of gestational ages that lambs were born. Due to unforeseeable circumstances at the time of experimentation (limited experimental space), UCO occurred at 132 – 134 days GA in the postnatal behaviour study compared to 130 – 132 days GA in the fetal behaviour study, however fetuses subjected to UCO were still born or ewe's went into labour significantly earlier compared to their respective control groups (which underwent the same conditions). Sex of the fetus could also explain some of the variability, however assessment of sex differences was beyond the scope of the study, and a larger cohort of animals would be required to investigate this further. It is important to highlight from both the studies (fetal and postnatal behaviour) described in this chapter that the responses to UCO result in variability of both physiological and behavioural parameters. Other researchers have also highlighted that in response to a severe insult (such as asphyxia or hypoxia) variability in the cardiovascular response be related to the behavioural differences seen long term (Gunn *et al.*, 1992; Mallard *et al.*, 1992; Harris *et al.*, 2009).

This study highlights that a single severe bout of hypoxia *in utero* can result in variable but persistent behavioural delays, both *in utero* and postnatally. In both studies, UCO also resulted in fetuses being more likely to be born earlier. Further studies detailing alterations of fetal breathing and body movements and postnatal outcome could help elucidate the behavioural consequences following an *in utero*, antepartum hypoxic event.

Chapter 7

GENERAL DISCUSSION

TABLE OF CONTENTS

The starting point for this thesis was that, while it is agreed that antepartum events affecting oxygenation of the fetus, such as cord complications and placental abruption significantly contribute to perinatal brain injury, there is little detail in the understanding of how this damage occurs at the cellular level. The studies detailed in this thesis aimed to investigate the role of cerebrovasculature responses in the fetal sheep brain to the injury that follows a global, severely hypoxic event late in gestation. It was also an aim of this thesis to provide information on the effects of such an event on brain function in the fetus leading up to parturition, and then on the behaviour of the newborn lamb.

7.1 MAJOR OUTCOMES

The studies detailed in Chapters 3 and 4 show that 48 h after a single but severe *in utero* hypoxic event (UCO) late in gestation there are significant regional responses that occur to the cerebral vasculature. Significant up-regulation of VEGF immunoreactivity occurred in blood vessels in both white and gray matter, suggesting that endothelial cells may be **more responsive** to low oxygen levels, and could provide an important mechanism by which endothelial cell permeability and proliferation is regulated in an autocrine manner. VEGF is commonly also referred to a vascular permeability factor, and the striking finding was that it was blood vessels in periventricular and subcortical white matter that showed a greater incidence of albumin extravasation. Interestingly, the assessment of vascular density and vessel morphology found that it was periventricular and subcortical white matter that showed a significant increase in vascular perimeter compared to controls. These are the first studies to show a significantly different response of the vasculature occurring in white matter of the fetal brain following an *in utero* **global** hypoxic insult late in gestation.

Following this, it was important to investigate if these changes evolved further or persisted in the days following UCO and prior to birth. The findings described in Chapter 5 show that increased vascular expression of VEGFR-2, but not VEGF, occurs which is consistent with

adult brain focal ischemia studies. Again, it is perhaps important that this increase of *vascular* VEGFR-2 expression occurred mainly in subcortical white matter, whereas *total* VEGFR-2 expression (i.e., all positive cellular VEGFR-2 staining, including neuronal and astrocytic expression) was significantly increased in the subventricular zone and periventricular white matter. This response could be neuroprotective, as studies investigating VEGF therapy suggest that the beneficial actions of VEGF are mediated by VEGFR-2. However, further investigation of the implications of VEGFR-2 up-regulation 5 – 10 following hypoxia is required. These findings strongly suggest that vascular cells (e.g., endothelial cells, pericytes) respond differently to hypoxia depending on brain region, and differently to neurons and astrocytes. Interestingly a large (although not quite significant increase in vascular expression of Epo) was observed only in the cortex, possibly contributing to regional **protection** of gray matter. Epo is a cytokine found to be promising as a treatment for brain injury in neonatal hypoxia. Furthermore, angpt-1, a key angiogenic protein important for vascular maturation and stabilization, was *decreased* in periventricular white matter only, a region known to be susceptible to haemorrhage and injury, following a mild or severe response to UCO.

The regional up-regulation of VEGFR-2 could highlight a protective response in the fetal brain, for both neurons and the vasculature. However down-regulation of angpt-1 only in periventricular white matter strongly suggests that this region is still vulnerable to hypoxic injury. The findings from the studies in Chapter 4 and 5 provide evidence that following *in utero* global hypoxia the white matter of the **late gestation** fetal brain may still be vulnerable to injury.

In addition, it was an interesting finding that during UCO fetuses responded in two distinct manners. This resulted in fetuses that were subjected to UCO being further sub-classified into a 'mild' or 'severe' response, immediately after UCO. This was based on responses of blood gas parameters (pO$_2$, pCO$_2$, pH, oxygen saturation and lactate) recorded at the end of the 10 min hypoxic challenge. Interestingly, regardless of the response to UCO (mild or severe), decreased

angpt-1 expression occurred in fetal brains, possibly suggesting that periventricular white matter could be vulnerable to hypoxia of any severity. However, changes in VEGFR-2 expression (vascular and total cell number) and fetal behaviour were only seen to occur following a severe UCO. The implications of this need to be further investigated.

Two sets of experiments were conducted to investigate the fetal and postnatal behavioural consequences that follow this model of acute *in utero* hypoxia in late gestation. Both in our newborn (lambs) and fetal behaviour experiments, animals subjected to UCO were born earlier, or labour was initiated earlier in ewes following UCO, regardless of the severity of UCO (mild or severe). Importantly UCO resulted in a variable but persistent change in fetal behaviour and delays postnatal behavioural parameters. The effect of severe UCO on fetal behaviour resulted in a significant increase in the amplitude of fetal breathing movements (FBM) from 18 to 26 h following severe UCO suggesting control centres in the brainstem may be vulnerable and injured following a hypoxic stress. The increase in the incidence of dissociated behaviour, electro-ocular (EOG) activity during high voltage electrocortical (HV ECoG) state, also suggests injury to the neural pathways mentioned above and including the brainstem. Following this, lambs that experienced *in utero* global hypoxia were delayed in being able to attain a stable standing position and some (2 out of 5 post-UCO lambs) failed to achieve important milestones such as feeding. The findings from these studies highlight, for the first time, that severe hypoxia late in gestation has persistent detrimental effects and significantly affect behaviour late in gestation and following birth in sheep.

7.2 GENERAL CONSIDERATIONS

7.2.1 Limitations

The experiments in this thesis primarily used immunohistochemistry to investigate cerebrovascular responses to UCO. Further investigation using *in vitro* techniques would aid in the investigation of the effects of VEGF in the developing fetal brain. Cell culture techniques primarily investigating the consequences of cellular (neuronal, astrocytic endothelial cells and pericytes) expression of VEGF could reveal the beneficial role that VEGF may play in the developing brain, and following hypoxia.

Difficulties also arose in finding an accurate endothelial cell marker in sheep in order to accurately identify endothelial cells. As this was not successful, we identified endothelial cells based on morphology. Once an appropriate marker is optimised for use in fetal sheep brain tissue, this would allow us to use fluorescent double labelling to accurately investigate endothelial expression of key proteins. Currently 'blood vessel associate expression' may include the expression in pericytes, which are always in close proximity to endothelial cells.

The use of fetal sheep does result in low numbers in experimental groups. In some instances a 'trend' or nearly significant result may have been significant if larger groups were used. In an attempt to maintain statistical power (to achieve power of 0.8) increasing the numbers in all groups (power analysis suggesting n > 10) would be sufficient for most of the experiments conducted for this thesis. However, mainly because of time and cost constraints, the group sizes are small.

From the studies conducted in Chapter 5 and 6, a key finding was the UCO resulted in ewes going into labour significantly earlier (~140 days GA) than the Control (Sham UCO; 144 days) group. The range of gestational days that the ewes came into labour was 136 – 144 days, however where significance existed, it strongly suggests that hypoxia, not gestational age,

resulted in the changes that were seen. Although the postnatal behaviour study did include a 'pre-term' control group to correct for this, the study of fetal behaviour did not, and this meant that the number of animals remaining as fetuses decreased as gestational age past 136 days. This also meant that statistical analysis was not possible after this.

7.2.2 Future directions

From the studies completed in Chapter 3, 4 and 5 further analysis is required to understand the consequence of the changes that have occurred. The regional differences seen in response to UCO (white matter versus gray matter) could be examined by further investigating the effect that VEGF has in the fetal brain following hypoxia in the late gestation. As previously stated, VEGF has been widely described as having both neuroprotective and detrimental actions. From our findings it appears that up-regulation of VEGF that occurs early (up to 48 h) results in increased blood brain barrier (BBB) permeability in white matter, and the up-regulation of VEGFR-2 that occurs 5 - 10 days after this is of unknown consequence. Neuroprotective responses of VEGF include stimulating neurogenesis and enhancing endothelial cell survival (decreased apoptotic cell death), importantly these actions involve the activation of VEGFR-2 (Hermann & Zechariah, 2009; Sentilhes *et al.*, 2010). Further investigation of the VEGF/VEGFR-2 system in the fetal brain is required to understand the functional role these genes play following a global hypoxic insult. These include their influence on cellular proliferation, cell death and possible repair mechanisms (such as vascular remodelling). From the findings in this thesis and following on from studies done in postnatal rats by Shimotake *et al.,* (2010), future experiments either inhibiting or up-regulating VEGF and/or VEGFR-2 would reveal if this hypoxia-sensitive angiogenic protein has predominantly protective or detrimental actions in the cerebral vasculature of the developing fetal brain. Preliminary quantitative real time PCR (qRT-PCR) was conducted to investigate HIF-1α, HIF-2α, VEGF and VEGFR-2 mRNA in fetal brains at 24 h following UCO (or Sham UCO) and in severe UCO (and Controls). This data is described and presented in Appendix 5 and 6. This data was not included

in the studies of this thesis due to variability of control tissues' gene expression; however the preliminary findings suggest that following the re-optimisation of the primers that were used, further investigation could reveal important mechanisms that are responsible for influencing VEGF and VEGFR-2 expression.

Further detailed investigation of cerebral blood flow at times beyond 72 h after UCO in late gestation fetal sheep is required. Experiments could be designed to use a quantifiable method of cerebral blood flow such as flow probes or microspheres. Based on the new knowledge obtained in Chapters 4 & 5 regarding the alterations in VEGF expression, further experiments could now use microspheres to obtain regional cerebral blood flow at (say) 2, 3 or 7 days after the UCO. However, this was not possible within the time-frame of the studies incorporated in this thesis.

Assessment of the neuropathology of fetal and 24 h old lamb brains is also required to further establish the relationship between the state of the brain in terms of injury and the behavioural changes that occur following UCO. The regional changes in expression of VEGF, VEGFR-2 and angpt-1 may also explain any damage or injury seen in brain regions.

The unexpected finding that white matter has a persistent response in the days following UCO must be further investigated. Importantly further assessment of the vasculature would help to explain the consequence of the changes in VEGF, VEGFR-2, Epo and angpt-1 that occurred, and may reveal possible regional vulnerability or protection in the late gestation fetal brain. The extent of increased vascular perimeter and an increase in the incidence of BBB permeability changes could be explored by investigating the interaction of matrix metalloproteinase's (MMP), which has been demonstrated to respond following a hypoxic insult, possibly explaining the alterations in the vasculature that have occurred. Structural analysis of the vasculature, including expression of tight junctions (that exists between endothelial cells) and pericytes (important for vascular maturity) could explain the consequence of the significant decrease of angpt-1 that occurred 5 – 10 days following UCO in periventricular white matter.

7.2.2.1 Matrix-Mellatoproteinase-9

Matrix metalloproteinase's (MMP) are zinc dependant proteases that play an important role in inflammation, platelet accumulation, oligodendrocytes process outgrowth, extracellular matrix and basement membrane degradation and the subsequent increase in BBB permeability following focal cerebral ischemia (Romanic *et al.*, 1998; Rosenberg *et al.*, 1998; Uhm *et al.*, 1998; Cheung *et al.*, 2006). They are activated by proteolysis and increase expression following oxidative stress, as seen after hypoxia, to break down and degrade tissue (Lukes *et al.*, 1999). MMP-2 and MMP-9 are the most researched isoforms with respect to brain injury following hypoxia-ischemia. VEGF induced changes in BBB permeability, involve MMP-9 induction and contribute to vascular destabilisation, loss of tight junctions and increased BBB permeability (Valable *et al.*, 2005; Bauer *et al.*, 2010). Degradation of the basal lamina constituent's laminin and collagen IV is mediated by increased MMP-2 and MMP-9 expression in endothelial cells, and subsequent treatment with hypothermia resulted in a decrease of MMP activation and a reduction in infarct size (Romanic *et al.*, 1998; Zalewska *et al.*, 2002; Hamann *et al.*, 2004). Limited research exists about the role of MMP-9 in the immature brain; however MMP-9 gene knockout in immature mice resulted in decreased inflammation and BBB leakage (Svedin *et al.*, 2007) implicating MMPs in vascular responses to hypoxia and possibly contributing to brain injury.

7.2.2.2 Tight junctional proteins

In the human brain the expression of tight junctional proteins claudin-5 and occludin as early as 12 weeks gestation; suggest that these are important in providing a structural barrier to prevent the entry of harmful substances into the brain parenchyma (Virgintino *et al.*, 2004; Ballabh *et al.*, 2005). The underlying changes that resulted in increased BBB permeability seen at 48 h following UCO (Chapter 4) remains to be further investigated. Although vascular permeability was not assessed in brains collected prior to birth (Chapter 5; as there was no change VEGF associated blood vessel expression) the response of key tight junctional proteins (claudin,

occludin and zona-occludin) could be significantly altered in the days following UCO. The consequences of the changes seen at 24 and 48 h following UCO and whether these result in a significant and persistent change of tight junction protein expression prior to birth and into the newborn period could reveal regions that are more susceptible to hypoxia induced permeability changes.

7.2.2.3 Pericytes

Limited research also exists into investigating the role and response of pericytes following hypoxia-ischemia in the **neonatal** brain. Pericytes have a key role in vessel maturity as well as BBB development, and more recently have been implicated in modulating cerebral blood flow (Hamilton *et al.*, 2010). From human studies the finding that the germinal matrix has fewer pericytes present during gestation in comparison to white matter and the cortex (Povlishock *et al.*, 1977; Braun *et al.*, 2007) highlighting that the role of these contractile cells needs to be further investigated in the fetal brain. Pericytes are some of the first cells to respond to hypoxia, within the hours following hypoxia in the adult, some pericytes also migrate away from vessels (Gonul *et al.*, 2002) resulting in decreased vascular support. *In vitro* and *in vivo* studies have shown that pericytes can express VEGF and exacerbate BBB disruption following acute hypoxia (Yamagishi *et al.*, 1999; Al Ahmad *et al.*, 2009; Al Ahmad *et al.*, 2010). Pericytes can also express angpt-1, whether pericyte migration occurred in the fetal brain following global hypoxia, particularly in periventricular white matter where angpt-1 was also significantly decreased (Chapter 5) could reveal the basis of vascular fragility (leading to an increased propensity to rupture).

7.3 CLINICAL IMPLICATIONS

The expression of VEGF by numerous cell types (neurons, astrocytes, pericytes and endothelial cells) and high expression during brain development strongly indicates that VEGF is important for functions including neurogenesis and angiogenesis (Virgintino *et al.*, 2003; Rosenstein & Krum, 2004; Sentilhes *et al.*, 2010). The key findings of this thesis suggest that late in gestation alterations in the expression of the VEGF/VEGFR-2 system occur following global hypoxia in the fetal sheep brain. Two clinical studies also suggest that VEGF could be important in determining the occurrence of hypoxic-ischemic encephalopathy. Samples of cord blood from birth asphyxiated infants showed a close correlation between increased circulating VEGF and the development of hypoxic-ischemic encephalopathy (Aly *et al.*, 2009). The findings from Aly *et al.,* (2009) suggest that circulating VEGF could be a predictor of hypoxic-ischemic encephalopathy (HIE) following birth asphyxia. However, assessment of HIE was done at 24 h after birth, and it may correlate with the time of alteration of blood brain barrier permeability, occurring as part of VEGF's 'early' response. Strikingly, in periventricular leukomalacia brains the presence of VEGF indicated neovascularisation at the foci of necrosis (Arai *et al.*, 1998). Arai *et al.,* (1998) suggested that VEGF localized in necrotic foci of PVL brains was indicative of neovascularisation, although the observations on these brains were made over times ranging from hours to a year after birth, and the actual time of the hypoxic event triggering the change in the brain cannot be known with any precision. However, in general these observations support the suggestion that the long-term effects of increased VEGF expression are associated with repair and protection of brain function. Further analysis is required to delineate the consequence of elevated VEGF in the hours and days following severe hypoxia and how this could contribute to the pathogenesis of encephalopathy and the recovery of the brain from these events.

VEGF is highly expressed in reactive astrocytes at the margins of necrotic tissue in brains of infants with periventricular leukomalacia (Arai *et al.*, 1998). Experiments in neonatal rats show that the developing brain responds to hypoxia with increased vascular permeability and VEGF-

mediated angiogenesis (Ment *et al.*, 1997). Furthermore, VEGF has been shown to induce rapid angiogenesis in the germinal matrix of pre-term rabbit pups, which was then associated with greater vascular fragility and propensity to haemorrhage (Ballabh *et al.*, 2007). These studies highlight that the measurement of VEGF from neonatal or cord blood could be used as a clinical indicator of the occurrence of hypoxic stress prior to, during or following birth.

The studies in this thesis investigated the consequence of a global hypoxic insult late in gestation and found considerable response of the vasculature in white matter. Although it is commonly thought that term infants are more vulnerable to gray matter injury, these findings strongly suggest that white matter is still considerably vulnerable to hypoxia in late gestation. Most importantly, the decreased expression of angpt-1 in periventricular white matter up to 10 days following *in utero* hypoxia in the near term fetus could explain the vulnerability of blood vessels in white matter to hypoxic-ischemic injury and subsequent rupture or bleeding, a finding of considerable importance also for the pre-term infant.

Clinically, fetal monitoring is limited to heart rate variability, gross fetal body movements and fetal breathing movements. From Chapter 6, persistent changes in fetal behaviour were seen - most notably in the amplitude of FBM following UCO. As heart rate had returned to pre-UCO values by 1 h after the UCO, further investigation of changes to body movement patterns and FBM following hypoxia could allow for future imaging techniques to be developed with high resolution to detect these changes. These measurements would provide evidence of the occurrence of fetal distress in addition to suggesting that injury may have occurred to deeper brain centres, such as the brainstem. In the adult, impaired BBB permeability, loss of tight junctions and albumin uptake by astrocytes and neurons has been observed in cases of epilepsy (Ivens *et al.*, 2007; Rigau *et al.*, 2007), and the contribution of these changes – all of which were observed in these fetal sheep after UCO – to the seizure activity which often occurs in the preterm infant who develops hypoxic-ischemic encephalopathy, would be a worthwhile avenue of investigation. Following on from the clinical implications of the fetal behaviour study (stated

above), the findings from the postnatal behaviour study highlight that a late gestation global hypoxia can result in fetuses being born days prior to term, with delays in important survival behaviours, such as standing and suckling. This suggests that *in utero* hypoxia can significantly contribute to the presentation of permanent behavioural delays in the hours following birth. Future long term studies would help determine the consequence of these behavioural delays, whether they recover, persist or become worse.

Currently the search for an ideal neuroprotective therapy to help prevent severe brain injury or aid in repair following a complicated pregnancy continues. Hamrick & Ferriero (2003) suggest that mediators of inflammation and anti-oxidants could protect the term brain from hypoxic injury. However from the findings of this thesis, targeting the response of hypoxia sensitive genes, such as VEGF and Epo, which appear to be responsive in the days following a global hypoxic insult, could improve outcome of the neonate following hypoxia-ischemia. Following neonatal stroke, treatment with recombinant Epo improved both brain injury and functional outcome (Chang *et al.*, 2005). Inhibition of VEGFR-2 resulted in increased cell death and brain injury and decreased endothelial cell proliferation (Shimotake *et al.*, 2010), highlighting that VEGFR-2 has potent neuroprotective actions. Translation into larger animal models such as fetal sheep or primates would also help investigate the possible neuroprotective role of these (Epo, VEGF, VEGFR-2 and angpt-1) important genes. The work outlined in this thesis provides invaluable information regarding the regional distribution of the cerebrovascular and behavioural responses that follow intra-uterine hypoxia in the fetus and the newborn.

7.4 Summary

The findings from this thesis highlight that an antepartum hypoxic event in late gestation can have both persistent and profound effects on both cerebral blood vessels and brain function of fetal and newborn sheep. Importantly, for the first time, it has been shown that a **global** hypoxic insult resulted in regional vascular responses predominantly seen in white matter of the term fetal sheep brain. Similar to studies conducted in the adult, the response of the fetal cerebrovasculature could influence other cells of brain, including neurons and astrocytes, following hypoxia-ischemia. When fetal cardiovascular and blood gas status return to basal in the hours following severe hypoxia, there is a persistent disorganisation of fetal behaviour and prolonged delays in the ability to stand and a failure to achieve key milestones immediately following birth. Together, the novel findings from these studies strongly suggest that the term infant is still vulnerable to injury and possible permanent deficit.

REFERENCES

Abraham CS, Deli MA, Temesvari P, Kovacs J, Szerdahelyi P, Joo F & Torpier G. (1999). Regional differences in asphyxia- and reperfusion-induced cytotoxic and vasogenic brain edema formation in newborn pigs. *Neuroscience Research Communications* **25,** 173-182.

Abrams RM, Gerhardt KJ & Burchfield DJ. (1991). Behavioral state transition and local cerebral blood flow in fetal sheep. *J Dev Physiol* **15,** 283-288.

Abrams RM, Post JC, Burchfield DJ, Gomez KJ, Hutchison AA & Conlon M. (1990). Local cerebral blood flow is increased in rapid-eye-movement sleep in fetal sheep. *Am J Obstet Gynecol* **162,** 278-281.

Aiello LP. (2005). Angiogenic pathways in diabetic retinopathy. *N Engl J Med* **353,** 839-841.

Al Ahmad A, Gassmann M & Ogunshola OO. (2009). Maintaining blood-brain barrier integrity: pericytes perform better than astrocytes during prolonged oxygen deprivation. *J Cell Physiol* **218,** 612-622.

Al Ahmad A, Taboada CB, Gassmann M & Ogunshola OO. (2010). Astrocytes and pericytes differentially modulate blood-brain barrier characteristics during development and hypoxic insult. *J Cereb Blood Flow Metab*.

Alcorn B & Shean R. (1995). The origins of cerebral palsy: a consensus statement. *Med J Aust* **162,** 384.

Alon T, Hemo I, Itin A, Pe'er J, Stone J & Keshet E. (1995). Vascular endothelial growth factor acts as a survival factor for newly formed retinal vessels and has implications for retinopathy of prematurity. *Nat Med* **1,** 1024-1028.

Altman DI, Powers WJ, Perlman JM, Herscovitch P, Volpe SL & Volpe JJ. (1988). Cerebral blood flow requirement for brain viability in newborn infants is lower than in adults. *Ann Neurol* **24,** 218-226.

Alvarez-Diaz A, Hilario E, de Cerio FG, Valls-i-Soler A & Alvarez-Diaz FJ. (2007). Hypoxic-ischemic injury in the immature brain--key vascular and cellular players. *Neonatology* **92,** 227-235.

Aly H, Hassanein S, Nada A, Mohamed MH, Atef SH & Atiea W. (2009). Vascular endothelial growth factor in neonates with perinatal asphyxia. *Brain Dev* **31,** 600-604.

Anagnostou A, Lee ES, Kessimian N, Levinson R & Steiner M. (1990). Erythropoietin has a mitogenic and positive chemotactic effect on endothelial cells. *Proc Natl Acad Sci U S A* **87,** 5978-5982.

Andre M, Lamblin MD, d'Allest AM, Curzi-Dascalova L, Moussalli-Salefranque F, T SNT, Vecchierini-Blineau MF, Wallois F, Walls-Esquivel E & Plouin P. (2010). Electroencephalography in premature and full-term infants. Developmental features and glossary. *Neurophysiol Clin* **40,** 59-124.

Arai Y, Deguchi K & Takashima S. (1998). Vascular endothelial growth factor in brains with periventricular leukomalacia. *Pediatr Neurol* **19,** 45-49.

Arany Z, Foo SY, Ma Y, Ruas JL, Bommi-Reddy A, Girnun G, Cooper M, Laznik D, Chinsomboon J, Rangwala SM, Baek KH, Rosenzweig A & Spiegelman BM. (2008). HIF-independent regulation of VEGF and angiogenesis by the transcriptional coactivator PGC-1alpha. *Nature* **451,** 1008-1012.

Ashwal S, Dale PS & Longo LD. (1984). Regional cerebral blood flow: studies in the fetal lamb during hypoxia, hypercapnia, acidosis, and hypotension. *Pediatr Res* **18,** 1309-1316.

Ashwal S, Majcher JS, Vain N & Longo LD. (1980). Patterns of fetal lamb regional cerebral blood flow during and after prolonged hypoxia. *Pediatr Res* **14,** 1104-1110.

Aurrand-Lions M, Johnson-Leger C, Wong C, Du Pasquier L & Imhof BA. (2001). Heterogeneity of endothelial junctions is reflected by differential expression and specific subcellular localization of the three JAM family members. *Blood* **98,** 3699-3707.

Back SA, Riddle A & Hohimer AR. (2006). Role of instrumented fetal sheep preparations in defining the pathogenesis of human periventricular white-matter injury. *J Child Neurol* **21,** 582-589.

Back SA, Riddle A & McClure MM. (2007). Maturation-dependent vulnerability of perinatal white matter in premature birth. *Stroke* **38,** 724-730.

Badawi N, Kurinczuk JJ, Keogh JM, Alessandri LM, O'Sullivan F, Burton PR, Pemberton PJ & Stanley FJ. (1998). Antepartum risk factors for newborn encephalopathy: the Western Australian case-control study. *BMJ* **317,** 1549-1553.

Baier RJ, Fajardo C, Alvarez J, Cates DB, Nowaczyk B & Rigatto H. (1992). The effects of gestational age and labour on the breathing and behaviour response to oxygen and umbilical cord occlusion in the fetal sheep. *J Dev Physiol* **18,** 93-98.

Balabanov R & Dore-Duffy P. (1998). Role of the CNS microvascular pericyte in the blood-brain barrier. *J Neurosci Res* **53,** 637-644.

Balabanov R, Washington R, Wagnerova J & Dore-Duffy P. (1996). CNS microvascular pericytes express macrophage-like function, cell surface integrin alpha M, and macrophage marker ED-2. *Microvasc Res* **52,** 127-142.

Ball RH, Parer JT, Caldwell LE & Johnson J. (1994). Regional blood flow and metabolism in ovine fetuses during severe cord occlusion. *Am J Obstet Gynecol* **171,** 1549-1555.

Ballabh P. (2010). Intraventricular hemorrhage in premature infants: mechanism of disease. *Pediatr Res* **67,** 1-8.

Ballabh P, Braun A & Nedergaard M. (2004a). Anatomic analysis of blood vessels in germinal matrix, cerebral cortex, and white matter in developing infants. *Pediatr Res* **56,** 117-124.

Ballabh P, Braun A & Nedergaard M. (2004b). The blood-brain barrier: an overview: structure, regulation, and clinical implications. *Neurobiol Dis* **16,** 1-13.

Ballabh P, Hu F, Kumarasiri M, Braun A & Nedergaard M. (2005). Development of tight junction molecules in blood vessels of germinal matrix, cerebral cortex, and white matter. *Pediatr Res* **58,** 791-798.

Ballabh P, Xu H, Hu F, Braun A, Smith K, Rivera A, Lou N, Ungvari Z, Goldman SA, Csiszar A & Nedergaard M. (2007). Angiogenic inhibition reduces germinal matrix hemorrhage. *Nat Med* **13,** 477-485.

Banerjee SK, Sarkar DK, Weston AP, De A & Campbell DR. (1997). Over expression of vascular endothelial growth factor and its receptor during the development of estrogen-induced rat pituitary tumors may mediate estrogen-initiated tumor angiogenesis. *Carcinogenesis* **18,** 1155-1161.

Baranova O, Miranda LF, Pichiule P, Dragatsis I, Johnson RS & Chavez JC. (2007). Neuron-specific inactivation of the hypoxia inducible factor 1 alpha increases brain injury in a mouse model of transient focal cerebral ischemia. *J Neurosci* **27,** 6320-6332.

Bassett JM & Thorburn GD. (1969). Foetal plasma corticosteroids and the initiation of parturition in sheep. *J Endocrinol* **44,** 285-286.

Bates DO & Curry FE. (1997). Vascular endothelial growth factor increases microvascular permeability via a Ca(2+)-dependent pathway. *Am J Physiol* **273,** H687-694.

Bates DO & Jones RO. (2003). The role of vascular endothelial growth factor in wound healing. *Int J Low Extrem Wounds* **2,** 107-120.

Bauer AT, Burgers HF, Rabie T & Marti HH. (2010). Matrix metalloproteinase-9 mediates hypoxia-induced vascular leakage in the brain via tight junction rearrangement. *J Cereb Blood Flow Metab* **30,** 837-848.

Beal MF. (1992). Mechanisms of excitotoxicity in neurologic diseases. *FASEB J* **6,** 3338-3344.

Beck H, Acker T, Wiessner C, Allegrini PR & Plate KH. (2000). Expression of angiopoietin-1, angiopoietin-2, and tie receptors after middle cerebral artery occlusion in the rat. *Am J Pathol* **157,** 1473-1483.

Bennet L, Peebles DM, Edwards AD, Rios A & Hanson MA. (1998). The cerebral hemodynamic response to asphyxia and hypoxia in the near-term fetal sheep as measured by near infrared spectroscopy. *Pediatr Res* **44,** 951-957.

Bennet L, Rossenrode S, Gunning MI, Gluckman PD & Gunn AJ. (1999). The cardiovascular and cerebrovascular responses of the immature fetal sheep to acute umbilical cord occlusion. *J Physiol* **517 (Pt 1),** 247-257.

Bergers G & Song S. (2005). The role of pericytes in blood-vessel formation and maintenance. *Neuro Oncol* **7,** 452-464.

Bernaudin M, Marti HH, Roussel S, Divoux D, Nouvelot A, MacKenzie ET & Petit E. (1999). A potential role for erythropoietin in focal permanent cerebral ischemia in mice. *J Cereb Blood Flow Metab* **19,** 643-651.

Bernstein JJ & Karp SM. (1995). Migrating fetal astrocytes do not intravasate since they are excluded from blood vessels by vital basement membrane. *Int J Dev Neurosci* **14,** 177-180.

Bissonnette JM, Hohimer AR & Willeke GB. (1989). Effect of asphyxia on respiratory activity in fetal sheep. *J Dev Physiol* **12,** 157-161.

Bjorkman ST, Miller SM, Rose SE, Burke C & Colditz PB. (2010). Seizures are associated with brain injury severity in a neonatal model of hypoxia-ischemia. *Neuroscience* **166,** 157-167.

Blair E. (1993). A research definition for 'birth asphyxia'? *Dev Med Child Neurol* **35,** 449-452.

Blood AB, Hunter CJ & Power GG. (2002). The role of adenosine in regulation of cerebral blood flow during hypoxia in the near-term fetal sheep. *J Physiol (Lond)* **543,** 1015-1023.

Blood AB, Hunter CJ & Power GG. (2003). Adenosine mediates decreased cerebral metabolic rate and increased cerebral blood flow during acute moderate hypoxia in the near-term fetal sheep. *J Physiol* **553,** 935-945.

Bocking AD. (1992). Fetal behavioral states: pathological alteration with hypoxia. *Semin Perinatol* **16,** 252-257.

Bocking AD. (2003). Assessment of fetal heart rate and fetal movements in detecting oxygen deprivation in-utero. *Eur J Obstet Gynecol Reprod Biol* **110 Suppl 1,** S108-112.

Bocking AD, Gagnon R, White SE, Homan J, Milne KM & Richardson BS. (1988). Circulatory responses to prolonged hypoxemia in fetal sheep. *Am J Obstet Gynecol* **159,** 1418-1424.

Bocking AD & Harding R. (1986). Effects of reduced uterine blood flow on electrocortical activity, breathing, and skeletal muscle activity in fetal sheep. *Am J Obstet Gynecol* **154,** 655-662.

Bocking AD, McMillen IC, Harding R & Thorburn GD. (1986). Effect of reduced uterine blood flow on fetal and maternal cortisol. *J Dev Physiol* **8,** 237-245.

Boddy K, Dawes GS, Fisher R, Pinter S & Robinson JS. (1974). Foetal respiratory movements, electrocortical and cardiovascular responses to hypoxaemia and hypercapnia in sheep. *J Physiol* **243,** 599-618.

Boer K, Troost D, Spliet WG, van Rijen PC, Gorter JA & Aronica E. (2008). Cellular distribution of vascular endothelial growth factor A (VEGFA) and B (VEGFB) and VEGF receptors 1 and 2 in focal cortical dysplasia type IIB. *Acta Neuropathol* **115,** 683-696.

Bogdanovic E, Nguyen VP & Dumont DJ. (2006). Activation of Tie2 by angiopoietin-1 and angiopoietin-2 results in their release and receptor internalization. *J Cell Sci* **119,** 3551-3560.

Bolanos JP & Almeida A. (1999). Roles of nitric oxide in brain hypoxia-ischemia. *Biochim Biophys Acta* **1411,** 415-436.

Boulton M, Foreman D, Williams G & McLeod D. (1998). VEGF localisation in diabetic retinopathy. *Br J Ophthalmol* **82,** 561-568.

Bradbury MW. (1984). The structure and function of the blood-brain barrier. *Fed Proc* **43,** 186-190.

Braun A, Xu H, Hu F, Kocherlakota P, Siegel D, Chander P, Ungvari Z, Csiszar A, Nedergaard M & Ballabh P. (2007). Paucity of pericytes in germinal matrix vasculature of premature infants. *J Neurosci* **27,** 12012-12024.

Breen S, Rees S & Walker D. (1997). Identification of brainstem neurons responding to hypoxia in fetal and newborn sheep. *Brain Res* **748,** 107-121.

Breier G. (2000). Functions of the VEGF/VEGF receptor system in the vascular system. *Semin Thromb Hemost* **26,** 553-559.

Breier G, Albrecht U, Sterrer S & Risau W. (1992). Expression of vascular endothelial growth factor during embryonic angiogenesis and endothelial cell differentiation. *Development* **114,** 521-532.

Breier G & Risau W. (1996). The role of vascular endothelial growth factor in blood vessel formation. *Trends Cell Biol* **6,** 454-456.

Brewer CA, Setterdahl JJ, Li MJ, Johnston JM, Mann JL & McAsey ME. (2000). Endoglin expression as a measure of microvessel density in cervical cancer. *Obstet Gynecol* **96,** 224-228.

Brightman M. (1991). Implication of astroglia in the blood-brain barrier. *Ann N Y Acad Sci* **633,** 343-347.

Burk J, Burggraf D, Vosko M, Dichgans M & Hamann GF. (2008). Protection of cerebral microvasculature after moderate hypothermia following experimental focal cerebral ischemia in mice. *Brain Res* **1226,** 248-255.

Camm EJ, Gibbs ME, Cock ML, Rees SM & Hardin R. (2000). Assessment of learning ability and behaviour in low birthweight lambs following intrauterine growth restriction. *Reprod Fertil Dev* **12,** 165-172.

Carmeliet P. (2003). Angiogenesis in health and disease. *Nat Med* **9,** 653-660.

Carmeliet P & Storkebaum E. (2002). Vascular and neuronal effects of VEGF in the nervous system: implications for neurological disorders. *Semin Cell Dev Biol* **13,** 39-53.

Castillo-Melendez M, Chow JA & Walker DW. (2004). Lipid peroxidation, caspase-3 immunoreactivity, and pyknosis in late-gestation fetal sheep brain after umbilical cord occlusion. *Pediatr Res* **55,** 864-871.

Castillo-Melendez M, Yan E & Walker DW. (2005). Expression of erythropoietin and its receptor in the brain of late-gestation fetal sheep, and responses to asphyxia caused by umbilical cord occlusion. *Dev Neurosci* **27,** 220-227.

Cavaglia M, Dombrowski SM, Drazba J, Vasanji A, Bokesch PM & Janigro D. (2001). Regional variation in brain capillary density and vascular response to ischemia. *Brain Res* **910,** 81-93.

Cerebral Palsy Australia. (2010). Cerebral Palsy - The Facts. Viewed January 2011. http://www.cpaustralia.com.au

Challis JR & Brooks AN. (1989). Maturation and activation of hypothalamic-pituitary adrenal function in fetal sheep. *Endocr Rev* **10,** 182-204.

Challis JR, Dilley SR, Robinson JS & Thorburn GD. (1976). Prostaglandins in the circulation of the fetal lamb. *Prostaglandins* **11,** 1041-1052.

Chang YS, Mu D, Wendland M, Sheldon RA, Vexler ZS, McQuillen PS & Ferriero DM. (2005). Erythropoietin improves functional and histological outcome in neonatal stroke. *Pediatr Res* **58,** 106-111.

Charonis AS, Tsilibary EC, Yurchenco PD & Furthmayr H. (1985). Binding of laminin to type IV collagen: a morphological study. *J Cell Biol* **100,** 1848-1853.

Chau A, Rose JC & Koos BJ. (1999). Adenosine modulates corticotropin and cortisol release during hypoxia in fetal sheep. *Am J Obstet Gynecol* **180,** 1272-1277.

Chavez JC, Baranova O, Lin J & Pichiule P. (2006). The transcriptional activator hypoxia inducible factor 2 (HIF-2/EPAS-1) regulates the oxygen-dependent expression of erythropoietin in cortical astrocytes. *J Neurosci* **26,** 9471-9481.

Chen J, Zhang C, Jiang H, Li Y, Zhang L, Robin A, Katakowski M, Lu M & Chopp M. (2005). Atorvastatin induction of VEGF and BDNF promotes brain plasticity after stroke in mice. *J Cereb Blood Flow Metab* **25,** 281-290.

Chen Q & Anderson DR. (1997). Effect of CO2 on intracellular pH and contraction of retinal capillary pericytes. *Invest Ophthalmol Vis Sci* **38,** 643-651.

Chen W, Jadhav V, Tang J & Zhang JH. (2008). HIF-1alpha inhibition ameliorates neonatal brain injury in a rat pup hypoxic-ischemic model. *Neurobiol Dis* **31,** 433-441.

Chen ZL & Strickland S. (1997). Neuronal death in the hippocampus is promoted by plasmin-catalyzed degradation of laminin. *Cell* **91,** 917-925.

Cheung PY, Stevens JP, Haase E, Stang L, Bigam DL, Etches W & Radomski MW. (2006). Platelet dysfunction in asphyxiated newborn piglets resuscitated with 21% and 100% oxygen. *Pediatr Res* **59,** 636-640.

Clancy B & Cauller LJ. (1998). Reduction of background autofluorescence in brain sections following immersion in sodium borohydride. *J Neurosci Methods* **83,** 97-102.

Clewlow F, Dawes GS, Johnston BM & Walker DW. (1983). Changes in breathing, electrocortical and muscle activity in unanaesthetized fetal lambs with age. *J Physiol* **341,** 463-476.

Cobbs CS, Chen J, Greenberg DA & Graham SH. (1998). Vascular endothelial growth factor expression in transient focal cerebral ischemia in the rat. *Neurosci Lett* **249,** 79-82.

Coomber BL & Stewart PA. (1984). Morphometric analysis of CNS microvascular endothelium. *Microvasc Res* **30,** 99-115.

Cowan F, Rutherford M, Groenendaal F, Eken P, Mercuri E, Bydder GM, Meiners LC, Dubowitz LM & de Vries LS. (2003). Origin and timing of brain lesions in term infants with neonatal encephalopathy. *Lancet* **361,** 736-742.

Cowell RM, Blake KR & Russell JW. (2007). Localization of the transcriptional coactivator PGC-1alpha to GABAergic neurons during maturation of the rat brain. *J Comp Neurol* **502,** 1-18.

Crossley KJ, Nicol MB, Hirst JJ, Walker DW & Thorburn GD. (1997). Suppression of arousal by progesterone in fetal sheep. *Reprod Fertil Dev* **9,** 767-773.

Cuevas P, Gutierrez-Diaz JA, Reimers D, Dujovny M, Diaz FG & Ausman JI. (1984). Pericyte endothelial gap junctions in human cerebral capillaries. *Anat Embryol (Berl)* **170,** 155-159.

Dawes G, Fox H, Leduc B, Liggins G & Richards R. (1972). Respiratory movements and rapid eye movement sleep in the fetal lambs. *J Physiol* **220,** 119-143.

Dawes GS, Gardner WN, Johnston BM & Walker DW. (1983). Breathing in fetal lambs: the effect of brain stem section. *J Physiol (Lond)* **335,** 535-553.

De Jong AS, Van Kessel-van Vark M & Raap AK. (1985). Sensitivity of various visualization methods for peroxidase and alkaline phosphatase activity in immunoenzyme histochemistry. *Histochem J* **17,** 1119-1130.

De Matteo R, Stacy V, Probyn ME, Brew N, Blasch N & Harding R. (2008). Does moderate preterm birth lead to altered arterial pressure? Studies in sheep. . *Clinical and Experimental Pharmacology and Physiology* **35,** 1426-1432.

De Reuck J. (1971). The human periventricular arterial blood supply and the anatomy of cerebral infarctions. *Eur Neurol* **5,** 321-334.

de Vries LS, Groenendaal F, Eken P, van Haastert IC, Rademaker KJ & Meiners LC. (1997). Infarcts in the vascular distribution of the middle cerebral artery in preterm and fullterm infants. *Neuropediatrics* **28,** 88-96.

Dehouck MP, Vigne P, Torpier G, Breittmayer JP, Cecchelli R & Frelin C. (1997). Endothelin-1 as a mediator of endothelial cell-pericyte interactions in bovine brain capillaries. *J Cereb Blood Flow Metab* **17,** 464-469.

del Zoppo GJ & Mabuchi T. (2003). Cerebral microvessel responses to focal ischemia. *J Cereb Blood Flow Metab* **23,** 879-894.

Dellian M, Witwer BP, Salehi HA, Yuan F & Jain RK. (1996). Quantitation and physiological characterization of angiogenic vessels in mice: effect of basic fibroblast growth factor, vascular endothelial growth factor/vascular permeability factor, and host microenvironment. *Am J Pathol* **149,** 59-71.

Dermietzel R, Krause D, Kremer M, Wang C & Stevenson B. (1992). Pattern of glucose transporter (Glut 1) expression in embryonic brains is related to maturation of blood-brain barrier tightness. *Dev Dyn* **193,** 152-163.

Derrick M, Luo NL, Bregman JC, Jilling T, Ji X, Fisher K, Gladson CL, Beardsley DJ, Murdoch G, Back SA & Tan S. (2004). Preterm fetal hypoxia-ischemia causes hypertonia and motor deficits in the neonatal rabbit: a model for human cerebral palsy? *J Neurosci* **24,** 24-34.

Derugin N, Ferriero DM & Vexler ZS. (1998). Neonatal reversible focal cerebral ischemia: a new model. *Neurosci Res* **32,** 349-353.

Dimberg A, Rolny C, van Meeteren L & Claesson-Welsh L. (2009). Vascular Endothelial Growth Factors and Receptors: Signaling in Vascular Development In *Handbook of Cell Signalling*, 2nd edn, ed. Bradshaw R & Dennis E, pp. 1927 - 1937. Academic Press.

Dobbing J & Sands J. (1979). Comparative aspects of the brain growth spurt. *Early Hum Dev* **3,** 79-83.

Dore-Duffy P. (2008). Pericytes: pluripotent cells of the blood brain barrier. *Curr Pharm Des* **14,** 1581-1593.

Dore-Duffy P, Katychev A, Wang X & Van Buren E. (2006). CNS microvascular pericytes exhibit multipotential stem cell activity. *J Cereb Blood Flow Metab* **26,** 613-624.

Dore-Duffy P, Owen C, Balabanov R, Murphy S, Beaumont T & Rafols JA. (2000). Pericyte migration from the vascular wall in response to traumatic brain injury. *Microvasc Res* **60,** 55-69.

Dumont DJ, Gradwohl GJ, Fong GH, Auerbach R & Breitman ML. (1993). The endothelial-specific receptor tyrosine kinase, tek, is a member of a new subfamily of receptors. *Oncogene* **8,** 1293-1301.

Duncan JR, Camm E, Loeliger M, Cock ML, Harding R & Rees SM. (2004). Effects of umbilical cord occlusion in late gestation on the ovine fetal brain and retina. *J Soc Gynecol Investig* **11,** 369-376.

Dvorak HF, Brown LF, Detmar M & Dvorak AM. (1995). Vascular permeability factor/vascular endothelial growth factor, microvascular hyperpermeability, and angiogenesis. *Am J Pathol* **146,** 1029-1039.

Dwyer CM, Dingwall WS & Lawrence AB. (1999). Physiological correlates of maternal-offspring behaviour in sheep: a factor analysis. *Physiol Behav* **67,** 443-454.

Dwyer CM & Lawrence AB. (2000). Effects of maternal genotype and behaviour on the behavioural development of their offspring in sheep. *Behaviour* **137,** 1629-1654.

Dwyer CM, Lawrence AB, Brown HE & Simm G. (1996). Effect of ewe and lamb genotype on gestation length, lambing ease and neonatal behaviour of lambs. *Reprod Fertil Dev* **8,** 1123-1129.

El-Khoury N, Braun A, Hu F, Pandey M, Nedergaard M, Lagamma EF & Ballabh P. (2006). Astrocyte end-feet in germinal matrix, cerebral cortex, and white matter in developing infants. *Pediatr Res* **59,** 673-679.

Elfont RM, Sundaresan PR & Sladek CD. (1989). Adrenergic receptors on cerebral microvessels: pericyte contribution. *Am J Physiol* **256,** R224-230.

Engelhardt B. (2003). Development of the blood-brain barrier. *Cell Tissue Res* **314,** 119-129.

Eriksdotter-Nilsson M, Bjorklund H & Olson L. (1986). Laminin immunohistochemistry: a simple method to visualize and quantitate vascular structures in the mammalian brain. *J Neurosci Methods* **17,** 275-286.

Estan J & Hope P. (1997). Unilateral neonatal cerebral infarction in full term infants. *Arch Dis Child Fetal Neonatal Ed* **76,** F88-93.

Fan LW, Lin S, Pang Y, Lei M, Zhang F, Rhodes PG & Cai Z. (2005). Hypoxia-ischemia induced neurological dysfunction and brain injury in the neonatal rat. *Behav Brain Res* **165,** 80-90.

Fan X, Heijnen CJ, van der Kooij MA, Groenendaal F & van Bel F. (2009). The role and regulation of hypoxia-inducible factor-1alpha expression in brain development and neonatal hypoxic-ischemic brain injury. *Brain Res Rev* **62,** 99-108.

Faraci FM & Heistad DD. (1998). Regulation of the cerebral circulation: Role of endothelium and potassium channels. *Physiol Rev* **78,** 53-97.

Feng Y, Rhodes PG & Bhatt AJ. (2008). Neuroprotective effects of vascular endothelial growth factor following hypoxic ischemic brain injury in neonatal rats. *Pediatr Res* **64,** 370-374.

Ferrari DC, Nesic OB & Perez-Polo JR. (2010). Oxygen resuscitation does not ameliorate neonatal hypoxia/ischemia-induced cerebral edema. *J Neurosci Res* **88,** 2056-2065.

Fischer S, Clauss M, Wiesnet M, Renz D, Schaper W & Karliczek GF. (1999). Hypoxia induces permeability in brain microvessel endothelial cells via VEGF and NO. *Am J Physiol* **276,** C812-820.

Fischer S, Wobben M, Marti HH, Renz D & Schaper W. (2002). Hypoxia-induced hyperpermeability in brain microvessel endothelial cells involves VEGF-mediated changes in the expression of zonula occludens-1. *Microvasc Res* **63,** 70-80.

Foran A, Cinnante C, Groves A, Azzopardi DV, Rutherford MA & Cowan FM. (2009). Patterns of brain injury and outcome in term neonates presenting with postnatal collapse. *Arch Dis Child Fetal Neonatal Ed* **94,** F168-177.

Forsythe JA, Jiang BH, Iyer NV, Agani F, Leung SW, Koos RD & Semenza GL. (1996). Activation of vascular endothelial growth factor gene transcription by hypoxia-inducible factor 1. *Mol Cell Biol* **16,** 4604-4613.

Foster KA, Colditz PB, Lingwood BE, Burke C, Dunster KR & Roberts MS. (2001). An improved survival model of hypoxia/ischaemia in the piglet suitable for neuroprotection studies. *Brain Res* **919,** 122-131.

Fox SB, Leek RD, Weekes MP, Whitehouse RM, Gatter KC & Harris AL. (1995). Quantitation and prognostic value of breast cancer angiogenesis: comparison of microvessel density, Chalkley count, and computer image analysis. *J Pathol* **177,** 275-283.

Fujimori K, Takanashi A, Endo C & Sato A. (2008). Stress hormone responses during 24-hour hypoxemia in preterm goat fetus. *Tohoku J Exp Med* **215,** 189-197.

Fujimoto E, Miki A & Mizoguti H. (1989). Histochemical study of the differentiation of microglial cells in the developing human cerebral hemispheres. *J Anat* **166,** 253-264.

Fukumura D, Gohongi T, Kadambi A, Izumi Y, Ang J, Yun CO, Buerk DG, Huang PL & Jain RK. (2001). Predominant role of endothelial nitric oxide synthase in vascular endothelial growth factor-induced angiogenesis and vascular permeability. *Proc Natl Acad Sci U S A* **98,** 2604-2609.

Furuse M, Hirase T, Itoh M, Nagafuchi A, Yonemura S & Tsukita S. (1993). Occludin: a novel integral membrane protein localizing at tight junctions. *J Cell Biol* **123,** 1777-1788.

Furuse M, Sasaki H & Tsukita S. (1999). Manner of interaction of heterogeneous claudin species within and between tight junction strands. *J Cell Biol* **147,** 891-903.

Gale NW, Thurston G, Hackett SF, Renard R, Wang Q, McClain J, Martin C, Witte C, Witte MH, Jackson D, Suri C, Campochiaro PA, Wiegand SJ & Yancopoulos GD. (2002). Angiopoietin-2 is required for postnatal angiogenesis and lymphatic patterning, and only the latter role is rescued by Angiopoietin-1. *Dev Cell* **3,** 411-423.

George EL, Georges-Labouesse EN, Patel-King RS, Rayburn H & Hynes RO. (1993). Defects in mesoderm, neural tube and vascular development in mouse embryos lacking fibronectin. *Development* **119,** 1079-1091.

Gerber HP, Condorelli F, Park J & Ferrara N. (1997). Differential transcriptional regulation of the two vascular endothelial growth factor receptor genes. Flt-1, but not Flk-1/KDR, is up-regulated by hypoxia. *J Biol Chem* **272,** 23659-23667.

Giussani DA, McGarrigle HH, Moore PJ, Bennet L, Spencer JA & Hanson MA. (1994). Carotid sinus nerve section and the increase in plasma cortisol during acute hypoxia in fetal sheep. *J Physiol* **477 (Pt 1),** 75-80.

Giussani DA, Spencer JA, Moore PJ, Bennet L & Hanson MA. (1993). Afferent and efferent components of the cardiovascular reflex responses to acute hypoxia in term fetal sheep. *J Physiol* **461,** 431-449.

Glass HC, Glidden D, Jeremy RJ, Barkovich AJ, Ferriero DM & Miller SP. (2009). Clinical Neonatal Seizures are Independently Associated with Outcome in Infants at Risk for Hypoxic-Ischemic Brain Injury. *J Pediatr* **155,** 318-323.

Gluckman PD & Johnston BM. (1987). Lesions in the upper lateral pons abolish the hypoxic depression of breathing in unanaesthetized fetal lambs in utero. *J Physiol* **382,** 373-383.

Goldstein GW. (1988). Endothelial cell-astrocyte interactions. A cellular model of the blood-brain barrier. *Ann N Y Acad Sci* **529,** 31-39.

Gonul E, Duz B, Kahraman S, Kayali H, Kubar A & Timurkaynak E. (2002). Early pericyte response to brain hypoxia in cats: an ultrastructural study. *Microvasc Res* **64,** 116-119.

Gonzalez H, Hunter CJ, Bennet L, Power GG & Gunn AJ. (2005). Cerebral oxygenation during postasphyxial seizures in near-term fetal sheep. *Journal of Cerebral Blood Flow and Metabolism* **25,** 911-918.

Gora-Kupilas K & Josko J. (2005). The neuroprotective function of vascular endothelial growth factor (VEGF). *Folia Neuropathol* **43,** 31-39.

Gould SJ & Howard S. (1988). An immunocytochemical study of the germinal layer vasculature in the developing fetal brain using Ulex europaeus 1 lectin. *J Pathol* **156,** 129-135.

Grunnet ML. (1989). Morphometry of blood vessels in the cortex and germinal plate of premature neonates. *Pediatr Neurol* **5,** 12-16.

Gunn AJ, Parer JT, Mallard EC, Williams CE & Gluckman PD. (1992). Cerebral histologic and electrocorticographic changes after asphyxia in fetal sheep. *Pediatr Res* **31,** 486-491.

Gustavsson M, Mallard C, Vannucci SJ, Wilson MA, Johnston MV & Hagberg H. (2007). Vascular response to hypoxic preconditioning in the immature brain. *J Cereb Blood Flow Metab* **27,** 928-938.

Hagberg H, Ichord R, Palmer C, Yager JY & Vannucci SJ. (2002). Animal models of developmental brain injury: relevance to human disease. A summary of the panel discussion from the Third Hershey Conference on Developmental Cerebral Blood Flow and Metabolism. *Dev Neurosci* **24,** 364-366.

Halliday HL, Ehrenkranz RA & Doyle LW. (2009). Early (< 8 days) postnatal corticosteroids for preventing chronic lung disease in preterm infants. *Cochrane Database Syst Rev*, CD001146.

Hamann GF, Burggraf D, Martens HK, Liebetrau M, Jager G, Wunderlich N, DeGeorgia M & Krieger DW. (2004). Mild to moderate hypothermia prevents microvascular basal lamina antigen loss in experimental focal cerebral ischemia. *Stroke* **35,** 764-769.

Hamann GF, Liebetrau M, Martens H, Burggraf D, Kloss CU, Bultemeier G, Wunderlich N, Jager G & Pfefferkorn T. (2002). Microvascular basal lamina injury after experimental focal cerebral ischemia and reperfusion in the rat. *J Cereb Blood Flow Metab* **22,** 526-533.

Hamann GF, Okada Y & del Zoppo GJ. (1996). Hemorrhagic transformation and microvascular integrity during focal cerebral ischemia/reperfusion. *J Cereb Blood Flow Metab* **16,** 1373-1378.

Hamann GF, Okada Y, Fitridge R & del Zoppo GJ. (1995). Microvascular basal lamina antigens disappear during cerebral ischemia and reperfusion. *Stroke* **26,** 2120-2126.

Hamel E. (2006). Perivascular nerves and the regulation of cerebrovascular tone. *J Appl Physiol* **100,** 1059-1064.

Hamilton NB, Attwell D & Hall CN. (2010). Pericyte-mediated regulation of capillary diameter: a component of neurovascular coupling in health and disease. *Front Neuroenergetics* **2**.

Hamm S, Dehouck B, Kraus J, Wolburg-Buchholz K, Wolburg H, Risau W, Cecchelli R, Engelhardt B & Dehouck MP. (2004). Astrocyte mediated modulation of blood-brain barrier permeability does not correlate with a loss of tight junction proteins from the cellular contacts. *Cell Tissue Res* **315,** 157-166.

Hamrick SE & Ferriero DM. (2003). The injury response in the term newborn brain: can we neuroprotect? *Curr Opin Neurol* **16,** 147-154.

Hansen TM, Moss AJ & Brindle NP. (2008). Vascular endothelial growth factor and angiopoietins in neurovascular regeneration and protection following stroke. *Curr Neurovasc Res* **5,** 236-245.

Harris TA, Healy GN, Colditz PB & Lingwood BE. (2009). Associations between serum cortisol, cardiovascular function and neurological outcome following acute global hypoxia in the newborn piglet. *Stress* **12,** 294-304.

Helou S, Koehler RC, Gleason CA, Jones MD, Jr. & Traystman RJ. (1994). Cerebrovascular autoregulation during fetal development in sheep. *Am J Physiol* **266,** H1069-1074.

Hermann DM & Zechariah A. (2009). Implications of vascular endothelial growth factor for postischemic neurovascular remodeling. *J Cereb Blood Flow Metab* **29,** 1620-1643.

Hippenstiel S, Krull M, Ikemann A, Risau W, Clauss M & Suttorp N. (1998). VEGF induces hyperpermeability by a direct action on endothelial cells. *Am J Physiol* **274,** L678-684.

Hirase T, Staddon JM, Saitou M, Ando-Akatsuka Y, Itoh M, Furuse M, Fujimoto K, Tsukita S & Rubin LL. (1997). Occludin as a possible determinant of tight junction permeability in endothelial cells. *J Cell Sci* **110 (Pt 14),** 1603-1613.

Hirschi KK & D'Amore PA. (1996). Pericytes in the microvasculature. *Cardiovasc Res* **32,** 687-698.

Holash J, Maisonpierre PC, Compton D, Boland P, Alexander CR, Zagzag D, Yancopoulos GD & Wiegand SJ. (1999). Vessel cooption, regression, and growth in tumors mediated by angiopoietins and VEGF. *Science* **284,** 1994-1998.

Hollingworth SA, Deayton JM, Young IR & Thorburn GD. (1995). Prostaglandin E2 administered to fetal sheep increases the plasma concentration of adrenocorticotropin (ACTH) and the proportion of ACTH in low molecular weight forms. *Endocrinology* **136,** 1233-1240.

Holmes K, Charnock Jones SD, Forhead AJ, Giussani DA, Fowden AL, Licence D, Kempster S & Smith GC. (2008). Localization and control of expression of VEGF-A and the VEGFR-2 receptor in fetal sheep intestines. *Pediatr Res* **63,** 143-148.

Hooper SB, Harding R, Deayton J & Thorburn GD. (1992). Role of prostaglandins in the metabolic responses of the fetus to hypoxia. *Am J Obstet Gynecol* **166,** 1568-1575.

Hori S, Ohtsuki S, Hosoya K, Nakashima E & Terasaki T. (2004). A pericyte-derived angiopoietin-1 multimeric complex induces occludin gene expression in brain capillary endothelial cells through Tie-2 activation in vitro. *J Neurochem* **89,** 503-513.

Hutchins KD, Dickson DW, Rashbaum WK & Lyman WD. (1992). Localization of microglia in the human fetal cervical spinal cord. *Brain Res Dev Brain Res* **66,** 270-273.

Hutton LC, Castillo-Melendez M & Walker DW. (2007). Uteroplacental inflammation results in blood brain barrier breakdown, increased activated caspase 3 and lipid peroxidation in the late gestation ovine fetal cerebellum. *Dev Neurosci* **29,** 341-354.

Hutton LC, Ratnayake U, Shields A & Walker DW. (2009). Neuropathology and functional deficits in a model of birth asphyxia in the precocial spiny mouse (Acomys cahirinus). *Dev Neurosci* **31,** 523-535.

Ikeda T, Murata Y, Quilligan EJ, Choi BH, Parer JT, Doi S & Park SD. (1998a). Physiologic and histologic changes in near-term fetal lambs exposed to asphyxia by partial umbilical cord occlusion. *Am J Obstet Gynecol* **178,** 24-32.

Ikeda T, Murata Y, Quilligan EJ, Parer JT, Doi S & Park SD. (1998b). Brain lipid peroxidation and antioxidant levels in fetal lambs 72 hours after asphyxia by partial umbilical cord occlusion. *Am J Obstet Gynecol* **178,** 474-478.

Inder TE & Volpe JJ. (2000). Mechanisms of perinatal brain injury. *Semin Neonatol* **5,** 3-16.

Ireland Z, Dickinson H, Fleiss B, Hutton LC & Walker DW. (2009). Behavioural effects of near-term acute fetal hypoxia in a small precocial animal, the spiny mouse (Acomys cahirinus). *Neonatology* **97,** 45-51.

Itskovitz J, LaGamma EF & Rudolph AM. (1987). Effects of cord compression on fetal blood flow distribution and O2 delivery. *Am J Physiol* **252,** H100-109.

Ivens S, Kaufer D, Flores LP, Bechmann I, Zumsteg D, Tomkins O, Seiffert E, Heinemann U & Friedman A. (2007). TGF-beta receptor-mediated albumin uptake into astrocytes is involved in neocortical epileptogenesis. *Brain* **130,** 535-547.

Iwai M, Cao G, Yin W, Stetler RA, Liu J & Chen J. (2007). Erythropoietin promotes neuronal replacement through revascularization and neurogenesis after neonatal hypoxia/ischemia in rats. *Stroke* **38,** 2795-2803.

Iyer NV, Kotch LE, Agani F, Leung SW, Laughner E, Wenger RH, Gassmann M, Gearhart JD, Lawler AM, Yu AY & Semenza GL. (1998). Cellular and developmental control of O2 homeostasis by hypoxia-inducible factor 1 alpha. *Genes Dev* **12,** 149-162.

Jakobsson L, Domogatskaya A, Tryggvason K, Edgar D & Claesson-Welsh L. (2008). Laminin deposition is dispensable for vasculogenesis but regulates blood vessel diameter independent of flow. *FASEB J* **22,** 1530-1539.

Janzer RC & Raff MC. (1987). Astrocytes induce blood-brain barrier properties in endothelial cells. *Nature* **325,** 253-257.

Jensen A, Garnier Y & Berger R. (1999). Dynamics of fetal circulatory responses to hypoxia and asphyxia. *Eur J Obstet Gynecol Reprod Biol* **84,** 155-172.

Jensen EC, Bennet L, Fraser M, Power GG, Hunter CJ & Gunn AJ. (2010). Adenosine A(1) receptor mediated suppression of adrenal activity in near-term fetal sheep. *Am J Physiol Regul Integr Comp Physiol* **298,** R700-706.

Jensen FE, Wang C, Stafstrom CE, Liu Z, Geary C & Stevens MC. (1998). Acute and chronic increases in excitability in rat hippocampal slices after perinatal hypoxia In vivo. *J Neurophysiol* **79,** 73-81.

Jin K, Zhu Y, Sun Y, Mao XO, Xie L & Greenberg DA. (2002). Vascular endothelial growth factor (VEGF) stimulates neurogenesis in vitro and in vivo. *Proc Natl Acad Sci U S A* **99,** 11946-11950.

Jin KL, Mao XO & Greenberg DA. (2000a). Vascular endothelial growth factor: direct neuroprotective effect in in vitro ischemia. *Proc Natl Acad Sci U S A* **97,** 10242-10247.

Jin KL, Mao XO, Nagayama T, Goldsmith PC & Greenberg DA. (2000b). Induction of vascular endothelial growth factor and hypoxia-inducible factor-1alpha by global ischemia in rat brain. *Neuroscience* **99,** 577-585.

Jost RG, Quilligan EJ, Yeh SY & Anderson GG. (1972). Intrauterine electroencephalogram of the sheep fetus. *Am J Obstet Gynecol* **114,** 535-539.

Juul SE, Aylward E, Richards T, McPherson RJ, Kuratani J & Burbacher TM. (2007). Prenatal cord clamping in newborn Macaca nemestrina: a model of perinatal asphyxia. *Dev Neurosci* **29,** 311-320.

Kadri H, Mawla AA & Kazah J. (2006). The incidence, timing, and predisposing factors of germinal matrix and intraventricular hemorrhage (GMH/IVH) in preterm neonates. *Childs Nerv Syst* **22,** 1086-1090.

Kanaan A, Farahani R, Douglas RM, LaManna JC & Haddad GG. (2006). Effect of chronic continuous or intermittent hypoxia and reoxygenation on cerebral capillary density and myelination. *Am J Physiol Regul Integr Comp Physiol* **290,** R1105-1114.

Kaneko M, White S, Homan J & Richardson B. (2003). Cerebral blood flow and metabolism in relation to electrocortical activity with severe umbilical cord occlusion in the near-term ovine fetus. *Am J Obstet Gynecol* **188,** 961-972.

Kappel A, Ronicke V, Damert A, Flamme I, Risau W & Breier G. (1999). Identification of vascular endothelial growth factor (VEGF) receptor-2 (Flk-1) promoter/enhancer sequences sufficient for angioblast and endothelial cell-specific transcription in transgenic mice. *Blood* **93,** 4284-4292.

Kaur C, Dheen ST & Ling EA. (2007). From blood to brain: amoeboid microglial cell, a nascent macrophage and its functions in developing brain. *Acta Pharmacol Sin* **28,** 1087-1096.

Kaur C & Ling EA. (2008). Blood brain barrier in hypoxic-ischemic conditions. *Curr Neurovasc Res* **5,** 71-81.

Kaur C & Ling EA. (2009). Periventricular white matter damage in the hypoxic neonatal brain: role of microglial cells. *Prog Neurobiol* **87,** 264-280.

Kaur C, Sivakumar V, Ang LS & Sundaresan A. (2006a). Hypoxic damage to the periventricular white matter in neonatal brain: role of vascular endothelial growth factor, nitric oxide and excitotoxicity. *J Neurochem* **98,** 1200-1216.

Kaur C, Sivakumar V, Zhang Y & Ling EA. (2006b). Hypoxia-induced astrocytic reaction and increased vascular permeability in the rat cerebellum. *Glia* **54,** 826-839.

Kawagoe Y, Green L, White S & Richardson B. (1999a). Intermittent umbilical cord occlusion in the ovine fetus near term: Effects on behavioral state activity. *American Journal of Obstetrics and Gynecology* **181,** 1520-1529.

Kawagoe Y, Green L, White S & Richardson B. (1999b). Intermittent umbilical cord occlusion in the ovine fetus near term: effects on behavioral state activity. *Am J Obstet Gynecol* **181,** 1520-1529.

Kaya D, Gursoy-Ozdemir Y, Yemisci M, Tuncer N, Aktan S & Dalkara T. (2005). VEGF protects brain against focal ischemia without increasing blood--brain permeability when administered intracerebroventricularly. *J Cereb Blood Flow Metab* **25,** 1111-1118.

Keck PJ, Hauser SD, Krivi G, Sanzo K, Warren T, Feder J & Connolly DT. (1989). Vascular permeability factor, an endothelial cell mitogen related to PDGF. *Science* **246,** 1309-1312.

Keep RF, Ennis SR, Beer ME & Betz AL. (1995). Developmental changes in blood-brain barrier potassium permeability in the rat: relation to brain growth. *J Physiol* **488 (Pt 2),** 439-448.

Keogh CL, Yu SP & Wei L. (2007). The effect of recombinant human erythropoietin on neurovasculature repair after focal ischemic stroke in neonatal rats. *J Pharmacol Exp Ther* **322,** 521-528.

Keunen H, Blanco CE, van Reempts JL & Hasaart TH. (1997). Absence of neuronal damage after umbilical cord occlusion of 10, 15, and 20 minutes in midgestation fetal sheep. *Am J Obstet Gynecol* **176,** 515-520.

Kilic E, Kilic U, Wang Y, Bassetti CL, Marti HH & Hermann DM. (2006). The phosphatidylinositol-3 kinase/Akt pathway mediates VEGF's neuroprotective activity

and induces blood brain barrier permeability after focal cerebral ischemia. *FASEB J* **20,** 1185-1187.

Kim H, Lee JM, Park JS, Jo SA, Kim YO, Kim CW & Jo I. (2008). Dexamethasone coordinately regulates angiopoietin-1 and VEGF: a mechanism of glucocorticoid-induced stabilization of blood-brain barrier. *Biochem Biophys Res Commun* **372,** 243-248.

Kim KJ, Li B, Winer J, Armanini M, Gillett N, Phillips HS & Ferrara N. (1993). Inhibition of vascular endothelial growth factor-induced angiogenesis suppresses tumour growth in vivo. *Nature* **362,** 841-844.

Klatzo I. (1987). Pathophysiological aspects of brain edema. *Acta Neuropathol* **72,** 236-239.

Knutson N & Wood CE. (2010). Interaction of PGHS-2 and glutamatergic mechanisms controlling the ovine fetal hypothalamus-pituitary-adrenal axis. *Am J Physiol Regul Integr Comp Physiol* **299,** R365-370.

Koelfen W, Freund M & Varnholt V. (1995). Neonatal stroke involving the middle cerebral artery in term infants: clinical presentation, EEG and imaging studies, and outcome. *Dev Med Child Neurol* **37,** 204-212.

Koos BJ, Maeda T & Jan C. (2001). Adenosine A(1) and A(2A) receptors modulate sleep state and breathing in fetal sheep. *Journal of Applied Physiology* **91,** 343-350.

Koos BJ, Maeda T, Jan C & Lopez G. (2002). Adenosine A(2A) receptors mediate hypoxic inhibition of fetal breathing in sheep. *American Journal of Obstetrics & Gynecology* **186,** 663-668.

Korzhevskii DE & Otellin VA. (2000). Initial stage of vascular bed development in telencephalon of human embryo. *Bull Exp Biol Med* **129,** 508-510.

Kremer C, Breier G, Risau W & Plate KH. (1997). Up-regulation of flk-1/vascular endothelial growth factor receptor 2 by its ligand in a cerebral slice culture system. *Cancer Res* **57,** 3852-3859.

Krugers HJ, Kemper RH, Korf J, Ter Horst GJ & Knollema S. (1998). Metyrapone reduces rat brain damage and seizures after hypoxia-ischemia: an effect independent of modulation of plasma corticosterone levels? *J Cereb Blood Flow Metab* **18,** 386-390.

Krupinski J, Kaluza J, Kumar P, Kumar S & Wang JM. (1994). Role of angiogenesis in patients with cerebral ischemic stroke. *Stroke* **25,** 1794-1798.

Kubonoya K & Power GG. (1997). Plasma adenosine responses during repeated episodes of umbilical cord occlusion. *American Journal of Obstetrics & Gynecology* **177,** 395-401.

Kulik T, Kusano Y, Aronhime S, Sandler AL & Winn HR. (2008). Regulation of cerebral vasculature in normal and ischemic brain. *Neuropharmacology* **55,** 281-288.

Kumar A, Mittal R, Khanna HD & Basu S. (2008). Free radical injury and blood-brain barrier permeability in hypoxic-ischemic encephalopathy. *Pediatrics* **122,** e722-727.

Kuroiwa T, Cahn R, Juhler M, Goping G, Campbell G & Klatzo I. (1985). Role of extracellular proteins in the dynamics of vasogenic brain edema. *Acta Neuropathol* **66,** 3-11.

Lagercrantz J, Farnebo F, Larsson C, Tvrdik T, Weber G & Piehl F. (1998). A comparative study of the expression patterns for vegf, vegf-b/vrf and vegf-c in the developing and adult mouse. *Biochim Biophys Acta* **1398,** 157-163.

Lai DM, Li H, Lee CC, Tzeng YS, Hsieh YH, Hsu WM, Hsieh FJ, Cheng JT & Tu YK. (2008). Angiopoietin-like protein 1 decreases blood brain barrier damage and edema following focal cerebral ischemia in mice. *Neurochem Int* **52,** 470-477.

Lamblin MD, Andre M, Challamel MJ, Curzi-Dascalova L, d'Allest AM, De Giovanni E, Moussalli-Salefranque F, Navelet Y, Plouin P, Radvanyi-Bouvet MF, Samson-Dollfus D & Vecchierini-Blineau MF. (1999). Electroencephalography of the premature and term newborn. Maturational aspects and glossary. *Neurophysiol Clin* **29,** 123-219.

Laurie GW, Leblond CP, Cournil I & Martin GR. (1980). Immunohistochemical evidence for the intracellular formation of basement membrane collagen (type IV) in developing tissues. *J Histochem Cytochem* **28,** 1267-1274.

Le Bras B, Barallobre MJ, Homman-Ludiye J, Ny A, Wyns S, Tammela T, Haiko P, Karkkainen MJ, Yuan L, Muriel MP, Chatzopoulou E, Breant C, Zalc B, Carmeliet P, Alitalo K, Eichmann A & Thomas JL. (2006). VEGF-C is a trophic factor for neural progenitors in the vertebrate embryonic brain. *Nat Neurosci* **9,** 340-348.

Lee HT, Chang YC, Tu YF & Huang CC. (2010). CREB activation mediates VEGF-A's protection of neurons and cerebral vascular endothelial cells. *J Neurochem* **113,** 79-91.

Lee J, Croen LA, Lindan C, Nash KB, Yoshida CK, Ferriero DM, Barkovich AJ & Wu YW. (2005). Predictors of outcome in perinatal arterial stroke: a population-based study. *Ann Neurol* **58,** 303-308.

Lenn NJ & Whitmore L. (1985). Gestational changes in the germinal matrix of the normal rhesus monkey fetus. *Pediatr Res* **19,** 130-135.

Lennmyr F, Ata KA, Funa K, Olsson Y & Terent A. (1998). Expression of vascular endothelial growth factor (VEGF) and its receptors (Flt-1 and Flk-1) following permanent and transient occlusion of the middle cerebral artery in the rat. *J Neuropathol Exp Neurol* **57,** 874-882.

Leonardo CC & Pennypacker KR. (2009). Neuroinflammation and MMPs: potential therapeutic targets in neonatal hypoxic-ischemic injury. *J Neuroinflammation* **6,** 13.

Leung DW, Cachianes G, Kuang WJ, Goeddel DV & Ferrara N. (1989). Vascular endothelial growth factor is a secreted angiogenic mitogen. *Science* **246,** 1306-1309.

Liesi P. (1985). Do neurons in the vertebrate CNS migrate on laminin? *EMBO J* **4,** 1163-1170.

Liesi P, Kaakkola S, Dahl D & Vaheri A. (1984). Laminin is induced in astrocytes of adult brain by injury. *EMBO J* **3,** 683-686.

Lin J, Wu PH, Tarr PT, Lindenberg KS, St-Pierre J, Zhang CY, Mootha VK, Jager S, Vianna CR, Reznick RM, Cui L, Manieri M, Donovan MX, Wu Z, Cooper MP, Fan MC, Rohas LM, Zavacki AM, Cinti S, Shulman GI, Lowell BB, Krainc D & Spiegelman BM. (2004). Defects in adaptive energy metabolism with CNS-linked hyperactivity in PGC-1alpha null mice. *Cell* **119,** 121-135.

Lin TN, Nian GM, Chen SF, Cheung WM, Chang C, Lin WC & Hsu CY. (2001). Induction of Tie-1 and Tie-2 receptor protein expression after cerebral ischemia-reperfusion. *J Cereb Blood Flow Metab* **21,** 690-701.

Lin TN, Wang CK, Cheung WM & Hsu CY. (2000). Induction of angiopoietin and Tie receptor mRNA expression after cerebral ischemia-reperfusion. *J Cereb Blood Flow Metab* **20,** 387-395.

Ling EA & Wong WC. (1993). The origin and nature of ramified and amoeboid microglia: a historical review and current concepts. *Glia* **7,** 9-18.

Low JA. (2004). Determining the contribution of asphyxia to brain damage in the neonate. *J Obstet Gynaecol Res* **30,** 276-286.

Low JA, Robertson DM & Simpson LL. (1989). Temporal relationships of neuropathologic conditions caused by perinatal asphyxia. *Am J Obstet Gynecol* **160,** 608-614.

Lukes A, Mun-Bryce S, Lukes M & Rosenberg GA. (1999). Extracellular matrix degradation by metalloproteinases and central nervous system diseases. *Mol Neurobiol* **19,** 267-284.

Lynch JK, Hirtz DG, DeVeber G & Nelson KB. (2002). Report of the National Institute of Neurological Disorders and Stroke workshop on perinatal and childhood stroke. *Pediatrics* **109,** 116-123.

Magyar DM, Fridshal D, Elsner CW, Glatz T, Eliot J, Klein AH, Lowe KC, Buster JE & Nathanielsz PW. (1980). Time-trend analysis of plasma cortisol concentrations in the fetal sheep in relation to parturition. *Endocrinology* **107,** 155-159.

Maher F, Vannucci SJ & Simpson IA. (1993). Glucose transporter isoforms in brain: absence of GLUT3 from the blood-brain barrier. *J Cereb Blood Flow Metab* **13,** 342-345.

Maisonpierre PC, Suri C, Jones PF, Bartunkova S, Wiegand SJ, Radziejewski C, Compton D, McClain J, Aldrich TH, Papadopoulos N, Daly TJ, Davis S, Sato TN & Yancopoulos GD. (1997). Angiopoietin-2, a natural antagonist for Tie2 that disrupts in vivo angiogenesis. *Science* **277,** 55-60.

Mallard EC, Gunn AJ, Williams CE, Johnston BM & Gluckman PD. (1992). Transient umbilical cord occlusion causes hippocampal damage in the fetal sheep. *Am J Obstet Gynecol* **167,** 1423-1430.

Mallard EC, Williams CE, Johnston BM & Gluckman PD. (1994). Increased vulnerability to neuronal damage after umbilical cord occlusion in fetal sheep with advancing gestation. *Am J Obstet Gynecol* **170,** 206-214.

Marti HH. (2004). Erythropoietin and the hypoxic brain. *J Exp Biol* **207,** 3233-3242.

Marti HH, Bernaudin M, Petit E & Bauer C. (2000a). Neuroprotection and Angiogenesis: Dual Role of Erythropoietin in Brain Ischemia. *News Physiol Sci* **15,** 225-229.

Marti HH & Risau W. (1998). Systemic hypoxia changes the organ-specific distribution of vascular endothelial growth factor and its receptors. *Proc Natl Acad Sci U S A* **95,** 15809-15814.

Marti HJ, Bernaudin M, Bellail A, Schoch H, Euler M, Petit E & Risau W. (2000b). Hypoxia-induced vascular endothelial growth factor expression precedes neovascularization after cerebral ischemia. *Am J Pathol* **156,** 965-976.

Martin-Padura I, Lostaglio S, Schneemann M, Williams L, Romano M, Fruscella P, Panzeri C, Stoppacciaro A, Ruco L, Villa A, Simmons D & Dejana E. (1998). Junctional adhesion molecule, a novel member of the immunoglobulin superfamily that distributes at intercellular junctions and modulates monocyte transmigration. *J Cell Biol* **142,** 117-127.

Massik J, Jones MD, Jr., Miyabe M, Tang YL, Hudak ML, Koehler RC & Traystman RJ. (1989). Hypercapnia and response of cerebral blood flow to hypoxia in newborn lambs. *J Appl Physiol* **66,** 1065-1070.

Mayhan WG. (1999). VEGF increases permeability of the blood-brain barrier via a nitric oxide synthase/cGMP-dependent pathway. *Am J Physiol* **276,** C1148-1153.

McClure MM, Riddle A, Manese M, Luo NL, Rorvik DA, Kelly KA, Barlow CH, Kelly JJ, Vinecore K, Roberts CT, Hohimer AR & Back SA. (2008). Cerebral blood flow heterogeneity in preterm sheep: lack of physiologic support for vascular boundary zones in fetal cerebral white matter. *J Cereb Blood Flow Metab* **28,** 995-1008.

McCrabb GJ & Harding R. (1995). Cerebral blood flow is increased throughout 12 h of hypoxaemia in the mid-gestation ovine fetus. *Reprod Fertil Dev* **7,** 463-467.

McKendry AA, Palliser HK, Yates DM, Walker DW & Hirst JJ. (2010). The effect of betamethasone treatment on neuroactive steroid synthesis in a foetal Guinea pig model of growth restriction. *J Neuroendocrinol* **22,** 166-174.

McLean C & Ferriero D. (2004). Mechanisms of hypoxic-ischemic injury in the term infant. *Semin Perinatol* **28,** 425-432.

Meek JH, Tyszczuk L, Elwell CE & Wyatt JS. (1999). Low cerebral blood flow is a risk factor for severe intraventricular haemorrhage. *Arch Dis Child Fetal Neonatal Ed* **81,** F15-18.

Meininger CJ, Schelling ME & Granger HJ. (1988). Adenosine and hypoxia stimulate proliferation and migration of endothelial cells. *Am J Physiol* **255,** H554-562.

Melgar MA, Rafols J, Gloss D & Diaz FG. (2005). Postischemic reperfusion: ultrastructural blood-brain barrier and hemodynamic correlative changes in an awake model of transient forebrain ischemia. *Neurosurgery* **56,** 571-581.

Ment LR, Stewart WB, Ardito TA & Madri JA. (1991). Beagle pup germinal matrix maturation studies. *Stroke* **22,** 390-395.

Ment LR, Stewart WB, Fronc R, Seashore C, Mahooti S, Scaramuzzino D & Madri JA. (1997). Vascular endothelial growth factor mediates reactive angiogenesis in the postnatal developing brain. *Brain Res Dev Brain Res* **100,** 52-61.

Miller SL, Chai M, Loose J, Castillo-Melendez M, Walker DW, Jenkin G & Wallace EM. (2007). The effects of maternal betamethasone administration on the intrauterine growth-restricted fetus. *Endocrinology* **148,** 1288-1295.

Miller SL, Yan EB, Castillo-Melendez M, Jenkin G & Walker DW. (2005). Melatonin provides neuroprotection in the late-gestation fetal sheep brain in response to umbilical cord occlusion. *Dev Neurosci* **27,** 200-210.

Miller SP, Weiss J, Barnwell A, Ferriero DM, Latal-Hajnal B, Ferrer-Rogers A, Newton N, Partridge JC, Glidden DV, Vigneron DB & Barkovich AJ. (2002). Seizure-associated brain injury in term newborns with perinatal asphyxia. *Neurology* **58,** 542-548.

Milligan DW. (1980). Failure of autoregulation and intraventricular haemorrhage in preterm infants. *Lancet* **1,** 896-898.

Milner R & Campbell IL. (2002). Developmental regulation of beta1 integrins during angiogenesis in the central nervous system. *Mol Cell Neurosci* **20,** 616-626.

Milner R, Hung S, Erokwu B, Dore-Duffy P, LaManna JC & del Zoppo GJ. (2008). Increased expression of fibronectin and the alpha 5 beta 1 integrin in angiogenic cerebral blood vessels of mice subject to hypobaric hypoxia. *Mol Cell Neurosci* **38,** 43-52.

Mishra OP & Delivoria-Papadopoulos M. (1999). Cellular mechanisms of hypoxic injury in the developing brain. *Brain Res Bull* **48,** 233-238.

Mito T, Konomi H, Houdou S & Takashima S. (1991). Immunohistochemical study of the vasculature in the developing brain. *Pediatr Neurol* **7,** 18-22.

Miyawaki T, Matsui K & Takashima S. (1998). Developmental characteristics of vessel density in the human fetal and infant brains. *Early Hum Dev* **53,** 65-72.

Mollace V, Muscoli C, Rotiroti D & Nistico G. (1997). Spontaneous induction of nitric oxide- and prostaglandin E-2-release by hypoxic astroglial cells is modulated by interleukin 1 beta. *Biochemical and Biophysical Research Communications* **238,** 916-919.

Morrison JL, Carmichael L, Homan J, White S & Richardson BS. (2005). Cerebral blood flow during spontaneous and cholinergically induced behavioral states in the sheep fetus. *Pediatric Research* **57,** 667-673.

Mu D, Jiang X, Sheldon RA, Fox CK, Hamrick SE, Vexler ZS & Ferriero DM. (2003). Regulation of hypoxia-inducible factor 1alpha and induction of vascular endothelial growth factor in a rat neonatal stroke model. *Neurobiol Dis* **14,** 524-534.

Murohara T, Horowitz JR, Silver M, Tsurumi Y, Chen D, Sullivan A & Isner JM. (1998). Vascular endothelial growth factor/vascular permeability factor enhances vascular permeability via nitric oxide and prostacyclin. *Circulation* **97,** 99-107.

Mustonen T & Alitalo K. (1995). Endothelial receptor tyrosine kinases involved in angiogenesis. *J Cell Biol* **129,** 895-898.

Myers RE. (1975). Fetal asphyxia due to umbilical cord compression. Metabolic and brain pathologic consequences. *Biol Neonate* **26,** 21-43.

Nag S, Takahashi JL & Kilty DW. (1997). Role of vascular endothelial growth factor in blood-brain barrier breakdown and angiogenesis in brain trauma. *J Neuropathol Exp Neurol* **56,** 912-921.

Nagy Z & Martinez K. (1991). Astrocytic induction of endothelial tight junctions. *Ann N Y Acad Sci* **633,** 395-404.

Nakagawa S, Deli MA, Nakao S, Honda M, Hayashi K, Nakaoke R, Kataoka Y & Niwa M. (2007). Pericytes from brain microvessels strengthen the barrier integrity in primary cultures of rat brain endothelial cells. *Cell Mol Neurobiol* **27,** 687-694.

Nico B, Corsi P, Vacca A, Roncali L & Ribatti D. (2002). Vascular endothelial growth factor and vascular endothelial growth factor receptor-2 expression in mdx mouse brain. *Brain Res* **953,** 12-16.

Nicol MB, Hirst JJ, Walker D & Thorburn GD. (1997). Effect of alteration of maternal plasma progesterone concentrations on fetal behavioural state during late gestation. *J Endocrinol* **152,** 379-386.

Nitsos I & Walker DW. (1999). Characterization of pontine neurons which respond to hypoxia in fetal sheep. *Neurosci Lett* **266,** 33-36.

Northington FJ, Tobin JR, Harris AP, Traystman RJ & Koehler RC. (1997). Developmental and regional differences in nitric oxide synthase activity and blood flow in the sheep brain. *J Cereb Blood Flow Metab* **17,** 109-115.

Nowak R, Murphy TM, Lindsay DR, Alster P, Andersson R & Uvnas-Moberg K. (1996). Development of a preferential relationship with the mother by the newborn lamb: importance of the sucking activity. *Physiol Behav* **62,** 681-688.

O'Brien JS & Sampson EL. (1965). Lipid composition of the normal human brain: gray matter, white matter, and myelin. *J Lipid Res* **6,** 537-544.

O'Regan M. (2005). Adenosine and the regulation of cerebral blood flow. *Neurol Res* **27,** 175-181.

Ogunshola OO, Stewart WB, Mihalcik V, Solli T, Madri JA & Ment LR. (2000). Neuronal VEGF expression correlates with angiogenesis in postnatal developing rat brain. *Brain Res Dev Brain Res* **119,** 139-153.

Oike Y, Yasunaga K & Suda T. (2004). Angiopoietin-related/angiopoietin-like proteins regulate angiogenesis. *Int J Hematol* **80,** 21-28.

Otrock ZK, Mahfouz RA, Makarem JA & Shamseddine AI. (2007). Understanding the biology of angiogenesis: review of the most important molecular mechanisms. *Blood Cells Mol Dis* **39,** 212-220.

Pan JR, Li Y, Pei Z, Li XP, Peng Y & Wang YD. (2010). Hypoxic tissues are associated with microvessel density following brain ischemia-reperfusion. *Neurol Sci* **31,** 765-771.

Papavassiliou E, Gogate N, Proescholdt M, Heiss JD, Walbridge S, Edwards NA, Oldfield EH & Merrill MJ. (1997). Vascular endothelial growth factor (vascular permeability factor) expression in injured rat brain. *J Neurosci Res* **49,** 451-460.

Papile LA, Rudolph AM & Heymann MA. (1985). Autoregulation of cerebral blood flow in the preterm fetal lamb. *Pediatr Res* **19,** 159-161.

Paravicini TM, Drummond GR & Sobey CG. (2004). Reactive oxygen species in the cerebral circulation: physiological roles and therapeutic implications for hypertension and stroke. *Drugs* **64,** 2143-2157.

Pardridge WM, Boado RJ & Farrell CR. (1990). Brain-type glucose transporter (GLUT-1) is selectively localized to the blood-brain barrier. Studies with quantitative western blotting and in situ hybridization. *J Biol Chem* **265,** 18035-18040.

Parer JT. (1998). Effects of fetal asphyxia on brain cell structure and function: limits of tolerance. *Comp Biochem Physiol A Mol Integr Physiol* **119,** 711-716.

Parikh NA, Katsetos CD, Ashraf QM, Haider SH, Legido A, Delivoria-Papadopoulos M & Mishra OP. (2003). Hypoxia-induced caspase-3 activation and DNA fragmentation in cortical neurons of newborn piglets: role of nitric oxide. *Neurochem Res* **28,** 1351-1357.

Pearce W. (2006). Hypoxic regulation of the fetal cerebral circulation. *J Appl Physiol* **100,** 731-738.

Pepper MS & Mandriota SJ. (1998). Regulation of vascular endothelial growth factor receptor-2 (Flk-1) expression in vascular endothelial cells. *Exp Cell Res* **241,** 414-425.

Peppiatt CM, Howarth C, Mobbs P & Attwell D. (2006). Bidirectional control of CNS capillary diameter by pericytes. *Nature* **443,** 700-704.

Perlman JM. (2004). Brain injury in the term infant. *Semin Perinatol* **28,** 415-424.

Pessin JE & Bell GI. (1992). Mammalian facilitative glucose transporter family: structure and molecular regulation. *Annu Rev Physiol* **54,** 911-930.

Pichiule P & LaManna JC. (2002). Angiopoietin-2 and rat brain capillary remodeling during adaptation and deadaptation to prolonged mild hypoxia. *J Appl Physiol* **93,** 1131-1139.

Plate KH, Beck H, Danner S, Allegrini PR & Wiessner C. (1999). Cell type specific upregulation of vascular endothelial growth factor in an MCA-occlusion model of cerebral infarct. *J Neuropathol Exp Neurol* **58,** 654-666.

Poschl E, Schlotzer-Schrehardt U, Brachvogel B, Saito K, Ninomiya Y & Mayer U. (2004). Collagen IV is essential for basement membrane stability but dispensable for initiation of its assembly during early development. *Development* **131,** 1619-1628.

Povlishock JT, Martinez AJ & Moossy J. (1977). The fine structure of blood vessels of the telencephalic germinal matrix in the human fetus. *Am J Anat* **149,** 439-452.

Ramaswamy V, Miller SP, Barkovich AJ, Partridge JC & Ferriero DM. (2004). Perinatal stroke in term infants with neonatal encephalopathy. *Neurology* **62,** 2088-2091.

Ramsauer M, Krause D & Dermietzel R. (2002). Angiogenesis of the blood-brain barrier in vitro and the function of cerebral pericytes. *FASEB J* **16,** 1274-1276.

Rankin JH, Landauer M, Tian Q & Phernetton TM. (1987). Ovine fetal electrocortical activity and regional cerebral blood flow. *Journal of Developmental Physiology* **9,** 537-542.

Remmers M, Schmidt-Kastner R, Belayev L, Lin B, Busto R & Ginsberg MD. (1999). Protein extravasation and cellular uptake after high-dose human-albumin treatment of transient focal cerebral ischemia in rats. *Brain Res* **827,** 237-242.

Rice JE, 3rd, Vannucci RC & Brierley JB. (1981). The influence of immaturity on hypoxic-ischemic brain damage in the rat. *Ann Neurol* **9,** 131-141.

Richardson BS & Bocking AD. (1998). Metabolic and circulatory adaptations to chronic hypoxia in the fetus. *Comp Biochem Physiol A Mol Integr Physiol* **119,** 717-723.

Richardson BS, Carmichael L, Homan J, Johnston L & Gagnon R. (1996). Fetal cerebral, circulatory, and metabolic responses during heart rate decelerations with umbilical cord compression. *Am J Obstet Gynecol* **175,** 929-936.

Richardson BS, Carmichael L, Homan J & Patrick JE. (1992). Electrocortical activity, electroocular activity, and breathing movements in fetal sheep with prolonged and graded hypoxemia. *Am J Obstet Gynecol* **167,** 553-558.

Richardson BS, Patrick JE & Abduljabbar H. (1985). Cerebral oxidative metabolism in the fetal lamb: relationship to electrocortical state. *Am J Obstet Gynecol* **153,** 426-431.

Rigau V, Morin M, Rousset MC, de Bock F, Lebrun A, Coubes P, Picot MC, Baldy-Moulinier M, Bockaert J, Crespel A & Lerner-Natoli M. (2007). Angiogenesis is associated with blood-brain barrier permeability in temporal lobe epilepsy. *Brain* **130,** 1942-1956.

Risau W. (1991). Induction of blood-brain barrier endothelial cell differentiation. *Ann N Y Acad Sci* **633,** 405-419.

Risau W & Lemmon V. (1988). Changes in the vascular extracellular matrix during embryonic vasculogenesis and angiogenesis. *Dev Biol* **125,** 441-450.

Risau W & Wolburg H. (1990). Development of the blood-brain barrier. *Trends Neurosci* **13,** 174-178.

Rodrigo J, Fernandez AP, Serrano J, Peinado MA & Martinez A. (2005). The role of free radicals in cerebral hypoxia and ischemia. *Free Radic Biol Med* **39,** 26-50.

Roelfsema V, Gunn AJ, Fraser M, Quaedackers JS & Bennet L. (2005). Cortisol and ACTH responses to severe asphyxia in preterm fetal sheep. *Exp Physiol* **90,** 545-555.

Romanic AM, White RF, Arleth AJ, Ohlstein EH & Barone FC. (1998). Matrix metalloproteinase expression increases after cerebral focal ischemia in rats: inhibition of matrix metalloproteinase-9 reduces infarct size. *Stroke* **29,** 1020-1030.

Rosenberg GA, Estrada EY & Dencoff JE. (1998). Matrix metalloproteinases and TIMPs are associated with blood-brain barrier opening after reperfusion in rat brain. *Stroke* **29,** 2189-2195.

Rosenstein JM & Krum JM. (2004). New roles for VEGF in nervous tissue--beyond blood vessels. *Exp Neurol* **187,** 246-253.

Rurak DW & Gruber NC. (1983). Increased oxygen consumption associated with breathing activity in fetal lambs. *J Appl Physiol* **54,** 701-707.

Sadowska GB, Malaeb SN & Stonestreet BS. (2010). Maternal glucocorticoid exposure alters tight junction protein expression in the brain of fetal sheep. *Am J Physiol Heart Circ Physiol* **298,** H179-188.

Sakagami K, Kawamura H, Wu DM & Puro DG. (2001). Nitric oxide/cGMP-induced inhibition of calcium and chloride currents in retinal pericytes. *Microvasc Res* **62,** 196-203.

Sakagami K, Wu DM & Puro DG. (1999). Physiology of rat retinal pericytes: modulation of ion channel activity by serum-derived molecules. *J Physiol* **521 Pt 3,** 637-650.

Sanes JR, Engvall E, Butkowski R & Hunter DD. (1990). Molecular heterogeneity of basal laminae: isoforms of laminin and collagen IV at the neuromuscular junction and elsewhere. *J Cell Biol* **111,** 1685-1699.

Schmid-Brunclik N, Burgi-Taboada C, Antoniou X, Gassmann M & Ogunshola OO. (2008). Astrocyte responses to injury: VEGF simultaneously modulates cell death and proliferation. *Am J Physiol Regul Integr Comp Physiol* **295,** R864-873.

Schoch HJ, Fischer S & Marti HH. (2002). Hypoxia-induced vascular endothelial growth factor expression causes vascular leakage in the brain. *Brain* **125,** 2549-2557.

Scholler K, Trinkl A, Klopotowski M, Thal SC, Plesnila N, Trabold R, Hamann GF, Schmid-Elsaesser R & Zausinger S. (2007). Characterization of microvascular basal lamina damage and blood-brain barrier dysfunction following subarachnoid hemorrhage in rats. *Brain Res* **1142,** 237-246.

Schulze C & Firth JA. (1993). Immunohistochemical localization of adherens junction components in blood-brain barrier microvessels of the rat. *J Cell Sci* **104 (Pt 3),** 773-782.

Semenza GL. (2009a). Regulation of oxygen homeostasis by hypoxia-inducible factor 1. *Physiology (Bethesda)* **24,** 97-106.

Semenza GL. (2009b). Vascular responses to hypoxia and ischemia. *Arterioscler Thromb Vasc Biol* **30,** 648-652.

Sentilhes L, Michel C, Lecourtois M, Catteau J, Bourgeois P, Laudenbach V, Marret S & Laquerriere A. (2010). Vascular endothelial growth factor and its high-affinity receptor (VEGFR-2) are highly expressed in the human forebrain and cerebellum during development. *J Neuropathol Exp Neurol* **69,** 111-128.

Shalak L & Perlman JM. (2004). Hypoxic-ischemic brain injury in the term infant-current concepts. *Early Hum Dev* **80,** 125-141.

Shapiro W, Wasserman AJ & Patterson JL, Jr. (1966). Human cerebrovascular response to combined hypoxia and hypercapnia. *Circ Res* **19,** 903-910.

Sheldon RA, Osredkar D, Lee CL, Jiang X, Mu D & Ferriero DM. (2009). HIF-1 alpha-deficient mice have increased brain injury after neonatal hypoxia-ischemia. *Dev Neurosci* **31,** 452-458.

Shi SR, Key ME & Kalra KL. (1991). Antigen retrieval in formalin-fixed, paraffin-embedded tissues: an enhancement method for immunohistochemical staining based on microwave oven heating of tissue sections. *J Histochem Cytochem* **39,** 741-748.

Shimotake J, Derugin N, Wendland M, Vexler ZS & Ferriero DM. (2010). Vascular endothelial growth factor receptor-2 inhibition promotes cell death and limits endothelial cell proliferation in a neonatal rodent model of stroke. *Stroke* **41,** 343-349.

Shinozuka N & Nathanielsz PW. (1998). Electrocortical activity in fetal sheep in the last seven days of gestation. *J Physiol* **513 (Pt 1),** 273-281.

Shweiki D, Itin A, Neufeld G, Gitay-Goren H & Keshet E. (1993). Patterns of expression of vascular endothelial growth factor (VEGF) and VEGF receptors in mice suggest a role in hormonally regulated angiogenesis. *J Clin Invest* **91,** 2235-2243.

Silver M & Fowden AL. (1991). Induction of labor in sheep by inhibition of 3-beta hydroxysteroid dehydrogenase - role of the fetal adrenal. *Journal of Developmental Physiology* **15,** 169-174.

Simon KE, Mondares RL, Born DE & Gleason CA. (2008). The effects of binge alcohol exposure in the 2nd trimester on the estimated density of cerebral microvessels in near-term fetal sheep. *Brain Res* **1231,** 75-80.

Sims ME, Turkel SB, Halterman G & Paul RH. (1985). Brain injury and intrauterine death. *Am J Obstet Gynecol* **151,** 721-723.

Skold MK & Kanje M. (2008). Vascular endothelial growth factor in central nervous system injuries - a vascular growth factor getting nervous? *Curr Neurovasc Res* **5,** 246-259.

Skuli N, Liu L, Runge A, Wang T, Yuan L, Patel S, Iruela-Arispe L, Simon MC & Keith B. (2009). Endothelial deletion of hypoxia-inducible factor-2alpha (HIF-2alpha) alters vascular function and tumor angiogenesis. *Blood* **114,** 469-477.

Skuli N & Simon MC. (2009). HIF-1alpha versus HIF-2alpha in endothelial cells and vascular functions: is there a master in angiogenesis regulation? *Cell Cycle* **8,** 3252-3253.

Smith-Swintosky VL, Pettigrew LC, Sapolsky RM, Phares C, Craddock SD, Brooke SM & Mattson MP. (1996). Metyrapone, an inhibitor of glucocorticoid production, reduces brain injury induced by focal and global ischemia and seizures. *J Cereb Blood Flow Metab* **16,** 585-598.

St-Pierre J, Drori S, Uldry M, Silvaggi JM, Rhee J, Jager S, Handschin C, Zheng K, Lin J, Yang W, Simon DK, Bachoo R & Spiegelman BM. (2006). Suppression of reactive oxygen species and neurodegeneration by the PGC-1 transcriptional coactivators. *Cell* **127,** 397-408.

Stanley F, Blair E, Rice G, Stone P, Robinson J, Henderson-Smart D, Yu V, Harbord M, Stern L, Chambers H & et al. (1995). The origins of cerebral palsy--a consensus statement: The Australian and New Zealand perinatal Societies. *Aust Coll Midwives Inc J* **8,** 19-25.

Stanley FJ & Watson L. (1992). Trends in perinatal mortality and cerebral palsy in Western Australia, 1967 to 1985. *BMJ* **304,** 1658-1663.

Stevenson BR, Siliciano JD, Mooseker MS & Goodenough DA. (1986). Identification of ZO-1: a high molecular weight polypeptide associated with the tight junction (zonula occludens) in a variety of epithelia. *J Cell Biol* **103,** 755-766.

Stewart PA & Hayakawa K. (1994). Early ultrastructural changes in blood-brain barrier vessels of the rat embryo. *Brain Res Dev Brain Res* **78,** 25-34.

Stolp HB, Dziegielewska KM, Ek CJ, Potter AM & Saunders NR. (2005). Long-term changes in blood-brain barrier permeability and white matter following prolonged systemic inflammation in early development in the rat. *Eur J Neurosci* **22,** 2805-2816.

Stonestreet BS, Burgess GH & Cserr HF. (1992). Blood-brain barrier integrity and brain water and electrolytes during hypoxia/hypercapnia and hypotension in newborn piglets. *Brain Res* **590,** 263-270.

Stonestreet BS, Patlak CS, Pettigrew KD, Reilly CB & Cserr HF. (1996). Ontogeny of blood-brain barrier function in ovine fetuses, lambs, and adults. *Am J Physiol* **271,** R1594-1601.

Stonestreet BS, Petersson KH, Sadowska GB, Pettigrew KD & Patlak CS. (1999). Antenatal steroids decrease blood-brain barrier permeability in the ovine fetus. *Am J Physiol* **276,** R283-289.

Sun Y, Jin K, Xie L, Childs J, Mao XO, Logvinova A & Greenberg DA. (2003). VEGF-induced neuroprotection, neurogenesis, and angiogenesis after focal cerebral ischemia. *J Clin Invest* **111,** 1843-1851.

Suri C, Jones PF, Patan S, Bartunkova S, Maisonpierre PC, Davis S, Sato TN & Yancopoulos GD. (1996). Requisite role of angiopoietin-1, a ligand for the TIE2 receptor, during embryonic angiogenesis. *Cell* **87,** 1171-1180.

Svedin P, Hagberg H, Savman K, Zhu C & Mallard C. (2007). Matrix metalloproteinase-9 gene knock-out protects the immature brain after cerebral hypoxia-ischemia. *J Neurosci* **27,** 1511-1518.

Szymonowicz W, Walker AM, Cussen L, Cannata J & Yu VY. (1988). Developmental changes in regional cerebral blood flow in fetal and newborn lambs. *Am J Physiol* **254,** H52-58.

Takahashi A, Park HK, Melgar MA, Alcocer L, Pinto J, Lenzi T, Diaz FG & Rafols JA. (1997). Cerebral cortex blood flow and vascular smooth muscle contractility in a rat model of ischemia: a correlative laser Doppler flowmetric and scanning electron microscopic study. *Acta Neuropathol* **93,** 354-368.

Takashima S & Tanaka K. (1978a). Development of cerebrovascular architecture and its relationship to periventricular leukomalacia. *Arch Neurol* **35,** 11-16.

Takashima S & Tanaka K. (1978b). Microangiography and vascular permeability of the subependymal matrix in the premature infant. *Can J Neurol Sci* **5,** 45-50.

Temesvari P, Hencz P, Joo F, Eck E, Szerdahelyi P & Boda D. (1984). Modulation of the blood-brain barrier permeability in neonatal cytotoxic brain edema: laboratory and morphological findings obtained on newborn piglets with experimental pneumothorax. *Biol Neonate* **46,** 198-208.

Thanabalasundaram G, Pieper C, Lischper M & Galla HJ. (2010). Regulation of the blood-brain barrier integrity by pericytes via matrix metalloproteinases mediated activation of vascular endothelial growth factor in vitro. *Brain Res* **1347,** 1-10.

Thurston G, Rudge JS, Ioffe E, Zhou H, Ross L, Croll SD, Glazer N, Holash J, McDonald DM & Yancopoulos GD. (2000). Angiopoietin-1 protects the adult vasculature against plasma leakage. *Nat Med* **6,** 460-463.

Thurston G, Suri C, Smith K, McClain J, Sato TN, Yancopoulos GD & McDonald DM. (1999). Leakage-resistant blood vessels in mice transgenically overexpressing angiopoietin-1. *Science* **286,** 2511-2514.

Timpl R, Rohde H, Robey PG, Rennard SI, Foidart JM & Martin GR. (1979). Laminin--a glycoprotein from basement membranes. *J Biol Chem* **254,** 9933-9937.

Tomanek RJ & Schatteman GC. (2000). Angiogenesis: new insights and therapeutic potential. *Anat Rec* **261,** 126-135.

Trollmann R & Gassmann M. (2009). The role of hypoxia-inducible transcription factors in the hypoxic neonatal brain. *Brain Dev* **31,** 503-509.

Trommer BL, Groothuis DR & Pasternak JF. (1987). Quantitative analysis of cerebral vessels in the newborn puppy: the structure of germinal matrix vessels may predispose to hemorrhage. *Pediatr Res* **22,** 23-28.

Tsiantos A, Victorin L, Relier JP, Dyer N, Sundell H, Brill AB & Stahlman M. (1974). Intracranial hemorrhage in the prematurely born infant. Timing of clots and evaluation of clinical signs and symptoms. *J Pediatr* **85,** 854-859.

Uhm JH, Dooley NP, Oh LY & Yong VW. (1998). Oligodendrocytes utilize a matrix metalloproteinase, MMP-9, to extend processes along an astrocyte extracellular matrix. *Glia* **22,** 53-63.

Unno N, Giussani DA, Hing WK, Ding XY, Collins JH & Nathanielsz PW. (1997). Changes in adrenocorticotropin and cortisol responsiveness after repeated partial umbilical cord occlusions in the late gestation ovine fetus. *Endocrinology* **138,** 259-263.

Unno N, Wu WX, Wong CH, Bennett PR, Shinozuka N & Nathanielsz PW. (1998). Prostaglandin regulation of fetal plasma adrenocorticotropin and cortisol concentrations in late-gestation sheep. *Biol Reprod* **58,** 514-519.

Val-Laillet D, Simon M & Nowak R. (2004). A full belly and colostrum: two major determinants of filial love. *Dev Psychobiol* **45,** 163-173.

Valable S, Bellail A, Lesne S, Liot G, Mackenzie ET, Vivien D, Bernaudin M & Petit E. (2003). Angiopoietin-1-induced PI3-kinase activation prevents neuronal apoptosis. *FASEB J* **17,** 443-445.

Valable S, Montaner J, Bellail A, Berezowski V, Brillault J, Cecchelli R, Divoux D, Mackenzie ET, Bernaudin M, Roussel S & Petit E. (2005). VEGF-induced BBB permeability is associated with an MMP-9 activity increase in cerebral ischemia: both effects decreased by Ang-1. *J Cereb Blood Flow Metab* **25,** 1491-1504.

Van den Broeck C, Himpens E, Vanhaesebrouck P, Calders P & Oostra A. (2007). Influence of gestational age on the type of brain injury and neuromotor outcome in high-risk neonates. *Eur J Pediatr* **167,** 1005-1009.

van Zwieten EJ, Ravid R, Swaab DF & Van de Woude T. (1988). Immunocytochemically stained vasopressin binding sites on blood vessels in the rat brain. *Brain Res* **474,** 369-373.

VanBel F, Sola A, Roman C & Rudolph AM. (1997). Perinatal regulation of the cerebral circulation: Role of nitric oxide and prostaglandins. *Pediatric Research* **42,** 299-304.

Vanhatalo S & Kaila K. (2006). Development of neonatal EEG activity: from phenomenology to physiology. *Semin Fetal Neonatal Med* **11,** 471-478.

Vannucci SJ, Seaman LB, Brucklacher RM & Vannucci RC. (1994). Glucose transport in developing rat brain: glucose transporter proteins, rate constants and cerebral glucose utilization. *Mol Cell Biochem* **140,** 177-184.

Veltkamp R, Bieber K, Wagner S, Beynon C, Siebing DA, Veltkamp C, Schwaninger M & Marti HH. (2006). Hyperbaric oxygen reduces basal lamina degradation after transient focal cerebral ischemia in rats. *Brain Res* **1076,** 231-237.

Vermeulen PB, Gasparini G, Fox SB, Toi M, Martin L, McCulloch P, Pezzella F, Viale G, Weidner N, Harris AL & Dirix LY. (1996). Quantification of angiogenesis in solid human tumours: an international consensus on the methodology and criteria of evaluation. *Eur J Cancer* **32A,** 2474-2484.

Vexler ZS, Sharp FR, Feuerstein GZ, Ashwal S, Thoresen M, Yager JY & Ferriero DM. (2006). Translational stroke research in the developing brain. *Pediatr Neurol* **34,** 459-463.

Virgintino D, Errede M, Robertson D, Capobianco C, Girolamo F, Vimercati A, Bertossi M & Roncali L. (2004). Immunolocalization of tight junction proteins in the adult and developing human brain. *Histochem Cell Biol* **122,** 51-59.

Virgintino D, Errede M, Robertson D, Girolamo F, Masciandaro A & Bertossi M. (2003). VEGF expression is developmentally regulated during human brain angiogenesis. *Histochem Cell Biol* **119,** 227-232.

Virgintino D, Robertson D, Benagiano V, Errede M, Bertossi M, Ambrosi G & Roncali L. (2000). Immunogold cytochemistry of the blood-brain barrier glucose transporter GLUT1 and endogenous albumin in the developing human brain. *Brain Res Dev Brain Res* **123,** 95-101.

Virgintino D, Robertson D, Monaghan P, Errede M, Ambrosi G, Roncali L & Bertossi M. (1998). Glucose transporter GLUT1 localization in human foetus telencephalon. *Neurosci Lett* **256,** 147-150.

Vogel J, Horner C, Haller C & Kuschinsky W. (2003). Heterologous expression of human VEGF165 in rat brain: dose-dependent, heterogeneous effects on CBF in relation to vascular density and cross-sectional area. *J Cereb Blood Flow Metab* **23,** 423-431.

Volpe JJ. (1989). Intraventricular hemorrhage and brain injury in the premature infant. Neuropathology and pathogenesis. *Clin Perinatol* **16,** 361-386.

Volpe JJ. (1998). Brain injury in the premature infant: overview of clinical aspects, neuropathology, and pathogenesis. *Semin Pediatr Neurol* **5,** 135-151.

von Wasielewski R, Werner M, Nolte M, Wilkens L & Georgii A. (1994). Effects of antigen retrieval by microwave heating in formalin-fixed tissue sections on a broad panel of antibodies. *Histochemistry* **102,** 165-172.

Wagner S, Tagaya M, Koziol JA, Quaranta V & del Zoppo GJ. (1997). Rapid disruption of an astrocyte interaction with the extracellular matrix mediated by integrin alpha 6 beta 4 during focal cerebral ischemia/reperfusion. *Stroke* **28,** 858-865.

Walker DW. (1995). Hypoxic inhibition of breathing and motor activity in the foetus and newborn. *Clin Exp Pharmacol Physiol* **22,** 533-536.

Waltenberger J, Mayr U, Pentz S & Hombach V. (1996). Functional upregulation of the vascular endothelial growth factor receptor KDR by hypoxia. *Circulation* **94,** 1647-1654.

Wang J & Milner R. (2006). Fibronectin promotes brain capillary endothelial cell survival and proliferation through alpha5beta1 and alphavbeta3 integrins via MAP kinase signalling. *J Neurochem* **96,** 148-159.

Wang W, Dentler WL & Borchardt RT. (2001). VEGF increases BMEC monolayer permeability by affecting occludin expression and tight junction assembly. *Am J Physiol Heart Circ Physiol* **280,** H434-440.

Watson CS, Schaefer R, White SE, Homan JH, Fraher L, Harding R & Bocking AD. (2002). Effect of intermittent umbilical cord occlusion on fetal respiratory activity and brain adenosine in late-gestation sheep. *Reprod Fertil Dev* **14,** 35-42.

Weidner N, Semple JP, Welch WR & Folkman J. (1991). Tumor angiogenesis and metastasis--correlation in invasive breast carcinoma. *N Engl J Med* **324,** 1-8.

Wick A, Wick W, Waltenberger J, Weller M, Dichgans J & Schulz JB. (2002). Neuroprotection by hypoxic preconditioning requires sequential activation of vascular endothelial growth factor receptor and Akt. *J Neurosci* **22,** 6401-6407.

Wiener CM, Booth G & Semenza GL. (1996). In vivo expression of mRNAs encoding hypoxia-inducible factor 1. *Biochem Biophys Res Commun* **225,** 485-488.

Wigglesworth JS & Pape KE. (1978). An integrated model for haemorrhagic and ischaemic lesions in the newborn brain. *Early Hum Dev* **2,** 179-199.

Willis CL, Leach L, Clarke GJ, Nolan CC & Ray DE. (2004). Reversible disruption of tight junction complexes in the rat blood-brain barrier, following transitory focal astrocyte loss. *Glia* **48,** 1-13.

Wolff JR, Rajan KT & Noack W. (1974). The fate and fine structure of fragments of blood vessels in CNS tissue cultures. *Cell Tissue Res* **156,** 89-102.

Xu H, Hu F, Sado Y, Ninomiya Y, Borza DB, Ungvari Z, Lagamma EF, Csiszar A, Nedergaard M & Ballabh P. (2008). Maturational changes in laminin, fibronectin, collagen IV, and perlecan in germinal matrix, cortex, and white matter and effect of betamethasone. *J Neurosci Res* **86,** 1482-1500.

Yalow RS & Berson SA. (1960). Plasma insulin concentrations in nondiabetic and early diabetic subjects. Determinations by a new sensitive immuno-assay technic. *Diabetes* **9,** 254-260.

Yamagishi S, Yonekura H, Yamamoto Y, Fujimori H, Sakurai S, Tanaka N & Yamamoto H. (1999). Vascular endothelial growth factor acts as a pericyte mitogen under hypoxic conditions. *Lab Invest* **79,** 501-509.

Yamaji R, Okada T, Moriya M, Naito M, Tsuruo T, Miyatake K & Nakano Y. (1996). Brain capillary endothelial cells express two forms of erythropoietin receptor mRNA. *Eur J Biochem* **239,** 494-500.

Yan E, Castillo-Melendez M, Nicholls T, Hirst J & Walker D. (2004). Cerebrovascular responses in the fetal sheep brain to low-dose endotoxin. *Pediatr Res* **55,** 855-863.

Yan EB, Baburamani AA, Walker AM & Walker DW. (2009). Changes in cerebral blood flow, cerebral metabolites, and breathing movements in the sheep fetus following asphyxia produced by occlusion of the umbilical cord. *Am J Physiol Regul Integr Comp Physiol* **297,** R60-69.

Yancopoulos GD, Davis S, Gale NW, Rudge JS, Wiegand SJ & Holash J. (2000). Vascular-specific growth factors and blood vessel formation. *Nature* **407,** 242-248.

Yang D, Nemkul N, Shereen A, Jone A, Dunn RS, Lawrence DA, Lindquist D & Kuan CY. (2009). Therapeutic administration of plasminogen activator inhibitor-1 prevents hypoxic-ischemic brain injury in newborns. *J Neurosci* **29,** 8669-8674.

Yang SZ, Zhang LM, Huang YL & Sun FY. (2003). Distribution of Flk-1 and Flt-1 receptors in neonatal and adult rat brains. *Anat Rec A Discov Mol Cell Evol Biol* **274,** 851-856.

Yao X, Miao W, Li M, Wang M, Ma J, Wang Y, Miao L & Feng H. (2010). Protective effect of albumin on VEGF and brain edema in acute ischemia in rats. *Neurosci Lett* **472,** 179-183.

Yawno T, Yan EB, Hirst JJ & Walker DW. (2010). Neuroactive steroids induce changes in fetal sheep behavior during normoxic and asphyxic states. *Stress*.

Yeo EJ, Cho YS, Kim MS & Park JW. (2008). Contribution of HIF-1alpha or HIF-2alpha to erythropoietin expression: in vivo evidence based on chromatin immunoprecipitation. *Ann Hematol* **87,** 11-17.

Young PP, Fantz CR & Sands MS. (2004). VEGF disrupts the neonatal blood-brain barrier and increases life span after non-ablative BMT in a murine model of congenital neurodegeneration caused by a lysosomal enzyme deficiency. *Exp Neurol* **188,** 104-114.

Yurchenco PD & Schittny JC. (1990). Molecular architecture of basement membranes. *FASEB J* **4,** 1577-1590.

Zalewska T, Ziemka-Nalecz M, Sarnowska A & Domanska-Janik K. (2002). Involvement of MMPs in delayed neuronal death after global ischemia. *Acta Neurobiol Exp (Wars)* **62,** 53-61.

Zhang ZG, Zhang L, Jiang Q & Chopp M. (2002a). Bone marrow-derived endothelial progenitor cells participate in cerebral neovascularization after focal cerebral ischemia in the adult mouse. *Circ Res* **90,** 284-288.

Zhang ZG, Zhang L, Jiang Q, Zhang R, Davies K, Powers C, Bruggen N & Chopp M. (2000). VEGF enhances angiogenesis and promotes blood-brain barrier leakage in the ischemic brain. *J Clin Invest* **106,** 829-838.

Zhang ZG, Zhang L, Tsang W, Soltanian-Zadeh H, Morris D, Zhang R, Goussev A, Powers C, Yeich T & Chopp M. (2002b). Correlation of VEGF and angiopoietin expression with disruption of blood-brain barrier and angiogenesis after focal cerebral ischemia. *J Cereb Blood Flow Metab* **22,** 379-392.

Zhu Y, Lee C, Shen F, Du R, Young WL & Yang GY. (2005). Angiopoietin-2 facilitates vascular endothelial growth factor-induced angiogenesis in the mature mouse brain. *Stroke* **36,** 1533-1537.

Zoellner H, Hofler M, Beckmann R, Hufnagl P, Vanyek E, Bielek E, Wojta J, Fabry A, Lockie S & Binder BR. (1996). Serum albumin is a specific inhibitor of apoptosis in human endothelial cells. *J Cell Sci* **109 (Pt 10),** 2571-2580.

APPENDICES

TABLE OF CONTENTS

APPENDIX 1 - CORTISOL REAGENTS

Cortisol Assay Buffer

PB (0.5M, pH 7.4)

Molarity		Made to 100 ml
0.5 M	di-Sodium hydrogen $NaH_2PO_4.H_2O$	12.48 g
0.5 M	Sodium di- Na_2HPO_4	45.12 g
	Distilled water	Up to 100 ml

Cortisol Assay Buffer (0.05M, pH 7.4)

Molarity		Made to 1000 ml
0.05 M	0.5 M - PB	100 ml
	Distilled water	Up to 900 ml

Store at 4°C for 4 weeks

^{3}H – Cortisol

Stock Solution – ^{3}H

Concentration		Made to 10 ml
1 part	250 µCi [1, 2, 6, 7-^{3}H] Cortisol	
9 parts	Toluene	9 ml

Store at -20°C

Working Solution – ^{3}H

Concentration	
^{3}H – Cortisol Stock (dry down)	~30 µl
Cortisol Assay Buffer	10 ml

Check on counter, want ~10000 cpm, dilute accordingly.

γ-Globulin

Molarity		Made to 500 ml
8 g/ml	γ-Globulin	40 g
	Cortisol Assay Buffer	Up to 1000 ml

Antiserum

Stock Solution - Antiserum - 1/50

Concentration		
1:50	Antiserum	10 mg
50%	Cortisol Assay Buffer	2.93 ml
50%	Glycerol	2.93 ml

Working Dilution- Antiserum - 1/5000

Concentration		
1:5000	Antiserum Stock	100 µl
	Cortisol Assay Buffer	10 ml

22% Polyethylene Glycol

Molarity		**Made to 1000 ml**
22%	Polyethylene Glycol 6000	220 ml
0.1%	Sodium Azide	1 g
	Distilled water	Up to 1000 ml (does expand)

APPENDIX 2 - IMMUNOHISTOCHEMISTRY REAGENTS

Phosphate Buffered Saline (PBS – pH 7.4)

PB (0.2M, pH 7.4)

Molarity		Made to 2000 ml
0.2 M	di-Sodium hydrogen $NaH_2PO_4.H_2O$	12.48 g
0.2 M	Sodium di- Na_2HPO_4	45.12 g
	Distilled water	Up to 2000 ml

PBS (0.1M, pH 7.4)

Molarity		Made to 2000 ml
0.1 M	0.2 M - PB	1000 ml
0.9%	NaCl	18 g
	Distilled water	Up to 1000 ml

Tris Buffered Saline (TBS, pH 10)

Molarity		Made to 1000 ml
0.05M	Tris Base	6.1 g
0.9%	NaCl	9 g
	Distilled water	Up to 1000 ml

Citric Acid Buffer (pH 6.0)

Molarity		Made to 1000 ml
0.01M	Citric Acid (MW 192.13) or (MW 210.14)	1.92 g 2.10 g
	Distilled water	Up to 1000 ml

Proteinase K (40 ug/ml) – Tris-EDTA

Tris-EDTA Buffer (pH 8.0)

Molarity		Made to 1000 ml
50mM	Tris Base	6.10 g
1mM	EDTA	0.37g
0.5%	Triton X-100	5 ml
	Distilled water	Up to 1000 ml

Mix to dissolve.

Store at room temperature.

Stock Solution - Proteinase K

Concentration		Made to 10 ml
400 µg/ml	Proteinase K	4 mg
	Tris-EDTA Buffer	5 ml
	Glycerol	5 ml

Mix well, aliquot and store at –20 °C for 2-3 years.

Working Solution – Proteinase K

Concentration		Made to 10 ml
40 µg/ml	Proteinase K	1 ml
	Tris-EDTA Buffer	9 ml

Mix well.

This solution is stable for 1 month at 4 °C.

Blocking Buffer – Goat/Rabbit

Concentration		Made to 100 ml	
2%	Normal goat serum or rabbit serum	2 ml	Blocking
1%	Bovine serum albumin (BSA)	1 g	
0.1%	Cold fish gelatin	0.1 g	Blocking
0.1%	Triton X-100	0.1 g	Penetration
0.05%	Tween 20	50 µl	Detergent
0.05%	Sodium Azide	0.05 g	Preservative
0.01M	PBS (pH 7.4)	Up to 100 ml	

Mix well and store at 4 ºC.

Primary Antibody Diluent

Concentration		Made to 100 ml	
1%	Bovine serum albumin (BSA)	1 g	
0.1%	Cold fish gelatin	0.1 g	Blocking
0.05%	Sodium Azide	0.05 g	Preservative
0.01M	PBS (pH 7.4)	Up to 100 ml	

Mix well and store at 4 ºC.

APPENDIX 3 – IMMUNOHISTOCHEMISTRY PROTOCOLS

	Albumin	Ki67	Epo	Laminin
Antigen Retrieval	-	Microwave	Microwave	Oven
Buffer	-	Citric acid buffer (pH 6.0)	Citric Acid Buffer (pH 6)	Proteinase K (40 µg/ml) in Tris-EDTA Buffer (pH 8.0)
Heat Time	-	3 x 10 min	2 x 5 min	30 min at 37°C
Cool Time	-	30 min at RT	30 min at RT	20 min at RT
Block endogenous peroxidises	3% H_2O_2 in 50% MeOH	3% H_2O_2 in dH_2O	3% H_2O_2 in 50% MeOH	0.3% H_2O_2 in 50% MeOH
Time/Temp	10 min at RT	10 min at RT	10 min at RT	15 min at RT
Blocking Solution	Protein free blocker (DAKO)	5% NGS + 2% BSA in PBS	5 % NGS + 2% BSA in PBS	NGSBB
Time/Temp	60 min at RT	45 min at RT	60 min at RT	30 min at RT
Primary Antibody	Rabbit anti-Sheep (Accurate Chemical and Scientific, USA)	Rabbit anti-Ki67 (Thermo, USA)	Rabbit anti-Epo (Santa Cruz, USA)	Rabbit anti-Laminin (Novus Biologicas, USA)
Dilution	1:1000	1:100	1:200	1:200
Diluent	DAKO Real Diluent	PBS	Dako REAL Diluent	Primary Antibody Diluent
Time/Temp	4°C O/N	4°C O/N	60 min at RT, O/N at 4°C	60 min at RT, O/N at 4°C
Secondary Antibody	Goat anti-Rabbit (Vector Laboratories, USA)	Goat anti-Rabbit (Vector Laboratories, USA)	Goat anti-Rabbit (Vector Laboratories, USA)	Goat anti-Rabbit (Vector Laboratories, USA)
Dilution	1:200	1:200	1:500	1:200
Time/Temp	60 min at RT	45 min at RT	60 min at RT	45 min at RT
Strep/HRP	Amersham Pharmacia Biotech, USA	Amersham Pharmacia Biotech, USA	Amersham Pharmacia Biotech, USA	Amersham Pharmacia Biotech, USA
Dilution	1:200	1:200	1:200	1:200
Time/Temp	30 min at RT	45 min at RT	30 min at RT	45 min at RT
Chromagen	DAB (Pierce, USA)	DAB (Pierce, USA)	DAB (Pierce, USA)	DAB (Pierce, USA)
Dilution	1:10	1:10	1:10	1:10
Time/Temp	10 – 15 min at RT	10 – 15 min at RT	10 – 15 min at RT	10 min at RT

	VEGF	VEGFR-2 (KDR-flt-1)	Angiopoietin-1
Antigen Retrieval	Microwave	Microwave	Microwave
Buffer	TBS (pH 10)	Citric Acid Buffer (pH 6)	Citric Acid Buffer (pH 6)
Heat Time	3 x 10 min	3 x 5 min	2 x 5 min
Cool Time	30 min at RT	30 min at RT	30 min at RT
Block endogenous peroxidases	0.3% H_2O_2 in PBS	3% H_2O_2 in 50% MeOH	3% H_2O_2 in 50% MeOH
Time/Temp	10 min at RT	10 min at RT	10 min at RT
Blocking Solution	NGSBB	5 % NGS + 2% BSA in PBS	DAKO Protein Block
Time/Temp	60 min	60 min at RT	60 min
Primary Antibody	Mouse anti-VEGF (Novus Biologicas, USA)	Rabbit anti-VEGFR-2 (Abcam, USA)	Rabbit anti-Angpt 1 (Abcam, USA)
Dilution	1:200	1:200	1:200
Diluent	True Vision (Sapphire Bioscience)	Dako REAL Diluent	DAKO Real Diluent
Time/Temp	60 min at RT, O/N at 4°C	60 min at RT, O/N at 4°C	60 min at RT, O/N at 4°C
Secondary Antibody	Goat anti-mouse (Dako, Australia)	Goat anti-Rabbit (Vector Laboratories, USA)	Goat anti-Rabbit (Vector Laboratories, USA)
Dilution	1:200	1:500	1:200
Time/Temp	60 min RT	60 min at RT	30 min RT
Strep/HRP	Amersham Pharmacia Biotech, USA	Amersham Pharmacia Biotech, USA	Amersham Pharmacia Biotech, USA
Dilution	1:200	1:200	1:200
Time/Temp	60 min at RT	30 min at RT	60 min at RT
Chromagen	DAB (Pierce, USA)	DAB (Pierce, USA)	DAB (Pierce, USA)
Dilution	1:10	1:10	1:10
Time/Temp	10 min at RT	5 min at RT	5 min at RT

APPENDIX 4 – COMPLETE BLOOD GAS TABLE FROM CHAPTER 6

	Treatment	-1 h	- 5 min	+5 min	+9 min	+30 min	+1 h	+2 h
pO_2 (mmHg)	*Control*	22.54 ± 1.02	22.56 ± 1.20	22.76 ± 0.96	24.08 ± 1.25	23.42 ± 1.10	22.48 ± 0.92	22.28 ± 0.98
	Mild UCO	22.20 ± 1.13	21.54 ± 1.01	12.20 ± 2.10*	14.58 ± 1.34*	21.82 ± 1.57	20.98 ± 1.69	20.96 ± 1.10
	Severe UCO	22.63 ± 1.57	22.72 ± 1.68	5.10 ± 1.47*[#]	5.25 ± 1.45*[#]	23.67 ± 2.26	23.63 ± 1.07	22.50 ± 1.55
pCO_2 (mmHg)	*Control*	50.34 ± 1.00	50.48 ± 0.70	50.92 ± 0.27	51.52 ± 0.94	50.86 ± 0.39	50.12 ± 0.56	49.68 ± 0.67
	Mild UCO	51.82 ± 1.15	51.50 ± 1.14	76.14 ± 7.11*	74.80 ± 9.04*	52.58 ± 1.30	50.38 ± 1.44	49.60 ± 1.06
	Severe UCO	50.63 ± 0.89	49.92 ± 0.70	101.52 ± 3.70*[#]	126.50 ± 3.00*[#]	55.43 ± 1.64	48.15 ± 48.20	48.20 ± 0.64
pH	*Control*	7.36 ± 0.00	7.35 ± 0.01	7.35 ± 0.01	7.35 ± 0.01	7.35 ± 0.01	7.36 ± 0.01	7.36 ± 0.01
	Mild UCO	7.36 ± 0.01	7.36 ± 0.01	7.20 ± 0.04*	7.16 ± 0.05*	7.29 ± 0.02	7.33 ± 0.01	7.36 ± 0.01
	Severe UCO	7.37 ± 0.01	7.37 ± 0.01	7.05 ± 0.02*[#]	6.92 ± 0.01*[#]	7.19 ± 0.01*	7.29 ± 0.02	7.33 ± 0.01
O_2 Sat (%)	*Control*	64.62 ± 2.83	63.10 ± 3.22	64.00 ± 2.27	67.26 ± 2.78	65.10 ± 3.44	63.54 ± 3.05	63.42 ± 2.43
	Mild UCO	58.40 ± 2.20	56.20 ± 2.35	18.22 ± 4.99*	23.78 ± 3.99*	52.26 ± 3.74	52.02 ± 4.80	53.92 ± 3.26
	Severe UCO	61.08 ± 4.59	61.20 ± 4.87	6.72 ± 1.56*[#]	5.93 ± 1.22*[#]	51.80 ± 6.68	59.63 ± 3.91	58.55 ± 5.10
Glucose (mmol/L)	*Control*	0.80 ± 0.10	0.80 ± 0.08	0.80 ± 0.08	0.84 ± 0.10	0.84 ± 0.13	0.92 ± 0.10	0.88 ± 0.10
	Mild UCO	1.04 ± 0.05	1.02 ± 0.04	1.36 ± 0.20	2.10 ± 0.49*	1.52 ± 0.23*	1.24 ± 0.14	1.34 ± 0.14
	Severe UCO	0.97 ± 0.06	1.02 ± 0.05	0.52 ± 0.07	1.38 ± 0.28[#]	1.83 ± 0.12*	1.50 ± 0.06*	1.63 ± 0.10*
Lactate (mmol/L)	*Control*	1.28 ± 0.04	1.26 ± 0.05	1.28 ± 0.04	1.22 ± 0.06	1.32 ± 0.10	1.32 ± 0.10	1.24 ± 0.07
	Mild UCO	1.56 ± 0.08	1.48 ± 0.13	3.28 ± 0.73*	4.02 ± 0.89*	4.28 ± 0.96*	3.46 ± 0.80*	2.56 ± 0.54
	Severe UCO	1.55 ± 0.08	1.53 ± 0.09	7.03 ± 0.67*[#]	9.57 ± 0.56*[#]	7.90 ± 0.24*[#]	6.52 ± 0.41*[#]	5.17 ± 0.57*[#]
Cortisol	*Control*	12.98 ± 5.09	5.43 ± 1.56	6.03 ± 2.26	9.66 ± 5.46	11.03 ± 5.71	5.33 ± 1.50	10.43 ± 4.61

Mild UCO	10.82 ± 2.48	15.44 ± 3.94	$38.83 \pm 6.52^*$	$48.92 \pm 3.41^*$	$61.67 \pm 11.17^*$	$42.84 \pm 15.65^*$	17.56 ± 2.49
Severe UCO	7.17 ± 2.46	5.07 ± 1.28	$7.27 \pm 2.79^{\#}$	$6.60 \pm 0.99^{\#}$	$33.27 \pm 5.90^{\#}$	$31.81 \pm 6.27^*$	31.01 ± 8.13

	Treatment	+4 h	+6 h	+8 h	+10 h	+12 h	+24 h	+48 h
pO_2 (mmHg)	*Control*	22.16 ± 0.80	22.22 ± 0.93	23.10 ± 0.94	24.44 ± 1.64	22.02 ± 1.14	22.06 ± 0.90	21.38 ± 1.00
	Mild UCO	21.30 ± 1.29	20.26 ± 1.11	21.38 ± 1.21	21.30 ± 1.14	21.16 ± 1.16	21.22 ± 1.39	20.44 ± 1.46
	Severe UCO	21.93 ± 1.91	22.08 ± 1.84	22.48 ± 1.78	21.82 ± 1.86	22.08 ± 1.74	22.72 ± 1.18	22.57 ± 1.42
pCO_2 (mmHg)	*Control*	49.86 ± 0.61	49.34 ± 0.55	51.00 ± 0.69	50.24 ± 0.77	51.74 ± 0.37	50.58 ± 0.37	51.86 ± 0.82
	Mild UCO	51.12 ± 1.09	51.52 ± 1.37	51.48 ± 1.44	50.74 ± 0.75	50.44 ± 1.21	51.62 ± 2.15	51.48 ± 1.00
	Severe UCO	47.85 ± 0.77	48.23 ± 0.76	48.38 ± 0.97	49.00 ± 0.98	48.43 ± 0.87	48.82 ± 1.37	48.82 ± 1.37
pH	*Control*	7.35 ± 0.00	7.36 ± 0.01	7.36 ± 0.01	7.37 ± 0.01	7.35 ± 0.00	7.35 ± 0.00	7.35 ± 0.00
	Mild UCO	7.37 ± 0.01	7.36 ± 0.01	7.36 ± 0.01	7.37 ± 0.01	7.37 ± 0.01	7.36 ± 0.01	7.38 ± 0.01
	Severe UCO	7.37 ± 0.01	7.38 ± 0.01	7.38 ± 0.01	7.38 ± 0.01	7.38 ± 0.01	7.37 ± 0.00	7.38 ± 0.01
O_2 Sat (%)	*Control*	62.44 ± 2.83	63.12 ± 3.58	64.82 ± 2.69	67.92 ± 3.08	61.56 ± 3.71	61.94 ± 3.29	58.98 ± 3.09
	Mild UCO	54.88 ± 3.07	51.42 ± 2.52	53.72 ± 2.92	54.46 ± 2.34	54.40 ± 2.87	54.94 ± 3.18	53.12 ± 4.33
	Severe UCO	57.72 ± 6.54	58.12 ± 5.34	61.05 ± 5.36	58.20 ± 6.07	59.22 ± 4.93	61.68 ± 3.55	61.08 ± 3.80
Glucose (mmol/L)	*Control*	0.96 ± 0.11	0.96 ± 0.11	1.04 ± 0.14	0.94 ± 0.12	0.98 ± 0.10	1.02 ± 0.10	0.94 ± 0.06
	Mild UCO	1.24 ± 0.12	1.22 ± 0.06	1.12 ± 0.06	1.08 ± 0.04	1.08 ± 0.05	1.02 ± 0.04	1.04 ± 0.10
	Severe UCO	1.62 ± 0.14*	1.53 ± 0.14*	1.37 ± 0.13	1.20 ± 0.12	1.20 ± 0.09	1.37 ± 0.08	1.18 ± 0.14
Lactate (mmol/L)	*Control*	1.36 ± 0.07	1.38 ± 0.09	1.46 ± 0.14	1.58 ± 0.30	1.50 ± 0.18	1.42 ± 0.11	1.58 ± 0.30
	Mild UCO	2.08 ± 0.42	1.86 ± 0.27	1.74 ± 0.23	1.68 ± 0.25	1.76 ± 0.20	1.70 ± 0.14	1.76 ± 0.15
	Severe UCO	4.32 ± 0.51*[#]	3.68 ± 0.52*[#]	2.85 ± 0.40	2.45 ± 0.39	2.08 ± 0.25	1.93 ± 0.13	1.53 ± 0.07
Cortisol	*Control*	5.64 ± 1.68	14.51 ± 9.37	14.84 ± 9.90	9.62 ± 4.08	13.00 ± 7.02	12.15 ± 3.88	8.41 ± 3.62
	Mild UCO	10.88 ± 1.93	23.22 ± 3.75	12.68 ± 2.44	12.07 ± 3.17	14.64 ± 4.66	14.64 ± 4.66	50.74 ± 41.63
	Severe UCO	29.76 ± 8.58*	24.84 ± 4.35	19.89 ± 4.21	12.25 ± 0.64	18.98 ± 6.38	38.36 ± 8.85*	16.84 ± 2.58

	Treatment	+3 days	+4 days	+5 days	+6 days	+7 days	+8 days	+9 days
pO_2 (mmHg)	*Control*	21.26 ± 0.67	21.26 ± 1.31	20.98 ± 1.20	20.92 ± 1.28	19.84 ± 1.56	20.66 ± 1.71	21.60 ± 2.15
	Mild UCO	18.33 ± 2.36	18.57 ± 3.41					
	Severe UCO	20.95 ± 1.88	19.42 ± 1.64	21.96 ± 1.75	19.73 ± 2.26	21.03 ± 2.94	24.30 ± 1.85	22.67 ± 0.78
pCO_2 (mmHg)	*Control*	51.46 ± 0.65	51.42 ± 1.25	50.26 ± 0.72	51.12 ± 0.92	51.78 ± 0.42	52.48 ± 0.96	49.90 ± 0.76
	Mild UCO	52.58 ± 1.28	56.07 ± 2.87					
	Severe UCO	50.07 ± 1.16	51.10 ± 1.74	48.34 ± 1.39	50.55 ± 1.43	51.88 ± 1.27	49.80 ± 1.00	50.90 ± 0.38
pH	*Control*	7.35 ± 0.00	7.35 ± 0.00	7.36 ± 0.00	7.37 ± 0.01	7.36 ± 0.00	7.35 ± 0.01	7.36 ± 0.01
	Mild UCO	7.36 ± 0.02	7.33 ± 0.04					
	Severe UCO	7.38 ± 0.01	7.38 ± 0.01	7.37 ± 0.01	7.37 ± 0.01	7.33 ± 0.03	7.37 ± 0.00	7.37 ± 0.01
O_2 Sat (%)	*Control*	58.54 ± 1.29	57.44 ± 4.26	58.28 ± 3.72	57.16 ± 4.01	52.70 ± 4.79	54.04 ± 5.63	57.30 ± 6.34
	Mild UCO	42.58 ± 6.72	42.53 ± 10.79					
	Severe UCO	55.88 ± 4.85	50.43 ± 6.17	57.32 ± 4.73	49.10 ± 7.72	51.03 ± 7.68	59.00 ± 3.79	54.23 ± 2.23
Glucose (mmol/L)	*Control*	0.98 ± 0.07	1.08 ± 0.07	0.84 ± 0.05	1.00 ± 0.08	0.94 ± 0.04	0.94 ± 0.04	3.77 ± 2.62
	Mild UCO	1.25 ± 0.10	1.73 ± 0.58					
	Severe UCO	1.25 ± 0.13	1.22 ± 0.23	1.12 ± 0.16	1.03 ± 0.12	0.98 ± 0.07	1.17 ± 0.18	1.07 ± 0.07
Lactate (mmol/L)	*Control*	1.44 ± 0.07	1.56 ± 0.19	1.54 ± 0.22	1.64 ± 0.19	1.86 ± 0.35	2.90 ± 1.55	1.57 ± 0.12
	Mild UCO	3.45 ± 1.46	3.83 ± 2.19					
	Severe UCO	1.60 ± 0.12	2.70 ± 1.05	1.74 ± 0.17	1.55 ± 0.10	1.60 ± 0.15	1.50 ± 0.15	1.43 ± 0.07
Cortisol	*Control*	9.62 ± 5.24	19.77 ± 12.14	20.42 ± 7.09	22.87 ± 10.73	8.95 ± 3.81	21.27 ± 14.52	31.30 ± 20.05
	Mild UCO							
	Severe UCO	7.70 ± 2.07	27.89 ± 12.06	36.63 ± 10.81	18.94 ± 7.78	19.31 ± 8.02		

	Treatment	**+10 days**	**+11 days**	**+12 days**	**+13 days**	**+14 days**
pO$_2$ (mmHg)	*Control*	20.47 ± 1.34	22.43 ± 0.64	21.40 ± 2.32	21.30 ± 3.07	21.73 ± 2.92
	Mild UCO					
	Severe UCO					
pCO$_2$ (mmHg)	*Control*	50.80 ± 1.46	47.73 ± 1.27	50.20 ± 51.50	51.50 ± 0.75	49.73 ± 0.94
	Mild UCO					
	Severe UCO					
pH	*Control*	7.36 ± 0.01	7.37 ± 0.01	7.36 ± 0.00	7.35 ± 0.01	7.37 ± 0.02
	Mild UCO					
	Severe UCO					
O$_2$ Sat (%)	*Control*	54.23 ± 4.77	59.73 ± 1.99	54.83 ± 6.93	53.00 ± 10.65	54.93 ± 9.19
	Mild UCO					
	Severe UCO					
Glucose (mmol/L)	*Control*	1.03 ± 0.03	1.00 ± 0.06	1.03 ± 0.03	1.03 ± 0.07	1.20 ± 0.17
	Mild UCO					
	Severe UCO					
Lactate (mmol/L)	*Control*	1.47 ± 0.12	1.40 ± 0.06	1.33 ± 0.20	1.30 ± 0.15	1.27 ± 0.12
	Mild UCO					
	Severe UCO					
Cortisol	*Control*	53.21 ± 22.97	45.14 ± 24.61			
	Mild UCO					
	Severe UCO					

APPENDIX 5 – QUANTITATIVE REAL-TIME POLYMERASE CHAIN

REACTION

Quantitative real-time polymerase chain reaction (qRT-PCR) was used to determine the relative amount of mRNA expression for VEGF, VEGFR-2 (Flk-1), HIF-1α and HIF-2α. These protocols were run with the kind assistance of Ms. Annie McDougall, Ms. Valerie Zahra and Ms. Maria Papiouannou (The Ritchie Centre, Monash Institute of Medical Research).

Total RNA extraction and DNase treatment of RNA

Total ribonucleic acids (RNA) were extracted from snap frozen brain tissue that was stored at -80°C, using an RNeasy midi RNA extraction kit (Qiagen, Australia). RNA extraction included the addition of DNase (Qiagen, Australia) to remove contaminating genomic DNA from the RNA sample; all solutions were provided in the kit. RNA was extracted using the specific protocol for animal tissues (pg. 41 RNeasy Midi Handbook, Qiagen, Australia).

In brief, brain tissue (0.1 g) was homogenised in 2 ml solution of β-mercaptoethanol and Buffer RLT (ratio 10µl:1ml respectively), centrifuged for 10 min at 4700 xg, with the supernatant collected and transferred to a 15ml collection tube. An equal volume of 70% ethanol was added and vigorously mixed, and the solution was transferred to an RNeasy midi column in another 15 ml collection tube. Tubes were centrifuged for 5 min at 4700 xg, washed with buffer RW1 (2 ml), and centrifuged (5 min at 4700 xg). DNase 1 solution (160µl, 1:7 dilution in buffer RDD) was added to each sample and incubated at room temp for 15 minutes to digest any genomic DNA present in the samples. Washed in buffer RW1 (2 ml) was added and samples were centrifuged (5 min at 4700 xg). Buffer RPE (2.5 ml; diluted 1:4 with 100% ethanol) was added to each midi column before they were centrifuged for 2 min (4700 xg); this step was repeated and then the tube was centrifuged for a further 2mins. The midi column was placed in a new collection tube and 150 µl RNase-free water was added to each sample. Samples were incubated on the bench for 1 min and centrifuged (3 min at 4700 xg). The supernatant was then run

through the column a second time to elute the DNase-treated RNA which was then stored at -70°C.

The RNA concentration and purity was determined by measuring the absorbance (optical density, OD) of each sample (1:20 dilution, 5 µl of RNA in 95 µl of mQH$_2$O) at 260 nm and 280 nm with a spectrophotometer (Eppendorf, Germany). The concentration of RNA was determined using the equation:

$$RNA\ concentration\ (\mu g/\mu l) = \frac{(OD_{260nm}\ x\ 40)\ x\ dilution\ factor}{1000}$$

RNA purity and degradation was determined by gel electrophoresis. RNA samples were diluted to ~1 µg total RNA in 4µl and were heated to 65°C for 5 mins to denature the RNA. 6x loading buffer (2 µl) was then added and each sample was loaded into a separate well on a 1% agarose gel containing gel Red (Biotium, USA) and electrophoresed for 30min at 80V. Gels were visualised on a gel documentation system (Chemidoc XRS, BioRad, USA)

cDNA synthesis

DNase-treated RNA was transcribed into complementary DNA (cDNA) using the Superscript III reverse transcription kit (Invitrogen, Australia) as per the manufacturer's instructions; all reagents were provided. Briefly, RNA (1 µg) was diluted to 11 µl in sterile RNase free water and incubated with 1µl of random hexamers and 1µl of dNTPs (concentration) at 65°C for 5 min to denature the RNA, then cooled on ice for 1 min. 5x reaction buffer (4 µl), DTT (1 µl), RNaseOUT (1 µl) and Superscript III reverse transcriptase enzyme (1 µl) were added to each RNA sample, giving a final volume of 20 µl (50 ng/µl of starting RNA). Each sample was incubated at room temperature for 5 minutes followed by 50°C for 60 minutes. The reaction was heat inactivated at 70°C for 15 min and the resulting cDNA was stored at -20°C. The final concentration of cDNA was 50 ng/µl used for VEGF, HIF 1α, HIF 2α, 18S and Rps29.

VEGFR2 qRT-PCR required 100 ng/µl cDNA, to achieve this 2 µg of RNA was diluted in the above protocol.

Primer Design and optimisation

Primers were designed and optimised by Ms. Valerie Zahra and Dr. Caitlin Filby (Filby et al., 2010) for real-time PCR using the computer program primer3 (http://frodo.wi.mit.edu/cgi-bin/primer3/primer3_www.cgi). For optimising primer quality Netprimer and to check for homology NCBI BLAST were used. For primer sequences see Table A1. To ensure precise and efficient amplification of the gene of interest primers were designed according to the principles below.

The optimum concentration of primers and cDNA (100, 50, 25, 10 ng/µl) for the most efficient reaction was determined for all genes of interest by selecting the combination that resulted in the highest plateau and the steepest replication curve and fastest replication. In addition, a melt curve analysis performed to ensure primer specificity to the gene of interest. Primers were reconstituted in 100µl of RNase-free water (Gibco, Australia). Each primer pair (forward and reverse) was then diluted to concentrations of 10µM.

Real-time PCR reaction

For all samples, qRT-PCR amplification was performed using the Fast Real Time PCR System (7900HT, Applied Biosystems). Each reaction contained 0.5 µl cDNA (50 ng/µl for VEGF, HIF-1α, HIF-2α and 100 ng/µl for VEGFR-2), 0.5 µl (10 µM) of each forward and reverse primers and 5 ml of SYBR green (Applied Biosystems) made up to 10 µl with sterile mQH2O. Following preparation of cDNA samples and all reagents were pipetted in triplicate on a 384 PCR plate (MicroAmp, Applied Biosystems, Singapore) using the Liquid Handler (Model CAS1200, Corbett, USA)

Table A5.1: Primers used for qRT-PCR

	Assecion #, Species,	Forward 5' – 3'	Reverse 5' – 3'	Annealing Temperature (°C)	cDNA Concentration (ng/µl)
VEGF	AF071015.1, Ovis aries	CGAAAGTCTGGAGTGTGTGC	TATGTGCTGGCTTTGGTGAG	60	50
VEGFR-2 (Flk-1)	AF534634, Ovis aries	CCCAATCAGAGACCCACG	GCCATCCTGTTGAGCGTTA	60	100
HIF-1α	BC126622, Bos Taurus	GGAAACTTCTGGATGCTGGT	GCAATTCATCTGTGCCTTCA	60	50
HIF-2α	AB018399, Bos Taurus	TGTCGGAGAACATCAGCAAG	CATGGTCACAGGGATGAGTG	60	50
18S	X01117, Rattus norvegicus	GTCTGTGATGCCCTTAGATGTC	AAGCTTATGACCCGCACTTAC	59 - 60	50
Rps29	NM174804 Rattus norvegicus/ Bos Taurus	CAGGGTTCTCGCTCTTGC	ACTGGCGGCACATATTGAG	60	50

Real-time PCR program

Quantitative real-time PCR was performed using Fast Real Time PCR System (7900HT, Applied Biosystems) with the following sequence:

An initial denaturation step at 50°C for 2 min and then 95°C for 10 min, followed by 50 cycles at 95°C for 15 sec, with a combination annealing and extension at the appropriate temperature (60°C) for the gene of interest for 60 sec; fluorescence was measured at the end of each cycle. Following the PCR program a melt curve was generated as follows to ensure a single product had been amplified per primer set: denaturation at 95°C for 15 sec, followed by a ramp-like increase in temperature from 60°C for 15 sec to 95°C, increasing by 0.5°C increments. No template reactions containing all reagents except the cDNA, were included to ensure no contaminating DNA was present.

The presence of double-stranded DNA was determined using the fluorescent dye SYBR Green, allowing for the quantification of the PCR products. Detection occurs at 494 nm at the end of the extension step of each cycle, resulting in an exponential increase in the amount of fluorescent with increasing cycle number. The level of fluorescence is plotted against the number of cycles, resulting in an amplification curve for each sample that can subsequently be analysed. The melt curve was analysed to determine if there was any non-specific binding of the primers to the cDNA, or if there was any primer-dimers forming. One peak in the melt curve of each sample indicated that the primer was only binding to the specific sequence of interest.

Real-time PCR analysis

The replication of each sample was analysed using Realplex systems analysis software (Applied Biosciences, USA). Each sample was performed in triplicate and analysed at the point at which the amplification plot crossed the 'threshold', which is set by the analysis software during the exponential replication phase, above the background fluorescence and below the plateau of replication. Triplicate values were averaged, if the standard deviation of these was >0.5 this

triplicate was excluded. Following this if the duplicate standard deviation was >0.5 then this sample was excluded.

The cycle number at which each sample crosses the threshold is referred to as the cycle threshold (C_T). Therefore a lower C_T value represents a higher level of mRNA, while a higher C_T means a lower mRNA level. To control for small differences in the amount of cDNA or global gene expression between samples, qRT-PCR was performed on each sample using either 18S or ribosomal protein 29 (Rps29) as housekeeping genes. The C_T of the housekeeping gene was subtracted from the C_T of the gene of interest (ΔC_T). The average C_T for the calibrator was subtracted from the ΔC_T of each sample ($\Delta\Delta C_t$). The mRNA levels for each sample were normalised (using the equation $2^{-\Delta\Delta C_T}$) and the results were expressed relative to the mean mRNA levels of the control group, allowing the C_T values and therefore the expression of the gene of interest to be compared between groups. The calculations are summarised in the equations below.

$$\Delta C_T = C_T \,(\text{Target gene}) - C_T \,(\text{House keeping gene})$$

$$\text{Normalised expression} = 2^{-\Delta\Delta C_T}$$

APPENDIX 6 – QUANTITATIVE REAL-TIME POLYMERASE CHAIN REACTION RESULTS

These preliminary qRT-PCR were run to investigate the mRNA expression of HIF-1α, HIF-2α, VEGF and VEGFR-2, from Control and 24 h post-UCO (Chapter 4), and controls and severe-UCO (Chapter 5) fetal sheep brains.

Chapter 4 - Analysis of HIF-1α, HIF-2α, VEGF and VEGFR-2 mRNA expression.

At 24 h post-UCO the expression of HIF-1α mRNA was significantly decreased (0.32 ± 0.13 relative expression) compared to controls ($p < 0.05$; Figure 1 A). VEGF and HIF-2α mRNA expression showed a trend to a decrease, however this was not significant (Figure 1 B, C). Statistical analysis was not done for VEGFR-2 because in this case the Control group, due to variable triplicate values, contained values from only 2 fetuses. However there appeared to be no change (Figure 1 D).
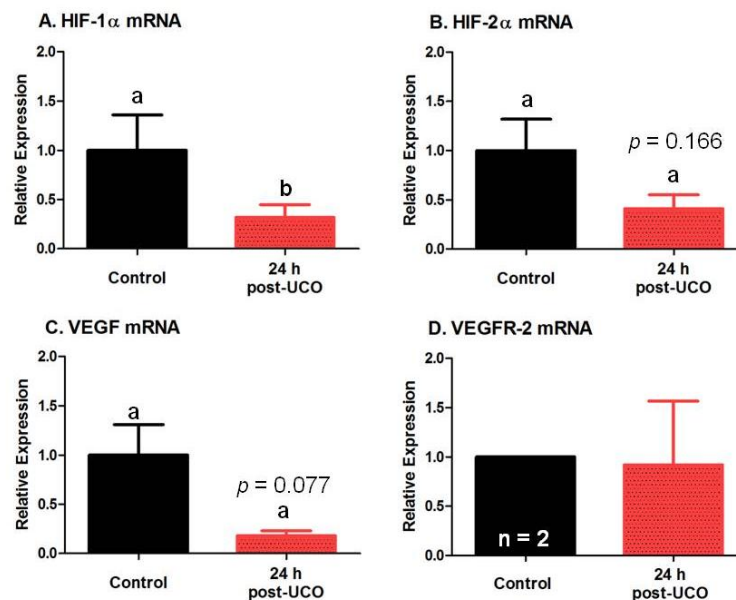

Figure A6.1: Gene expression of VEGF, VEGFR-2, HIF-1α and HIF-2α from fetal sheep brains. VEGF (A), VEGFR-2 (B), HIF-1α (C), HIF-2α (D) mRNA relative gene expression in Control (black) and 24 h post- UCO (red) fetal brains. All mRNA data are normalised to Rps29. Mean ± SEM.

Chapter 5 - Analysis of HIF-1α, HIF-2α, VEGF and VEGFR-2 mRNA expression.

Fetal brains were collected when ewe's were in labour or at 145 days GA. qRT-PCR was done on section of brain from Control (n = 5) and severe UCO (n = 5) fetuses to get an preliminary indication of mRNA expression.

No significant differences were seen in VEGF or VEGFR-2 mRNA expression between UCO Severe and Control fetal brain samples (Figure 2 A, B). There was also no significant difference in HIF-1α or HIF-2α mRNA relative expression between groups (Figure 2 C, D). Although this appears to be significant, when statistical analysis were run a failure to achieve homogeneity of variance (Levene's test) resulted in *p>*.05.
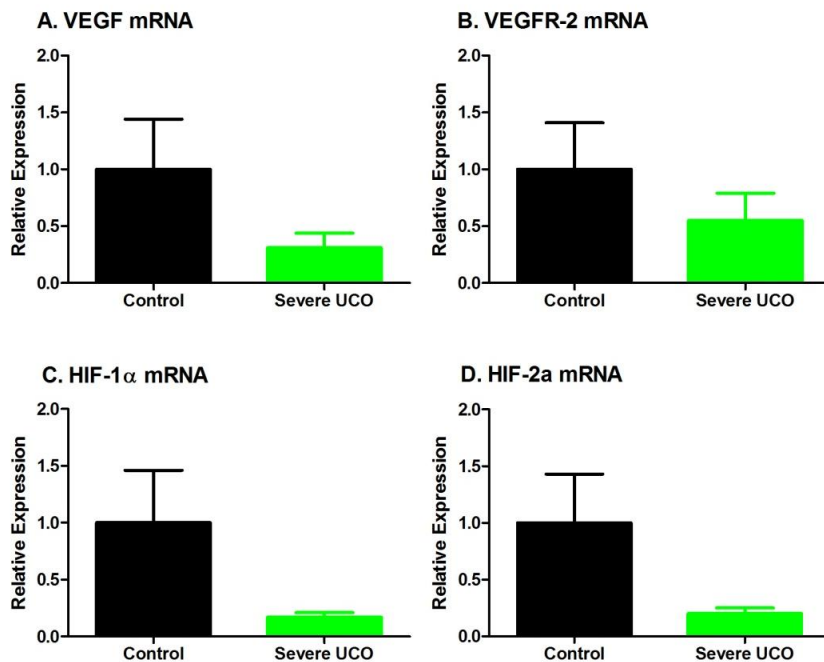
Figure A6.2: Gene expression of VEGF, VEGFR-2, HIF-1α and HIF-2α from fetal sheep brains. VEGF (A), VEGFR-2 (B), HIF-1α (C), HIF-2α (D) mRNA relative gene expression in Control (black) and severe UCO (green) fetal brains. All mRNA data are normalised to Rps29. Mean ± SEM.

Interestingly, there was a significant **decrease** of HIF-1α and a trend to a decrease of VEGF mRNA expression 24 h post-UCO. Due to the high standard error of control values, re-optimisation of the primers and conditions used is required to accurately make inferences from this data. The data does suggest that further investigation is required to understand the mechanisms that result in up-regulation of VEGF and VEGFR-2 following hypoxia in the fetal brain.

APPENDIX 7 – CHAPTER 5 AND 6 - CONTROL AND UCO SYSTEMIC & PREGNANCY OUTCOME DATA.

Response to UCO

Blood gases

Fetuses that were assigned to the UCO group (n=11) experienced hypoxia, hypercapnia and acidosis during UCO (Figure 1 A, B, C, D) when compared to controls (n=5). The arterial blood pO_2, pCO_2 and oxygen saturation returned to pre-UCO values by 30 mins after the end of UCO (Figure 1 A, B and D), but a significant arterial acidosis was present until 30 min post-UCO (7.23 ± 0.02).

Blood glucose concentration (Figure 1 E) significantly increased in UCO fetuses at 9 (1.71 ± 0.28 mmol/L), 30 min (1.69 ± 0.12 mmol/L) and at 2 h (1.50 ± 0.09 mmol/L) when compared to controls (0.84 ± 0.10 mmol/L, 0.84 ± 0.13 mmol/L, 0.88 ± 0.10 mmol/L respectively). Blood lactate concentration (Figure 1 F) was significantly increased in fetuses that experienced UCO from 5 mins (5.33 ± 2.5 mmol/L) until 2 h (3.98 ± 0.56 mmol/L) post-UCO, peaking at 9 min during UCO (7.05 ± 0.99 mmol/L), compared to the control fetuses (5 mins, 1.28 ± 0.04 mmol/L; 9 mins, 1.22 ± 0.06 mmol/L; 2 h, 1.32 ± 0.10 mmol/L (2 h).

There were no significant differences between groups for these measurements from 2 h after the UCO until the experiment ended, which was either 145 days or when the ewe came into labour.
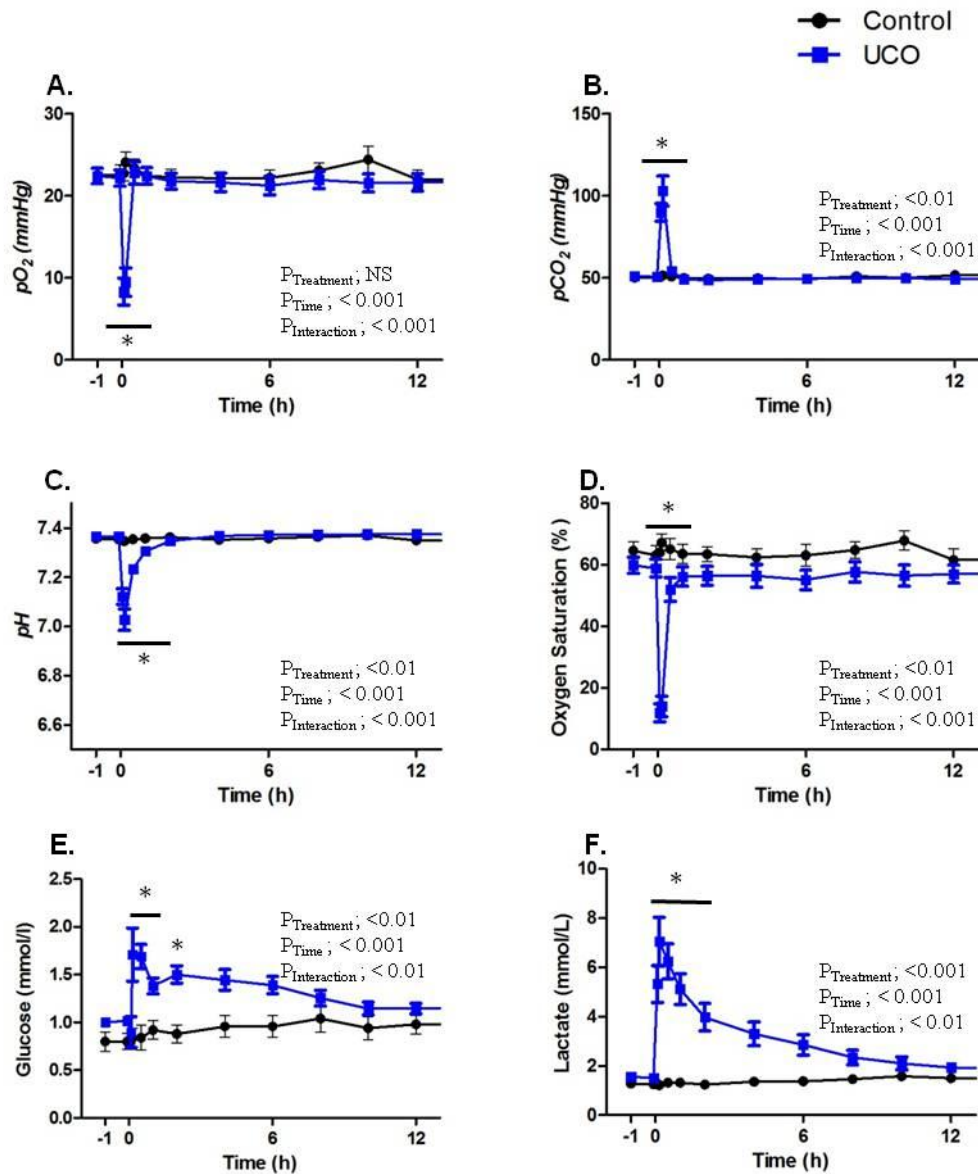
Figure A7.1: Fetal systemic blood gases in response to Sham or 10 min UCO. Fetuses subjected to a sham UCO (Control; black, n=5) or UCO (blue, n=11) responses to pO_2 (A), pCO_2 (B), pH (C), O_2 saturation (D), plasma glucose (E) and plasma lactate (F) from -1 h to +12 h. Time 0 indicates start of UCO (or Sham UCO). * indicates significant ($p < 0.05$) differences compared to controls. Mean $\pm$ SEM.

Mean Arterial Pressure and Heart Rate

The UCO resulted in an initial increase of MAP peaking at 3 min following the start of cord occlusion (59.81 ± 4.22 mmHg vs. 42.37 ± 0.56 mmHg), after which the arterial pressure began to decrease. On release of the umbilical cord cuff MAP significantly increased again at 13 min

(51.11 ± 2.20 mmHg), following this MAP returned to pre-UCO values and by 15 min after UCO, after which there was no significant differences between groups (Figure 2 A).

Fetuses responded to the UCO with a significant bradycardia, with heart rate reaching a minimum at 2 min during UCO (111.86 ± 7.76 beats/min vs. 167.44 ± 15.67 beats/min). Although heart rate appeared to be more variable after the UCO, there was no significant difference between the control and the UCO groups up to 24 h after this intervention (Figure 2 B).
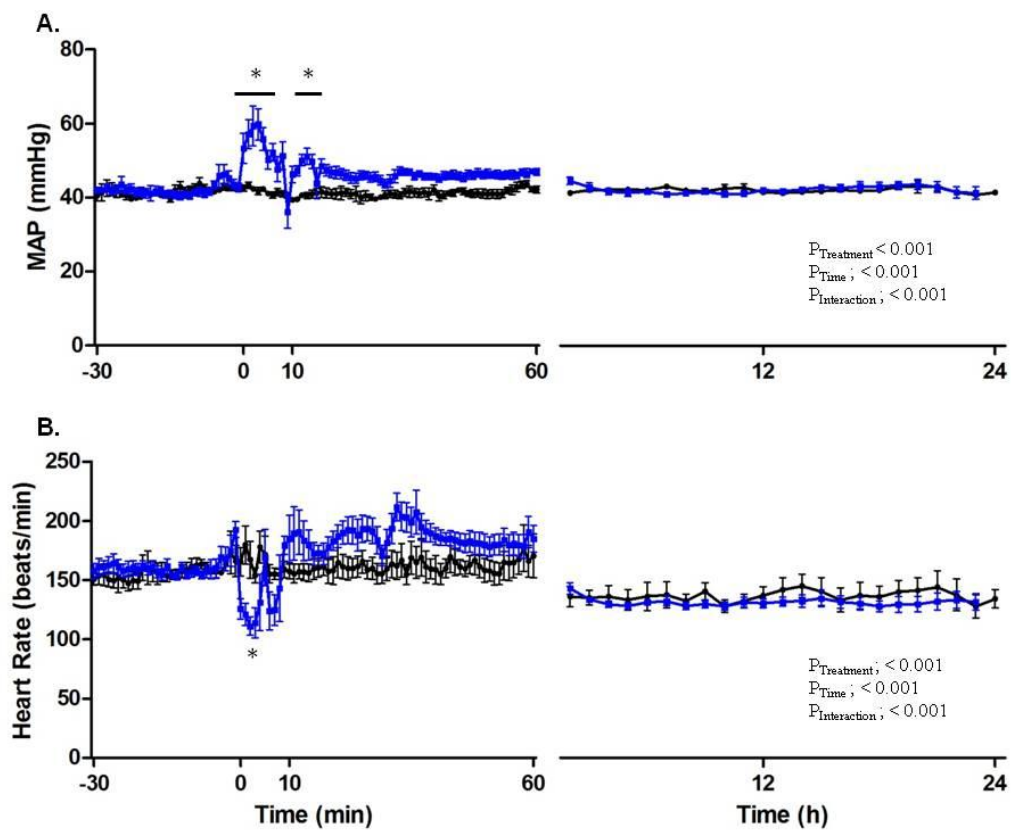

Figure A7.2: Fetal physiological responses to UCO. Mean arterial blood pressure (MAP; A) and heart rate (HR; B) monitored from -30 min to 24 h post-UCO. Time 0 indicates start of UCO (or Sham UCO). * indicates significant ($p < 0.05$) differences compared to controls (black) and UCO (blue). Mean ± SEM. Note x axis scales from minutes to hours.

Outcome of Pregnancy

Following the UCO or sham procedure on days 130–132 gestation, all fetuses were allowed to recover and continue development *in utero.* Figure 3 shows the 'survival plot' for the gestational age when all ewes came into labor. Ewes with fetuses that had experienced UCO went into labour significantly earlier (139.5 ± 1.0 days) than those where the sham UCO (control) procedure was done (144.0 ± 1 days; Table 1), although one of the control ewes went into labour at 140 days GA; the fetus appeared healthy so was included in the analysis. Pregnancy for the remaining 4 control fetuses continued until 145 days, when 2 of the ewes were in labour; all 4 ewes were electively killed at this time. Shown in Figure 3, the ewes whose fetuses experienced UCO went into labour at 136 days gestation (n=2), 137 days (n=3), 138 days (n=1), 140 days (n=1), 142 days (n=1), 143 days (n=1), and 144 days gestation (n=2). One of the 136 day fetuses died while the ewe was in early stage labour; the remainder were all alive immediately prior to post mortem.
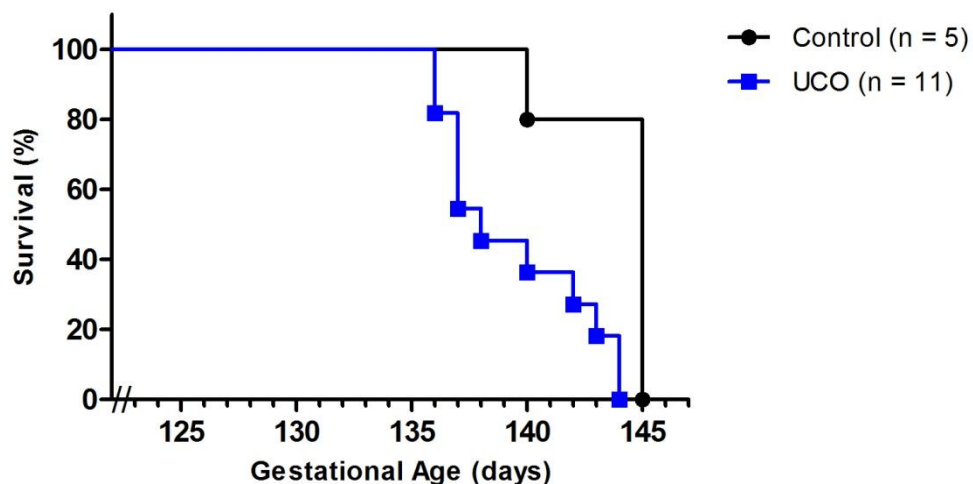

Figure A7.3: Survival plot showing gestational age ewes' went into labour. Fetal sheep surgery was done between 124 – 126 days GA, 10 min UCO (or Sham) occurred between 130 – 132 days GA for Control (n=5; black) and UCO (n=11; blue) groups.

The control group of fetuses consisted of 3 males and 2 females, while the UCO group had 7 males and 4 females (Table 1). Fetuses that experienced UCO had a significantly greater brown fat:body weight ratio (4.97 ± 0.19 vs 3.60 ± 0.60). No other significant differences were seen in fetal body weight or organ:body weight ratio between groups for the brain, heart, liver, adrenals (both left and right combined for each fetus) and kidneys (both left and right combined for each fetus; Table 1).

Table A7.1: Outcome of pregnancy. GA in labour, birth weight, male:female ratio, nose-rump length and organ to body weight ratios for Control (n=5) and UCO (n=11). * $p < 0.05$ difference compared to controls. Mean $\pm$ SEM.

	Control (n = 5)	UCO (n = 11)
GA in labour (days) - Median	145	138
GA in labour (days) - Mean	144 ± 1	139.5 ± 1.0*
Birth weight (kg)	5.59 ± 0.40	4.78 ± 0.32
Male / Female Ratio	3 / 2	7 / 4
Nose-rump length (cm)	65.50 ± 2.36 (n=3)	61.68 ± 1.39
Organ (g):body weight (kg) ratio		
Brain	9.31 ± 0.55	10.67 ± 0.54
Lungs	30.26 ± 0.94	24.07 ± 2.70
Heart	7.06 ± 0.35	7.02 ± 0.41
Liver	27.28 ± 2.26	31.36 ± 2.21
Brown Fat	3.60 ± 0.60	4.97 ± 0.19*
Kidneys	5.14 ± 0.32	5.45 ± 0.20
Adrenal Glands	0.18 ± 0.02	0.20 ± 0.02